In vitro photodynamic effect of gallium, indium and iron phthalocyanine chloride on different cancer cell lines

Submitted in fulfilment of the requirements of the degree of Doctor of Philosophy: Biotechnology in the Faculty of Applied Sciences at the Durban University of Technology

Kaminee Maduray

Supervisor: ..... Date: .....
Professor B Odhav (PhD)

ABSTRACT

Photodynamic therapy (PDT) is emerging as a viable alternative to invasive anti-cancer treatment regimens such as surgery, chemotherapy or radiotherapy. A series of metal – based phthalocyanine complexes have been discovered that may be used as a drug or photosensitizer in photodynamic therapy for the treatment of cancers. During photodynamic therapy the photosensitizer is administrated intravenously or topically to the patient before laser treatment at an appropriate wavelength is delivered to the cancerous site to activate the photosensitizer. The activated photosensitizer will react with oxygen typically present in the cancerous tissue to produce reactive oxygen species for the eradication of the cancerous tissue. This is the first study where gallium (GaPcCl), indium (InPcCl) and iron (FePcCl) Pc chloride complexes were used for photodynamic research. These metal – based phthalocyanine complexes were investigated using different cancer cell lines (Caco-2, MCF-7, melanoma and A549). Also, the baseline cellular uptake and photodynamic effect of these complexes were established on healthy normal cells (human fibroblast cells).

Fluorescent spectrophotometry showed that all three photosensitizers accumulated in a time-dependent manner in Caco-2, MCF-7, melanoma and A549 cancer cells, as well as in healthy normal fibroblast cell in amounts which increased over a period of 24 hours, with emission peaking at 24 hours for all cell lines. Dark toxicity effects and photodynamic therapy efficacy were established with a MTT assay. High concentrations of inactive GaPcCl, InPcCl and FePcCl was toxic to Caco-2, melanoma, A549 and fibroblast cells. However, all three photosensitizers were in its inactive state at low and high photosensitizing concentrations were highly toxic to MCF-7 cancer cells. On the other hand, *in vitro* photodynamic therapy treatment with both low and high concentrations of GaPcCl, InPcCl and FePcCl were observed to be potently cytotoxic towards all four cancer

cell lines upon exposure to laser light for 22 seconds (2.5 J/cm^2), 39 seconds (4.5 J/cm^2) and 74 seconds (8.5 J/cm^2). These results revealed that all three photosensitizers reacts to photodynamic therapy in a concentration-dependent (photosensitizer) and dose-dependent (light dose/time) manner.

At 24 hours after photodynamic therapy, the most effective treatment parameters were laser treatment for 74 seconds with FePcCl concentrations from 60 µg/ml - 100 µg/ml which resulted in 0% cell survival of Caco-2 cancer cells. A short laser treatment time of 74 seconds for activation of FePcCl (20 µg/ml) resulted in 0% cell survival of MCF-7 cancer cells. Similarly, FePcCl (40 µg/ml - 100 µg/ml) activated for 22 seconds, 39 seconds and 74 seconds resulted in 100% cell death of A549 cancer cells. Photodynamic therapy treatment with GaPcCl and InPcCl were very effective in reducing the cell viability of melanoma cancer cells. Healthy normal fibroblast cells survived *in vitro* photodynamic therapy treatment with all three photosensitizers much better than the cancer (Caco-2, MCF-7, melanoma and A549) cells. This confirms the previously reported results that photosensitizers such as phthalocyanines and its metal-based complexes preferentially accumulate in cancer cells than normal healthy cells.

All three photosensitizers localized in mitochondria and lysosomes of the Caco-2, MCF-7 and A549 cancer cells. In melanoma cancer cells InPcCl also localized in the mitochondria and lysosome, but GaPcCl and FePcCl localized in mitochondria only. Apoptosis was identified via microscopical and flow cytometric investigations, as the dominant mode of cell death induced by GaPcCl, InPcCl and FePcCl mediated photodynamic therapy in cancer cell lines tested. Therefore, this study concludes that GaPcCl, InPcCl and FePcCl are effective photosensitizers for the *in vitro* PDT treatment of cancer cells. The effective *in*

vitro PDT treatment for each cell line was dependent on the photosensitizer concentration and illumination period for each of the different photosensitizers.

DECLARATION

I, Kaminee Maduray hereby declare that this thesis is my own work and effort. It has not been submitted in any form to another academic institution. Where information was used from other sources, the authors have been acknowledged and referenced accordingly.

_____
Student: Kaminee Maduray (Miss)

Approved for final submission

_____
Supervisor: Professor B Odhav (Ph.D.)

DEDICATION

I dedicate this work to:

My Mrs. S Maduray (mum) and Mr. Y Maduray (dad) for their continuous support and motivation. I am truly blessed to have you as parents.

ACKNOWLEDGEMENTS

I would like to express my gratitude and thanks to my supervisor Professor Odhav for her guidance, supervision, assistance, patience and above all encouragement throughout my undergraduate study.

I am indebted to the Department of Biotechnology and Food Technology for giving me the opportunity to study and conduct my Doctorate Degree research project at the postgraduate plant group research laboratory. My special appreciation is for Professor Suren Singh and Professor Kugen Permaul for their on-going support. I would like to also thank all the postgraduate students (plant and enzyme group) and staff of Department of Biotechnology and Food Technology for their assistance during experimental work.

A special thanks to Dr Celia Synman for proofreading and correcting my thesis. I wish to extend my sincere appreciation to Dr Yen-Ju, Natasha Kolesnikova, Dr Bronwyn C Joubert and Dr A D Marais for kindly providing me with cell lines for my experiments. I would like to acknowledge Christopher from the UKZN (laboratory for microscopy and microanalysis) for his assistance with the Transmission Electron Microscopy and Prof T Naickar from K-RITH her assistance with the Fluorescence Microscopy.

I am tremendously grateful to my family (Sally, Roy, Sivashin, Dhiya and Ravina Maduray) for their support, blessings and prayers. I have successfully completed this degree with their constant encouragement and faith in me. To God, thank you for giving me the strength to complete this degree and guiding me through the many obstacles in my path. Thank you for your protection and for your many signs along the way.

TABLE OF CONTENTS

LIST OF FIGURES

Chapter 1

LIST OF TABLES

Chapter 1

Chapter 2

Chapter 3

ABBREVATIONS

PS	Photosensitizer
PSs	Photosensitizers
PDT	Photodynamic therapy
h	hour
sec	second
min	minute
MTT	Methyl-thiazolyl-tetrazolium
DMSO	Dimethylsulfoxide
ROS	Reactive oxygen species
A.U.	Arbitrary units
Pc	Phthalocyanine
Pcs	Phthalocyanines
J/cm^2	Joules per centimeter square
nm	nanometers
GaPcCl	Gallium (III) phthalocyanine chloride
InPcCl	Indium (III) phthalocyanine chloride
FePcCl	Iron (III) phthalocyanine chloride
BPD	Benzoporphyrin derivatives
m – THPc	meta-tetrahydroxyphenyl chlorin
ALA	5-Aminolevulinic acid
HpD	Hematoporphyrin derivative
HPPH	2-[hexyloxyethyl-2 devinyl pyropheophorbide-α
Zn	Zinc

Al	Aluminum
Ga	Gallium
In	Indium
Si	Silicon
Cu	Copper
Fe	Iron
Co	Cobalt
VO	Vanadium
ER	Endoplasmic reticulum
DMEM	Dulbecco’s MEM
FBS	Fetal bovine serum
PBS	Phosphate buffered saline
MCF-7	Michigan cancer foundation

LIST OF PUBLICATIONS

Maduray, K., Odhav, B. 2012 Efficacy of gallium phthalocyanine as a photosensitizing agent in photodynamic therapy for the treatment of cancer. *SPIE,* 8553, 1-7, doi: 10.1117/12.2001266.

Maduray, K., Odhav, B. 2013 The *in vitro* photodynamic effect of laser activated gallium, indium and iron phthalocyanine chlorides on human lung adenocarcinoma cells. *Journal of Photochemistry and Photobiology B: Biology*, 128, 58‑63.

Maduray, K., Odhav, B. 2014 Metal-based phthalocyanines as a potential photosensitizing agent in photodynamic therapy for the treatment of melanoma skin cancer. *SPIE,* 8931, 1-7, doi: 10.1117/12.2044382.

CHAPTER 1

LITERATURE REVIEW

1.1 INTRODUCTION

Light has been known for its therapeutic benefits for more than three thousand years now. Light therapy (phototherapy) was practiced in ancient Egypt, India, Greece and China to treat various diseases, including psoriasis, rickets, vitiligo and skin cancer. At the end of the nineteenth century, Niels Finsen further developed “phototherapy’’ or the use of light to treat diseases in Denmark. He discovered that light exposure in the red visible range prevents the formation and discharge of smallpox pustules and can be used to treat this disease. Niels Finsen also found that ultraviolet light from the sun could be used to treat cutaneous tuberculosis. This was the beginning of the modern light therapy, and, in 1903, Finsen was awarded a Nobel Prize for his phototherapy discoveries (Dolmans *et al*., 2003).

In 1903, Professor Herman Von Tappeiner treated skin tumors with topically applied eosin and white light. The term “photodynamic action” was introduced in 1904 by Professor Herman Von Tappeiner (Dolmans *et al*., 2003). This term indicated the damage or destruction of cancerous tissue by visible light in the presence of a nontoxic sensitizer or chemical, emphasizing the requirement of oxygen for the process (Dolmans *et al*., 2003). Therefore, the term photodynamic therapy (PDT) is currently used. In another study, 25 patients with a total of 113 primary or secondary skin tumors were PDT treated with haematoporphyrin derivative (HPD). A complete response was observed in 98 tumors, a partial response was observed in 13 tumors and 2 tumors were found to be PDT treatment resistant (Dolmans *et al*., 2003). Following the preliminary successes in treating bladder

and skin tumors, Hayata and colleagues used PDT to treat obstructing lung tumors (Dolmans *et al*., 2003). Bronchoscopic analysis showed tumor growth delay in most patients, but only one out of fourteen patients was cured. In 1984, McCaughan and colleagues used PDT to treat patients with oesophageal tumors; Balchum and colleagues used PDT to treat patients with lung tumors; and Hayata and colleagues used PDT to treat patients with gastric carcinoma (Dolmans *et al*., 2003). These studies displayed promising responses in early stage patients, therefore PDT was recommended for patients with early stage cancers that were inoperable, due to other complications (Dolmans *et al*., 2003). Patients with breast, gynecological, intraocular, brain, head, neck, colorectal intraperitoneal, mesothelioma, cholangiocarcinoma and pancreatic tumors were subsequently treated with PDT. However, this therapy has only shown limited success in further studies, due to issues surrounding specificity and potency of photosensitizers (PSs). Another confounding factor is that PDT has been tested largely in patients with advanced stage diseases that are refractory to other treatments (Dolmans *et al*., 2003). In such cases, a local effect can usually not significantly alter the outcome of a systemic disease. More selective and potent sensitizers have been developed, which are now under investigation in clinical trials. With new lines of drugs, as well as with improved localization methods, improved protocols and equipment, the efficacy of PDT might be enhanced (Dolmans *et al*., 2003).

1.2 OVERVIEW OF CANCER AND CONVENTIONAL ONCOLOGY TREATMENTS

In modern medicine, the term malignant neoplasm (cancer) refers to the formation of an abnormal mass of tissue (tumor) as a result of cells undergoing uncontrolled proliferation due to gain of mutated proto-oncogenes (oncogenes) and loss of function of tumor suppressor genes (Alison, 2001). Healthy normal cells growth is controlled by proto-oncogenes that produce protein products which generally control how often a cell divides,

the degree to which it differentiates (or specializes in a specific function in the body) as well as genes that slow down cell division, repair DNA errors or instruct the cells when to die (by a process known as apoptosis or programmed cell death), suppressing uncontrolled cell proliferation (Alison, 2001). Generally, in damaged cells the uncontrolled and often rapid proliferation of cells can lead to tumors that are either benign (non-cancerous) or malignant (cancerous). The major differences between benign and malignant tumors are (Alison, 2001):

- Benign tumors usually have a slower growth rate than malignant tumors
- Benign tumors lack the ability to invade neighboring healthy normal tissue compared to malignant tumors which usually invade into surrounding healthy normal tissue (locally invasive cancer) as well as distant tissue or organs (metastatic cancer)

Metastatic cancer is of great importance since most cancer deaths are caused by the spread of the cancer to other secondary organs (Alison, 2001). In most cases, cancer patients with localized cancer have a better chance of survival than those with metastatic cancer (Alison, 2001). A histopathologist will 'grade' the tumor in terms of its state of differentiation because poorly differentiated (high grade) tumors show little or no resemblance to the tissue of origin (Alison, 2001). These tumors tend to be more aggressive, grow faster and are more likely to have metastasized prior to diagnoses or treatment. The presence of metastatic tumors immediately assigns the patient to the most advanced stage of cancer, irrespective of the size of the primary tumor (Alison, 2001). Therefore the management or treatment for cancer is dependent upon the following information (Alison, 2001):

- The site of the primary tumor or tissue of origin
- Tumor grade and stage

- Benign or Malignant tumor (local or metastatic)

Surgery is recommended as primary treatment for the removal of benign tumors and malignant solid tumors (Urruticoechea *et al*., 2010). An additional concern about malignant solid tumors is that adjuvant (after) or neoadjuvant therapy (before) may need to be given in combination with surgery (primary treatment) to reduce the risk of cancer recurrence. The common adjuvant and neoadjuvant treatment options used by many specialists are chemotherapy and radiotherapy (Urruticoechea *et al*., 2010). Systemic chemotherapy is used for more diffused tumors such as leukemia with circulating tumor cells. The new generation treatment modalities include targeted therapies or nanotechnology, hormonal therapy, immunotherapy and cancer vaccines (Aly, 2012). Despite numerous improvements made in cancer detection and treatment, the number of deaths from cancer is still high worldwide and a cure is still needed. All the conventional cancer treatments including new generation therapeutic modalities show a lack of efficiency in terms of adverse side effects, toxicity, resistance or toxicity due to non-specific effects on normal cells (Hu and Fu, 2012). In contrast, PDT is becoming recognized as an emerging alternative to all previously used therapies (Konopka and Goslinski, 2007). Although still emerging, it is now a successful and clinically approved therapeutic modality used for the management or treatment of specific malignant neoplastic diseases (Agostinis *et al*., 2011); as well as in several precancerous diseases and non-cancerous diseases (e.g. cardiovascular, dermatological, ophthalmic and infectious diseases) (Ethirajan *et al*., 2011) in several countries (e.g. United States, European Union, Canada, Russia and Japan) (Postiglione *et al*., 2011). The major advantages of PDT over conventional anti-cancer therapies are (Konopka and Goslinski, 2007):

- It is non-invasive
- Convenient for the patient

- Can be performed in outpatient or day-case (inpatient) settings
- It can improve quality and lengthen survival of patients in the advanced cancer stage
- Treatment can be repeated without compromising its efficacy
- Moderate to no sides effects
- Can have excellent cosmetic results since treatment involves in minimal or no scarring
- Can offer organ-sparing treatment worldwide, with very little investment in infrastructure

PDT is still considered to be an evolving and promising cancer treatment strategy. Its full potential has yet to be revealed, and its collection of medical applications alone or in combination with other clinically approved or experimental therapeutic approaches is definitely not exhausted (Agostinis *et al*., 2011). The other advantages of PDT compared with surgery, chemotherapy or radiation therapy are reduced long term morbidity and the fact that PDT does not compromise future treatment options with residual or recurrent disease (Agostinis *et al*., 2011).

1.3 PRINCIPLES OF PHOTODYNAMIC THERAPY

PDT is a photochemistry-based approach that uses an inactive photosensitizer (PS), light from a laser source emitting at an appropriate wavelength and oxygen to impart cytotoxicity via the generation of reactive molecular species such as reactive oxygen species (ROS) and excited state singlet oxygen in cancerous tissue (Celli *et al*., 2010). In clinical settings, the inactive PS is typically administrated intravenously or topically, which is preferentially taken up by rapidly proliferating tissue such as cancerous tissue rather than healthy normal tissue. This may be due to the fact that cancerous tissues have leaky

neovasculature allowing for enhanced permeability and accumulation of the PS specifically in the tumor region (Celli *et al*., 2010). A time interval (drug-light interval) is required to allow PS uptake ranging from a few minutes up to twenty four hours or more depending on the specific PS and the disease to treat. This is followed by light treatment (irradiation) or PS activation using a laser delivery system suitable for the anatomical site being treated (Celli *et al*., 2010). Typically, the applicable range of wavelengths for therapeutic activation of the PS is from 600 nm to 800 nm to avoid interference by endogenous chromophores within the body (Celli *et al*., 2010). During laser treatment, the activated PS can directly react with a substrate (e.g. cell membrane or molecule) and transfer a proton or hydrogen atom to form free radicals (Juarranz *et al*., 2008). These radicals will react with oxygen present in the tissue to produce ROS. Alternatively, the activated PS can transfer its energy directly to molecular oxygen (a triplet form in the ground state), to form an excited state singlet oxygen (Juarranz *et al*., 2008). This highly reactive form of oxygen (excited state singlet oxygen) will react with many biological molecules (e.g. lipids, proteins or nucleic acids). Both these photochemical reactions can occur simultaneously to generate ROS and excited state singlet oxygen (Juarranz *et al*., 2008). PDT efficiency is highly dependent on several factors including the amount of ROS and excited state singlet oxygen produced, which are the primary cytotoxic agents responsible for the eradication of cancerous tissue by inducing irreversible tumor cell death via necrosis, apoptosis or autophagy (Juarranz *et al*., 2008). Other factors influencing efficacy include the type of photosensitizing agent, its preparation and characteristics, the concentration of and administration of the photosensitizing agent, the type of light used for tumor irradiation and its parameters (energy intensity or light dose, power, fluence rate or power intensity, wavelength and time exposure) (Mihaela *et al*., 2009).

Compared with conventional oncology treatments, PDT can achieve equivalent efficacy in the treatment of certain cancers, particularly in the head, neck and mouth as well as skin lesions and basal cell carcinoma with great reduced morbidity and excellent cosmetic outcomes (Cabuy, 2012). Due to the ability to offer endoscopic delivery of light to hollow structures, PDT has been successful in the treatment of early gastrointestinal cancers, such as oesophageal cancer and lung cancer (Cabuy, 2012). Current evidence suggests that there are no major safety concerns associated with PDT, with no reports on the production of second malignant neoplasms. Laser treatment during PDT is a cold photochemical process which does not cause tissue heating or damage to connective tissues such as collagen and elastin (Cabuy, 2012). However, PDT is not yet an established treatment option in most countries and for many cancers presumably due to the lack of large randomized clinical trials (Cabuy, 2012). Researchers continue to explore ways to improve the effectiveness of PDT and expand it to other cancers. Other ways to improve PDT include optimization of PDT protocols such as fractionation of light or PS, well designed clinical trials and the development of new PSs (Cabuy, 2012).

1.4 BASIC COMPONENTS OF PDT

Clinically, PDT is relatively simple to perform. In reality PDT requires complex interaction between three components (PS, light and oxygen) to be available during treatment. Below is a review two key components of PDT (i.e. PSs and light sources).

1.4.1 PHOTOSENSITIZERS

Nontoxic, fluorescent and photosensitive chemical compounds, drugs or dyes are used as PS agents during PDT. Each PS molecule with the absorption of a single photon of light is promoted to an excited singlet state (e.g. S_1), and higher excited states can also be produced depending on the PS as well as the excitation wavelength used (Sharman *et al*.,

1999) as illustrated in Figure 1.1. This electronic excitation state of a PS can stimulate cytotoxic effects as well as emit fluorescence during relaxation from its excited singlet state back to its ground state (Celli *et al*., 2010). Therefore, in addition to therapeutic agents for PDT, PSs can be used as diagnostic imaging agents for selective visualization of tumors as PSs preferentially accumulate in neoplastic tissues and fluoresce upon excitation with the appropriate wavelength (Celli *et al*., 2010).

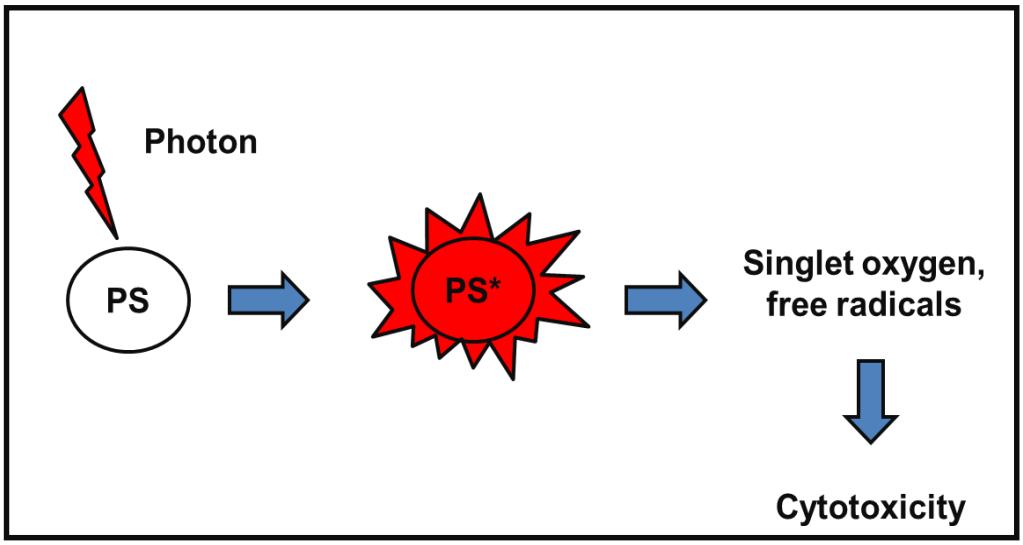

Figure 1.1 The events in PDT. Energy photons from a laser or a light source are absorbed by molecules (PS – ground state) which are activated by light. The activated PS (PS* - triplet state) leads to the formation of reactive molecular species that stimulate cytotoxicity (Hasan *et al*., 2011).

In general, the ideal PS is characterized on the basis of toxicity, selectivity, wavelength and cost (Allison *et al*., 2004a) as outlined in Table 1.1. While no PS can be expected to fulfil all of these guidelines, numerous PSs (e.g. natural dyes, synthetic dyes, plant pigments and complex synthetic macrocycles) fulfilling some of these criteria have been discovered. Many are known to be potential and excellent PDT agents but only a few are commercialized or clinically approved PSs (Sharman *et al*., 1999). Most of these identified

PSs (based directly on its chemical structure) are categorized into three main classes including derivatives; namely, porphyrin; chlorophyll and phthalocyanines (Pcs) (Table 1.2).

Porphyrins are commonly known as first-generation PSs with PSs developed in the 1970s and early 1980s were regarded as first-generation PSs (Allison *et al*., 2004a). Second – generation PSs were developed in the late 1980s to minimize the drawbacks of first-generation PSs and to improve PDT (Allison *et al*., 2004a). These second generation PSs include porphyrins, expanded porphyrins, chlorophyll with derivatives, phthalocyanines (Pcs) and phthalocyanine (Pc) derivatives. More recently, targeting strategies have been shown to improve the specificity of PS accumulation in cancerous tissue only. Therefore, targeted PDT approaches has led to conjugating pre-existing PSs (first-generation and second-generation) to antibodies and nanoparticles to form third-generation PSs (Allison *et al*., 2004a). Thus, the use of third-generation PSs in PDT promises to deliver the benefits of conventional PDT combined with the specificity and potency of antibody therapy or drug delivery therapy (Allison *et al*., 2004a).

Table 1.1 The characteristics of an ideal PS for PDT with regard to clinical relevance (adapted from Allison *et al*., 2004a)

	Characteristics of an ideal PS	Reference
Toxicity	Should not be a toxic chemical and metabolism of the PS should not create new toxic byproducts.	(Allison *et al*., 2004a)
Dark toxicity	It is not cytotoxic or has minimal cytotoxicity in the absence of light.	(Sharman et al., 1999)
Mutagenicity / Carcinogenicity	Should not locate in the nuclei, cure one disease and create another.	(Allison *et al*., 2004a)
Elimination	Be eliminated from the body appropriately and quickly to avoid generalized skin photosensitization.	(Allison *et al*., 2004a)
Selectivity	Selectively accumulate in diseased tissue.	(Allison *et al*., 2004a)
Targeted Intracellular localization	Intracellular targets, e.g. mitochondria of the diseased cell will lead to cell death via programmed death by apoptosis.	(Allison *et al*., 2004a)
Sunlight precautions	Exhibit low absorption at wavelengths from 300-400 nm (spectral range where daylight intensity is the highest) leading to potentially low or no skin photosensitivity after PDT treatment.	(Allison *et al*., 2004a)
Administration	Administration options should be versatile; topical, intravenously or oral depending on the clinical situation and affected area. In all cases, minimal administrative toxicity (i.e. hypotension and allergic reactions) and ease of administration.	(Allison *et al*., 2004a)
Reliability	Composition must be known and constant. Pure compound.	(Allison *et al*., 2004a)
Stability	Chemically stable and photostable.	(Allison *et al*., 2004a)
Biochemistry	Soluble in harmless aqueous solvent mixtures or water. Have a high photochemical reactivity, with high triplet state yields and long triplet state lifetimes and produce a high quantum yield of ROS which is often mediated by singlet oxygen. A high extinction coefficient in the 600 – 800 nm range.	(Kudinova and Berezov, 2010)
Safety	Should not induce adverse side effects (e.g. morbidity or clots, strokes, heart attacks, etc.).	(Allison *et al*., 2004a)
Activation Wavelength	High absorption peak between 600 nm – 800 nm to provide enough energy to excite oxygen molecules to its singlet state for a substantial yield of ROS; maximum skin penetration to treat deep-seated tumors and minimal to no skin photosensitivity.	(Allison *et al*., 2004a)
Integrative ability	To be used as photosensitizing agent during PDT treatment only; as well as in conjunction with other forms of oncology treatments.	(Allison *et al*., 2004a)
Availability / Cost	Must be commercial available and able to be reconstituted by a local pharmacy. Cost-effective.	(Allison *et al*., 2004a)

Table 1.2 PS families and the generation gap between each family (Allison *et al*., 2004a)

Family	PSs	Generation
Porphyrin	Hp (hematoporphyrin)	First-Generation
	HpD (hematoporphyrin derivatives)	First-Generation
	ALA (5 – aminolevulinic acid)	First-Generation
	BPD (benzoporphyrin derivative)	Second-Generation
	Texaphyrins	Second-Generation
Chlorophyll	Chorins	Second-Generation
	Purpurins	Second-Generation
	Bacteriochlorins	Second-Generation
Phthalocyanines	Napthalocyanine	Second-Generation
	Metallophthalocyanines	Second-Generation

1.4.1.1 FIRST-GENERATION PHOTOSENSITIZERS

Porphyrins are tetrapyrrolic (Figure 1.2) molecules with a heterocyclic macrocycle core skeleton known as a porpine (Josefsen and Boyle, 2008b). These are naturally occurring groups of intensely coloured compounds that are involved in a number of biological processes such as oxygen transport and photosynthesis. It also has applications in the medical field (e.g. PDT and fluorescence imaging). The characteristic spectrum of porphyrins consists of an intense narrow absorption band (ε > 200 000 mol^{-1} cm^{-1}) at around 400 nm (Soret or B Band) and weaker absorptions (ε > 200 000 mol^{-1} cm^{-1}) from 450 nm to 700 nm referred to as Q bands (Josefsen and Boyle, 2008b). Hematoporphyrin (Hp) and hematoporphyrin derivatives (HpD) are examples of first – generation porphyrin based PSs (Juzeniene *et al*., 2007).

The most common clinically used PS is a HpD (Figure 1.2) known as Porfimer sodium (Photofrin®) which is mixture of mono and oligomeric porphyrins (Allison and Sibata, 2010). This photosensitizing agent is considered reliable, can be light activated, pain free, relatively safe and nontoxic (Allison *et al*., 2004a). It has been accepted in several countries for the treatment of bladder, cervical, lung, oesophageal and gastric cancer

(Sharman *et al*., 1999). In addition, Photofrin® is being investigated as a possible photosensitizing agent for PDT treatment of Kaposi's sarcoma, head, neck, brain, intestinal, breast and skin cancer (Sharman *et al*., 1999). In clinical practice, Photofrin® is infused at 2 mg/kg and about 48 hours later illumination via laser treatment occurs generally by a diffusing fibre or more rarely by micro lens (Allison *et al*., 2004a). A treatment light dose of 150 J/cm^2 (lens) or 200 – 300 J/cm^2 (diffuser) is used during illumination, which largely depends on the clinical situation (Allison *et al*., 2004a). A photosensitizing concentration of 2 mg/kg has been the standard to achieve high tumor response as well as high rates of acute normal tissue toxicity (Allison and Sibata, 2010). At 2 mg/kg Photofrin® is taken up by healthy normal tissue with slightly higher concentrations in cancerous tissue (Allison and Sibata, 2010).

Other disadvantages of Photofrin® include its weak absorption at the therapeutic wavelength of 630 nm and absorption spectra of Photofrin® overlaps with melanin (Allen *et al*., 2001). This means Photofrin® - mediated PDT may be ineffective therapy for highly pigmented cancers such as melanoma cancer (Allen *et al*., 2001). It is, however, associated with significant prolonged skin photosensitivity (4 – 8 weeks) after treatment (Yano *et al*., 2011). Several studies, employing Photofrin® at lower concentrations (i.e. 1.2 mg/kg or 0.8 mg/kg) resulted in far more selective tumor destruction with minimal healthy normal tissue toxicity (Allison and Sibata, 2010). At these levels Photofrin® ablates tumors but spares healthy normal tissue, making these lower photosensitizing concentrations highly selective. It should be noted that the use of lower photosensitizing concentrations requires higher treatment light doses (Allison and Sibata, 2010). Higher light doses will allow for the delivery of additional light photons to the cancerous tissue for enhanced tissue penetration. Skin photosensitivity may also be eliminated as well but this has been poorly documented (Allison and Sibata, 2010).

Another first-generation prodrug is 5-Aminolevulinic acid (ALA, Figure 1.2) commercially known as Levulan and produced by DUSA Pharmaceuticals (Josefsen and Boyle, 2008b). This naturally occurring amino acid is enzymatically converted to the protoporphyrin IX (PPIX; active state) *in vivo*, which is then converted to heme (Allison and Sibata, 2010). ALA also shows low cytotoxicity in its inactive state and endogenously produced PPIX is rapidly cleared from the body (24 – 48 h) by natural clearance mechanisms which exist *in vivo* (Juzeniene *et al*., 2007). It can be administrated systemically (intravenously and orally) or topically. A short time interval of 1 – 8 h, which largely depends on the mode of administration, is required for the maximal accumulation of PPIX in the diseased tissue after ALA administration (Juzeniene *et al*., 2007). When ALA is administrated topically it does not penetrate to great depth, which limits its application. However, skin photosensitivity is limited to the area of application (Juzeniene *et al*., 2007). With systemic administration skin photosensitivity will occur for about 48 h and gastrointestinal upset as recognized side effect (Allison and Sibata, 2010). Clinically, ALA mediated PDT has been approved for the treatment of actinic keratosis, superficial basal cell lesions, nodular basal cell tumors, squamous cell tumors, head tumors, neck tumors, Barrett's oesophagus, bladder and prostate cancer (Allison and Sibata, 2010).

In addition, a methylated version ALA or ALA methyl ester (methyl-aminolevulonic acid, M-ALA) commercially called Metvix (Photocure ASA, Norway) is widely used for the PDT treatment of basal cell carcinoma and other skin lesions (Allison and Sibata, 2010). M-ALA has enhanced lipohylicity which allows for deeper tissue penetration (Allison and Sibata, 2010). It is topically applied for 3 h followed by red light laser treatment (Allison *et al*., 2004a). However, pain still remains a common disadvantage during treatment (Allison *et al*., 2004a). New ALA derivatives are continuously being designed and in the future low

doses of ALA-PDT will be employed for photorejuvenation as well as for the photochemoprevention of skin tumors (Allison and Sibata, 2010).

The disadvantages associated with clinically approved first-generation PSs (e.g. ALA and Photofrin®) are skin photosensitivity, weak absorption at therapeutic wavelengths, pain and ineffectiveness as photosensitizing agents for certain cancers have not prevented the successful PDT treatment of other cancers or diseases. The development of second-generation PSs are designed to improve PDT and overcome these disadvantages of ALA, Photofrin® and other first-generation PSs (Allison *et al*., 2004a).

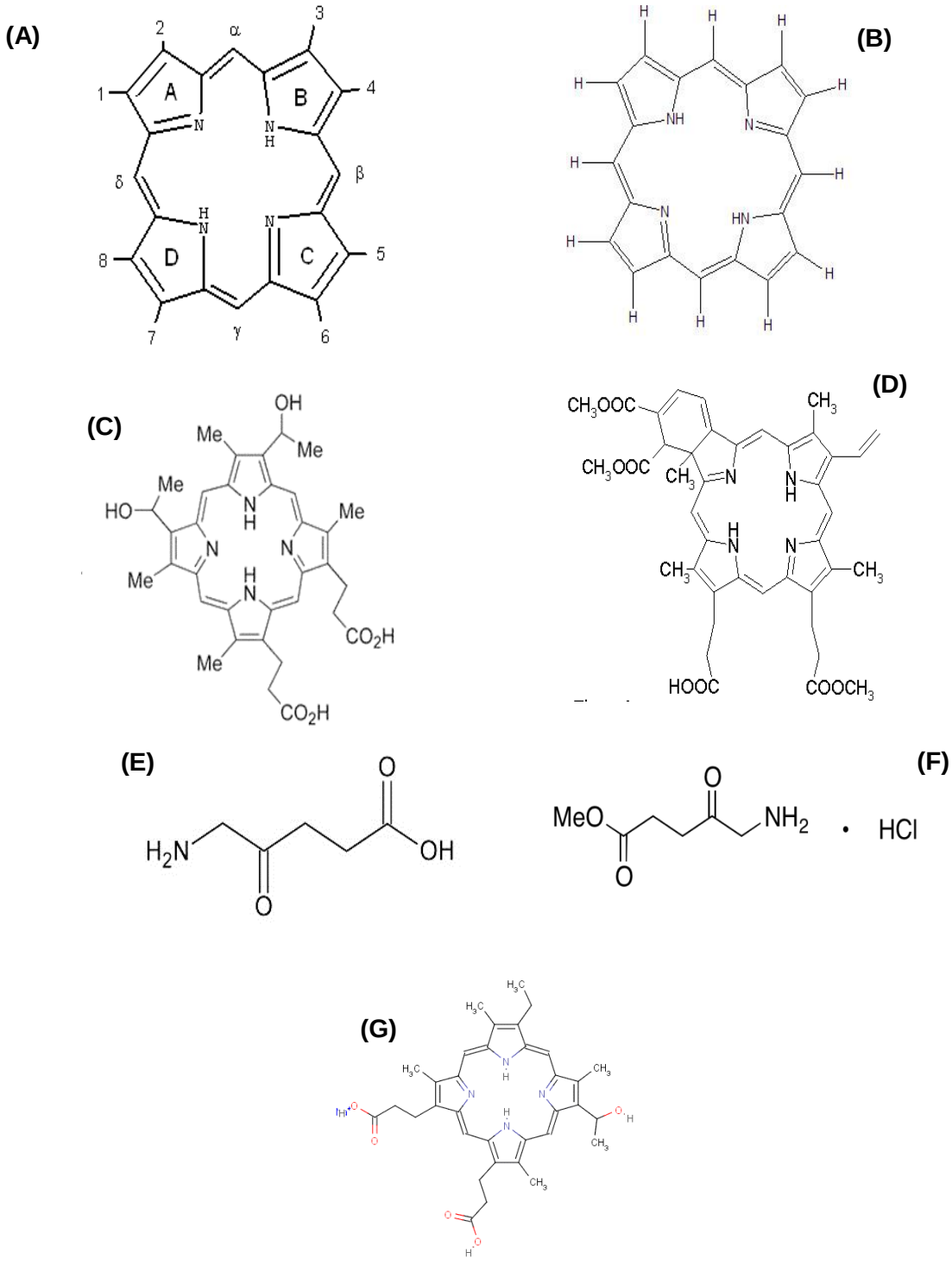

Figure 1.2 The chemical structure of (A) Tetrapyrrolic (B) porphyrin (C) hematoporphyrin (D) benzoporphyrin derivative (E) 5-aminolevulinic acid (F) 5-aminolevulinic acid methyl ester and (G) Photofrin (Josefsen and Boyle, 2012).

1.4.1.2 SECOND-GENERATION PHOTOSENSITIZERS (PSS)

The chlorophyll family (Figure 1.3) consists of a wide range of intensely developed second-generation PSs that includes chorins, purpurins and baceriochlorins (Kudinova and Berezov, 2010). One of the most widely utilized chlorin PS is Foscan® (trade name) also known as Temoporfin or tetra (m-hydroxyphenyl) for PDT (Yano *et al*., 2011). The most noted advantages are that it is a pure compound and yields an extraordinary amount of singlet oxygen at 652 nm, using low drug concentrations with low light doses during PDT treatment (Yano *et al*., 2011). Clinically, it is commonly used to treat neck and head cancers (Yano *et al*., 2011).

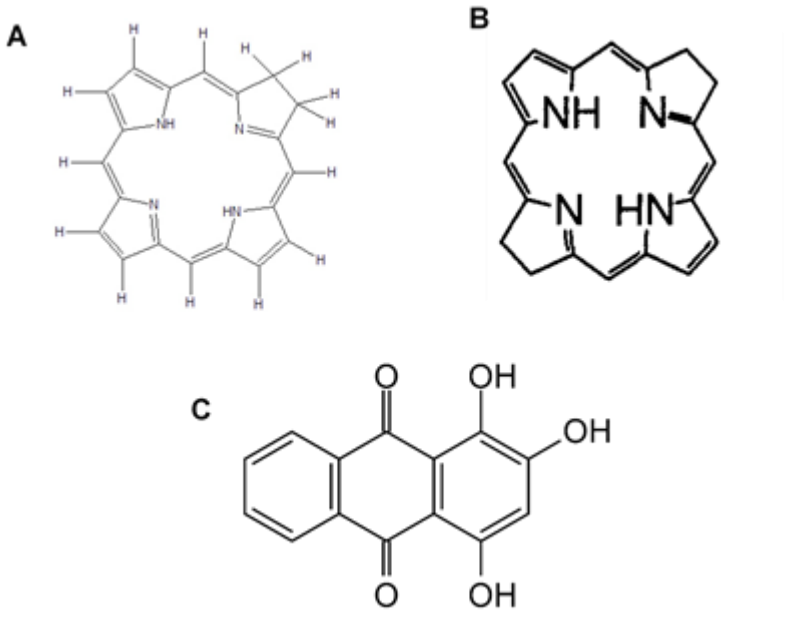

Figure 1.3 The structure of (A) chlorins (B) bacteriochlorins and (C) purpurins (Josefsen and Boyle, 2012).

In comparison to Photofrin®, a photodynamic response can be achieved with 0.1 mg/ kg of Foscan® and a treatment light dose of 5 J/cm^2 (Josefsen and Boyle, 2008b). Therefore, Foscan® is approximately hundred-fold more potent and photoactive than (2 - 5 mg/ kg and 100 – 300 J/cm^2) Photofrin® (Josefsen and Boyle, 2008b). Unfortunately, Foscan® may be administrated only intravenously during PDT and is associated with pain (Allison *et al*., 2004a). Clinically, it takes about 4 days to achieve accumulation of Foscan® in the tumor and clearance from normal healthy tissue in order for laser treatment to proceed (Allison *et al*., 2004a). It requires a long clearance time of 4 - 6 weeks from human plasma after injection (Yano *et al*., 2011). Prolonged photosensitivity from 2 weeks to 6 weeks can occur after Foscan® mediated PDT treatment. However much lower Foscan® concentrations administrated during PDT treatment of tumors can prevent prolonged photosensitivity (Yano *et al*., 2011).

Laserphyrin® (mono-L-aspartylchlorin-e_6) is another second-generation PS but a chlorin derivative (Yano *et al*., 2011). This chlorin derivative has numerous names including MACE, NPe6, LS11, Litx™, Photolon and Apoptosin™ (Allison and Sibata, 2010). Laserphyrin® was approved to be used as photosensitizing agent in PDT for the treatment of early-stage lung cancer in 2003 in Japan (Yano *et al*., 2011). It is also under phase II studies for liver, recurrent neck and head cancer (Yano *et al*., 2011). This PS is active at a long wavelength of 664 nm and a short interval of 2 - 4 h post infusion prior to laser treatment. In addition, it generates singlet oxygen very efficiently and is water-soluble. In PDT, a low PS concentration of Laserphyrin® (0.5 mg/kg – 3.5 mg/kg) and a treatment light dose of 150 J/cm^2 are used (Yano *et al*., 2011). Laserphyrin® also has a very short clearance time (3 – 7 days) and low accumulation in the skin which reduces or prevents skin photosensitivity after PDT treatment (Yano *et al*., 2011). This PS is excreted through the bile and appears to be safe (Allison and Sibata, 2010). 2-[hexyloxyethyl]-2 devinyl

pyropheophorbide-α (HPPH or Photochlor) is also a second-generation chlorine derivate (Allison *et al*., 2004a).

Clinically, this chlorine-based PS has successfully treated a number of naturally occurring tumors in cats and dogs (Allison and Sibata, 2010). This PS is hydrophobic and lipophilic in nature (Allison *et al*., 2004a). It is highly active at 665 nm (Allison and Sibata, 2010). HPPH selectively accumulates in tumors (Allison *et al*., 2004a). Photosensitizing concentrations range from 2.5 – 6 mg/m^2 and treatment light doses of 44.4 J/cm^2 – 133.2 J/cm^2 is necessary for the PDT treatment of tumors (Allison and Sibata, 2010). The PS can be intravenously administrated with minimal toxicity and laser treatment at 48 h post infusion (Allison *et al*., 2004a). Minimal skin photosensitivity is achieved with high and low HPPH photosensitizing concentrations (Allison and Sibata, 2010). It is relatively easy to synthesis, fairly safe, has minimal photosensitivity, a high level of tumor accumulation and has suitable activation wavelength for surface or deep-seated tumors. These features make HPPH an excellent PDT second-generation PS for clinical use (Allison and Sibata, 2010).

Tin etiopurpurin (Purlytin®) or SNET2 is a synthetic purpurin which is a degradation product of chlorophyll (Allison *et al*., 2004a). This pure PS (Allison *et al*., 2004a) is hydrophilic and is often formulated with an egg based carrier for PDT treatment (Allison and Sibata, 2010). Purlytin® has a high singlet oxygen quantum yield and peak absorbance at 660 nm because of its central heavy metal ion (tin) (Yano *et al*., 2011). Clinically, this PS is effective for PDT treatment of basal cell carcinoma, squamous cell carcinoma, chest wall metastasis and Kaposi sarcoma (Allison and Sibata, 2010). In general, Purlytin® at a photosensitizing concentration of 1.2 mg/kg is infused and accumulates in the cellular membranes (Allison and Sibata, 2010). After 24 h, laser

treatment is applied using a treatment dose of 200 J/cm^2 (Yano *et al*., 2011) and pain is minimal or non-existent (Allison *et al*., 2004a). This PS remains in the skin for a maximum of 14 days post infusion (Allison and Sibata, 2010).

Interestingly, photosynthetic pigments that occur in photosensitive bacteria were also discovered to have photodynamic therapy properties (Allison and Sibata, 2010). These were referred to as Padeliporfin or Padoporfin, which are bacteriophorbide derivatives of bacteriochlorines belonging to the chlorophyll family of second-generation PSs (Allison and Sibata, 2010). They are commercial known as WST9 or Tookad® and WST11. These PSs have a strong absorption at approximately 763 nm (Allison and Sibata, 2010). Tookad® is hydrophobic and requires a carrier during infusion (Allison and Sibata, 2010). WST11 is hydrophilic and can be administrated with ease. Both these PSs clear rapidly from the blood stream within 20 min therefore skin photosensitivity is negligible in most cases. Tookad has received much attention as a potential photosensitizing agent for the PDT of prostate cancer (Yano *et al*., 2011).

Verteporfin (Visudyne®) is a benzoporhyrin derivative (BPD) which has been extensively investigated for the PDT treatment of wet age-related macular degeneration, cutaneous non-melanoma skin cancers, multiple sclerosis, rheumatoid arthritis and Barrett's oesophageal adenocarcinoma (Yano *et al*., 2011). Visudyne® has also been employed with success for ophthalmic astrocytoma, choroidal melanoma and various cutaneous malignancies, including highly vascular tumors (e.g. canine osteosarcoma) (Allison and Sibata, 2010). This second-generation PS offer better advantages over first-generation PSs like Photofrin®. It is rapidly absorbed by the cancerous tissue and laser treatment is administrated 3 – 5 h after injection (Yano *et al*., 2011). Visudyne® is also rapidly cleared from the body and this minimizes skin photosensitivity from occurring in PDT treated

patients. For clinical activity, this hydrophobic PS is formulated with liposomes and activation at 690 nm is possible with Visudyne® allowing for deeper tissue penetration (Allison and Sibata, 2010). To date, Visudyne® mediated PDT has been approved for clinical use against age-related macular degeneration and rheumatoid arthritis in 26 countries (Yano *et al*., 2011).

Lutrin® (Texaphyrins, Motexafin, Lutetium or Lu-Tex) is a synthetic and expanded porphyrin-based second generation PS (Allison and Sibata, 2010). The main advantages of using Lutrin® as photosensitizing agent in PDT are associated with the following features (Allison and Sibata, 2010):

- It has high tumor selectivity
- It is water soluble
- It is rapidly excreted from the body
- Has maximum absorption at 732 nm
- Can be used for the treatment of large tumors
- It is an excellent singlet oxygen producer
- Can be administrated topically or intravenously
- Does not cause skin photosensitivity after PDT treatment

During PDT treatment, a low concentration (0.6 mg/kg – 7.2 mg/kg) of Lutrin® is administrated for 3 h before laser treatment is applied using a treatment dose of 150 J/cm^2 at 732 nm (Yano *et al*., 2011). Lutrin® mediated PDT has been approved for clinical use against recurrent prostate and cervical cancer. It has been investigated in phase I, II or III clinical trials against breast cancer, recurrent breast cancer, melanoma cancer and Kaposi's sarcoma (Yano *et al*., 2011). It is also used as an agent for diagnostic imaging in

the medical field (Yano *et al*., 2011). For example, a gadolinium (III) complex of texaphyrin (Xcytrin™) has been developed for use as MRI (Magnetic Resonance Imaging) agent. Xcytrin™ playing a role as radiosensitizer and chemosensitizer has also been investigated in a phase III clinical trial against brain metastases as well as in primary brain tumors (Yano *et al*., 2011).

Pcs (Figure 1.4) are also promising photosensitizing agents that resemble the porphyrin structure and belong to the group of second-generation PSs (Spikes, 1986). These are classical industrial dyes which have been found to have useful medical, optical and electrical applications (Lo *et al*., 2007). To name a few, Pcs are being used as molecular electronic devices, sensors, optical recording materials, non-linear optics, catalysts for oxidative degradation of pollutants and PSs for PDT (Lo *et al*., 2007). These compounds are made up of isoindoles rather than pyrroles, have a longer conjugate pathway around the ring structure, and therefore absorb at longer wavelengths than porphyrins (Spikes, 1986). Porphyrin displays a strong absorption at 410 nm – 450 nm together with a number of weaker Q bands at 500 nm – 700 nm, while Pcs show the corresponding absorptions at 320 nm – 360 nm (weak absorption bands) and 670 nm – 700 nm (strong absorption bands). Pcs are regarded as azaporphyrins (Figure 1.4) with potentially low or no skin photosensitivity after PDT treatment, because these compounds tend to exhibit low absorption at wavelengths (300 nm – 400 nm) in a spectral range where daylight intensity is the highest (Sekkat *et al*., 2011). These compounds are considered to be chemically, thermally and photochemically stable (Grobosch *et al*., 2010). Therefore, the photophysical as well as the redox reactions of Pcs and porphyrins are very different, despite their structural similarity. The properties of Pcs can be altered readily by adding the peripheral substituents and metal ions to the centre of the structure (Durmuş and Nyokong, 2007a).

More than 70 different kinds of metal or metalloid atoms can be inserted into the central ring of Pcs in place of the two hydrogens present in non-metallo Pcs to form metal-based Pc complexes or metallophthalocyanines (MPcs) (Claessens *et al*., 2001). These metal-based Pc complexes are known to be more stable in the presence of light and oxygen (Josefsen and Boyle, 2012). The type and presence of the inserted central metal ion in the Pc structure strongly influences its PDT properties (Durmuş and Nyokong, 2007a). For example, Pcs containing closed d shell, or diamagnetic ions such as zinc (Zn^{2+}), aluminum (Al^{3+}), gallium (Ga^{3+}), indium (In^{3+}) and silicon (Si^{4+}) form metal-based Pc complexes with high triplet quantum yields and long triplet lifetimes, which are essential for efficient generation of cytotoxic agents during PDT treatment (Durmuş and Nyokong, 2007c). In contrast, Pcs with open shell or paramagnetic metal ions such as copper (Cu^{2+}), iron (Fe^{2+}), cobalt (Co^{2+}) and vanadium (VO^{2+}) form metal-based Pc complexes with shortened triplet lifetimes (Durmuş and Nyokong, 2007a). Furthermore, diamagnetic heavy metals ions such as Ga^{3+} (Durmuş and Nyokong, 2007a) and In^{3+} (Chauke *et al*., 2007) play a major role in photosensitizing and optical limiting mechanisms as they enhance intersystem crossing through spin orbit coupling (San *et al*., 2011). This is a desirable feature for PSs as it improves the chances of getting a large population in the triplet state during PDT treatment (Durmuş and Nyokong, 2007a). Also, metal-based Pc complexes with Ga and In are able to host axial ligands which act as spacers between the rings. Axial ligands in metal-based Pc complexes are responsible for preventing or minimizing intermolecular interactions which causes aggregation in solution (San *et al*., 2011). Aggregation can result in the fast decay of excited states or reduction of singlet-oxygen quantum yield (Durmuş and Nyokong, 2007a). Major disadvantages associated with most Pcs including some metal-based Pc complexes are their low solubility potential and their ability to aggregate in certain solvents (e.g. water and organic solvents). However, metal-based Pc complexes or Pc derivatives of increased solubility can be produced by using

substituents such as alkyl, alkoxy, alkylthio chains and bulky groups (Durmuş and Nyokong, 2007b). Peripheral substitution with bulky groups or long alkyl, alkoxy or alkylthio chains leads to Pc complexes which are soluble in apolar solvents. The incorporation of sulfo or quaternary ammonium groups in Pc complexes enhances its solubility in a wide pH range of aqueous solutions (Durmuş and Nyokong, 2007b). The size of the substituents, nature of the substituents and the change in symmetry caused by the substituents are also important criteria for the solubility of the substituted Pcs (Durmuş and Nyokong, 2007b). Tetra substituted Pcs are more soluble than symmetrically octa substituted ones, due to the formation of four positional isomers in the case of tetra substituted analogues (Durmuş and Nyokong, 2007b).

The architectural flexibility, photophysics and photochemistry properties of various Pcs including metal-based Pc complexes are well documented and show clearly that these compounds could make valuable PSs for the PDT treatment of tumors (Çamur *et al*., 2011, Yanık *et al*., 2009, Durmuş *et al*., 2009, Nyokong, 2007, Nyokong, 2011, Sekkat *et al*., 2011). Pcs bearing a central Al, Zn or Si metal ion have been extensively studied *in vitro* as well as *in vivo* for their PDT activity against different cancers because of their desirable photophysical properties (Table 1.3). These metal-based complexes displayed potent photodynamic activity on different cells lines including human melanoma cells (G361), human fibrosarcoma cells (HT-1080), human breast cancer cells (MCF-7), human larynx carcinoma cells (Hep2) and oesophageal cancer (SHO); as well *as in vivo* studies using colorectal carcinoma in nude mice, hybrid mice with tumors and tumor models with EMT-6 cells of a murine mammary sarcoma induced in Balb/c mice (Table 1.3). Unfortunately, only a small amount of preliminary *in vitro* studies seems to be available on the photodynamic activity of a number of metal-based Pc complexes (e.g. Cr, Ni, Ge, Ga, Cu, Co, In, V, Mg, Cd, Ti, Fe and Sn Pcs.

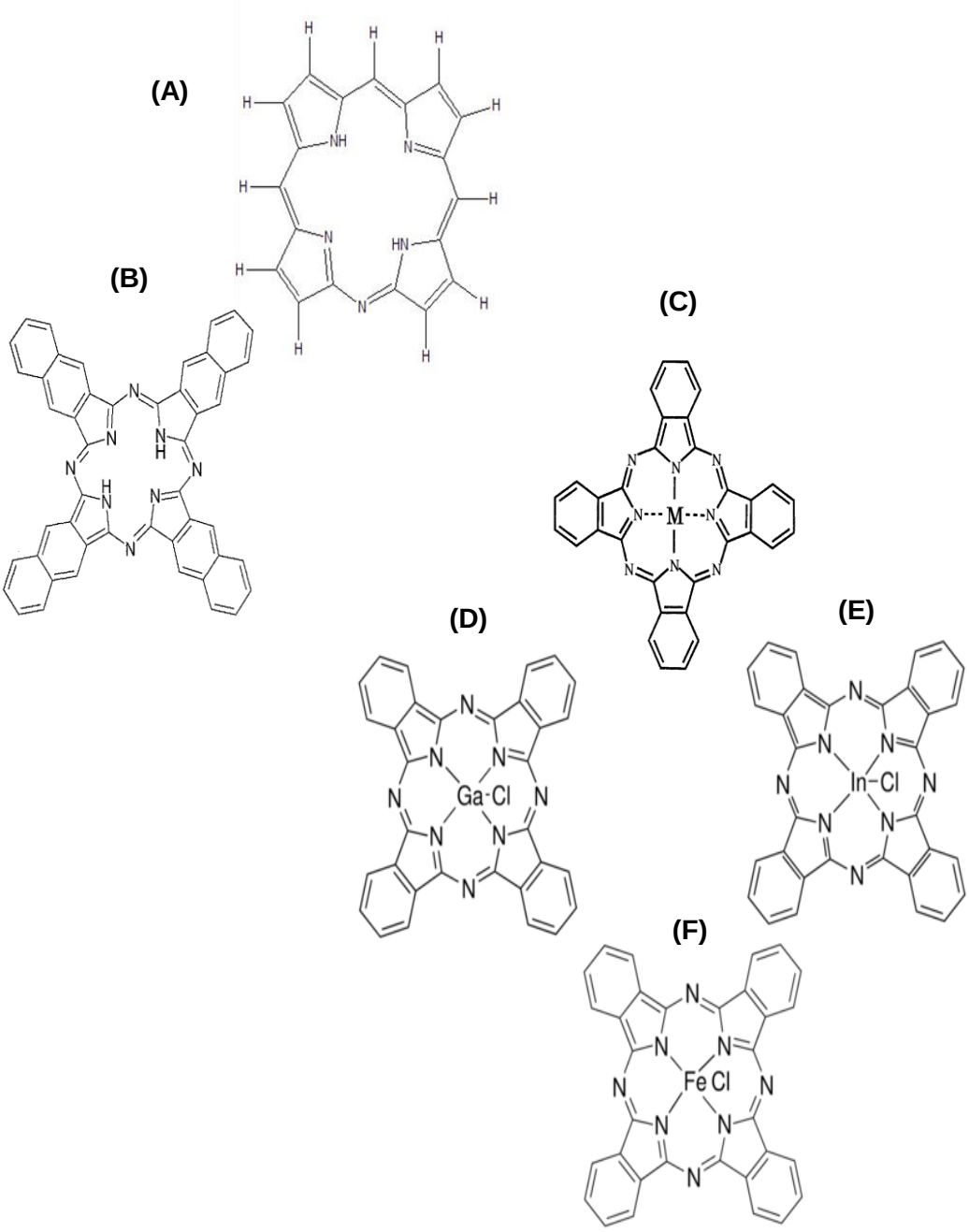

Figure 1.4 The structure of (A) azaporphyrins (B) phthalocyanine (C) metal-based phthalocyanine complex (Nyman and Hynninen, 2004) (D) gallium phthalocyanine chloride (E) indium phthalocyanine chloride and (F) iron phthalocyanine chloride (Sigma-Aldrich catalogue).

To date, mixtures of Al chloride Pcs with sulphonated side-groups (Photosens®) are clinically approved for the PDT treatment of a number of cancers (e.g. skin, breast, lung, head, neck, cervical, etc.) in Russia (Sekkat *et al*., 2011). Clinically, Photosens®-mediated PDT is performed according to a procedure similar to that described for Photofrin® but considerably lower Photosens® concentrations (0.5 - 0.8 mg/kg) are used and 24 – 72 h after Photosens® administration lower treatment light doses (150 J/cm^{-2} - 200 J/cm^{-2}) at peak wavelength of 675 nm are applied (Yano *et al*., 2011). This PS can be formulated for intravenous administration, direct lesion injection or for aerosol formulation. It has also been reported that Photosens®-mediated PDT is a painless and successful treatment for many cancers (Allison and Sibata, 2010). Recently, in attempts to enhance tissue selectivity, a liposomal formulation of ZnPc (CGP55847) has been developed and has been investigated in a phase III clinical trial against squamous cell carcinoma of the upper aerodigestive tract in Switzerland (Yano *et al*., 2011).

Another Pc under clinical trial is a Si complex (Pc4) for the sterilization of blood components (Sharman *et al*., 1999), against human cancers (e.g. colon, breast, and ovarian) and glioma (Josefsen and Boyle, 2012). Also, an extended Pc derivative termed naphthalocyanines was developed in efforts to increase peak absorption wavelength of Pcs (Josefsen and Boyle, 2012). Naphthalocyanines advantageously absorb at a higher wavelength (740 nm – 780 nm) than Pcs (including MPcs), further increasing the light penetration through skin. This absorption in the near infrared region makes naphthalocyanines potential candidates for *in vivo* imaging agents (Josefsen and Boyle, 2012). Furthermore, naphthalocyanines can be used as photosensitizing agents for the PDT treatment of highly pigmented tumors, including melanomas, which present significant problems with respect to transmission of visible light. Naphthalocyanines are generally less stable than its Pc relatives; they readily decompose in the presence of light

or oxygen and metal-based naphthalocyanines which lack axial ligands and have a tendency to form H-aggregates in solution (Josefsen and Boyle, 2012). These H-aggregates are inactive and comprise the photodynamic efficacy of naphthalocyanines (Josefsen and Boyle, 2012). Unfortunately, there are some disadvantages that are associated with naphthalocyanines that should be taken into consideration and explored further for improvement (Josefsen and Boyle, 2012).

Table 1.3 Published treatment parameters and data for *in vitro*, *in vivo* and clinical studies demonstrating the photodynamic effect of different metal-based Pc complexes for treatment of various different cancers. The most commonly studied metal-based Pc complexes are Al, Zn, Si, Ge and Sn Pc complexes indicated by the amount of published data available on these above mentioned metal-based Pc complexes

Cell Lines	**PS**	**[PS]**	**Laser (ʎ)**	**Light treatment**	**Results**	**Reference**
Human Leukemia T cells (CCRF & MOLT 4)	AlPcCl, ZnPc, MgPc	10^{-5} M	HeNe (632.8 nm)	1 h (7.2 J/cm^2), 2 h, 3 h	A small difference in the membrane of the cell influences the efficiency of dye incorporation and on the photodynamic reaction.	(Wiktorowicz *et al*., 2004)
Human epidermoid carcinoma (A431), Fibrosarcoma, Breast cancer (MCF-7)	Silicon Pc	0.5 µM	300 W Halogen lamp (675 nm)	20 kj/cm^2	Up regulation of apoptotic cells within 1 h	(Kalka *et al.*, 2000)
Clinical Trial Skin, breast, tongue, oral mucosa, lower lip, larynx, lung, stomach, bladder, rectum & other locations	Photosense (AlPc)	0.5 – 1.5 mg/kg	Solid state laser (670 nm)	100 J/cm^2 400 J/cm^2 250 J/cm^2	Rate of response Av-98.4% ; Rate of complete recovery Av -55.5%	(Stranadko *et al*., 1999)

Cell Lines	PS	[PS]	Laser (λ)	Light treatment	Results	Reference
Human epidermoid carcinoma (A431)	$AlPcS_4$	40 µM	Diode laser (660 nm)	1.5 J/cm^2	DT: >2 µM caused a drop in cellular survival below 80%; 100 µM cell survival is less than 1%; 40 µM + 0.35 Jcm^{-2} no effect; higher light doses cell survival of 6%; cellular uptake abrupt rise within the first hour of incubation followed by a nearly linear increase up to 30 h.	(Berlanda *et al*., 2010)
Human larynx carcinoma (Hep2)	$AlPcS_4$ ZnPc	10 µM	LID prototype (640 nm)	4.5 J/cm^2	DT: AlPc – 0 h (98.3%) & 3 h (75.2%); ZnPc – 0 h (77.6 %) & 3 h (94.3%) PDT: AlPc – 0 h (37.8%) & 3 h (13.2%); ZnPc – 0 h (41.4%) & 3 h (49.8%)	(Machado *et al*., 2009)
Human cervical carcinoma cells (SiHa)	ZnPc	-	Diode laser (665 nm)	3 J/cm^2	IC_{50} : 171 - 375 µM IC_{75} : 320 - 683 µM IC_{90}: 0.49 - 2.02 mM	(Haywood-Small *et al*., 2006)
Breast cancer (MCF-7)	AlPcSmix GePcSmix	0 - 40 µM 0 -120 µM	Diode laser (680 nm)	15 J/cm^2	AlPcSmix: 35 µM GePcSmix: lower concentrations	(Horne *et al*., 2012)
Breast cancer (MCF-7)	ZnPcSmix	0.05-1 µM	Diode laser (680 nm)	5 J/cm^2 10 J/cm^2 15 J/cm^2	Effective PDT: 0.5 - 1 µM + 10 & 15 J/cm^2	(Tynga *et al*., 2013)

Cell Lines	PS	[PS]	Laser (λ)	Light treatment	Results	Reference
Human oesophageal carcinoma (SNO)	$SiPcS_{mix}$ $GePcS_{mix}$ $SnPcS_{mix}$	20 µg/ml	Diode laser (670 nm)	3 min	GePcS mix showed the best PDT effect against SNO cells.	(Seotsanyana-Mokhosi *et al*., 2006)
Human amelanotic melanoma cell line (M6), Healthy human melanocytes & keratinocytes	SiPc	2×10^{-9} M	250 W halogen lamp (480 nm)	20 min 12 J/cm^2	20% cell viability.	(Decréau *et al*., 1999)
RIF-1 tumors in C3H mice	SiPc (10, 12, 18)	0.63-0.86 mg/kg	Argon pumped dye laser (675 nm)	135 J/cm^2	Pc 18 PDT treatment showed 72% complete tumor regression. Pc 10 & Pc 12 PDT showed 100% complete response. Doesn't produce cutaneous photosensitivity.	(Anderson *et al*., 1998)
Mouse murine cell lines (NIH/3T3 & UV-2237)	Al – chloro sulphonated – Pc	5 – 100 µg/ml	Fluorescent tubes (600 nm)	0 – 60 min	Less toxic in the dark. Uptake is time dependent. PDT treated cells (30 min) resulted in 0% survival at day 3.	(Chan *et al*., 1986)

Cell Lines	PS	[PS]	Laser (λ)	Light treatment	Results	Reference
Colorectal carcinoma in nude mice (32)	Disulfonated hydroxyl – AlPc	2.5 mg/kg	Xenon lamp (675 nm)	120 J/cm^2	87% success rate after a single dose. Regrowth of tumor was seen with one mouse. No side effects were seen after PDT treatment.	(Stukavec *et al*., 2009)
Hairless mice albino (SKH – HR 1) & with melanin (SKH – HR2) Used UV A (5 mW/cm^2) & UV B (4.5 mW/cm^2) to induce basal (10%) & squamous (80%) cell carcinoma	AlClPc	40 µl/cm^2	Diode laser (670 nm)	75 J/cm^2 150 J/cm^2 250 J/cm^2	Scarring was seen after PDT treatment. AlClPc was not detected in healthy normal tissue (biopsies). No photosensitivity or toxicity was seen. Recurrence of cancer in the treated area was not observed. 5 mice in each group were cured completely.	(Kyriazi *et al.,* 2008)
Mouse fibroblast (NIH3T3); Mouse melanoma (B16), Human breast carcinoma (MCF-7)	$ClAlPcS_4$	1 – 10 µg/ml	Semi – conductor (675 nm)	30 J/cm^2	Cell viability of all cell lines decreased proportionally to concentration increase.	(Kolarova *et al*., 2007)

Cell Lines	PS	[PS]	Laser (λ)	Light treatment	Results	Reference
Human keratinocytes	Chloro – AlPc	5 µM	Diode laser (670 nm)	5 min 25 J/cm^2	2 h after PDT: cell death of 80%; 24 h after PDT: cell death of 100%	(Tapajós *et al*., 2008)
Hybrid mice	Disulphonated - AlPc	5 mg/kg	Argon laser (685 nm)	10 min	Cured all tumors at 3 h & 12 h.	(Cubeddu *et al*., 2001)
Human cervical cancer (HeLa)	Chloro – Pc (liposomal)	5 mM	Diode laser (670 nm)	4.5 J/cm^2	PDT treatment induced photodamage to the mitochondria, endoplasmic reticulum & actin filaments of the cytoskeleton, suggesting loss of cell viability.	(Maftoum-Costa *et al*., 2008)
Oesophageal cancer (SNO)	GePcS mix AlPcS mix	10 µM 50 µM 100 µM 200 µM 300 µM	Diode laser (680 nm)	20 J/cm^2	Cells treated with 100,200 & 300 µM of inactive GePcS mix decreased in cell viability after 24 h. Cell viability decreased in a dose dependent manner after PDT.	Kresfelder *et*. *al*., 2009
Colon cancer (DLD-1) Lung cancer (A549)	ZnPcSmix	5 µM 10 µM 20 µM 40 µM	Diode laser (677 nm)	2 J/cm^2 5 J/cm^2 10 J/cm^2 20 J/cm^2	Significant decrease in cell viability of A549 with all concentrations and light doses. Significant decrease in cell viability of DLD-1 with 20 – 40 µM.	(Manoto *et al*., 2012)

Cell Lines	PS	[PS]	Laser (λ)	Light treatment	Results	Reference
Human keratinocytes & oral squamous cell carcinoma (H 376)	AlS_2Pc	25 µg/ml	Diode laser (675 nm)	1 J/cm^2	Able to directly kill H376 cancer cells *in vitro* via apoptosis.	(Kresfelder *et al*., 2009)
Human keratinocytes cells (UP)	AlS_2Pc	5 µg/ml 25 µg/ml 50 µg/ml 100 µg/ml	Fluorescent tubes (660 – 700 nm)	0 min 2.5 min 5 min 10 min 15 min 20 min	Cytotoxic effect of AlS2Pc is dose dependent. 25 µg/ml with 0.6 J/cm^2 reduced cell viability to 100%.	(Soukos *et al*., 1994)
Tumor model (EMT - 6 cells of a murine mammary sarcoma induced in Balb/c mice)	AlPc (chloride) $AlPc_1$ $AlPc_2$	0.5 & 0.25 2 1 µmol/kg	Xenon lamp (650 – 700 nm)	400 J/cm^2	No recurrent of tumor at 20 days post – PDT. 100% tumor response.	(Chan *et al*., 1997)
Human epidermoid carcinoma cells (A431)	$AlPcS_4$	2.5 µM	PDT – 1200 red light device (600 nm)	2.5 – 3.5 J/cm^2	50% of the cells were found to undergo apoptosis after irradiation with light doses from 2.5 to 3.5 J/cm^2, other 50% necrosis.	(Plaetzer *et al*., 2002)

Cell Lines	PS	[PS]	Laser (λ)	Light treatment	Results	Reference
Human breast cancer cells	ZnPc (Poll)	1 µM	Light emitting diode (670 – 675 nm)	0.5 – 20 J/cm^2	Decrease of cell survival from 92% to 30%. Induction of cell death via apoptosis.	(Vittar *et al*., 2010)
Human adenocarcinoma cell line (HCT 116)	ZnPc1 – ZnPc8	5 x 10^{-5} M	Halogen lamp (380 – 780 nm)	158.4 J/cm^2	IC_{50}: ZnPc1 – 4 & 8 > 1000 ng/ml ZnPc 5: 18.20 ng/ml ZnPc: 90.00 ng/ml ZnPc 7: 151.30 ng/ml Cell death : apoptosis	(Banfi *et al*., 2007)
Human fibroblast (HT-1080); Keratinocytes (HaCaT); Mouse embryo fibroblasts (Balb/3T3)	ZnPc	0.5 – 5 µM	Halogen lamp (600 -700 nm)	1 min	Complete cell lethality after 1 min irradiation with 3 µM of ZnPc.	(Fabris *et al*., 2006)
6.1 – 7.8 kg Beagle dogs (24)	ZnPc	0.5 mg/kg 1.5 mg/kg 4.5 mg/kg	SDS – DL3 laser (670 nm)	7 J/cm^2	1.5 mg/kg of ZnPc appeared to be a safe and promising approach for clinical use.	(Liu *et al*., 2007)

Cell Lines	PS	[PS]	Laser (λ)	Light treatment	Results	Reference
18 – 20 g Balb/c mice tumor model	ZnPc	0.12 mg/kg	Quartz/ halogen lamp (600 – 700 nm)	300 J/cm^2	Apoptosis 24 h and 48 h after tumor tissue is seriously damaged and a large number of dead tumor cells are present.	(Zhou *et al*., 1996)
Human melanoma cells (G361)	$ZnTPPS_4$ + cyclodextrin	10 µM	Halogen lamp (360 – 2700 nm)	12.5 J/cm^2	DNA damage. The use of irradiation in the absence of PS does not induce DNA damage.	(Kolarova *et al*., 2005)
Normal skin fibroblast cells HT-1080 fibrosarcoma cells	AlPcS	3 – 400 µg/ml	Argon laser (625 – 697 nm)	0.1 – 50 J/cm^2	DT: AlPcS is non – toxic at concentrations up to 25 µg/ml. Optimized PDT: 3 µg/ml of AlPcS for 8 h with 4 – 8 J/cm^2 of light dose.	(Glassberg *et al*., 1990)
Human laryngeal carcinoma (Hep-2)	Octal – bromide – ZnPc	1 µmol/l	Diode semi – conductor (676 nm)	4.5 J/cm^2	Significant morphologic changes in PDT treated cells were observed.	(Machado *et al*., 2010)
Human laryngeal carcinoma (Hep-2)	$AlPcS_4$ ZnPc	10 µM	LED prototype (640 nm)	4.5 J/cm^2	$AlPcS_4$ induced intrinsic death pathway and ZnPc induced prostanoid – mediated activation of death machinery after PDT treatment.	(Machado *et al*., 2009)

Cell Lines	PS	[PS]	Laser (ʎ)	Light treatment	Results	Reference
Human liver carcinoma (Hep G2) Human gastric carcinoma (BGC 823) Human neuroblastoma (SH-SY5Y) Normal non-carcinoma human gastric epithelial cells (GES-1) Human embryonic lung fibroblast (HELF)cells	$ZnPcS_2P_2$ ZnPc $ZnPcS_3P_1$ $ZnPcS_4$	10 nmol/ – 100 nmol/l	Diode laser (670 nm)	1.5 J/cm^2	IC_{50}: 0.5 – 10 µmol/l. Cell death is dependent on PS concentration. $ZnPcS_2P_2$ is now under clinical trials in China.	(Shao *et al*., 2012)
Human Larynx carcinoma (Hep2)	ZnPc (3) ZnPc (4)	0.1 µM	Projector (670 nm)	0.5 & 15 min	No DT with 0.1 µM. DT: 0.5 µM was toxic. A higher photocytotoxic effect was found for ZnPc (3) with respect to ZnPc (4) – (32% & 70% cell survival after 15 min of irradiation)	(Yslas *et al*., 2007)

Cell Lines	PS	[PS]	Laser (ʎ)	Light treatment	Results	Reference
C6 Glioma model in Wistar rats	AlSPc	0.05 mg/kg 1 mg/kg 5 mg/kg	Argon – ion pumped red dye laser (675 nm)	800 J/cm^2	No PDT effect on normal or tumor in the brain area if the PS concentration was less than 0.5 mg/kg. Selective necrosis of tumor was evident 6 h post – photosensitization at an AlSPc concentration up to 1 mg/kg with light dose up to 200 J/cm^2. Necrosis occurred in the normal brain tissue at higher AlSPc concentration and light dose.	(Stylli *et al*., 1995)
Rat pheochromoc-ytoma PC 12 & Human Lymphoblastoid CCRF-CEM cells	AlPc $AlPcS_4$	1 µM 25 µM	2 000 W Tungsten/ Halogen Lamp (600 nm)	0 J/cm^2 2 J/cm^2 4 J/cm^2 6 J/cm^2 8 J/cm^2	Photosensitization efficiency of Pc was much higher with a 24 h pre – incubation period was used, with light dose of 5 mW/cm^2. With a light dose of 10 mW/cm^2, the photosensitization efficiency of $AlPcS_4$ was independent of the pre – incubation time (6 h vs 24 h) with Pc. AlPc for 10 min or 6 h and lights doses of 10 mW/cm^2 or 5 mW/cm^2 on CCRF – CEM cells.	(Gomes *et al*., 1999)

Cell Lines	PS	[PS]	Laser (λ)	Light treatment	Results	Reference
Human melanoma cancer cells Human fibroblast cells Human keratinocytes cells	ZnTSPc	10 µg/ml – 100 µg/ml	Diode laser (672 nm)	4.5 J/cm^2	Optimized *in vitro* PDT: 50 µg/ml + 4.5 J/cm^2 Cell death induced: apoptosis.	(Maduray *et al*., 2011)
Myeloma cells & Chinese hamster ovary cells	ZnPc	25 µg/ml 100 µg/ml	Iodine tungsten lamp (610 nm)	15 min	The higher the concentration the greater the photodynamic effect. 100 µg/ml cells were killed after PDT treatment.	(Gao *et al*., 2001)
Human melanoma cancer cells Human fibroblast cells Human Keratinocytes cells	AlTSPc	10 µg/ml – 100 µg/ml	Diode laser (672 nm)	4.5 J/cm^2	Optimized *in vitro* PDT: 40 µg/ml + 4.5 J/cm^2 Cell death induced: apoptosis.	(Maduray *et al*., 2012)
Chinese hamster ovary (CHO – K1) & Human cervix carcinoma (HeLa)	$AlPcS_4$	10 mM	Semi – conductor (670 nm)	35 sec 0.5 J/cm^2	Induction of apoptosis (CHO – K1) and necrosis (HeLa) after PDT treatment.	(de CastroPazos *et al*., 2003)

Cell Lines	PS	[PS]	Laser (λ)	Light treatment	Results	Reference
Melanoma cancer (UACC-62) Breast cancer (MCF-7) Non- small lung cancer (NCl 460) Leukemic cancer (K562) Ovarian cancer (OVCAR-3) Prostate cancer (PC-03) Colon cancer (HT-29) Kidney cancer (786-0); Ovarian cancer (NCl-ADR/RES) Sheep red blood cells	Liposome bound ZnPc	1 x 10^{-3} mol/dm^3	Projector (600 nm)	2.1 J/cm^2 10 min	0.97 µmol/dm^{-3} causes major decrease in a number of the cells in all cell lines. Total cell growth inhibition only at concentrations higher than 250 µmol/dm^{-3}.	(De Oliveira *et al*., 2010)

Hypericin is known as one of the most powerful second-generation PSs to be found in nature because it has the ability to generate singlet oxygen or ROS upon irradiation with light (Koren *et al*., 1996). The hypericin molecule is a natural photoactive pigment which plays a role as an effective photoreceptor in *Saint John's Wort* plant as well as in other plant species of the *Hypericum* (Kubin *et al*., 2005). This plant pigment has long been used in traditional medicine for the treatment of depression and wound healing (Guedes and Eriksson, 2005). Its photodynamic effects were observed in the 20th century, when grazing cows, have ingested plants containing hypericin, and were diagnosed with "hypericism syndrome" a condition of severe sensitivity to light. It was also noticed that the photosensitizing effect of hypericin caused skin irritation, elevated body temperatures and in extreme cases death of the animal (Guedes and Eriksson, 2005). However, hypericin seems to display antiviral, antibacterial, antipsoriatic and antitumor activity including potential to be used as a diagnostic tool for fluorescence detection of malignant tissue (Kubin *et al*., 2005). As a photosensitizing agent it has good phototoxic efficiency with minimal dark toxicity and is activated around 600 nm. It has the ability to induce apoptosis (cell death) very effectively (Agostinis *et al*., 2002).

Hypericin might prove useful for treatment of skin cancer by inducing apoptosis without provoking a massive inflammatory response. The *in vitro* and *in vivo* photodynamic effects of hypericin have been studied and results prove that it shows great clinical potential as a photosensitizing agent for the PDT treatment of different cancers (Kubin *et al*., 2005). Despite all of its benefits and its strong photosensitizing ability, the application of hypericin in PDT suffers from two main disadvantages: isolation process is expensive and low solubility. Thus, over the last decade several efforts have been undertaken to synthesize new hypericin derivatives with increased solubility, longer wavelength absorption bands,

enhanced photosensitizing potential and applicability in a more wide-spread field (Karioti and Bilia, 2010).

1.4.1.3 THIRD-GENERATION PHOTOSENSITIZERS

Most recently, first-generation and second-generation PSs have been conjugated to various delivery models such as biologically active molecules, antibodies, liposomes and nanoparticles to form third-generation PSs (Paszko *et al*., 2011). Third-generation PSs have been designed to precisely deliver PSs to tumor cells at increased concentrations, and to minimize or prevent PS accumulation in healthy normal tissue (Josefsen and Boyle, 2008a). Also, a number of promising first-generation and second-generation PSs have poor solubility in aqueous media which prevents their intravenous delivery, and affects their efficacy (Josefsen and Boyle, 2008a). It would be advantageous for delivery models to facilitate the selectively transportation of these potentially useful PSs to the cancerous tissue or targeted site (Josefsen and Boyle, 2008b). One of the targeting strategies of third-generation PSs involve delivering the PS specifically to certain cellular organelles (e.g. mitochondria and nucleus) within the cancerous cell. Since the mitochondria efficiently stimulates apoptosis (preferred mode of cell death) and nuclear damage can also lead to rapid induction of cell death (Josefsen and Boyle, 2012).

Another option is conjugating PSs to antibodies to improve affinity and specificity of PSs (Josefsen and Boyle, 2012). Antibodies work by selectively targeting complimentary biomarkers which are expressed on the surface of healthy normal cells (Josefsen and Boyle, 2012). Cancerous cells commonly over-express certain biomarkers (e.g. antigens) on their surface against which antibodies can be produced and conjugated to PSs. This will facilitate the direct targeting of the PS towards specific bioreceptors and may even reduce the dose of PS that would be necessary for an observable PDT effect (Josefsen

and Boyle, 2012). Low density lipoprotein (LDL) receptors are also overexpressed in cancerous cells or tumor vasculature cells (Josefsen and Boyle, 2012). Low density lipoproteins (LDLs) contain a hydrophobic lipid core, outer shell of polar lipids and apoproteins (Josefsen and Boyle, 2012). These are biocompatible, biodegradable and non-immunogenic that serve as the main transporter of cholesterol molecules to mammalian cells. Therefore, LDLs are generally used as a carrier for targeted drug delivery in the field of medicine (Josefsen and Boyle, 2012). Thus, LDL can be used to deliver hydrophobic and amphiphilic PSs to cancerous cells in PDT. LDL complexes or conjugates also exhibit selective accumulation in cellular sites such as the mitochondria (Josefsen and Boyle, 2012). The incorporation of PSs into the LDL structure is anticipated to enhance tumor uptake and PDT activity of the PS (Josefsen and Boyle, 2012). It is also known that tumor cells have high energy requirements and tumor proliferation is often dependent on glucose uptake, because glycolysis rates are much higher in cancerous cells compared to healthy normal cells (Josefsen and Boyle, 2012). The idea of coupling sugars to PSs also show promise in the selective targeting of cancerous cells or tumors (Josefsen and Boyle, 2012).

Another possibility is to encapsulate the PS in delivery agents such as liposomes, micelles, ceramic based nanoparticles, gold nanoparticles and polymer nanoparticles (Paszko *et al*., 2011). Liposomes are able to encapsulate hydrophobic and hydrophilic PSs. Liposomal formulations of PSs display the ability to decrease the tendency of PS to aggregate and improve tumor-selective accumulation of PS (Paszko *et al*., 2011). Micelles also have the ability to specifically deliver the PS to cancerous cells and can be used to encapsulate PSs that have poor solubility in water (Paszko *et al*., 2011). Nanoparticles or nanosized carriers function on a similar principle to liposomes and share a similar composition (outer hydrophilic and inner hydrophobic region). These nanoparticles have a

strong ability to protect encapsulated drugs such as PSs; are compatible with biological systems and their surface can be easily modified with functional groups (e.g. antibodies or other ligands) to improve tumor selectivity (Paszko *et al*., 2011). Moreover, nanoparticles are stable in water and possess substantial capacity for drug loading. They are also suitable for controlled PS delivery due to their ability to slowly and consistently release drugs (Paszko *et al*., 2011).

Nevertheless, the basic aspects of targeted PDT or nano PDT for third-generation PSs stills needs to be explored in more detail. More *in vitro* and *in vivo* studies need to be conducted on the mechanisms of action, efficacy, associated toxicity, distribution and long term effects of these targeting strategies (Wojtyk *et al*., 2006).

1.4.2 LIGHT SOURCES

The type of light source and light delivery systems are of vital importance in PDT (Juzeniene *et al*., 2007). The choice of light source depends on the depth of the lesion, and the chosen wavelength of light (nm) has to be within the absorption band of the PS. The wavelength of light used in PDT is usually in the range of 600 – 800 nm, known as the therapeutic window. Also, in this wavelength range the energy of each photon (*hv*) is high enough (> 1.5 eV) to activate or excite the PS and yet is low enough so the light has sufficient penetration into the tissue (Zhu and Finlay, 2008). A number of different light sources have been used in PDT which can be classified into non-coherent (e.g. conventional arc lamps, LEDs and slide projectors) or coherent (e.g. lasers) light sources (Sibata *et al*., 2000).

Non-coherent sources for PDT include halogen xenon arc lamps, metal halide lamps, fluorescent tubes, light emitting diodes (LEDs), slide projectors equipped with filters and

intense pulsed light sources (IPL) (Huang, 2005). They can generate spectra of wavelengths to accommodate different PSs and can be used in conjunction with optical filters to output selective wavelength or wavelengths (Huang, 2005). These are safer, easy to use and less expensive. LEDs can produce high energy light of desired wavelengths; can be arranged in a range of geometries and sizes (Huang, 2005). For the PDT treatment of brain tumors the LED-probe is arranged in a cylinder tip to fit into a balloon catheter, whereas for intestinal PDT treatment the small and flexible light delivery LED catheter can be implanted into the tumor percutaneously (Huang, 2005). The larger LED arrays are more suitable for flat surface illumination of wide-area superficial lesions (Huang, 2005). The disadvantages of non-coherent sources include significant thermal effects, low light intensity and controlling light dose. In contrast, light exposure or light doses using coherent light sources (laser) at a defined wavelength offers accurate light dosimetry at the surface of the treated lesion (Huang, 2005). For non-coherent or broad band sources the depth of penetration, the extinction coefficient of the PS and the spectral intensity can all vary across the bandwidth of light used. Therefore, the light doses reported with coherent light sources are more precise compared to non-coherent light sources (Huang, 2005).

The most commonly used PDT coherent light source is lasers. Lasers produce high intensity and monochromatic light of a specific wavelength (Peng *et al*., 2008). They can emit either continuous or pulsed light, and the pulsed lengths are measured in femtoseconds (fs) (Peng *et al*., 2008). Most importantly, laser delivery systems can be used to transmit the laser beam to a targeted tissue (Peng *et al*., 2008). For example, the laser light can be focused, passed down an optical fibre or directly delivered to the target site using a specially designed illuminator tip (e.g. a microlens, a cylindrical or spherical diffuser). The wavelength, operating power, desired spot size and accessibility of the treatment site will influence the choice of laser delivery system used during treatment

(Peng *et al*., 2008). The use of lasers in medical treatments consists mainly of photothermal and PDT applications (Peng *et al*., 2008). It is also applied in both cases in almost all disciplines of medicine including dermatology, ophthalmology, dentistry, otolaryngology, gastroenterology, urology, gynecology, cardiology, neurosurgery and orthopedics (Peng *et al*., 2008). Gas lasers, argon lasers, helium-neon lasers, metal-vapor lasers (e.g. copper and gold) and solid state lasers (e.g. diode and potassium titanium oxide phosphate) are used for clinical PDT worldwide (Peng *et al*., 2008). The gold lasers (ʎ = 630 nm) have been used for porphyrin-mediated PDT and is the most frequently used laser in PDT. Fluorescence diagnostics and PDT are the typical application fields for diode lasers because wavelengths from UV to infrared can be obtained (Peng *et al*., 2008). Diode laser systems are also low in capital cost, negligible in running costs, highly reliable, small in size and portable (Peng *et al*., 2008). These features make diode laser systems very attractive light sources for scientific PDT studies, clinical and pre-clinical PDT treatments (Peng *et al*., 2008).

1.5 PHOTOPHYSICS AND PHOTOCHEMISTRY OF PDT

The photochemical and photophysical processes involved in PDT have been well documented and extensively studied (Sharman *et al*., 1999). Most PSs in their inactive state or ground state have two electrons with opposite spins positioned in an energetically most favorable molecular orbital (Castano *et al*., 2004). During the absorption of light or PS activation one electron is transferred to a higher energy orbital. The activated PS in its excited state is considered unstable and emits this excess energy as fluorescence and/or heat (Castano *et al*., 2004). Alternatively, the excited PS may undergo intersystem crossing to form a more stable triplet state PS with inverted spin of one electron (Castano *et al*., 2004). This excited triplet state PS can proceed through two different reaction pathways characterized as Type l and Type ll reactions (Castano *et al*., 2004).

In Type l reaction, the excited triplet state PS can react directly with a substrate (e.g. cell membrane or a molecule) and transfer a proton or an electron to form a radical anion or radical cation respectively (Sharman *et al*., 1999). These radical species are generally highly reactive and may further react with molecular oxygen (present in biological or cancerous tissue) to either produce ROS such as superoxide anions or hydroxyl radicals or cause irreparable biological damage (Sharman *et al*., 1999). It is these Type l photoreactions that lead to oxidative damage and cell death. It has also been noted that in an anoxic environment (total depletion of oxygen) excited triplet state PS can directly react with an organic substrate and reduced PS by electron exchange generating an oxidized substrate and reduced PS (P^-) (Sharman *et al*., 1999). Whereas, in an hypoxic environment (low oxygen concentration) the reduced PS (P^-) reacts with molecular oxygen to form superoxide anions (O^-_2) which then forms the highly reactive hydroxyl radical. Type l photoreactions depend on the amount of oxygen present in the treated biological tissue and on the availability of target-substrate concentration (Macdonald and Dougherty, 2001).

The Type ll reactions involve the energy transfer between the excited triplet state of the PS and ground state molecular oxygen (present in biological tissue) to produce excited state singlet oxygen (Sharman *et al*., 1999). This excited state singlet oxygen is a highly reactive form of oxygen and reacts with a large number of biological substrates (e.g. lipids, proteins or nucleic acids) to induce oxidative damage and cell death (Sharman *et al*., 1999). Type ll reactions are dependent on oxygen concentration. During PDT treatment, both Type l and Type ll photochemical reactions can occur simultaneously to generate ROS and excited state singlet oxygen (Sharman *et al*., 1999). The ratio between these two pathways depends on the type of PS used, the concentration of substrate and molecular oxygen availability in the treated biological tissue (Castano *et al*., 2004). Although Type ll reactions are known to be more dominate during PDT, Type l reactions may become more

dominate under situations where PS are highly concentrated in treated tissue or under hypoxic conditions (low oxygen concentration) (Macdonald and Dougherty, 2001). The photophysical and photochemical mechanisms of PDT are diagrammatic illustrated in Figure 1.5.

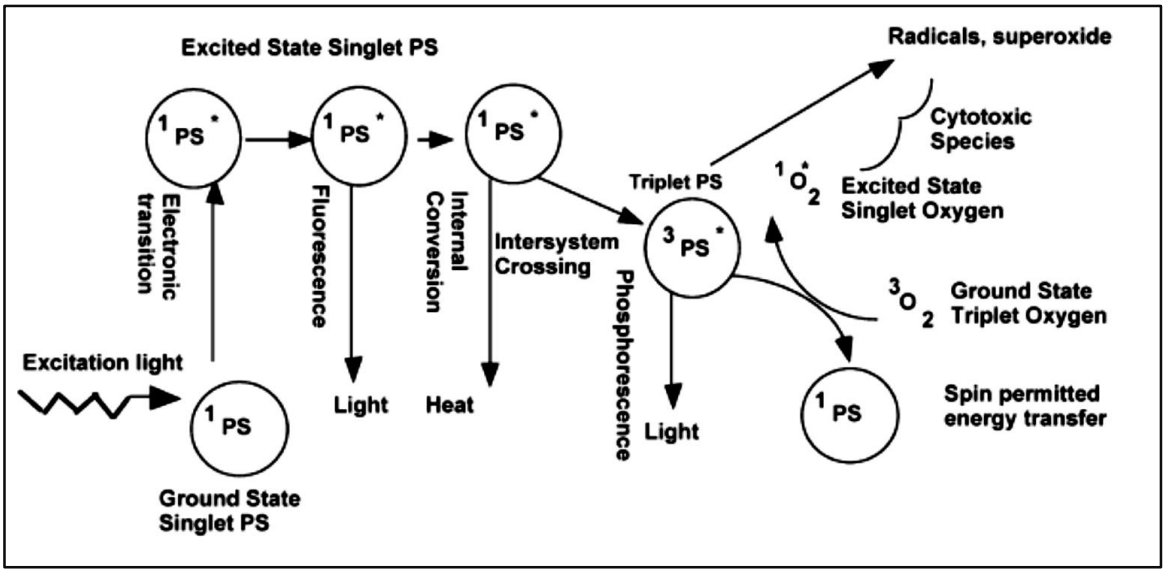

Figure 1.5 The processes of light absorption and energy transfer that occur during PDT. Upon absorption of light of a specific wavelength one of the ground state PS electrons is boosted into a high-energy orbital (first excited singlet state; $^{1}PS^{*}$). This is a short lived species and loses its energy by emitting fluorescence or internal conversion into heat. The excited singlet state PS may also undergo intersystem crossing to form the relatively long-lived excited triplet state $^{3}PS^{*}$. This long-lived excited triplet state PS can effectively interact with its surroundings, either by Type I or by Type II reactions to generate reactive species (free radicals and reactive oxygen species) which causes oxidative damage and cell death (Castano *et al*., 2004).

1.6 PHOTOBIOLOGY OF PDT

The most important factor governing the outcome of PDT is how the PS interacts with cancerous cells in the targeted tissue or tumor, and the key aspects of this interaction is the subcellular localization of the PS as well as the mode of PDT induced cell death

responsible for tumor destruction (Castano *et al*., 2004). Also, the cellular uptake of PSs by cancerous or other cells is essential for effective PDT (Castano *et al*., 2004). PSs which are hydrophobic with two or less negative charges can diffuse across the plasma membrane, and then relocate to other intracellular membranes or sites in the cell (Castano *et al.*, 2004). Those PSs which are less hydrophobic and have > 2 negative charges are too polar to diffuse across the plasma membrane and therefore taken up by endocytosis (Castano *et al*., 2004).

1.6.1 SUBCELLULAR LOCALIZATION OF PSS

ROS and excited state singlet oxygen have short half-lifes and act close to their site of generation (Castano *et al*., 2004). Therefore, the degree of photodamage and type of photodamage that occurs in cancerous cells after PDT treatment depends on the subcellular localization of the PS within the cell (Castano *et al*., 2004). Since most PSs are fluorescent, PS localization can be easily studied and determined by fluorescence microscopy (Castano *et al*., 2004). Mitochondria, lysosomes, plasma membrane, endoplasmic reticulum (ER) and Golgi apparatus are preferential target sites for PSs (Castano *et al*., 2004). None of the clinically approved PSs for PDT localize in the nuclei. Therefore, PDT has a low potential of causing DNA damage, mutations, carcinogenesis and developing resistant clones (Allison *et al*., 2004b).

Several photosensitizing agents localize in lysosomes and upon laser illumination (laser treatment) they can cause cell death via two different ways (Mroz *et al*., 2011). These include the release of lysosomal enzymes in the cytosol or the relocalization of the PS after illumination to other non-lysosomal sites in the cell. PSs that readily aggregate are more likely to be taken up by pinocytosis and/or endocytosis and therefore localize in lysosomes (Moor, 2000). Also, PSs that have net anionic characteristics localize in the

lysosomes, whilst those with cationic character localize in the mitochondria (Castano *et al*., 2004). Mitochondria is considered to be a very important subcellular target for many PS used in PDT. This is related to the tendency of many PS to induce programmed cell death (apoptosis) by mitochondrial damage after laser treatment (Castano *et al*., 2004). The earliest apoptosis event observed after laser treatment is the release of cytochrome C from mitochondria (Mroz *et al*., 2011). Cytochrome C release can cause the initiation of a cascade leading to the activation of caspases 9 and 3 followed by the final stages of apoptosis modulated by Bcl-2 family (Mroz *et al*., 2011). Thus, PDT treatments with PSs localized in mitochondria are very rapid inducers of apoptosis (Chiaviello *et al*., 2011). A preferred subcellular localization for hydrophobic PSs is the mitochondria and the plasma membrane (Castano *et al*., 2004). The effect of PDT on cancerous cells with plasma membrane localized PSs was found to disrupt the plasma and swelling of the cell wall after PDT treatment. Disruption of the plasma and swelling of the cell wall are profound morphological characteristics of apoptosis (Castano *et al*., 2004). In some cases, it was observed that the damage of the plasma membrane induced-necrosis like cell death (Chiaviello *et al*., 2011).

In eukaryotes, endoplasmic reticulum (ER) is known as a repository of calcium ions and plays a role in signaling (Chiaviello *et al*., 2011). Any disturbances in the functions of ER lead to ER stress. However, if ER stress persist program cell death is activated. The localization of PS in ER and laser treatment causes ER photodamage with the release of sufficient calcium ions which creates interactions with the mitochondrial matrix resulting in apoptosis (Chiaviello *et al*., 2011).

Another method of cell death is autophagy. It is another response to ER photodamage perhaps serving to eradicate cancerous cells not initially removed by apoptosis (Mroz *et*

al., 2011). Thus, many of the second-generation photosensitizing agents are designed to target specific sites within a cancerous cell. This would help in the rapid initiating of cellular signals required for the induction of cell death (Kessel, 2006). For example, monocationic porphyrin was designed to localize in the plasma membrane of photosensitized cells. Other specifically designed second-generation PSs include chorin derivatives (e.g. NPe6 and lysyl chlorin p diester) and expanded porphyrin based PSs (e.g. LuTex) localize in lysosomes (Kessel, 2006). Pcs such as the Pc 4 and BPD localize in the mitochondria and ER (Kessel, 2006). Whereas, Al Pc complexes including tin etiopurpurin are designed to localize in ER and lysosome. HPPH and mTHPC localize in the ER (Kessel, 2006).

1.6.2 MODES OF CELL DEATH INDUCED BY PDT

PDT treatment can induce three mechanisms of cell death, namely apoptosis, necrosis and autophagy (Mroz *et al*., 2011). PDT-induced cell death may vary not only with the cell type or its genetic or metabolic potential but also with the experimental parameters, total treatment light dose delivered, types of PSs and their intracellular localization (Moor, 2000, Mroz *et al*., 2011). The initial cellular site of PDT related damage may determine which cell death pathway is triggered. The efficacy of PDT related cellular damage may also regulate how the PDT treated cells respond (Mroz *et al*., 2011). The PDT treated cells have to be damaged beyond repair for apoptosis to occur. Otherwise, autophagy is activated to initiate cell survival or serve as rescue or repair mechanisms. PDT at its highest dose possibly leads to necrosis as the proteins that are involved in apoptosis or autophagy pathways may be destroyed and cellular integrity damaged (Mroz *et al*., 2011). Additionally, PDT treatment may cause the shutdown of tumor vessels which results in the local depletion of nutrients and oxygen, and therefore activating necrosis. Lastly, PDT can also lead to activation of a tumor directed immune response; some cancerous cells are

eradicated via apoptosis by cytotoxic T cells (Mroz *et al*., 2011). This is clearly summarized in Table 1.4.

Key molecular effectors or signaling molecules regulating the induction of apoptosis, necrosis or autophagic cell death pathways (Mroz *et al*., 2011) are triggered by PDT as seen in Figure 1.6. These signaling molecules modulating the induction of apoptosis, necrosis or autophagy can become useful targets to stimulate or increase photokilling in cancer cells during PDT treatment (Mroz *et al*., 2011).

Table 1.4 Major cell death pathways and key players activated by PDT (Mroz *et al*., 2011)

	ORGANELLES	CELL DEATH
Direct Cell Damage	**Mitochondria :** Cytochrome c release; Bcl -2 damage	**Apoptosis**
	Cytoplasm: Beclin 1; mTOR activation	**Autophagy**
	Cell membrane disintegration	**Necrosis**
Vascular Shutdown	Local depletion of oxygen and nutrients	**Apoptosis Necrosis Autophagy**
Activation Of Immune Response	Cytotoxic T cells	Granzyme mediated **Apoptosis**

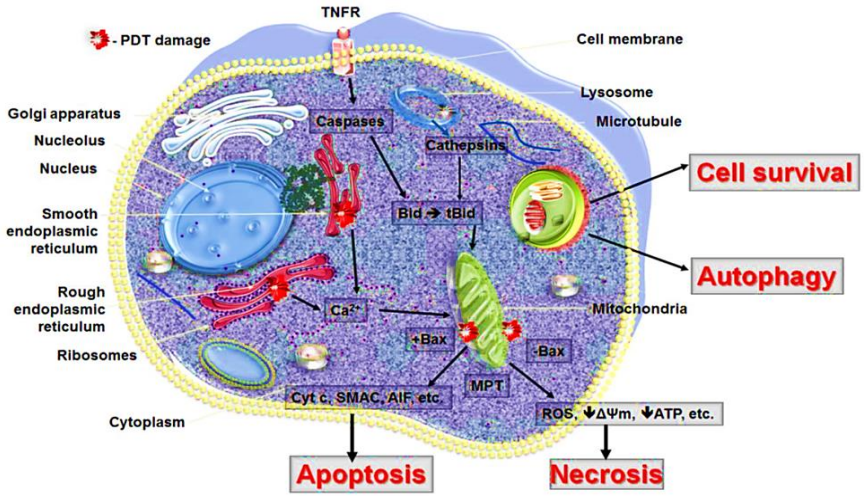

Figure 1.6 The modes of cell death observed after PDT. It depends on the intracellular localization of the PS and PDT related damage to organelles. PDT with PS localizing in the mitochondria will lead to loss of membrane permeability and release of pro-apoptotic mediators. PDT damage to ER will release cellular deposits of calcium. Accumulation of PS in the lysosome releases proteolytic enzymes upon laser treatment (autophagy). Necrosis and autophagy may be dominating cell death modes when apoptosis is dysfunctional. Several PS may locate in more than one organelle at the same time and the cell death pathways may occur concurrently (Mroz *et al*., 2011).

1.6.2.1 PDT AND PROGRAMMED CELL DEATH (APOPTOSIS)

Apoptosis is a process of cell death initiated through either the activation of death receptors or the mitochondrial release of cytochrome c (Rustin, 2002). Both these events eventually lead to activation of caspase cascades called “executioner caspases” such as caspase 3, caspase 6 and caspase 7 (Mroz *et al*., 2011). These active executioner caspases cleave cellular substrates, which causes distinct biochemical and morphological changes in observed dying cells (Rathmell and Thompson, 1999). Morphological characteristics for apoptosis include cell shrinkage, membrane blebbing, chromatin condensation and nuclear fragmentation (Savill and Fadok, 2000). During apoptosis, Bax and Bak (pro-apoptotic proteins in the Bcl-2 family) oligomerize in the outer membrane of

the mitochondria and releasing other pro-apoptotic proteins like cytochrome c from mitochondria, which allows for the activation of caspase 9 (killer proteases). Accumulating research have shown that PDT is an efficient inducer of apoptosis in many different cancer cell lines however, the lack of the ability to undergo apoptosis does not protect cell lines from lethal effects of PDT treatment (Mroz *et al*., 2011). Also, it appears that the post-mitochondrial regulators (e.g. Bax proteins), trigger late events of the apoptotic response. Thus, PDT treatment that can trigger an increase in Bax/Bcl-2 ratios in cancerous cells is regarded as a successful treatment (Mroz *et al*., 2011).

A family of death receptors known as TNFR superfamily (tumor necrosis factor receptor) is also involved in the signaling process of apoptosis (Mroz *et al*., 2011). TNFR signaling is an important factor in immune responses. This signaling contains other members like Fas and APO2/TRAIL to induce apoptosis through a p53 independent mechanism (Mroz *et al*., 2011). These death receptors activate the apoptotic pathway by caspase 8 mediated cleavage of the Bcl-2 family member BID. BID interacts with Bax and Bak for the mitochondrial release of cytochrome c and SMAC/DIABLO to activate caspase 9 and caspase 3. There is strong evidence that APO2/TRAIL is also involved in PDT mediated apoptosis (Mroz *et al*., 2011).

1.6.2.2 PDT AND NECROSIS

Necrosis is now also considered as a form of programmed cell death (Zong and Thompson, 2006). Some of the characteristic features of necrotic cell death include cytoplasmic swelling, destruction of cellular organelles and disruption of plasma membrane causing the release of intracellular contents which leads to inflammation (Danial and Korsmeyer, 2004). Investigating the factors and parameters that activate cellular necrosis after PDT is not as easy as investigating those factors which lead to

apoptosis. One contributing factor is that high doses of PDT (either a high PS concentration or a high treatment dose or both) tends to induce cell death by necrosis, while PDT administrated at lower doses tend to induce apoptotic cell death (Mroz *et al*., 2011). Another consideration is that with PS localization in the plasma membrane the photosensitization process can rapidly switch the balance towards necrotic cell death, likely due to loss of plasma membrane integrity and the rapid intracellular ATP depletion (Mroz *et al*., 2011). Also, high doses of PDT can possible photochemically inactivate key enzymes and other components of the apoptotic cascade such as caspases or inhibit apoptosis by interfering with lamin phosphorylation or by photodynamic cross-linking of lamins. Thus, high doses of PDT leads to photodamage of cancerous cells through necrotic cell death pathways (Mroz *et al*., 2011).

1.6.2.3 PDT AND AUTOPHAGY

Autophagy is also considered as cell death mechanism. The morphologic features of this type of cell death include chromatin condensation, accompanied by massive autophagic vacuolization of the cytoplasm (Mroz *et al*., 2011). The vacuoles contain double membranes and degenerating cytoplasmic organelles or cytosol (Mroz *et al*., 2011). This cell death mechanism is a catabolic cellular process that allows the cell to maintain a balance between the synthesis, degradation and recycling of cellular products (Mroz *et al*., 2011). A number of autophagic processes exist, which lead to lysosomal degradation of cellular organelles and proteins. The autophagy process involves the following steps (Kroemer *et al*., 2005):

- A double membrane structure called autophagosome surrounds the region of target
- Creating a vesicle that separates its contents from the rest of the cytoplasm

- This vesicle is then transported and fused to the lysosome forming autophagolysosome
- The contents of which are subsequently degraded by lysosomal hydrolases

Beclin1 is an essential protein for autophagy and is also known as tumor suppressor gene. Therefore, autophagy suppresses tumor growth through the generation of Beclin1 (Maiuri *et al*., 2010). This role changes as the role becomes more advanced; autophagy starts to promote tumor progression by supplying the tumor cells in the central low nutrient part of the tumor with energy that is needed for these cells to stay alive. Autophagy also has the ability to block apoptotic pathways, thereby protecting the cells from treatment (Mroz *et al*., 2011). In contrast, some cancer therapies can induce autophagic cell death in the treated tumor cells. Since mammalian cells uses autophagy as a defense against ROS mediated damage by clearing the cell of damaged organelles depending on the type of ROS and degree of oxidative injury PDT may stimulate autophagy as cell death mechanism or cytoprotector (Mroz *et al*., 2011). Autophagy can also play a role in the induction of other cell death mechanisms such as apoptosis. Furthermore, autophagy seems to play a pro-survival role in tumor cells that are capable of apoptosis and promote cell death (autophagy or necrosis) in cells that are apoptosis deficient (lack or absence of Bax/Bak apoptotic factors) (Mroz *et al*., 2011).

Based on the *in vitro* studies using various cancer lines and PSs it can be concluded that PDT directly triggers autophagy (Mroz *et al*., 2011). This is independent of the subcellular localization of the PS, as PDT mediated autophagy was seen with PSs that localized in the ER, mitochondria, lysosome and endosomes (Mroz *et al*., 2011). Literature also states that apoptosis often occurs in cells that are already undergoing autophagy as a result of PDT treatment. Most importantly, autophagy signaling proteins (Beclin1, Atg 5) are not

photodamaged by PDT. The rate of autophagic cell death if induced by PDT is influenced by the type of cancer cell, PS and treat light dose (Mroz *et al*., 2011).

1.7 SAFETY AND ADVANTAGES OF PDT

In principle PDT is ablating a lesion and creating a wound that requires healing. Clinical PDT has been associated with good healing and absences of scars (Cabuy, 2012). This is due to the fact that PDT is a cold photochemical process with no tissue heating and connective tissues such as collagen and elastin are not negatively affected during treatment. PDT also has excellent cosmetic outcomes and greatly reduced disfigurement making it an ideal treatment of skin lesions and lesions of the head, neck, and oral cavity. The ability to use endoscopic delivery of light to hollow structures makes PDT a safe and success treatment modality for early gastrointestinal cancers, oesophageal cancer and lung cancer (Cabuy, 2012).

Importantly, PDT does not cause second malignant neoplasms (Cabuy, 2012). It also does not compromise future treatment options for patients in need of other adjuvant or neoadjuvant therapy in combination with PDT (Cabuy, 2012). The only side effect evident in PDT is mild to moderate photosensitivity experienced after PDT treatment. For the topical application of the PS a local bandage is used to prevent exposure of the treated site to sunlight. In the case of systemic PS application during PDT treatment patients are advised to avoid direct sunlight for various lengths of time depending on the type of PS and PS dose (Cabuy, 2012). The side effects of PDT should be considered as manageable; when compared to the side effects experienced by cancer patients receiving surgery, radiation therapy and chemotherapy or combination therapies (Cabuy, 2012). However, PDT is not yet legalized in many countries presumably owing to the lack of research and clinical trials in those countries (Cabuy, 2012).

For PDT to become a treatment option for many other cancers (e.g. melanoma) and diseases, research needs to continue in order to expand and improve PDT photosensitizing agents and clinical protocols. In the future, it is most likely that PDT will continue to be used as a stand-alone modality or in combination with other conventional treatment modalities (e.g. chemotherapy, surgery or radiation therapy) or with new strategies. In conclusion, it is clear that the majority of disadvantages associated with PDT is linked to the photosensitizing agent used during therapy. Therefore, it is important to optimize certain parameters specifically wavelength, PS administration concentrations (low) and laser treatment times (short).

1.8 PROJECT AIM

One of the most efficient PS, aluminum phthalocyanine, exhibits high photodynamic activities, both *in vivo* and *in vitro*, against a range of model cell lines and tumors (Table 1.3). However, the photodynamic activity of a wide range of other metal-based Pcs still needs to be explored. Therefore, the aim of this *in vitro* study was to assess the effectiveness of gallium, indium and iron Pc chloride complexes as photosensitizing agents for PDT.

To achieve this aim the following objectives were set out:

- To identify the absorption and fluorescence (emission and excitation) profile of gallium, indium and iron phthalocyanine chlorides using spectrophotometric analysis
- To investigate the cellular uptake of gallium, indium and iron phthalocyanine chlorides by five different cell lines (four cancer cell lines and one healthy normal cell line) using a fluorescence spectrophotometer

- To assess the cytotoxic effects of different concentrations of inactive gallium, indium and iron phthalocyanine chlorides (in the absence of laser treatment) on the five different cell lines using the MTT cell viability assay
- To investigate the photodynamic effect of different concentrations of gallium, indium and iron phthalocyanine chlorides activated at different light doses with a diode laser (ʎ = 661 nm) on the five cell lines using the MTT cell viability assay
- To evaluate the potential mode of cell death induced by *in vitro* gallium, indium and iron phthalocyanine chlorides mediated PDT in the different cancer cell lines by electron transmission microscopy and flow cytometric analysis
- To determine the subcellular localization sites of gallium, indium and iron phthalocyanine chlorides within the four different cancer cell lines using fluorescent markers or probes for specific intracellular organelles and fluorescent microscopy for visualization.

The following cancer cell lines were used; colon (Caco-2), breast (MCF-7), skin (melanoma) and lung (A549). It is known that all cancer cells have an initial mutation that makes them immortal and a secondary mutation that results in tumorigenicity. In addition to cancer cell lines primary cultured human fibroblast cells (healthy normal cells isolated from patients at a laboratory in UCT) were used as a non-tumorigenic control cell line for the *in vitro* PDT experiments.

CHAPTER 2

RESEARCH DESIGN

Research design is the framework that outlines the methods that are followed for research. This chapter describes the cell lines, experimental procedures and specific PDT methods used to achieve the planned objectives of the study.

2.1 PHOTOSENSITIZERS

Gallium (III) phthalocyanine chloride (GaPcCl); indium (III) phthalocyanine chloride (InPcCl) and iron (III) phthalocyanine chloride (FePcCl) were purchased from Sigma Aldrich® (South Africa). Stock solutions (100 µg/ml) of each photosensitizer was prepared using dimethylsulfoxide (DMSO – Sigma®, United Kingdom) and culture media, which was further diluted in culture media to obtain treatment concentrations ranging from 2 µg/ml to 80 µg/ml.

2.2 ABSORPTION, FLOURESCENCE EMISSION AND EXCITATION PROFILING OF THE PHOTOSENSITIZERS

All spectrophotometric experiments were carried out using DMSO as a solvent. The absorption spectrum for GaPcCl, InPcCl and FePcCl were recorded on a spectrophotometer (Cary 100) in the spectral range of 300 nm – 900 nm at room temperature. Fluorescence excitation and emission spectrum for GaPcCl, InPcCl and FePcCl were measured using a fluorescence spectrophotometer (Cary Eclipse, Varian) at room temperature. The emission spectra were acquired for GaPcCl, InPcCl and FePcCl in the spectral range of 300 nm – 900 nm with excitation wavelengths set at 600 nm, 605 nm and 680 nm respectively.

2.3 CELL CULTURE

Four different adherent human cancer cell lines were used in this study namely, colon carcinoma (Caco-2); breast adenocarcinoma (MCF-7); malignant melanoma and lung adenocarcinoma (A549) cells. The healthy normal cell line used during this study was adherent human fibroblast cells. This mycoplasma-free cell lines were obtained from the following sources:

- Caco-2 cells were kindly donated by Dr Yen-Ju (Hollis) Shen from Medical Research Council (MRC) in Durban
- MCF-7 and melanoma cancer cells were kindly provided by Natasha Kolesnikova from the Biosciences at CSIR in Pretoria
- A549 cancer cells kindly donated by Dr Bronwyn C Joubert from University of KwaZulu - Natal
- Human fibroblast cells (primary culture) were kindly provided Dr A D Marais from Department of Chemical Pathology at University of Cape Town

Caco-2, melanoma, A549 and fibroblast cells were cultured in T-75 flasks (Corning, USA) containing Dulbecco's MEM medium (DMEM – Biochrome, Berlin) composed of sodium bicarbonate, glucose, glutamine, pyruvate and supplemented with 10% fetal bovine serum (FBS – Highveld Biological Pty, Ltd., South Africa) as well as 1% antibiotics (Penicillin/Streptomycin - Biochrome, Berlin) at 37°C in humidified atmosphere with 5% CO_2. MCF-7 were routinely grown in T-75 flasks (Corning, USA) containing RPMI 140 (Biochrome, Berlin) medium comprising of sodium bicarbonate, glutamine and supplemented with 10% fetal bovine serum (FBS – Highveld Biological Pty, Ltd., South Africa) as well as 1% antibiotics (Penicillin/Streptomycin - Biochrome, Berlin) at 37°C in humidified atmosphere with 5% CO_2. Flasks containing cells were examined on a daily basis for turbidity and colour changes in medium. Cell growth or proliferation was

monitored with an inverted microscope (Nikon, Japan) and cells were either passaged (sub-cultured) or harvested for experiments when they reached 80% confluency in the flask. Cell were passaged by removing media and washing cells with 5 ml of phosphate buffered saline (PBS – Sigma®, United Kingdom) before adding 4 ml of trypsin/versene (0.125% : 0.1% - Highveld Biological Pty, Ltd., South Africa) solution to detach the cells from the bottom of the flask. Flasks were incubated for approximately 5 min at 37°C in humidified atmosphere with 5% CO_2. After 5 min, the flasks were viewed under inverted microscope before supplemented culture media was added to the flask to inactivate the trypsin/versene. The cell solution was transferred to 50 ml centrifuge tubes (Corning, USA) and centrifuged at 1200 rpm or 152 g for 5 min. Thereafter, supernatant was discarded and the pellet was re-suspended in 5 ml of supplemented culture media. 100 µl of this cell solution was stained with trypan blue dye (Sigma®, United Kingdom) to manually count the number of viable or live cells using a haemocytometer under the inverted microscope. Cells were either sub-cultured into new T-75 flask containing appropriate supplemented media or cells were harvested for experimental purposes. All experiments were performed with cells of passage numbers from 48 to 57 for the A549 cancer cell line and the other cell lines were passaged 15 times or less for experiments.

2.4 CELLULAR UPTAKE OF PHOTOSENSITIZERS

The cellular uptake of GaPcCl, InPcCl and FePcCl by the four different cancer cells (Caco-2, MCF-7, melanoma and A549) and the healthy normal cells (fibroblast) were determined by using a Cary Eclipse fluorescence spectrophotometer (Varian). For experiments, cells that reach 80% confluency were seeded in 24-well tissue culture plates (Costar, USA) at a cell density of 2 x 10^4 cells/well. Cells were allowed to attach overnight at 37°C in humidified atmosphere with 5% CO_2. After 24 h, cells were photosensitized with 100 µg/ml of GaPcCl, InPcCl or FePcCl for 30 min, 1 h, 2 h, 4 h, 6 h, 8 h, 10 h, 12 h, 14 h, 16 h, 18 h,

20 h, 22 h and 24 h. At the end of each incubation period, the photosensitized cells were thoroughly washed in PBS to remove any extracellular traces of PSs before detaching the cells from the surface of the plate with 1 ml of trypsin/versene. Plates were incubated for approximately 5 min at 37°C in humidified atmosphere with 5% CO_2. After 5 min, the plates were viewed under inverted microscope before supplemented culture media was added to the appropriate wells to inactivate the trypsin/versene. The cell solution was transferred to 15 ml centrifuge tubes (Corning, USA) and centrifuged at 1200 rpm for 5 min. Thereafter, supernatant was discarded and the collected cell pellet was re-suspended in 2 ml of DMSO (to exact intracellular PSs and lyse the cells) and incubated at room temperature for 10 min. Then samples were vortexed and centrifuged for 2 min at 6000 rpm. The DMSO supernatant containing the extracted intracellular GaPcCl, InPcCl or FePcCl was collected into another amber microtube and the pellet was discarded. The DMSO supernatant was analyzed for traces of extracted GaPcCl, InPcCl or FePcCl using a fluorescence spectrophotometer at specific excitation wavelengths of 600 nm, 605 nm and 680 nm respectively. Simultaneously, supernatants from untreated control cells (not pre-incubated with PSs) were measured as a control at similar excitation wavelengths for each exposure time. The presence of emitted fluorescence peaks are an indication of PS uptake by cells and the fluorescence intensity (arbitrary units, a.u.) readings of the emitted peaks are proportional to the amount of PS being taken up by the cells.

2.5 DARK TOXICITY ASSAY

A PS in its inactive form (without laser activation or treatment) may have anti-proliferative and/or cytotoxic effects which can be determined by conducting a dark toxicity assay as described below.

Cells (Caco-2, MCF-7, melanoma, A549 and fibroblast) at a density of 2 x 10^4 cells per well were seeded in 24-well tissue culture plates and allowed to attach overnight at 37°C in humidified atmosphere with 5% CO_2. The next day, cells were treated with GaPcCl, InPcCl or FePcCl at different photosensitizing concentrations (2 µg/ml - 100 µg/ml) for 2 h at 37°C in humidified atmosphere with 5% CO_2. Each concentration was tested in triplicate and plates were wrapped in aluminum foil before incubating. Untreated control cells that were not exposed to GaPcCl, InPcCl or FePcCl (0 µg/ml) were included for each set of experiments. After 2 h of incubation cells were washed twice with PBS and the cell viability was measured using the MTT (methyl-thiazolyl-tetrazolium) colorimetric assay. For the MTT assay, 500 µl of culture medium and 100 µl of MTT solution (1 mg/ml in PBS) were added to each well. The plates were incubated for 4 h allowing for the MTT to be metabolized to formazan by the succinate-tetrazolim reductase system that is active only in viable cells. At the end of the fourth hour, the medium was removed and the resultant formazan crystals were dissolved in 500 µl of DMSO. The absorbance intensity of each well was measured using a standard microplate reader (Biohit) set at a wavelength 490 nm with a reference wavelength of 620 nm. The relative cell viability (%) for each sample was expressed as a percentage relative to the untreated control cells. Therefore, percentage of viable cells for each well was calculated using the formula [1].

$$\boldsymbol{Cell\ Viability}\ (\%) = \left(\frac{\boldsymbol{abs\ of\ sample}}{\boldsymbol{abs\ of\ control}}\right) \times \mathbf{100} \quad \text{..... [1]}$$

2.6 *IN VITRO* PDT

Cells (Caco-2, MCF-7, melanoma, A549 and fibroblast) that reached 80% confluence were seeded in 24-well tissue culture plates (Costar, USA) at a cell density of 2 x 10^4 cells/well. Cells were allowed to attach overnight at 37°C in humidified atmosphere with 5% CO_2.

After 24 h of cell growth the culture medium from each well was removed and the cells were washed twice with PBS. Cells were treated with GaPcCl, InPcCl or FePcCl at different photosensitizing concentrations (2 µg/ml - 100 µg/ml) for 2 h. Each concentration was tested in triplicate and plates were wrapped in aluminum foil and incubated at 37°C in humidified atmosphere with 5% CO_2. After two hour incubation period, cells in monolayer cultures were irradiated with diode laser (continuous wave laser) system emitting at a wavelength 661 nm (Coherent cube laser system, USA). The laser set-up is shown in Figure 2.1. The output power of the laser beam was 90 mW for all experiments. For all experiments, the laser beam was measured before and after laser treatment using a laser power meter (Coherent, USA). A spot size or laser beam of 1 cm in diameter was used to deliver treatment lights of 2.5 J/cm^2, 4.5 J/cm^2 and 8.5 J/cm^2. The irradiation time (s) was calculated to deliver a light of 2.5 J/cm^2, 4.5 J/cm^2 and 8.5 J/cm^2 in 22 sec, 39 sec and 74 sec respectively (Table 2.1 and Figure 2.2). All irradiations were performed at room temperature in the dark. Cells to be used as untreated control cells (0 µg/ml) were not exposed to the photosensitizers and laser irradiation. Laser irradiated cells that were not pre-treated with the photosensitizers served as the laser controls. Post-irradiated and control cells were incubated for 24 h before cell viability was measured using the MTT cell viability assay as described above.

2.7 CYTOLOGIC ANALYSIS OF PDT TREATED CELLS USING AN INVERTED MICROSCOPE

Cells (Caco-2, MCF-7, melanoma, A549 and fibroblast cells) were seeded in 24-well tissue culture plates at a cell density of 2 x 10^4 cells/well. Cells were allowed to attach overnight at 37°C in humidified atmosphere with 5% CO_2. After 24 h, culture medium from each well before washing with PBS. Cells were photosensitized with either GaPcCl, InPcCl or InPcCl at concentrations listed in Table 2.1 with accordance to cell type and plates were

incubated at 37°C in humidified atmosphere with 5% CO_2 for 2 h. After 2 h, cells were irradiated with diode laser emitting at a wavelength of 661 nm. The measured output of 1 cm spot size was 90 mW for all laser treatments and the treatment light dose in accordance to cell type is listed in Table. After laser treatment plates were further incubated at 37°C in humidified atmosphere with 5% CO_2 for 24 h. Untreated cells that were not exposed to PDT treatment were used as a control for each set of experiments. Thereafter, the changes in cell morphology were evaluated by analyzing 24 h post-PDT treated cancer cells including the untreated control cells under inverted microscope and capturing images.

Figure 2.1 Set-up of the red light diode laser system at a wavelength of 661 nm with a spot size of 1 cm (diameter) used to deliver light doses of 2.5 J/cm^2, 4.5 J/cm^{2}and 8.5 J/cm^2 to monolayer of cells seeded in 24-well plates.

Table 2.1 Laser parameters used in PDT experiments

Parameters	Unit	22 sec	39 sec	74 sec
Wavelength	nm	661	661	661
Wave emission	-	continuous	continuous	continuous
Power output	mW	90	90	90
Power density	mW/cm^2	114.59×10^{-3}	114.59×10^{-3}	114.59×10^{-3}
Spot size	cm^2	0.7854	0.7854	0.7854
Light dose	**J/cm^2**	**2.5**	**4.5**	**8.5**

Area of Spot Size (cm^2) = πr^2

Power Density (W/cm^2) = [Power (mW) / Area of spot size (cm^2)] x 10^{-3}

Irradiation Time (sec) = Required Light Dose (J/cm^2) / Power Density (W/cm^2)

Figure 2.2 Equations used to calculate the irradiation parameters.

2.8 ANALYSIS OF CELL DEATH MECHANISMS INDUCED BY PDT

Various techniques are available with which the mechanism of induced cell death may be assessed. Morphologic evaluation on cancer cells after GaPcCl, InPcCl and FePcCl mediated PDT treatment was performed using inverted microscope. The ultra-structural changes induced by GaPcCl, InPcCl and FePcCl mediated PDT treatment in the different cancer cell lines were also observed using a transmission electron microscope (TEM). Also, cell death modes can be successfully determined by flow cytometric analysis using the Annexin V-FITC/propidium iodide assay.

2.8.1 EVALUATION OF ULTRA-STRUCTURAL CHANGES IN CANCER CELLS AFTER PDT TREATMENT USING THE TEM

Cells (Caco-2, MCF-7, melanoma and A549) were seeded in Lab-Tek® II chamber slide (2 well glass slide) system (Nalge Nunc international Cooperation, USA) at a cell density of 2

x 10^4 cells/well. Cells were allowed to attach overnight at 37°C in humidified atmosphere with 5% CO_2. After 24 h, cells were PDT treated as described in section 2.6.

PDT treated cells and untreated control cells were processed and analyzed at the University of KwaZulu-Natal in the laboratory for microscopy and microanalysis. Culture medium was removed from wells and cells were washed twice with PBS. Then cells were washed with 0.1 M phosphate buffer (pH 7.4) for 5 min. After 5 min, 0.1 M phosphate buffer (pH 7.4) was removed and a primary fixative (2.5% gluteraldehyde in 0.1 M phosphate buffer) was added to each well for 2 h. The next step included washing the cells in 0.1 M phosphate buffer (pH 7.4) for 5 min and this step was repeated three times. After washing, cells were post-fixed in 0.5% osmium tetroxide in 0.1 M phosphate buffer for 1 h at room temperature. Cells were washed again in 0.1 M phosphate buffer (pH 7.4) for 5 min which was repeated three times. The dehydration of samples included the following steps:

- 50% ethanol for 5 min (repeated twice)
- 75% ethanol for 5 min (repeated twice)
- 90% ethanol for 5 min (repeated twice)
- 100% ethanol for 10 min (repeated twice)

Samples were then infiltrated by adding resin and incubating overnight at room temperature. The next day the resin was removed and fresh resin was added to samples and samples were incubated for a further 4 h at room temperature. After 4 h, the resin was removed and fresh resin was added before polymerizing samples for 8 h in an oven set at 70°C. The cured resins were removed from slides and an ultra-thin section (EM UC7 RT, Leica) of each resin was placed onto grids. Grids were stained with uranyl acetate for 15 min and lead citrate for 15 min before viewing under TEM (Jeol Jem 1010 EM). Digital images were captured for sample.

2.8.2 ANALYSIS OF APOPTOSIS USING DUAL FITC ANNEXIN V AND PROPIDIUM IODIDE STAINS

Cells (Caco-2, MCF-7, melanoma and A549) were cultured in T-25 flasks (Corning, USA) containing the appropriate supplemented cultured medium at 37°C in humidified atmosphere with 5% CO_2. 80% confluent cells were PDT treated as described in section 2.6. Untreated cells that were not exposed to PDT treatment were used as a control for each set of experiments. At 24 h post-PDT treatment, cells were processed for flow cytometric analysis using the FITC Annexin V Apoptosis Detection Kit I (BD Biosciences, USA). The kit contained Annexin V binding buffer (10x); FITC Annexin V staining solution; PI staining solution and a detailed protocol.

Firstly, cells were prepared by removing the culture media from each flask. Thereafter, the adherent cells were washed in PBS before adding 2 ml of Accutase™ cell detachment solution (BD Biosciences, USA) for the detaching of the cells from the bottom of the flask. Flasks containing the cell suspension were incubated for 5 min at 37°C in humidified atmosphere with 5% CO_2. Each flask was viewed under the inverted microscope to see if the cells had detached before supplemented with culture medium. Cells were centrifuged at 1200 rpm for 5 min. The supernatant was discarded and the pellet was washed twice with cold PBS before re-suspending cells in binding buffer (1x) at a concentration of $1x10^6$ cells/ml. 100 µl of this solution was transferred to a 5 ml culture tube for labelling. 5 µl of FITC Annexin and 5 µl of PI were added to each tube and cells were gently vortexed before incubation for 5 min at room temperature (25 °C) in the dark. After 5 min, 400 µl of binding buffer (1x) was added to each tube and samples were analyzed using the Accuri C6 Flow Cytometer. Intensity distribution graphs were generated and analyzed with intensity of PI on the y-axis and FITC Annexin V on the x-axis. Cells that are considered viable, stain FITC Annexin V negative and PI negative (lower left quadrant); cells that are

in early or later stage apoptosis stain FITC Annexin V positive and PI negative (lower right quadrant); and cells that are in the late apoptosis stage or already dead stain FITC Annexin V positive and PI positive (upper right quadrant). The upper left quadrant (FITC Annexin V negative and PI positive) displays events which correspond to cellular debris.

2.9 SUBCELLULAR LOCALIZATION OF PHOTOSENSITIZERS

The localization sites of GaPcCl, InPcCl and FePcCl in the different cancer cell lines were determined using fluorescent markers or probes for intracellular organelles. Mitotracker® Green FM (M7514, Invitrogen) was used for mitochondria and Lysotracker® Green DND-26 (L7526, Invitrogen) for lysosomes. A 1 mM stock solution of Mitotracker solution was prepared by adding 74, 4 µl of DMSO to a vial containing 50 µg of Mitotracker® Green FM and further diluted in pre-warmed culture medium to obtain a final working concentration of 79 µM. The Lysotracker staining solution was prepared by combining 39.5 µl of 1 mM Lysotracker® Green DND-26 with 500 µl of pre-warmed culture medium in an eppendorf tube for a working concentration of 79 µM. The nucleus was stained with the ProLong® gold antifade reagent with DAPI (Invitrogen).

Experimentally, to determine the cellular localization site of GaPcCl, InPcCl and FePcCl cells (Caco-2, MCF-7, melanoma and A549) were grown on a Lab-Tek® II chamber slide system (Nalge Nunc international Cooperation, USA) composing of eight chambers mounted onto a single glass slide with a coverlid for 24 h at 37°C in humidified atmosphere with 5% CO_2. The next day cells were treated either with GaPcCl, InPcCl or FePcCl at a photosensitizing concentration of 100 µg/ml for a period of 2 h at 37°C in humidified atmosphere with 5% CO_2. After 2 h, cells were washed twice with PBS before staining mitochondria or lysosomes of the untreated control cells and photosensitized cells with the fluorescent probes. 200 µl of 79 µM Mitotracker staining solution or 150 µl of 79 µM

Lysotracker staining solution was added to the appropriate wells containing the untreated control cells and photosensitized cells for 15 min at 37°C in humidified atmosphere with 5% CO_2. After 15 min, culture medium containing the probe was removed and cells were washed with PBS before removing the chamber from the slides. Then, nuclei were counter stained using DAPI and cover slips were placed on slides before fluorescence visualization using Zeiss Axioscope A1 fluorescent microscope interfaced with Axiovision Rel 4.8 image analysis software program. Organelle markers and PSs were excited at the following wavelengths namely, 405 nm for DAPI; 488 nm for Mitotracker and Lysotracker; and 568 nm for PSs. All images were captured on 40 x initial magnification.

2.10 STATISTICAL ANALYSIS

Each test was done in triplicate and repeated. The mean, standard deviation and standard error were calculated using Microsoft Excel 2010 software. Further, statistical analysis was performed using Instat software (GraphPad prism 6) by one-way analysis of Variance (ANOVA). The Tukey-Kramer Multiple Comparisons Test was used to determine the significant changes between experimental groups and respective controls.

CHAPTER 3

RESULTS

3.1 ABSORPTION, FLOURESCENCE EMISSION AND EXCITATION PROFILING OF THE PHOTOSENSITIZERS

Auto fluorescence compounds like metal-based Pcs can be identified on the basis of its excitation and emission properties. The ground state electronic spectra of GaPcCl (Figure 3.1) showed characteristic absorption in the Q band region at a wavelength of 678 nm with a lower absorbance at 611 nm. InPcCl dissolved in DMSO showed the highest absorption peak at 685 nm accompanied by lower absorption peaks at 350 nm and 616 nm (Figure 3.2). The ground state electronic spectra of FePcCl dissolved in DMSO displayed absorption at 325 nm, 642 nm and 675 nm (Figure 3.3). Based on these absorption spectra a commercially available laser system emitting at a set wavelength of 661 nm was purchased to activate the PSs during PDT treatment studies.

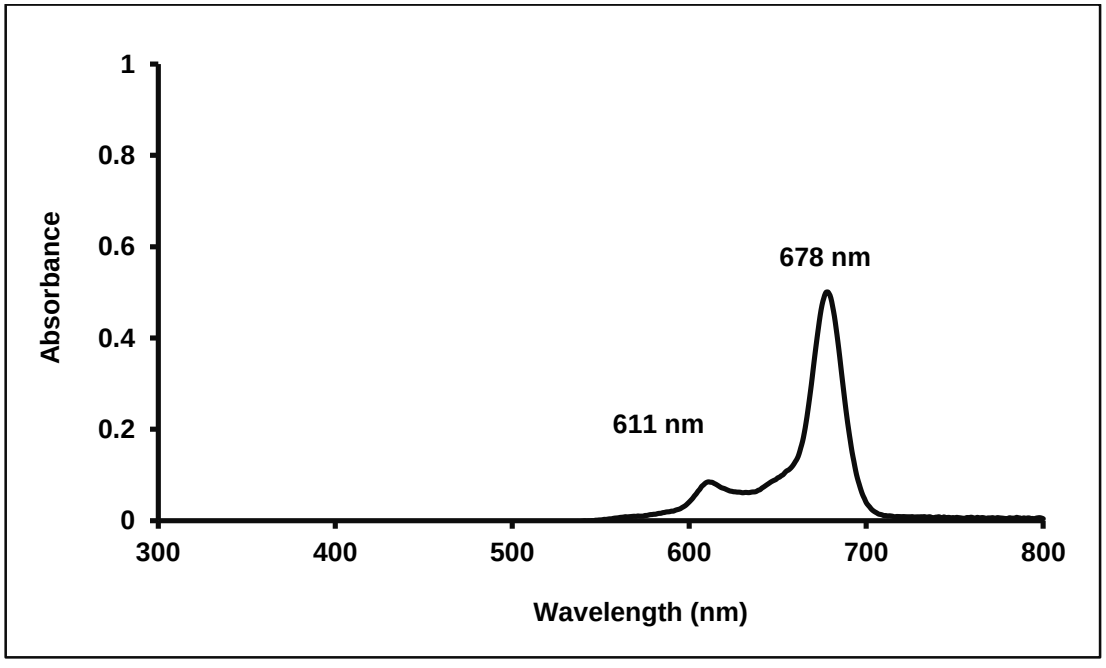

Figure 3.1 The absorption spectrum of GaPcCl.

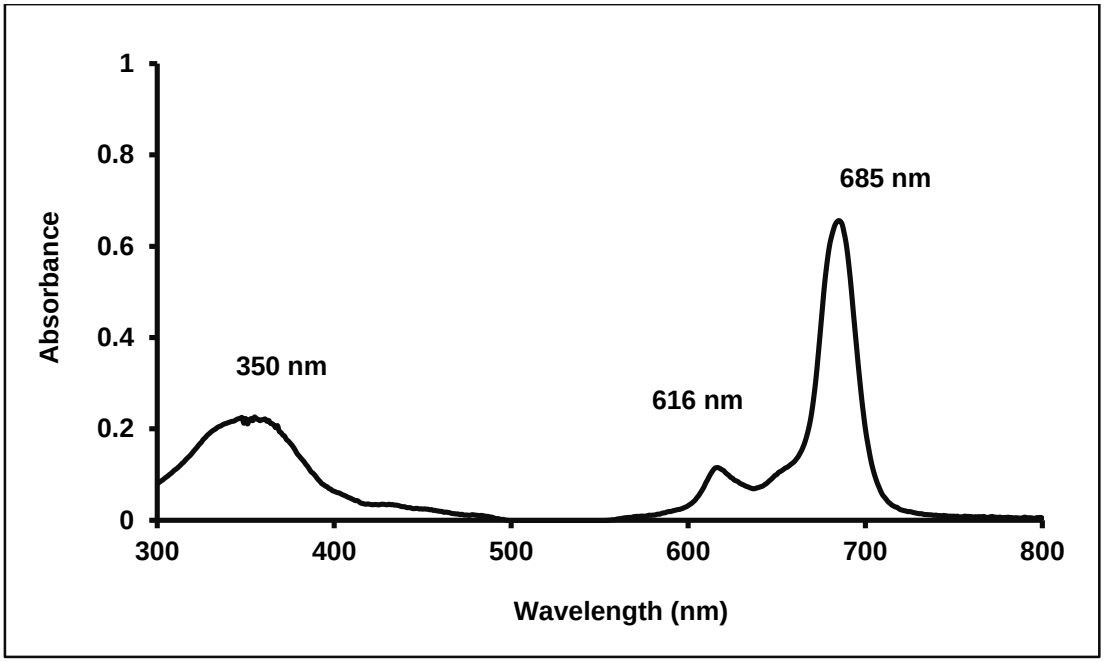

Figure 3.2 The absorption spectrum of InPcCl**.**

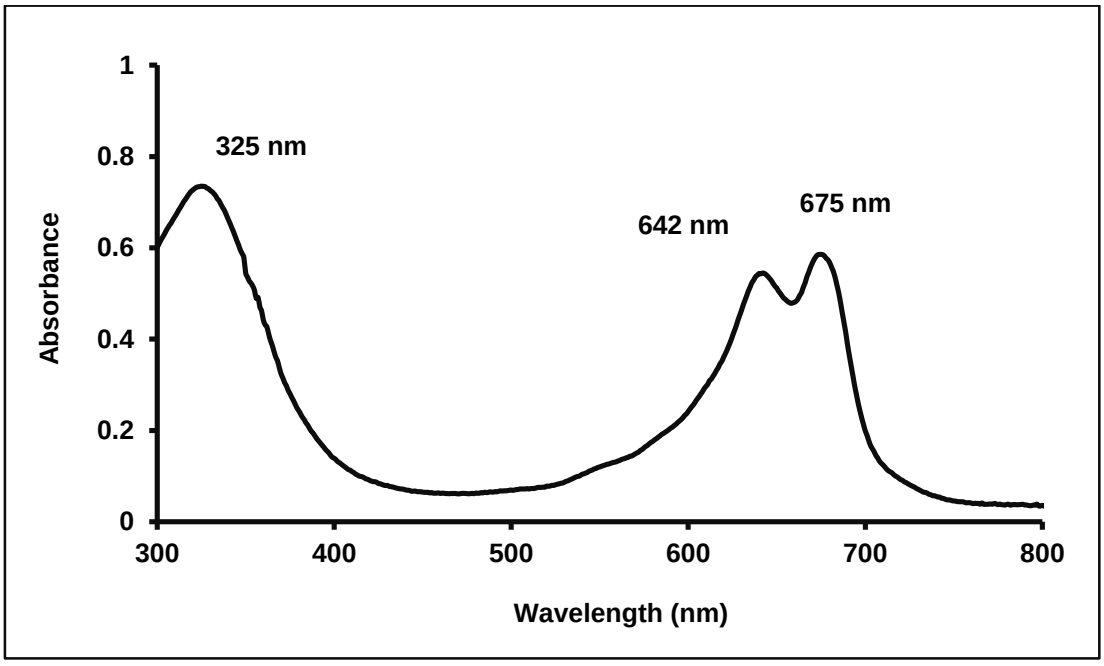

Figure 3.3 The absorption spectrum of FePcCl.

The low absorption spectra of 325 nm and 350 nm observed for InPcCl and FePcCl cannot be used in PDT due to the high energy of these wavelengths. All PSs absorbed light with wavelengths between 611 nm and 685 nm. Therefore, excitation wavelengths of 600 nm, 605 nm and 680 nm were used to examine the emission spectra of the selected PSs. GaPcCl (Figure 3.4), InPcCl (Figure 3.5) and FePcCl (Figure 3.6) displayed detectable emission peaks/fluorescence when excited at a fixed wavelength of 600 nm, 605 nm and 680 nm respectively. The fluorescence profile of GaPcCl (Figure 3.4) in DMSO exhibits two distinct emission peaks at 700 nm and 746 nm with an excitation wavelength of 600 nm. Excitation of InPcCl with an excitation wavelength of 605 nm gave an intense emission peak at 701 nm and minor peak at 750 nm (Figure 3.5). A fluorescence emission peak was observed at 750 nm for FePcCl in DMSO (Figure 3.6) with an excitation wavelength of 680 nm.

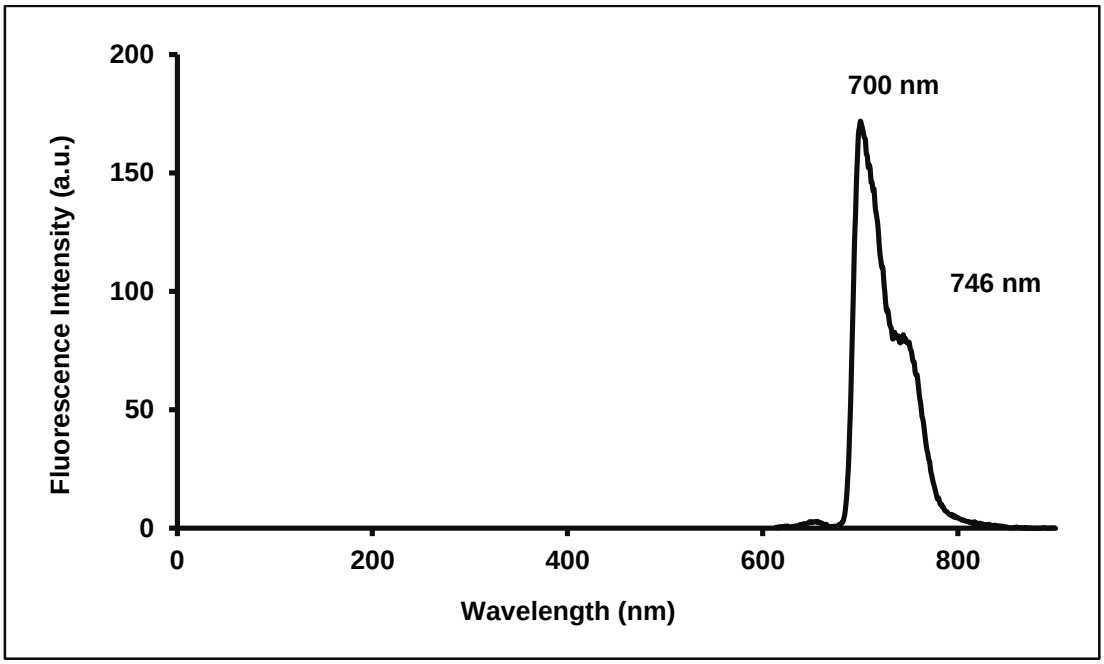

Figure 3.4 The fluorescence emission spectrum of GaPcCl in DMSO determined by using a fluorescence spectrophotometer with a fixed excitation wavelength of 600 nm.

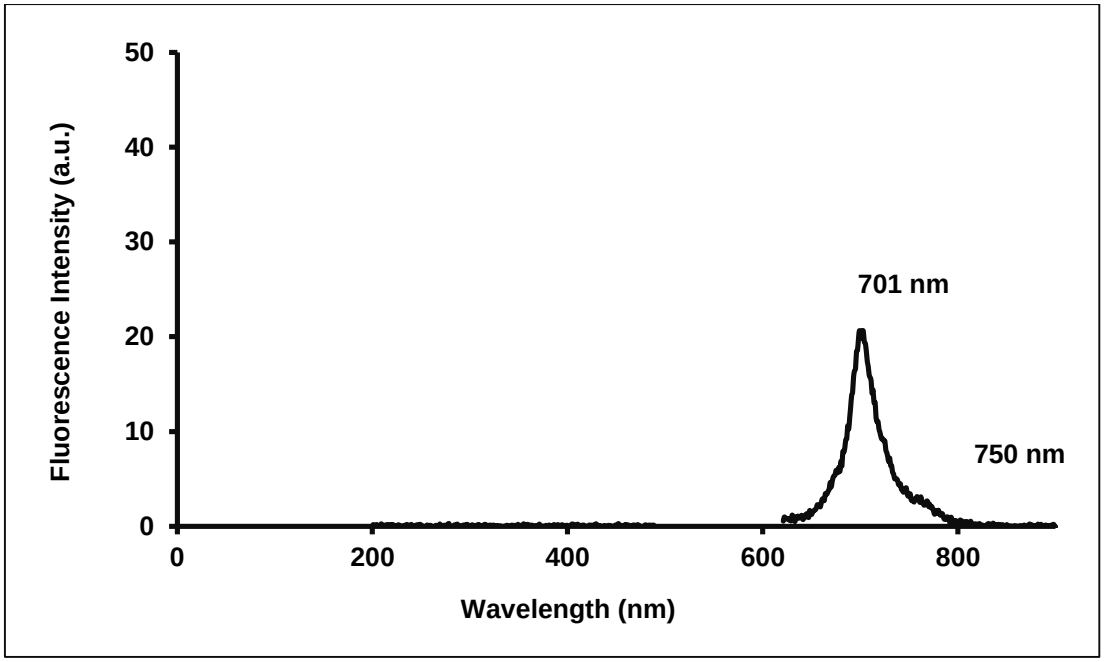

Figure 3.5 The fluorescence emission spectrum of InPcCl in DMSO determined by using a fluorescence spectrophotometer with a fixed excitation wavelength of 605 nm.

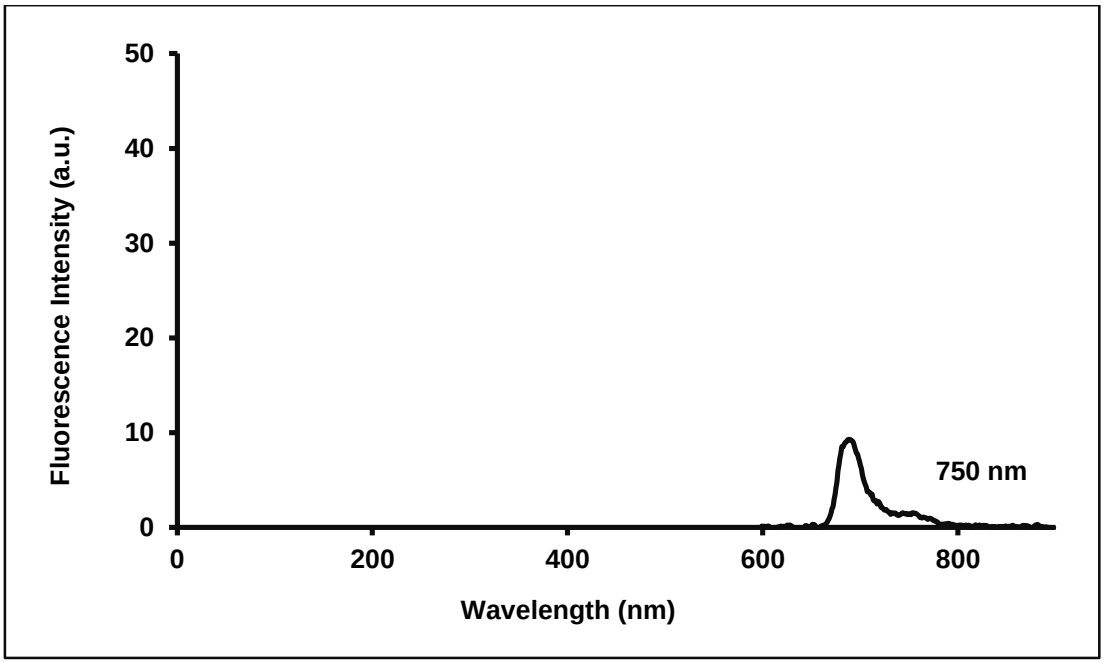

Figure 3.6 The fluorescence emission spectrum of FePcCl in DMSO determined by using a fluorescence spectrophotometer with a fixed excitation wavelength of 680 nm.

3.2 CELLULAR UPTAKE OF PHOTOSENSITIZERS

One of the underlying principles of PDT is the uptake or accumulation of the PS by cancer cells, prior to the laser treatment stage. Accumulation over time was correlated to the increasing fluorescence intensity of the emission spectra. All three PSs selected for this present *in vitro* study were accumulated by Caco-2 (Figure 3.7 – 3.9), MCF-7 (Figure 3.10 – 3.12), melanoma (Figure 3.13 – 3.15) and A549 (Figure 3.16 – 3.18) cancer cells in amounts which steadily increased over a 24 h period. The time dependence for the intracellular accumulation of GaPcCl, InPcCl and FePcCl in all four cancer cells are graphical illustrated below.

All three metal-based Pc chloride complexes showed a rapid cellular uptake during the first 30 min, followed by a slow but increasing uptake during the next 24 hours. The results also indicate that the cellular uptake of GaPcCl, InPcCl and FePcCl by all four cancer cells are time-dependent. The highest fluorescence intensity (arbitrary unit - a.u.) for the emission peaks of GaPcCl, InPcCl and FePcCl were observed at 24 h for all four cancer cell lines. The emission peaks for extracted intracellular FePcCl from Caco-2 (Figure 3.9 B), MCF-7 (Figure 3.12 B) and A549 (Figure 3.18 B) cancer cells when compared to the other two PSs showed the highest fluorescence intensity at 24 hours. Emission peaks for intracellular InPcCl from Caco-2 (Figure 3.9), MCF-7 (Figure 3.12) and A549 (Figure 3.18) cancer cells showed lower fluorescence intensities (a.u.) when compared FePcCl and GaPcCl. This indicating that a greater quantity of FePcCl is being taken up with GaPcCl showing slightly lower uptake and FePcCl being the least taken up by these three cancer cell lines over 24 hours. In contrast, the emission peaks for intracellular GaPcCl (Figure 3.12) showed the highest fluorescence intensities and emission peaks for intracellular InPcCl (Figure 3.13) showed the lowest fluorescence intensities from melanoma cancer

cells over 24 hours. Intracellular GaPcCl (Figure 3.14) showed emission peaks with slightly lower fluorescence intensities compared to InPcCl in melanoma cancer cells.

The emission peaks and fluorescence intensity (a.u.) of intracellular GaPcCl, InPcCl and FePcCl in DMSO extracted from healthy normal cells (fibroblast cells) is displayed in Figure 3.19, Figure 3.20 and Figure 3.21 respectively. Each PS had a very fast uptake since emission peaks with low fluorescence intensity (a.u.) was achieved after 30 min incubation with fibroblast cells. For periods of incubation longer than 30 min, the emission peaks associated with GaPcCl, InPcCl and FePcCl showed increased fluorescence intensity (a.u.) indicating an increased cellular uptake of PS by fibroblast cells. The results also indicate that the cellular uptake of GaPcCl, InPcCl and FePcCl by fibroblast cells is time-dependent.

The uptake of InPcCl and FePcCl was higher by cancer cells compared to healthy normal fibroblast cells. A lower uptake of InPcCl is also observed in fibroblast cells which was much lower than the amounts being taken up by the different cancer cells. In addition, a lower uptake of FePcCl was also observed in fibroblast cells which was also much lower than the amounts being taken up by three of the different cancer cell lines (Caco-2, MCF-7 and A549). Unfortunately, a higher uptake of GaPcCl by fibroblast cells than each of the different cancer cells cancer cells is detected by the higher fluorescence intensities of the emission peaks for each time point.

Interestingly, at an uptake time of 24 h the emission peak for extracted intracellular FePcCl from A549 cells showed the highest fluorescence intensity (982 a.u.) when compared to the emission peaks for extracted intracellular GaPcCl and InPcCl from all five cell lines.

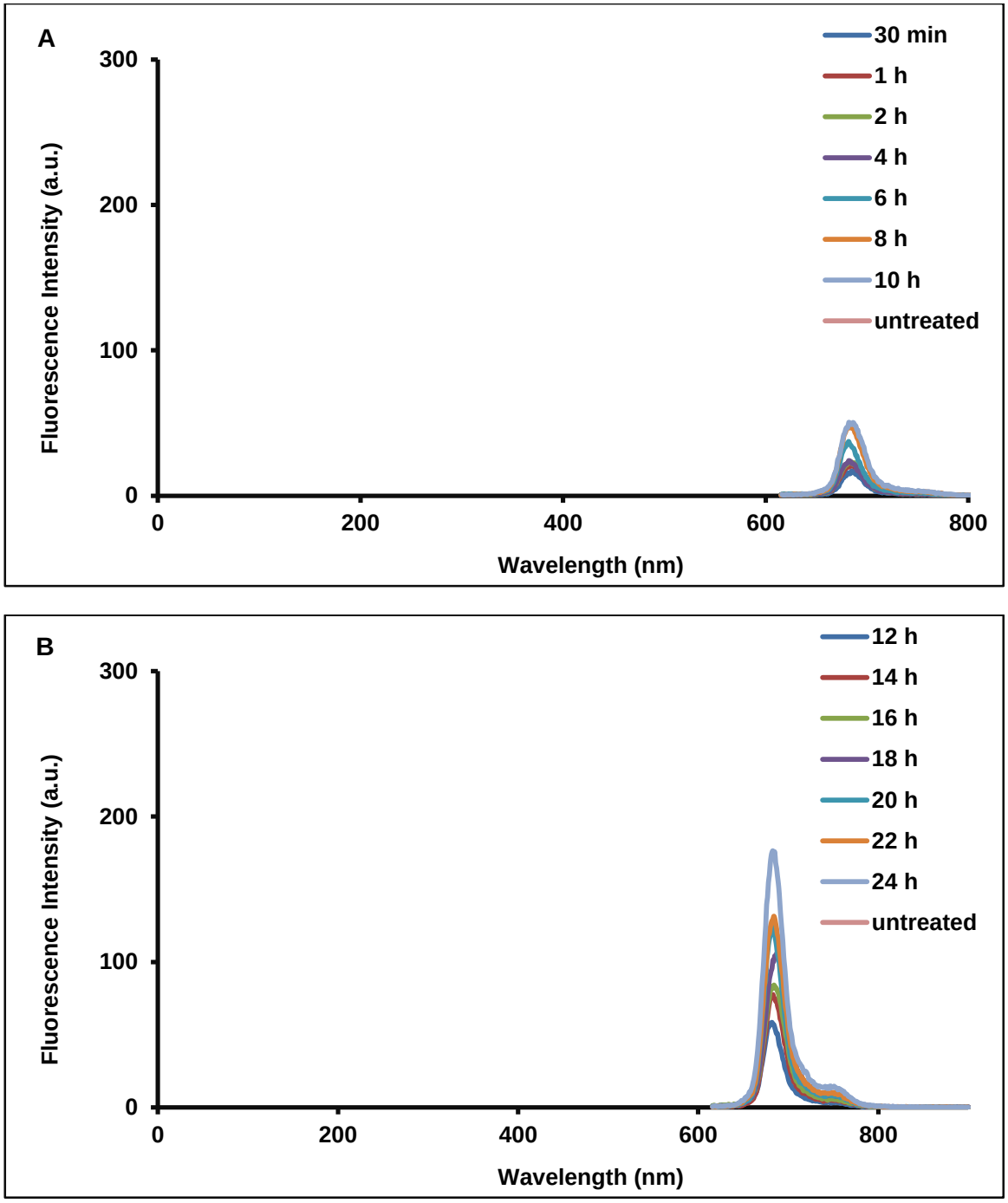

Figure 3.7 The emission peaks and fluorescence intensities (a.u.) of extracted intracellular GaPcCl (100 µg/ml) from Caco-2 cancer cells over (A) 30 min to 10 h and (B) 12 h to 24 h incubation periods measured using a fluorescence spectrophotometer with an excitation wavelength set at 600 nm. Untreated = untreated control cells not exposed to GaPcCl.

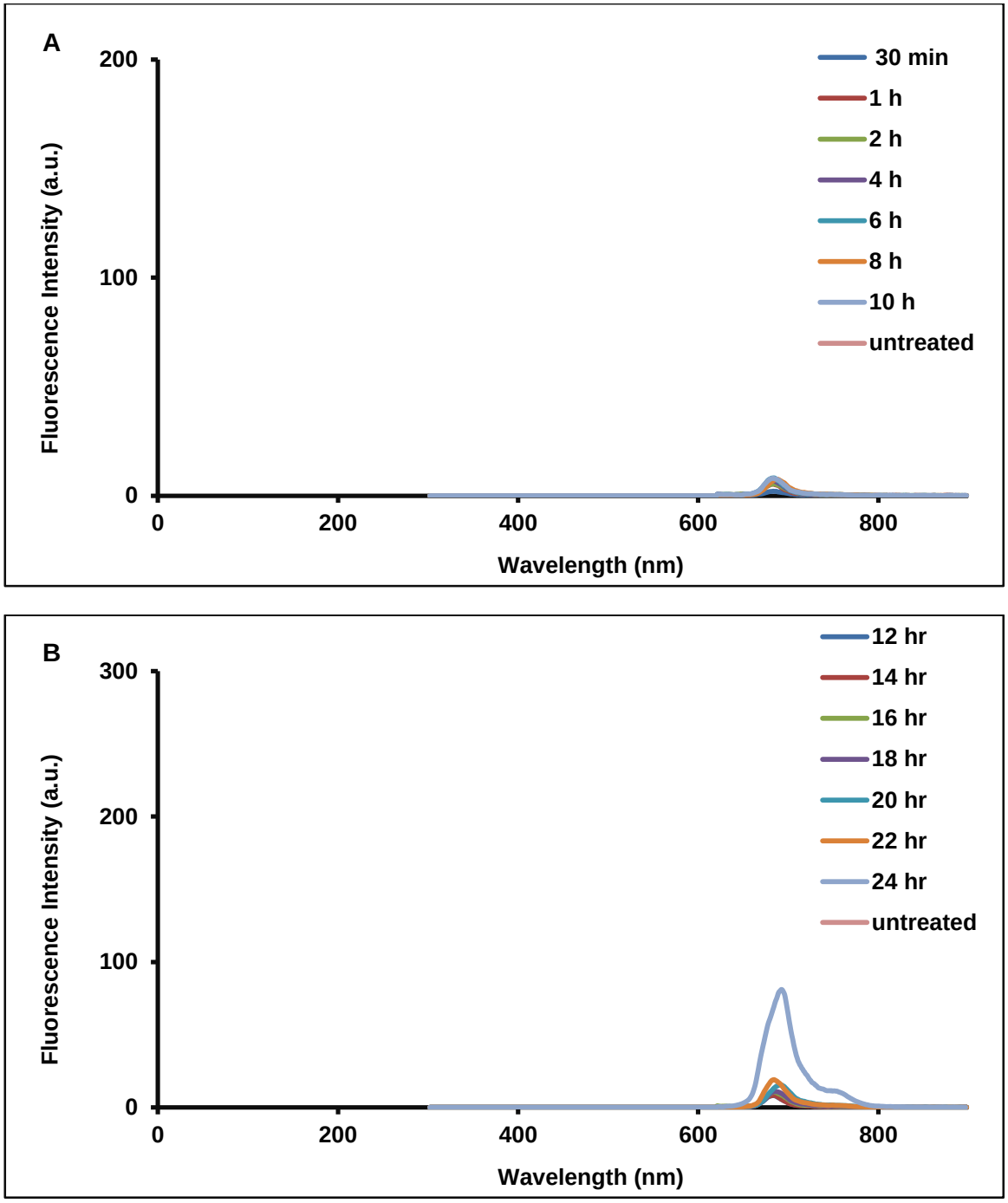

Figure 3.8 The emission peaks and fluorescence intensities (a.u.) of extracted intracellular InPcCl (100 µg/ml) from Caco-2 cancer cells over (A) 30 min to 10 h and (B) 12 h to 24 h incubation periods measured using a fluorescence spectrophotometer with an excitation wavelength set at 605 nm. Untreated = untreated control cells not exposed to InPcCl.

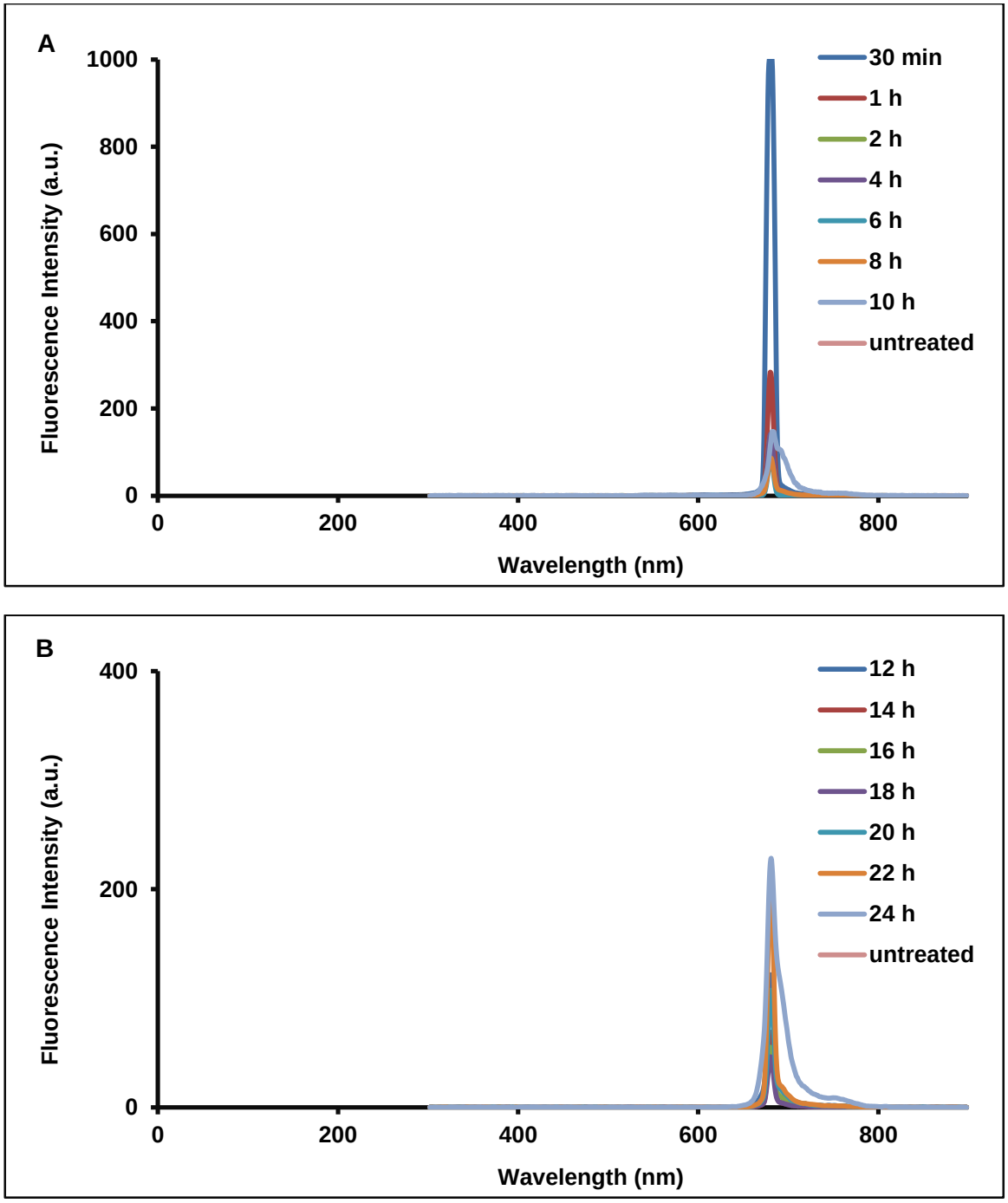

Figure 3.9 The emission peaks and fluorescence intensities (a.u.) of extracted intracellular FePcCl (100 µg/ml) from Caco-2 cancer cells over (A) 30 min to 10 h and (B) 12 h to 24 h incubation periods measured using a fluorescence spectrophotometer with an excitation wavelength set at 680 nm. Untreated = untreated control cells not exposed to FePcCl.

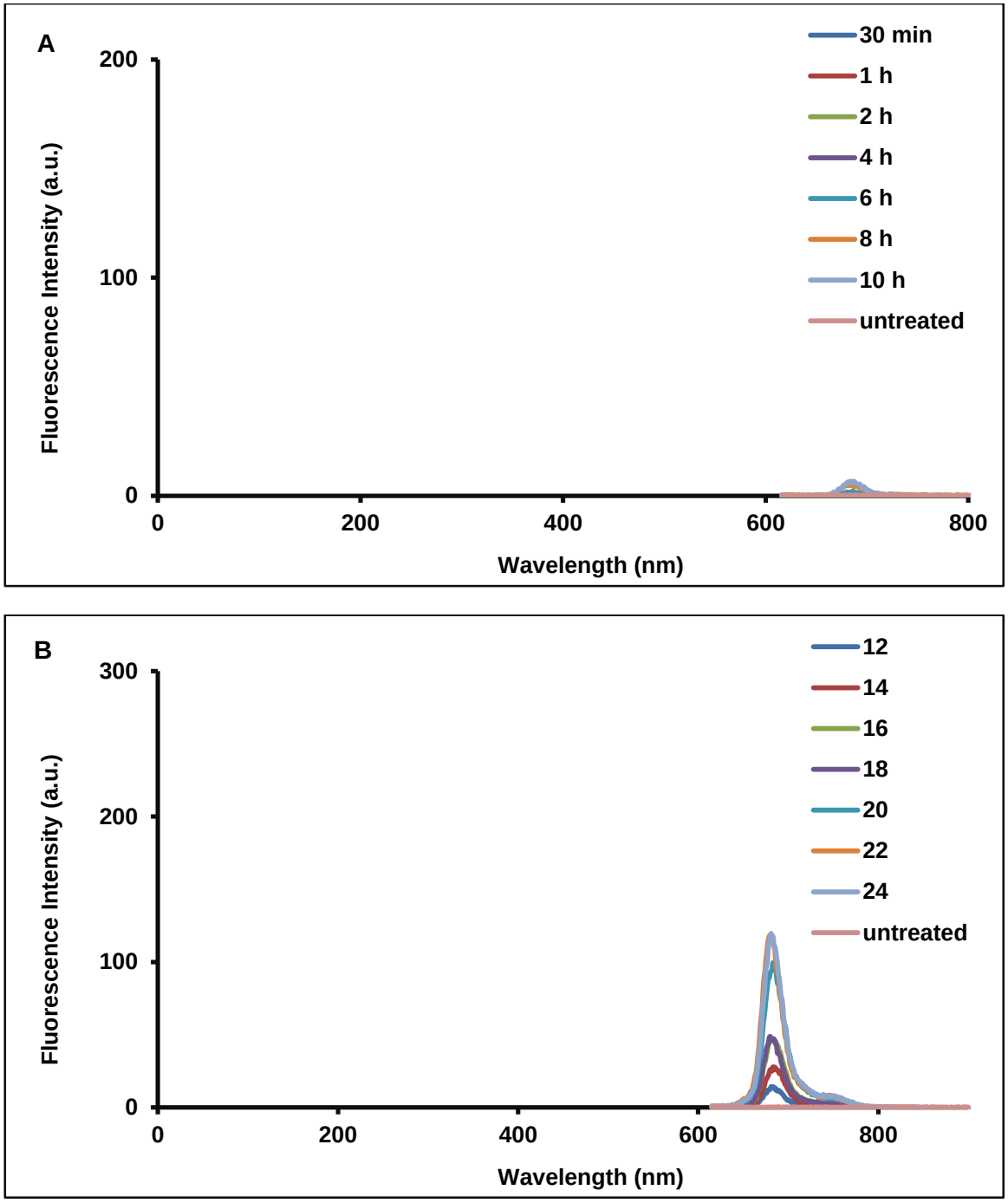

Figure 3.10 The emission peaks and fluorescence intensities (a.u.) of extracted intracellular GaPcCl (100 µg/ml) from MCF-7 cancer cells over (A) 30 min to 10 h and (B) 12 h to 24 h incubation periods measured using a fluorescence spectrophotometer with an excitation wavelength set at 600 nm. Untreated = untreated control cells not exposed to GaPcCl.

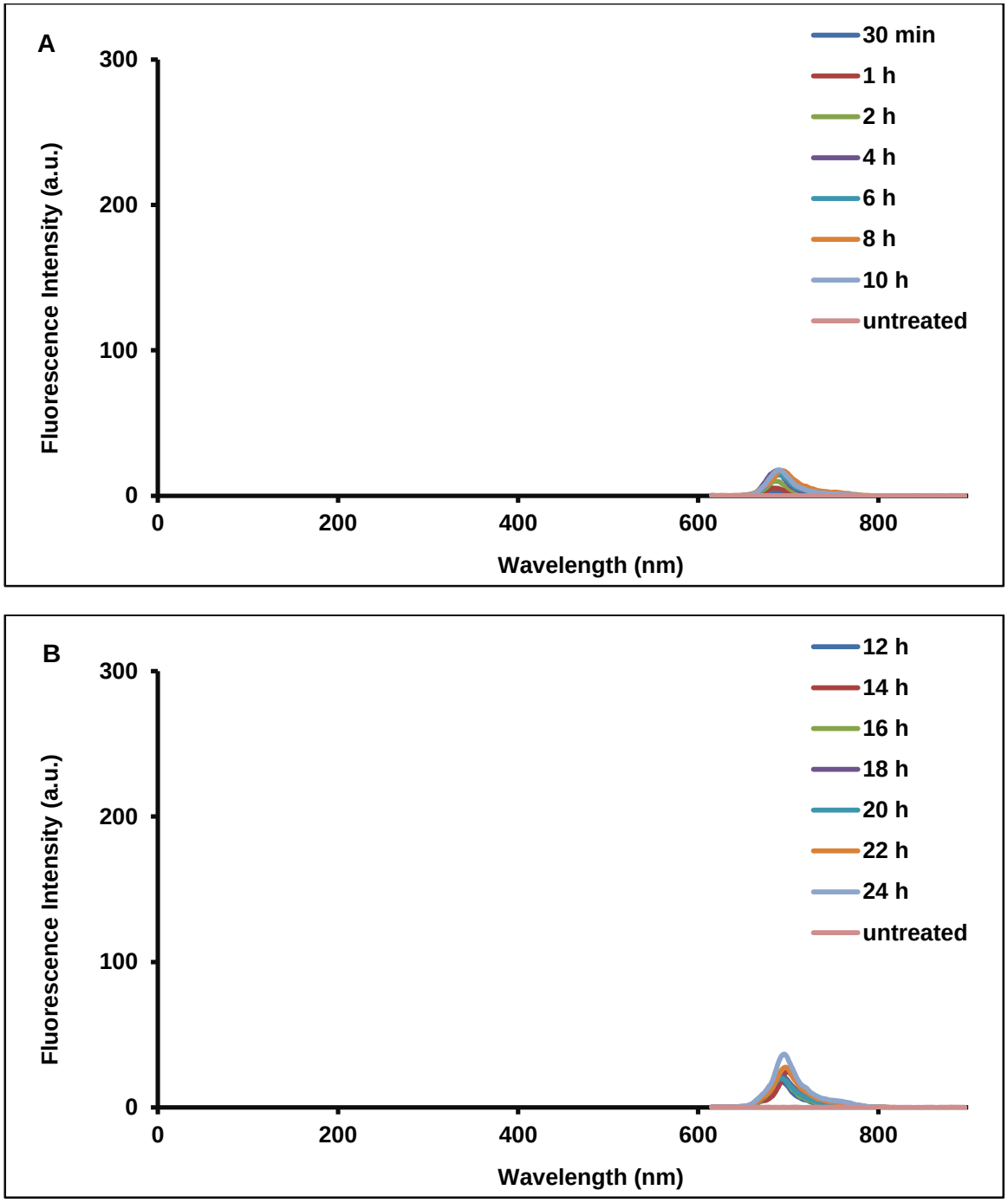

Figure 3.11 The emission peaks and fluorescence intensities (a.u.) of extracted intracellular InPcCl (100 µg/ml) from MCF-7 cancer cells over (A) 30 min to 10 h and (B) 12 h to 24 h incubation periods measured using a fluorescence spectrophotometer with an excitation wavelength set at 605 nm. Untreated = untreated control cells not exposed to InPcCl.

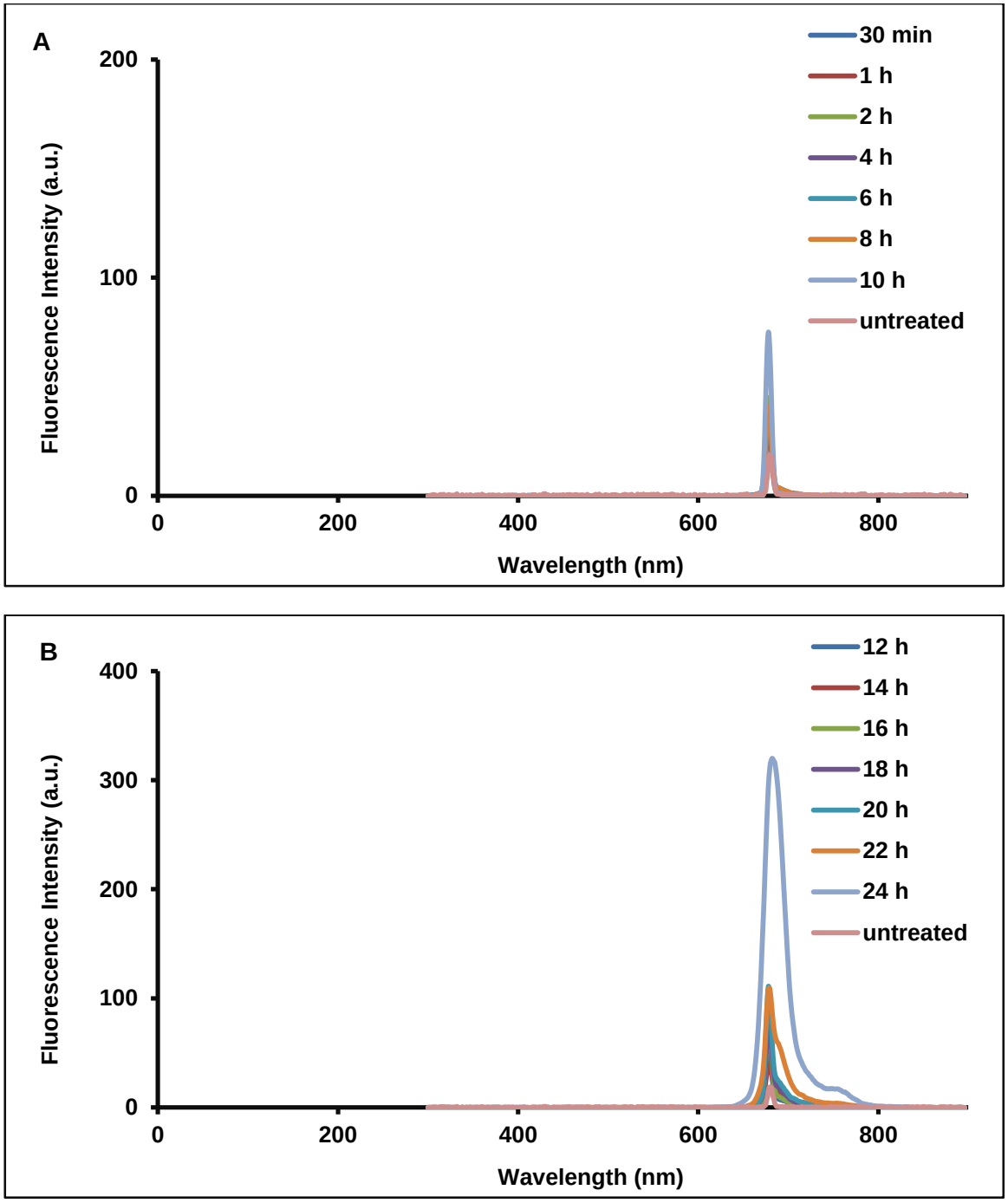

Figure 3.12 The emission peaks and fluorescence intensities (a.u.) of extracted intracellular FePcCl (100 µg/ml) from MCF-7 cancer cells over (A) 30 min to 10 h and (B) 12 h to 24 h incubation periods measured using a fluorescence spectrophotometer with an excitation wavelength set at 680 nm. Untreated = untreated control cells not exposed to FePcCl.

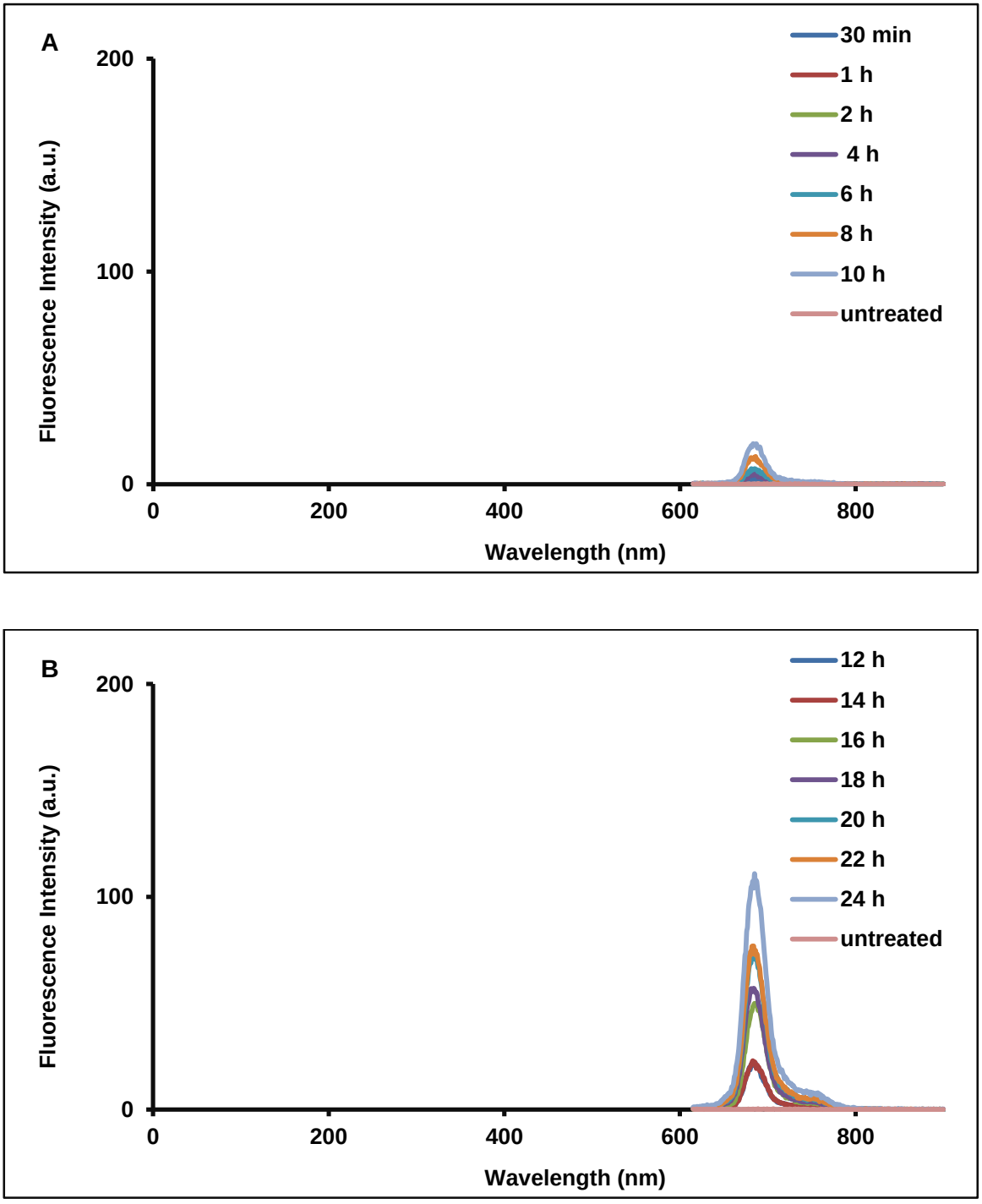

Figure 3.13 The emission peaks and fluorescence intensities (a.u.) of extracted intracellular GaPcCl (100 µg/ml) from melanoma cancer cells over (A) 30 min to 10 h and (B) 12 h to 24 h incubation periods measured using a fluorescence spectrophotometer with an excitation wavelength set at 600 nm. Untreated = untreated control cells not exposed to GaPcCl.

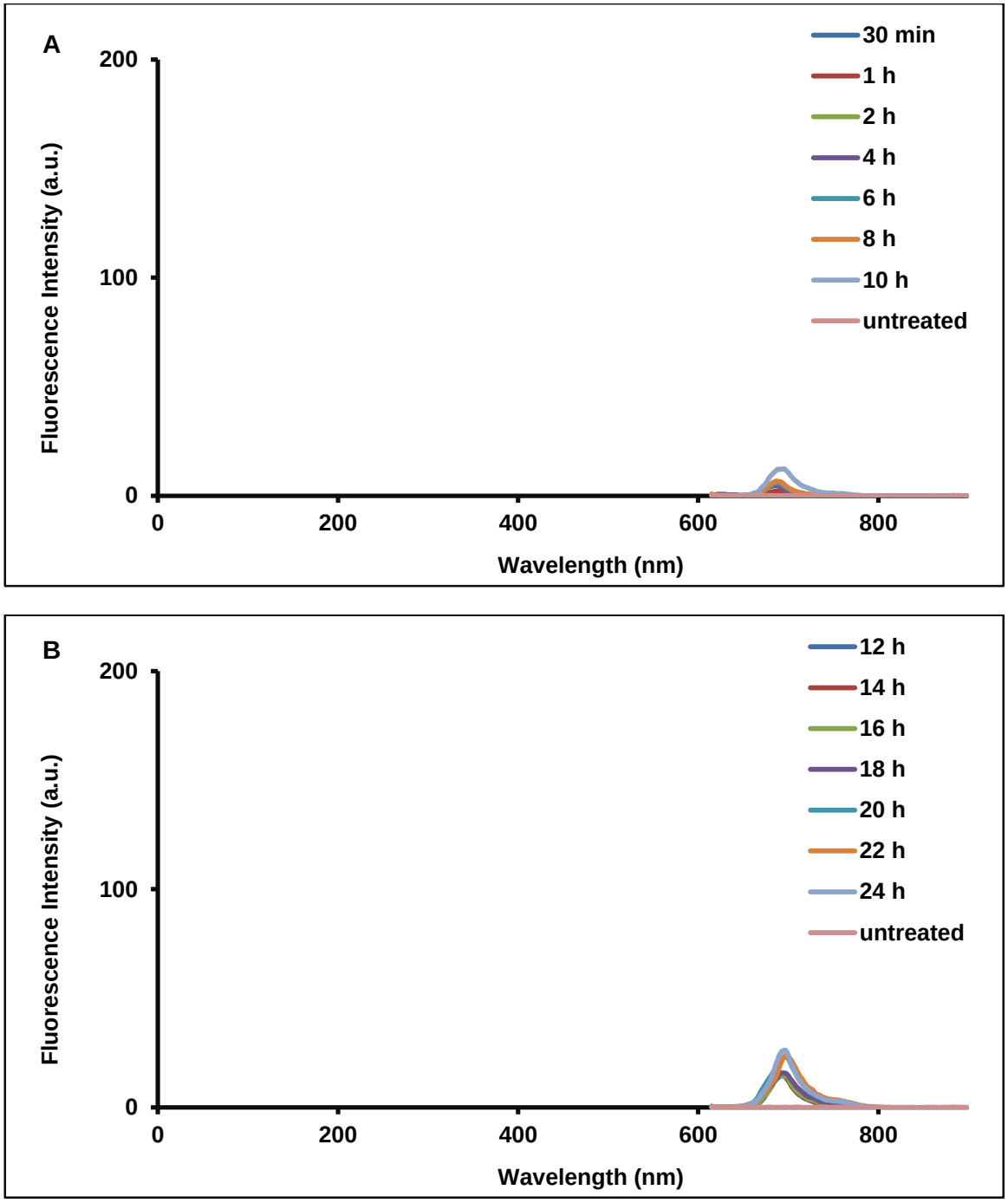

Figure 3.14 The emission peaks and fluorescence intensities (a.u.) of extracted intracellular InPcCl (100 µg/ml) from melanoma cancer cells over (A) 30 min to 10 h and (B) 12 h to 24 h incubation periods measured using a fluorescence spectrophotometer with an excitation wavelength set at 605 nm. Untreated = untreated control cells not exposed to InPcCl.

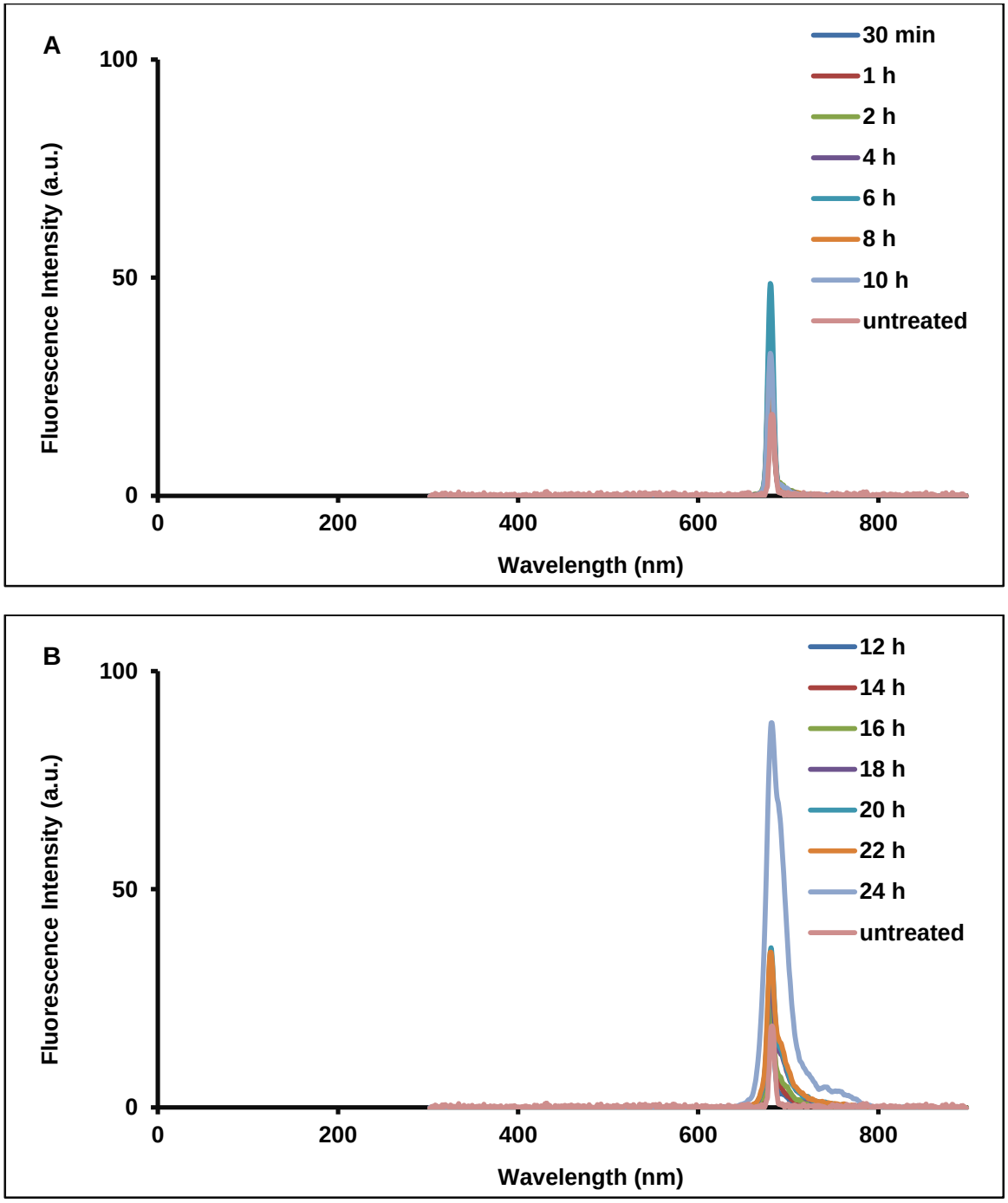

Figure 3.15 The emission peaks and fluorescence intensities (a.u.) of extracted intracellular FePcCl (100 µg/ml) from melanoma cancer cells over (A) 30 min to 10 h and (B) 12 h to 24 h incubation periods measured using a fluorescence spectrophotometer with an excitation wavelength set at 680 nm. Untreated = untreated control cells not exposed to FePcCl.

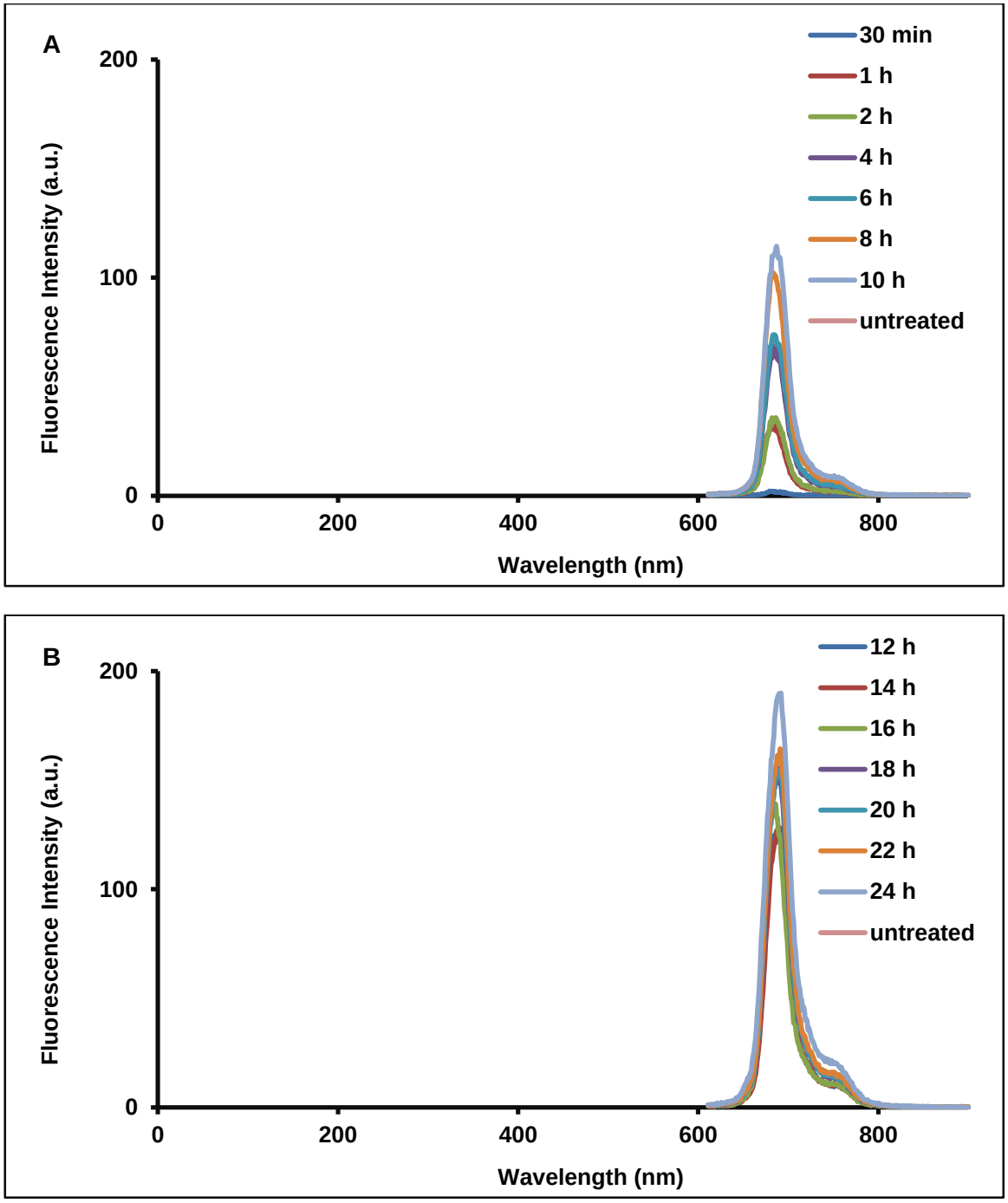

Figure 3.16 The emission peaks and fluorescence intensities (a.u.) of extracted intracellular GaPcCl (100 µg/ml) from A549 cancer cells over (A) 30 min to 10 h and (B) 12 h to 24 h incubation periods measured using a fluorescence spectrophotometer with an excitation wavelength set at 600 nm. Untreated = untreated control cells not exposed to GaPcCl.

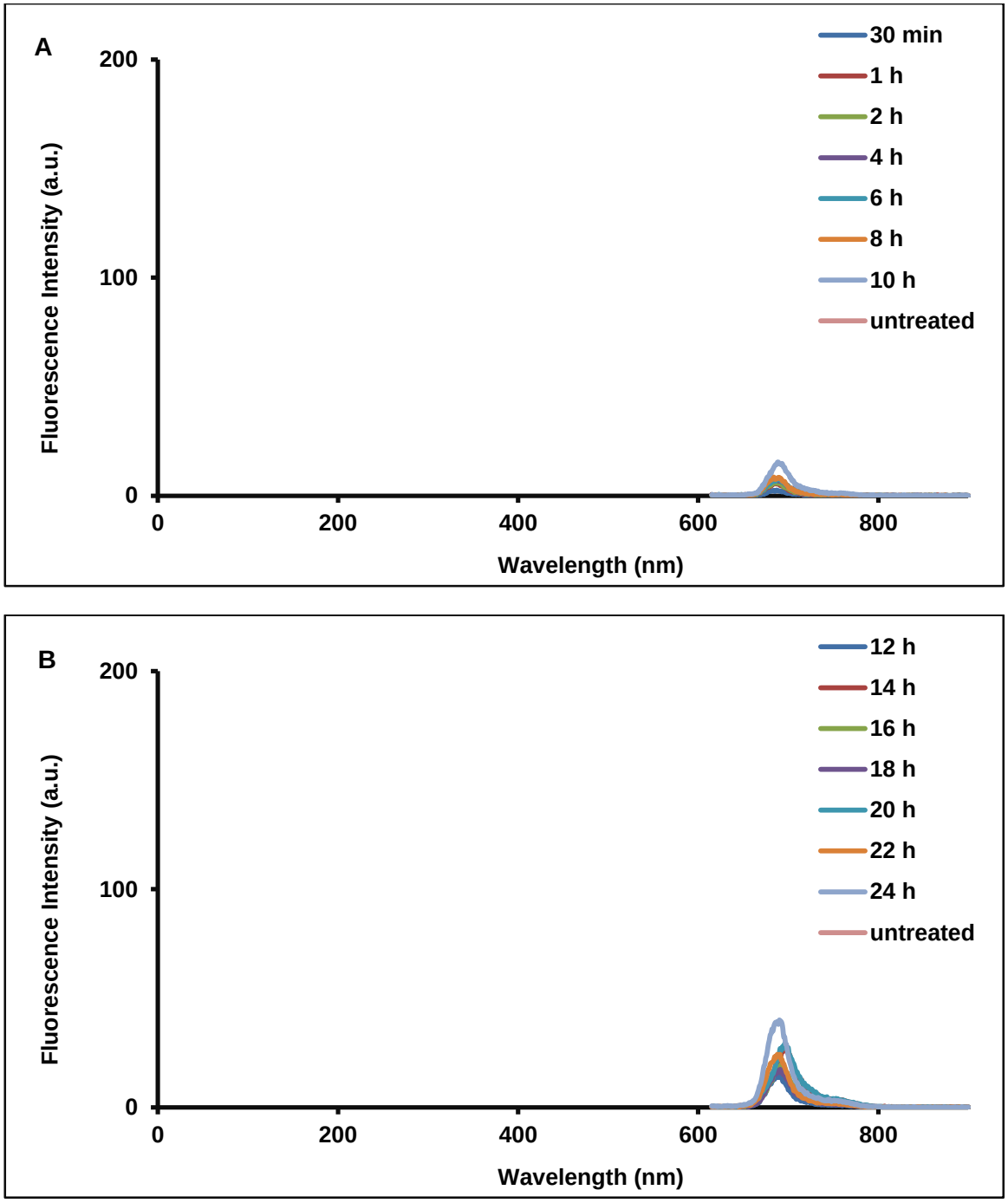

Figure 3.17 The emission peaks and fluorescence intensities (a.u.) of extracted intracellular InPcCl (100 µg/ml) from A549 cancer cells over (A) 30 min to 10 h and (B) 12 h to 24 h incubation periods measured using a fluorescence spectrophotometer with an excitation wavelength set at 605 nm. Untreated = untreated control cells not exposed to InPcCl.

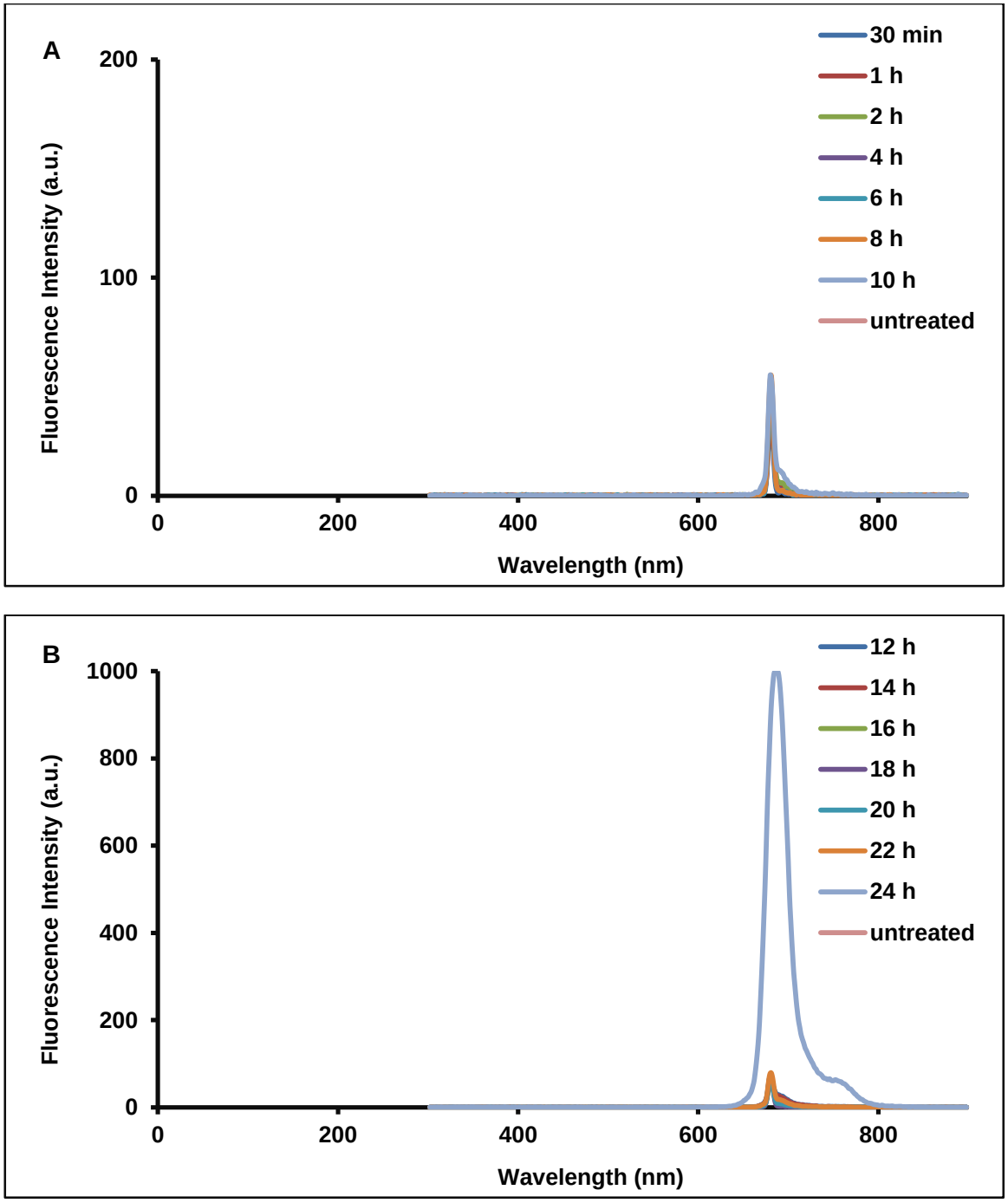

Figure 3.18 The emission peaks and fluorescence intensities (a.u.) of extracted intracellular FePcCl (100 µg/ml) from A549 cancer cells over (A) 30 min to 10 h and (B) 12 h to 24 h incubation periods measured using a fluorescence spectrophotometer with an excitation wavelength set at 680 nm. Untreated = untreated control cells not exposed to FePcCl.

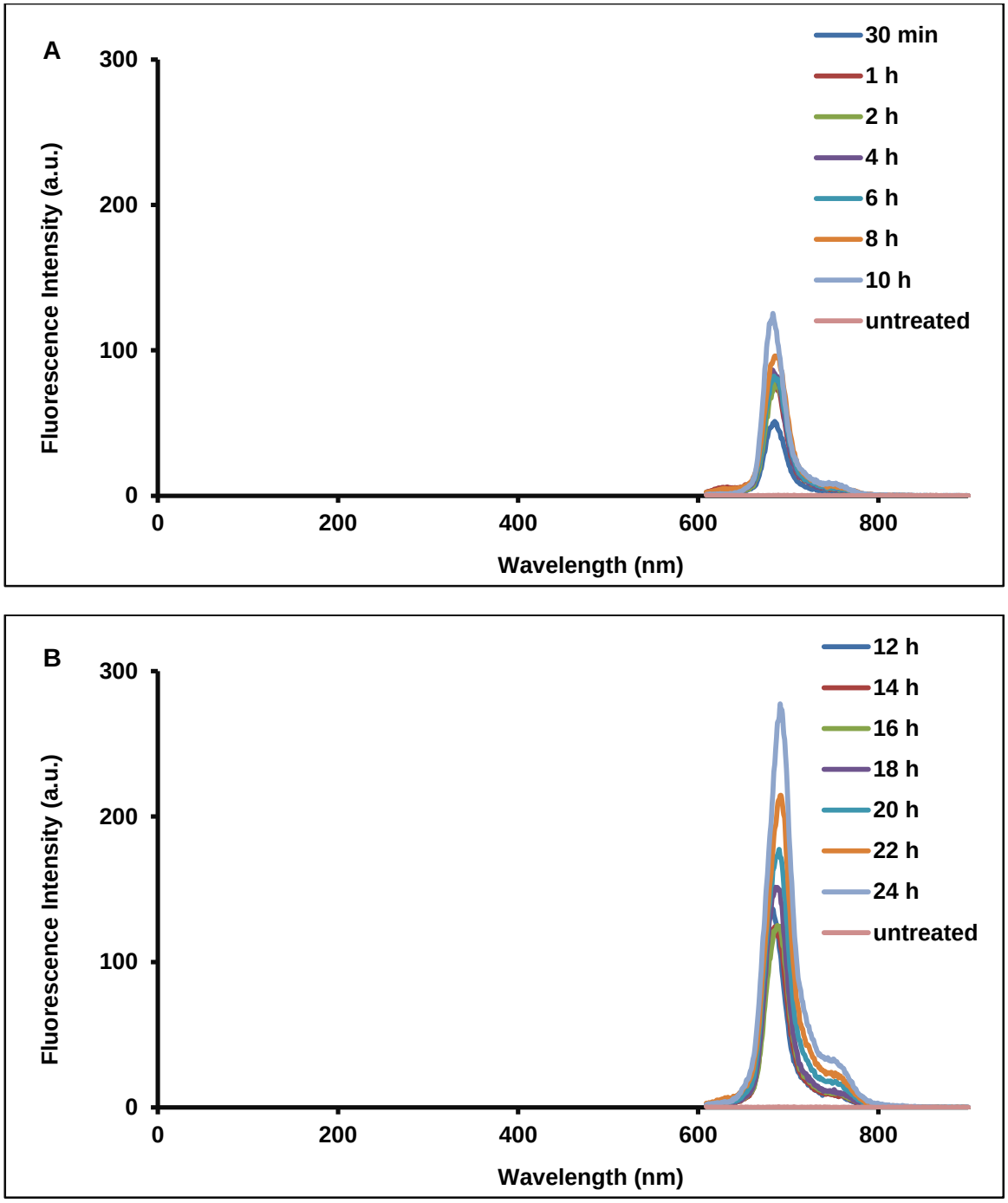

Figure 3.19 The emission peaks and fluorescence intensities (a.u.) of extracted intracellular GaPcCl (100 µg/ml) from fibroblast cells (healthy normal cells) over (A) 30 min to 10 h and (B) 12 h to 24 h incubation periods measured using a fluorescence spectrophotometer with an excitation wavelength set at 600 nm. Untreated = untreated control cells not exposed to GaPcCl.

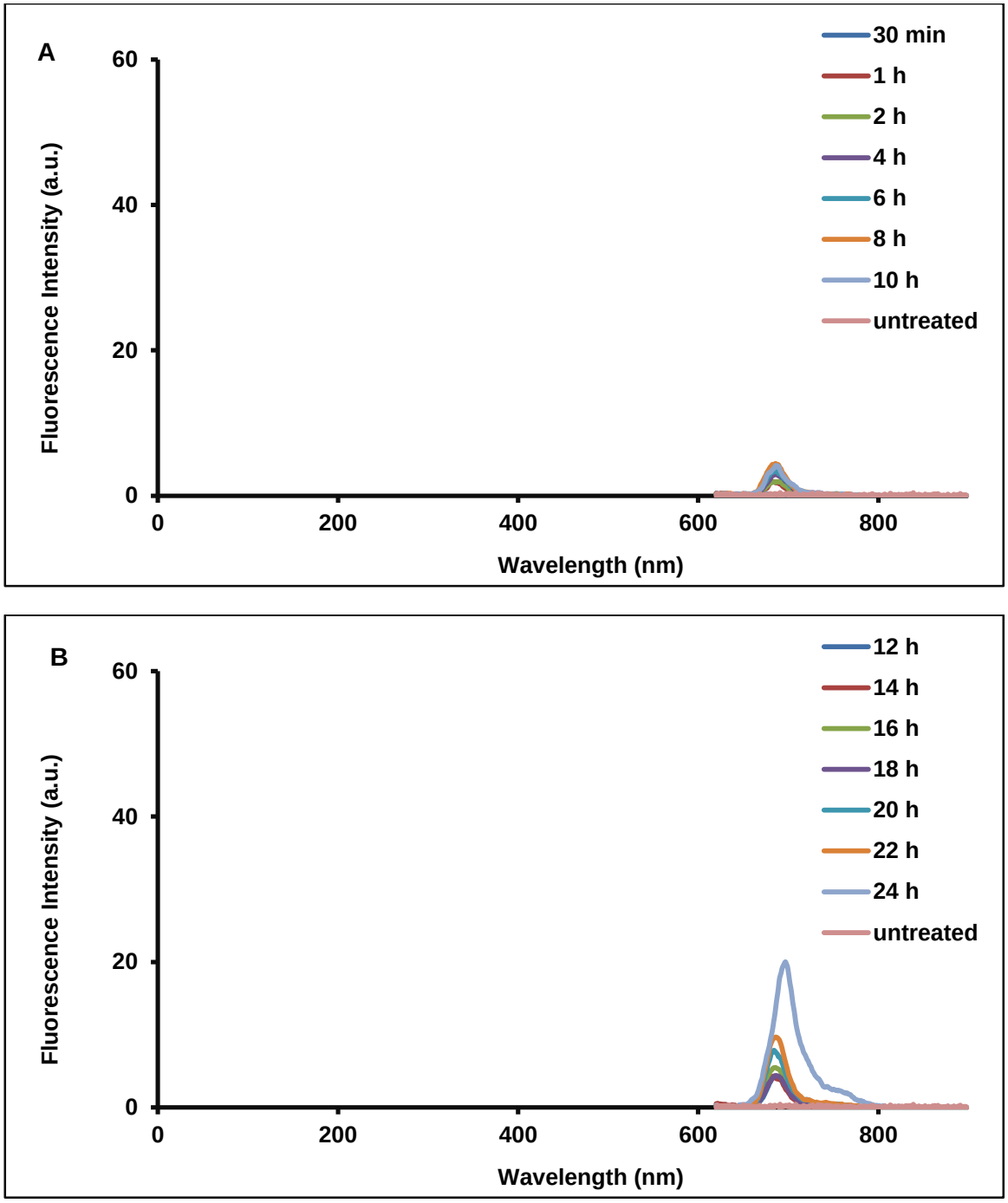

Figure 3.20 The emission peaks and fluorescence intensities (a.u.) of extracted intracellular InPcCl (100 µg/ml) from fibroblast cells (healthy normal cells) over (A) 30 min to 10 h and (B) 12 h to 24 h incubation periods measured using a fluorescence spectrophotometer with an excitation wavelength set at 605 nm. Untreated = untreated control cells not exposed to InPcCl.

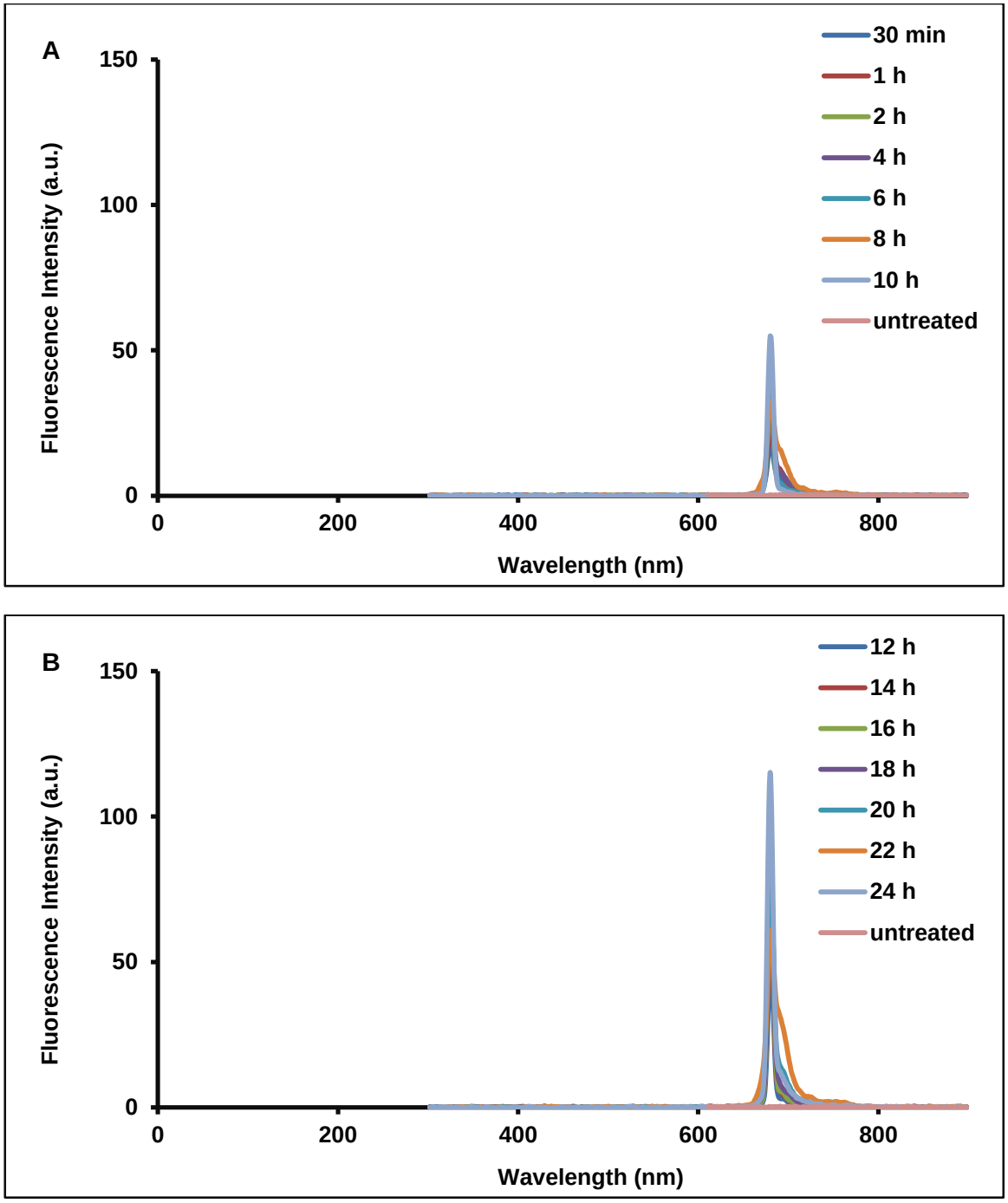

Figure 3.21 The emission peaks and fluorescence intensities (a.u.) of extracted intracellular FePcCl (100 µg/ml) from fibroblast cells (healthy normal cells) over (A) 30 min to 10 h and (B) 12 h to 24 h incubation periods measured using a fluorescence spectrophotometer with an excitation wavelength set at 680 nm. Untreated = untreated control cells not exposed to FePcCl.

3.3 DARK TOXICITY ASSAY

The cytotoxic effect of inactive GaPcCl, InPcCl and FePcCl at different photosensitizing concentrations (without laser treatment) on different cancer cell lines compared to healthy normal cell line is presented in Figure 3.22 – Figure 3.36. In all cases, a detectable decrease in the cell viability of cancer and healthy normal cells was caused by incubation of the cells in the dark with the different concentrations of each photosensitizer.

GaPcCl is toxic to Caco-2 cancer cells at all concentrations (2 µg/ml – 100 µg/ml) as showed in figure 3.22. Caco-2 cancer cells showed a fairly good survival with InPcCl at concentrations less than 20 µg/ml, whereas concentrations higher than 20 µg/ml were toxic to Caco-2 cancer cells. FePcCl toxicity was only detected from a concentration of 20 µg/ml with Caco-2 cancer cells. It is significantly evident that GaPcCl (Figure 3.25), InPcCl (Figure 3.26) and FePcCl (Figure 3.27) in its inactive state at low and high photosensitizing concentrations are highly cytotoxic to MCF-7 cancer cells.

Negligible cytotoxicity was detected with lower concentrations of inactive GaPcCl, InPcCl and FePcCl with melanoma cancer cells. GaPcCl, InPcCl and FePcCl were highly toxic to melanoma cancer cells reducing cell viability to 50% or below at concentrations from 40 µg/ml, 100 µg/ml and 60 µg/ml respectively (Figures 4.28 – 4.30). A significant decrease in the cell viability of A549 cancer cells are seen with GaPcCl, InPcCl and FePcCl at 20 µg/ml, 6 µg/ml and 8 µg/ml respectively (Figures 4.31 – 4.33). In the case of fibroblast cells (healthy normal cells), only concentrations ranging from 8 µg/ml to 100 µg/ml induced a decrease in cell viability (Figures 4.34 – 3.6).

100 µg/ml of GaPcCl, InPcCl and FePcCl in its inactive state decreased cell viability of healthy normal cells (fibroblast cells) to 57% (Figure 3.34), 50% (Figure 3.35) and 55%

(Figure 3.36) respectively. At the same photosensitizing concentration GaPcCl, InPcCl and FePcCl (inactive state) decreased cell viability of Caco-2 cancer cells to 44% (Figure 3.22), 21% (Figure 3.23) and 41% (Figure 4.24) respectively. Similarly, inactive GaPcCl, InPcCl and FePcCl at a concentration of 100 µg/ml decreased the cell viability of melanoma cancer cells to 31% (Figure 3.28), 42% (Figure 3.29) and 21% (Figure 3.30). A549 cancer cells to 46%, 55% and 26% respectively. The data in Figure 3.31 – Figure 3.33 indicate that inactive GaPcCl, InPcCl and FePcCl at a concentration of 100 µg/ml decreased the cell viability of A549 cancer cells to 46%, 55% and 26% respectively.

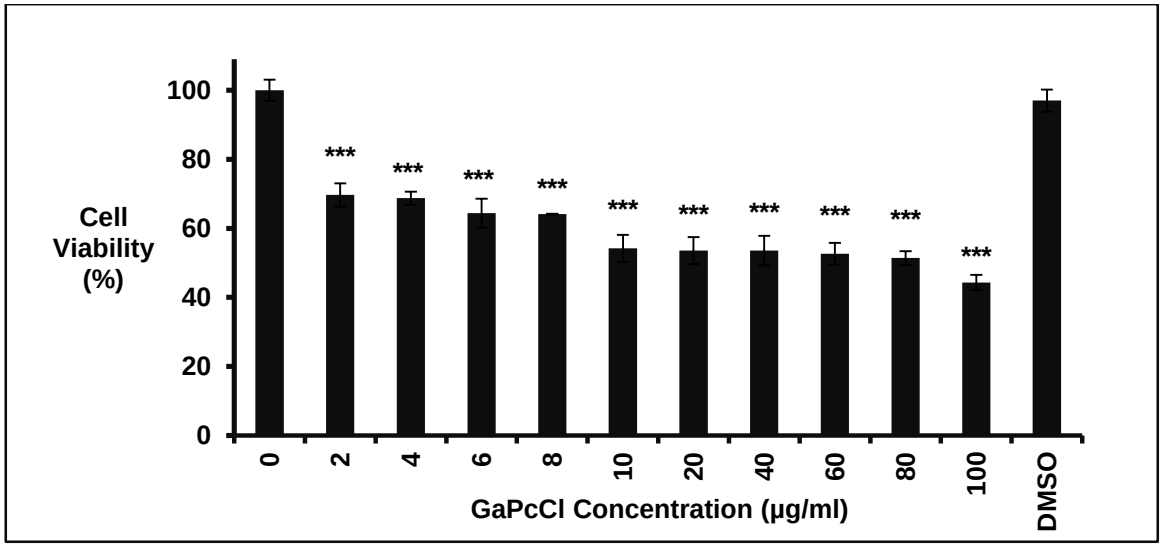

Figure 3.22 The cell viability (%) of Caco-2 cancer cells after incubation with different concentrations of GaPcCl for 2 h without laser treatment. 0 µg/ml = Caco-2 cancer cells that were not exposed to GaPcCl (untreated control cells); DMSO (control). Significant differences between the untreated cell control and each of the different treatment concentrations are represented in graph as (***) $P \leq 0.001$.

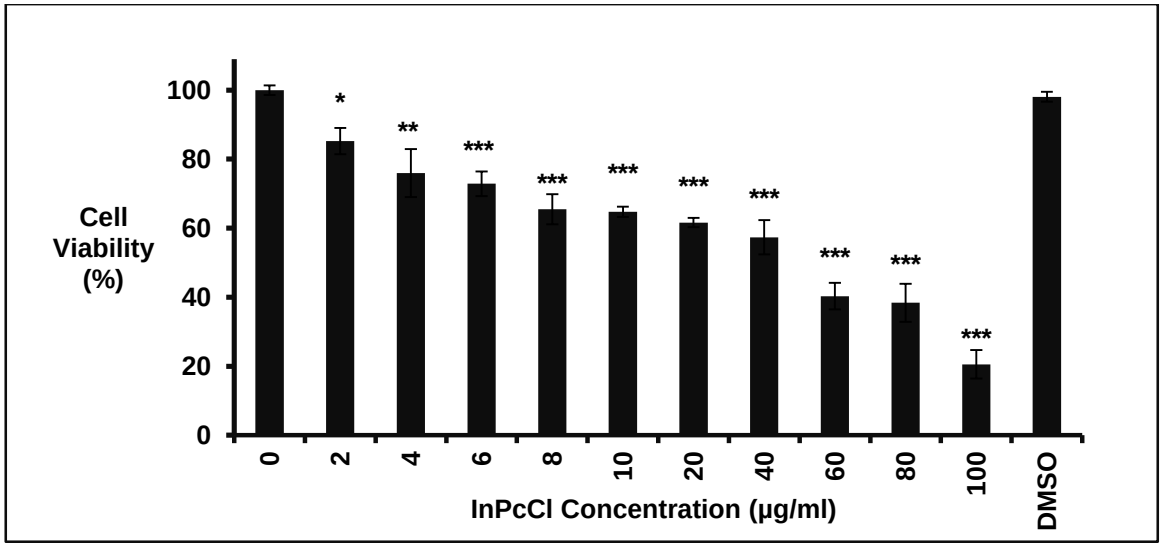

Figure 3.23 The cell viability (%) of Caco-2 cancer cells after incubation with different concentrations of InPcCl for 2 h without laser treatment. 0 µg/ml = Caco-2 cancer cells that were not exposed to InPcCl (untreated control cells); DMSO (control). Significant differences between the untreated cell control and each of the different treatment concentrations are represented in graph as (*) $P \leq 0.05$, (**) $P \leq 0.01$ and (***) $P \leq 0.001$.

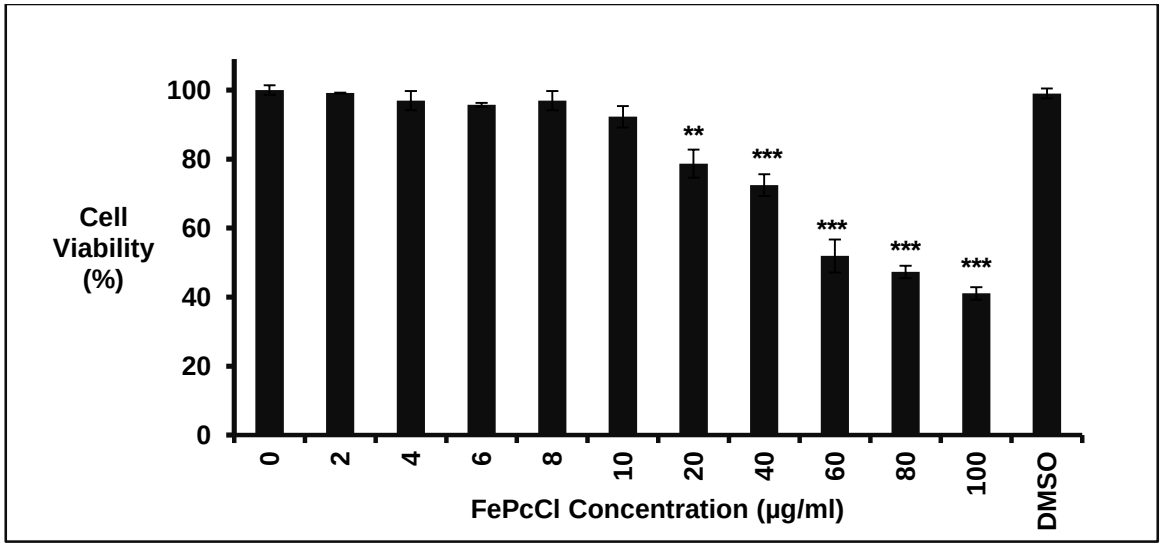

Figure 3.24 The cell viability (%) of Caco-2 cancer cells after incubation with different concentrations of FePcCl for 2 h without laser treatment. 0 µg/ml = Caco-2 cancer cells that were not exposed to FePcCl (untreated control cells); DMSO (control). Significant differences between the untreated cell control and each of the different treatment concentrations are represented in graph as (**) $P \leq 0.01$ and (***) $P \leq 0.001$.

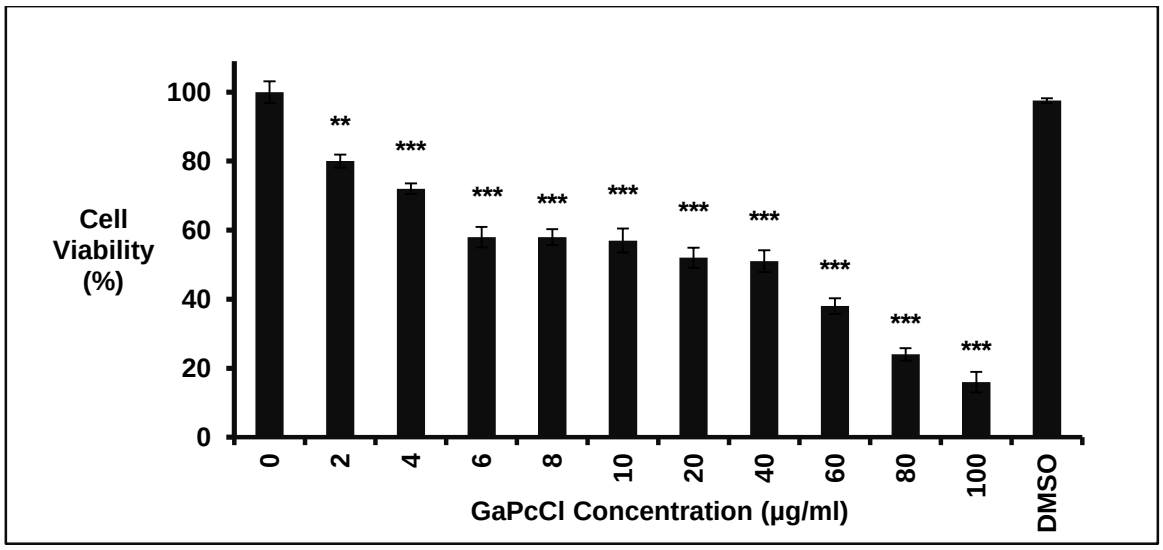

Figure 3.25 The cell viability (%) of MCF-7 cancer cells after incubation with different concentrations of GaPcCl for 2 h without laser treatment. 0 µg/ml = MCF-7 cancer cells that were not exposed to GaPcCl (untreated control cells); DMSO (control). Significant differences between the untreated cell control and each of the different treatment concentrations are represented in graph as (**) $P \leq 0.01$ and (***) $P \leq 0.001$.

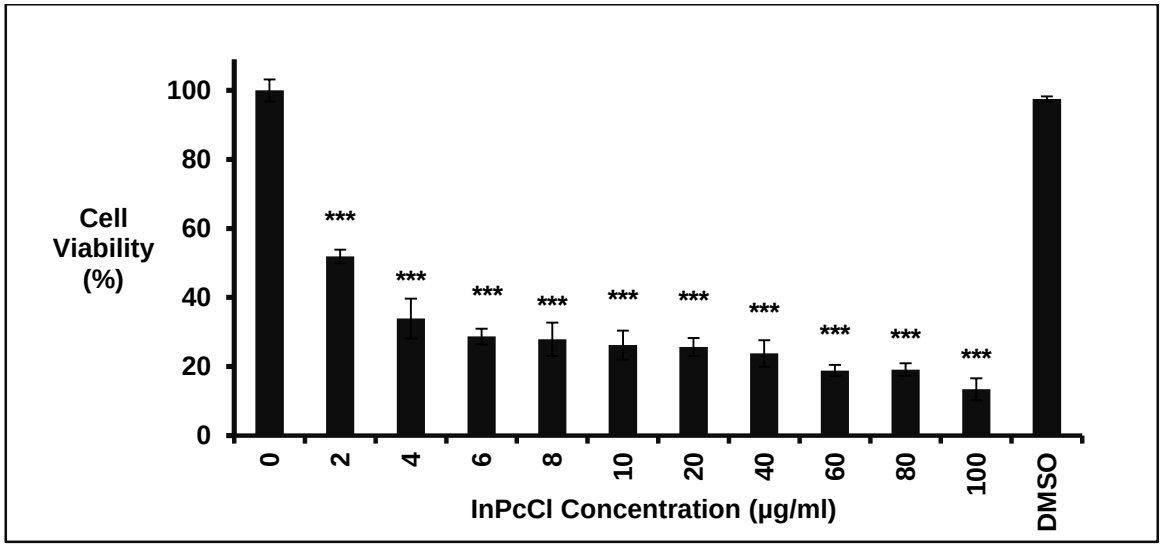

Figure 3.26 The cell viability (%) of MCF-7 cancer cells after incubation with different concentrations of InPcCl for 2 h without laser treatment. 0 µg/ml = MCF-7 cancer cells that were not exposed to InPcCl (untreated control cells); DMSO (control). Significant differences between the untreated cell control and each of the different treatment concentrations are represented in graph as (***) $P \leq 0.001$.

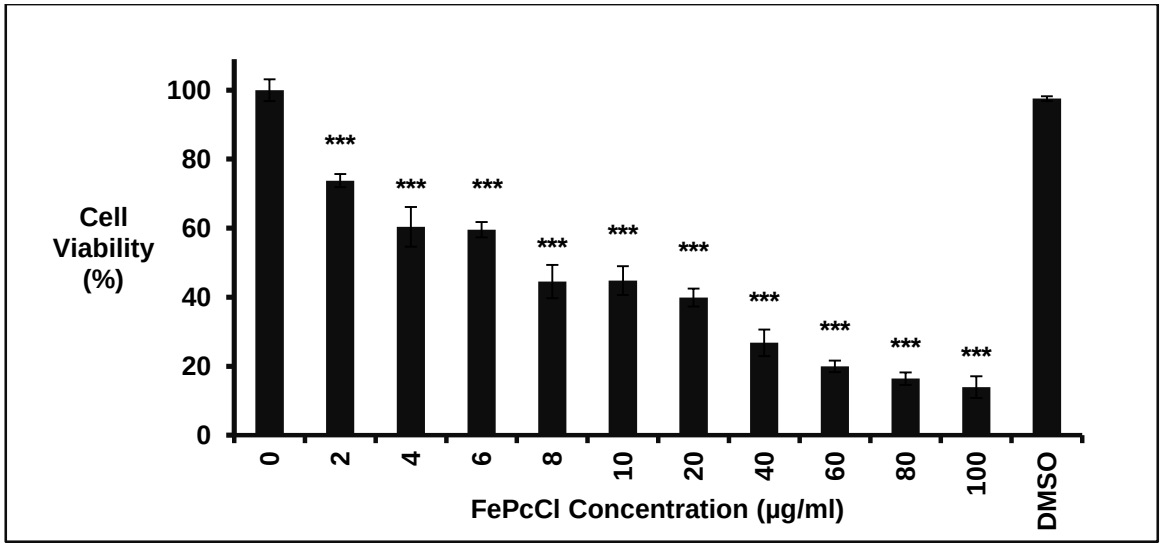

Figure 3.27 The cell viability (%) of MCF-7 cancer cells after incubation with different concentrations of FePcCl for 2 h without laser treatment. 0 µg/ml = MCF-7 cancer cells that were not exposed to FePcCl (untreated control cells); DMSO (control). Significant differences between the untreated cell control and each of the different treatment concentrations are represented in graph as (***) P ≤ 0.001.

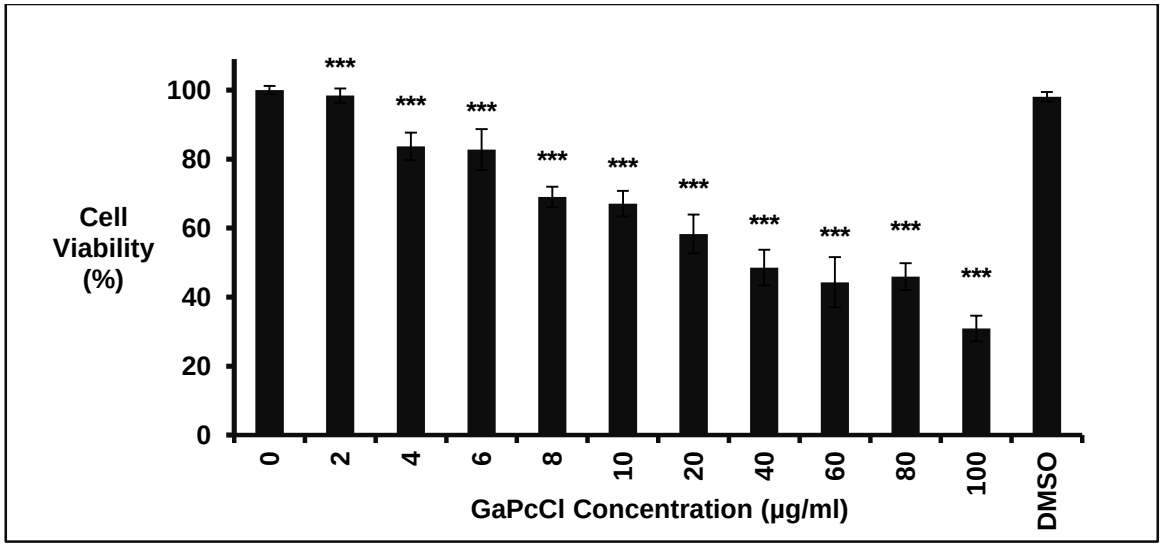

Figure 3.28 The cell viability (%) of melanoma cancer cells after incubation with different concentrations of GaPcCl for 2 h without laser treatment. 0 µg/ml = melanoma cancer cells that were not exposed to GaPcCl (untreated control cells); DMSO (control). Significant differences between the untreated cell control and each of the different treatment concentrations are represented in graph as (***) P ≤ 0.001.

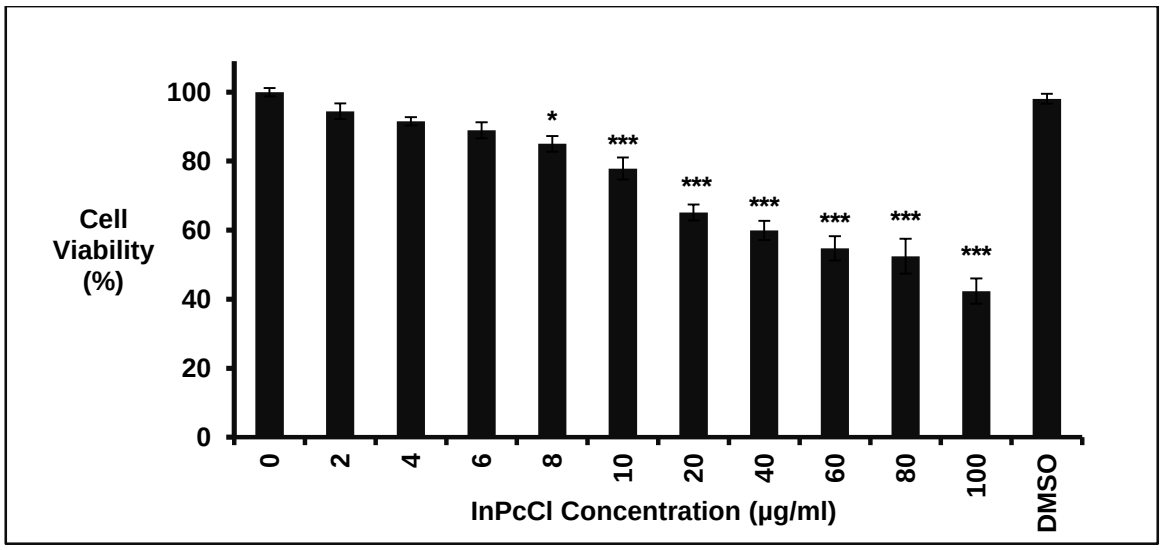

Figure 3.29 The cell viability (%) of melanoma cancer cells after incubation with different concentrations of InPcCl for 2 h without laser treatment. 0 µg/ml = melanoma cancer cells that were not exposed to InPcCl (untreated control cells); DMSO (control). Significant differences between the untreated cell control and each of the different treatment concentrations are represented in graph as (*) $P \leq 0.05$ and (***) $P \leq 0.001$.

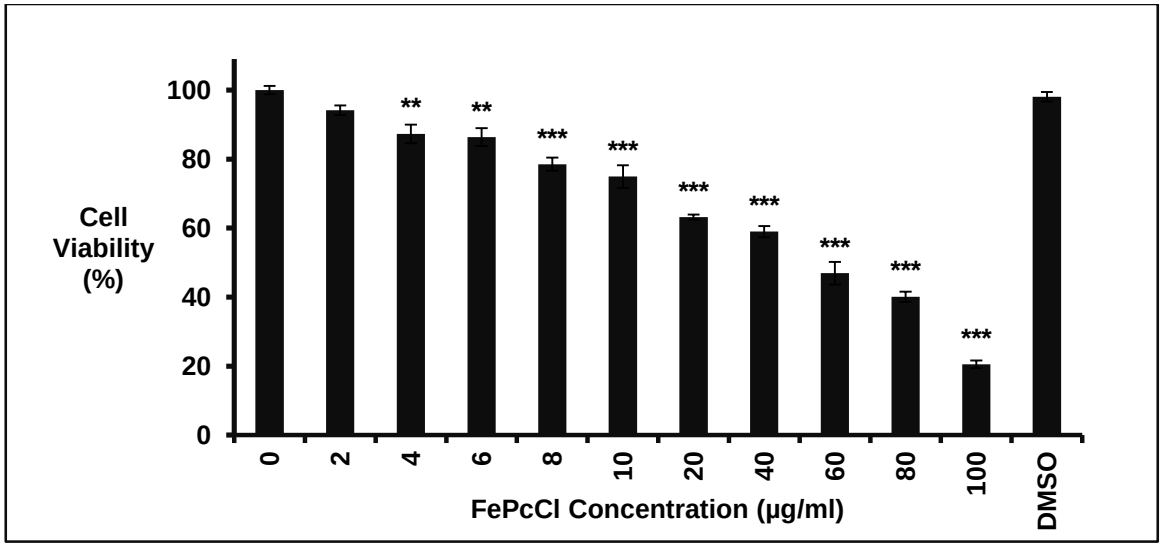

Figure 3.30 The cell viability (%) of melanoma cancer cells after incubation with different concentrations of FePcCl for 2 h without laser treatment. 0 µg/ml = melanoma cancer cells that were not exposed to FePcCl (untreated control cells); DMSO (control). Significant differences between the untreated cell control and each of the different treatment concentrations are represented in graph as (**) $P \leq 0.01$ and (***) $P \leq 0.001$.

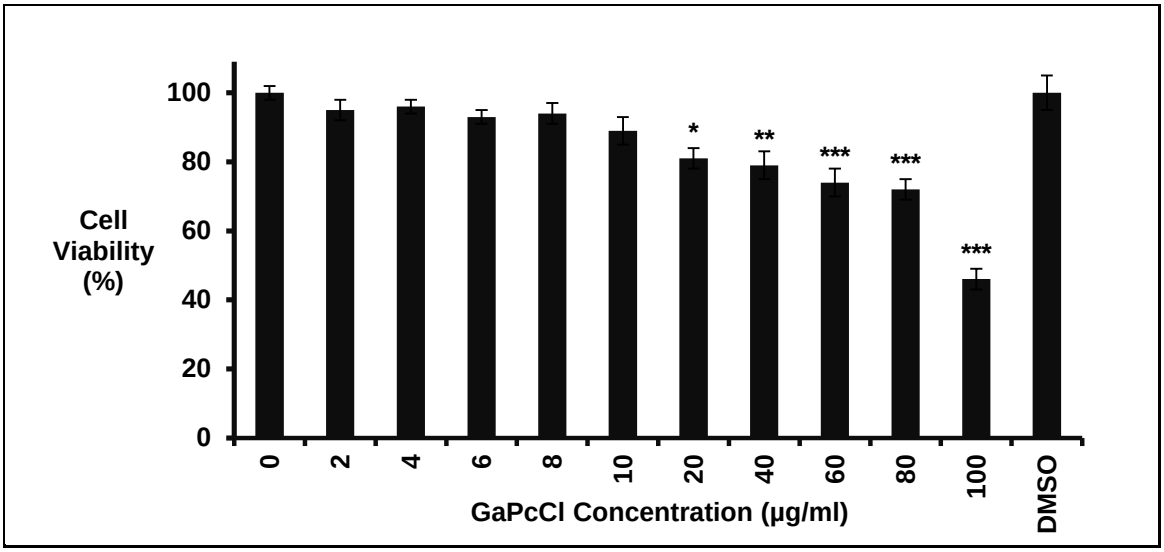

Figure 3.31 The cell viability (%) of A549 cancer cells after incubation with different concentrations of GaPcCl for 2 h without laser treatment. 0 µg/ml = A549 cancer cells that were not exposed to GaPcCl (untreated control cells); DMSO (control). Significant differences between the untreated cell control and each of the different treatment concentrations are represented in graph as (*) $P \leq 0.05$, (**) $P \leq 0.01$ and (***) $P \leq 0.001$.

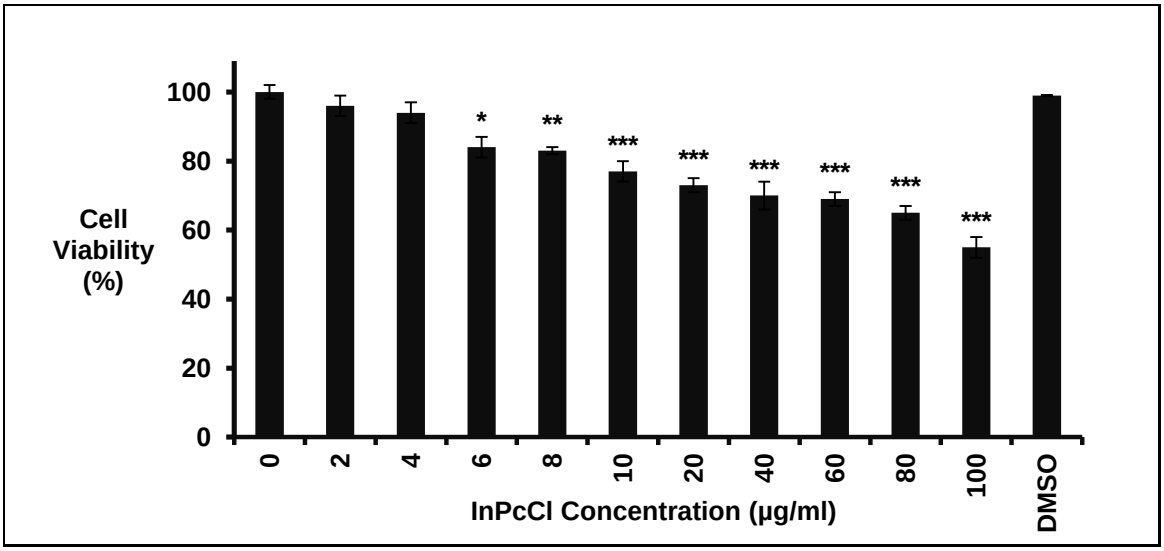

Figure 3.32 The cell viability (%) of A549 cancer cells after incubation with different concentrations of InPcCl for 2 h without laser treatment. 0 µg/ml = A549 cancer cells that were not exposed to InPcCl (untreated control cells); DMSO (control). Significant differences between the untreated cell control and each of the different treatment concentrations are represented in graph as (*) $P \leq 0.05$, (**) $P \leq 0.01$ and (***) $P \leq 0.001$.

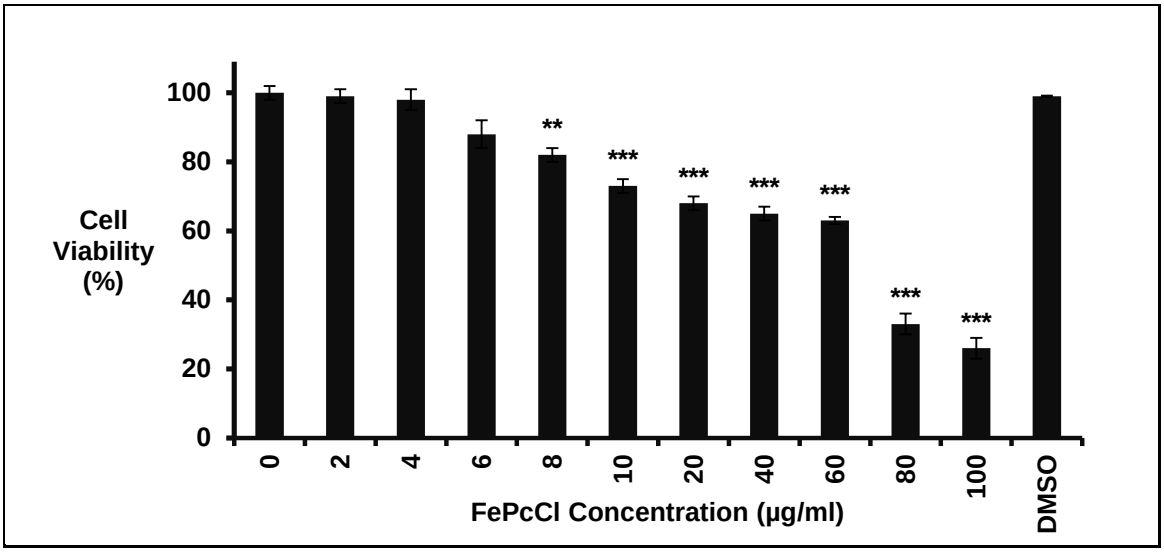

Figure 3.33 The cell viability (%) of A549 cancer cells after incubation with different concentrations of FePcCl for 2 h without laser treatment. 0 µg/ml = A549 cancer cells that were not exposed to FePcCl (untreated control cells); DMSO (control). Significant differences between the untreated cell control and each of the different treatment concentrations are represented in graph as (**) $P \leq 0.01$ and (***) $P \leq 0.001$.

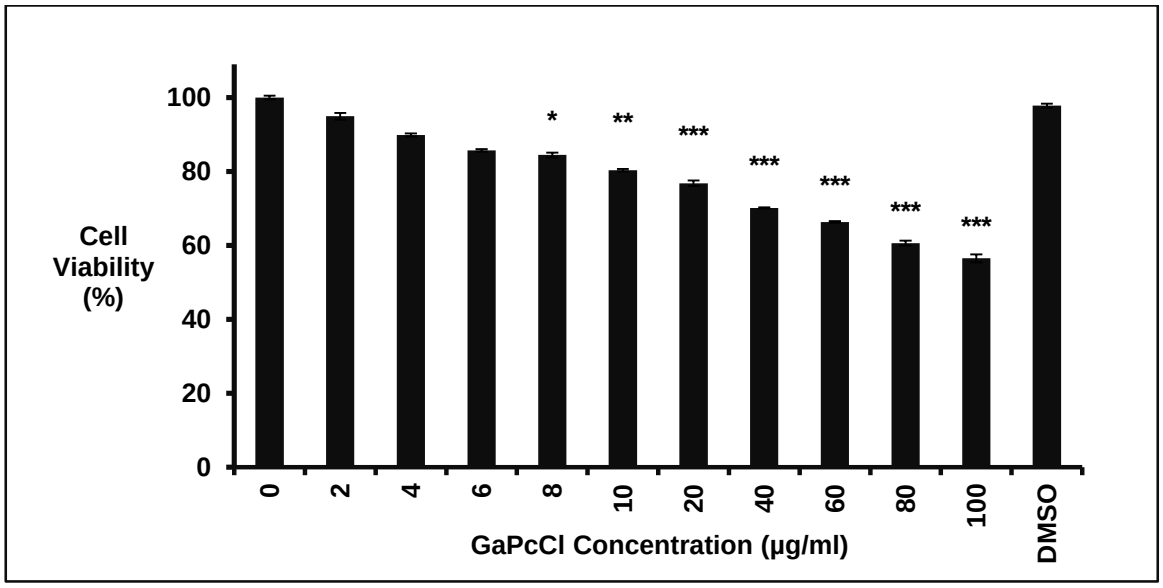

Figure 3.34 The cell viability (%) of fibroblast cells after incubation with different concentrations of GaPcCl for 2 h without laser treatment. 0 µg/ml = fibroblast cells that were not exposed to GaPcCl (untreated control cells); DMSO (control). Significant differences between the untreated cell control and each of the different treatment concentrations are represented in graph as (*) $P \leq 0.05$, (**) $P \leq 0.01$ and (***) $P \leq 0.001$.

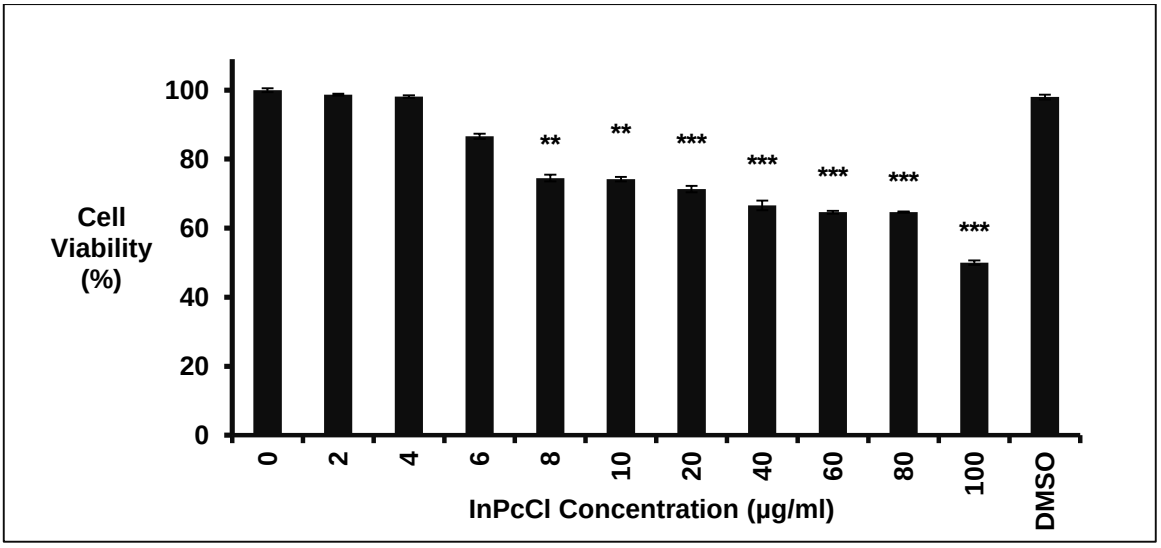

Figure 3.35 The cell viability (%) of fibroblast cells after incubation with different concentrations of InPcCl for 2 h without laser treatment. 0 µg/ml = fibroblast cells that were not exposed to InPcCl (untreated control cells); DMSO (control). Significant differences between the untreated cell control and each of the different treatment concentrations are represented in graph as (**) $P \leq 0.01$ and (***) $P \leq 0.001$.

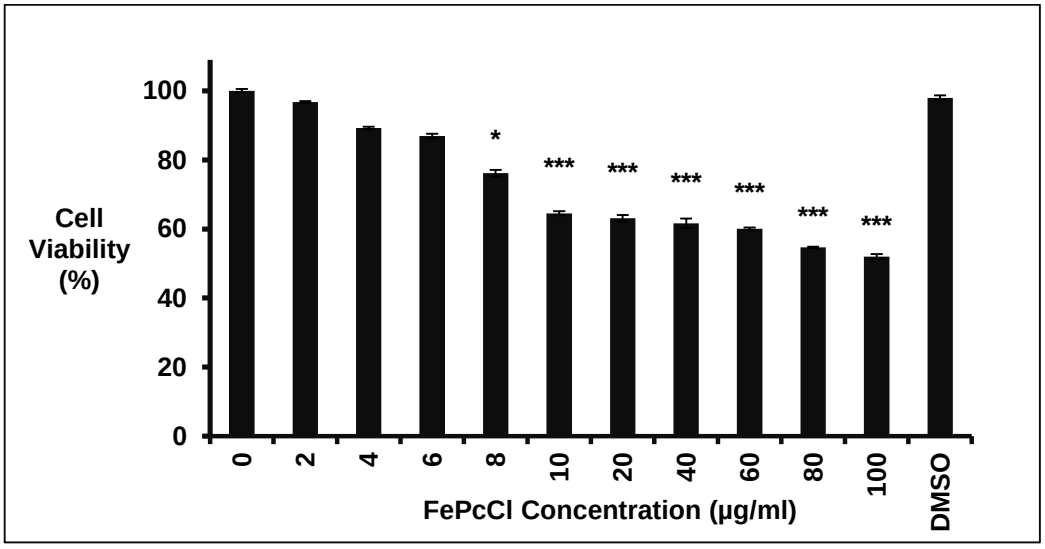

Figure 3.36 The cell viability (%) of fibroblast cells after incubation with different concentrations of FePcCl for 2 h without laser treatment. 0 µg/ml = fibroblast cells that were not exposed to FePcCl (untreated control cells); DMSO (control). Significant differences between the untreated cell control and each of the different treatment concentrations are represented in graph as (*) $P \leq 0.05$, (**) $P \leq 0.01$ and (***) $P \leq 0.001$.

Results also show that FePcCl was not toxic to Caco-2 cancer cells at concentrations lower than 20 µg/ml. Both GaPcCl and FePcCl are toxic to MCF-7 cancer cells with InPcCl being highly toxic at all concentrations. Melanoma cancer cells only displayed relative good cell survival with all PSs, especially FePcCl, where cell viability dropped to below 50% only with concentrations higher than 60 µg/ml. A549 cancer cells showed the least toxicity to all three PSs, with concentrations of 80 µg/ml - 100 µg/ml causing cell death of more than 50% of the cell population. Healthy normal cells (fibroblasts) showed good survival rates with GaPcCl, InPcCl and FePcCl at concentrations less than 8 µg/ml.

3.4 *IN VITRO* PDT

The cell viability of GaPcCl, InPcCl or FePcCl photosensitized cancer cells after laser treatment was significantly reduced when compared to the untreated controls. Cells (in the absence of PSs) exposed to the laser and cells treated with DMSO only are compared to untreated cells to rule out the possibility that the laser or DMSO is responsible for the destruction of the cells.

Caco-2 cancer cells photosensitized with different concentrations of GaPcCl, InPcCl or FePcCl showed a significant decrease in the cell viability when irradiated for 22 sec (2.5 J/cm^2), 39 sec (4.5 J/cm^2) and 74 sec (8.5 J/cm^2) as shown in Figure 3.37 – Figure 3.39. At a GaPcCl concentration of 2 µg/ml cell viability was decreased to 60%, 70% and 65%; 24 h after laser for treatment for 22 sec, 39 sec and 74 sec respectively (Figure 3.37). In comparison to a higher treatment concentration of 100 µg/ml cell viability was further decreased to 41%, 40% and 27%; 24 h after light treatment for 22 sec, 39 sec and 74 sec respectively (Figure 3.37). Also, the decrease in cell viability of Caco-2 cells to 50% and lower are actually due to PDT treatment with GaPcCl concentrations ranging from 4 µg/ml to 100 µg/ml in combination with laser exposure for 74 sec (8.5 J/cm^2), not due to

laser exposure only. In Figure 3.38, effective PDT treatment is also indicated by lower cell viability (%) values seen with Caco-2 cells after treatment with InPcCl at different concentrations in combination with both 39 sec and 74 sec laser treatment. High concentrations such as 100 µg/ml of InPcCl with a treatment light dose of 2.5 J/cm^2, 4.5 J/cm^2 and 8.5 J/cm^2 reduced cell viability to 5%, 4% and 5% respectively. Results also showed that cell survival of Caco-2 decreased to 0% after PDT treatment with photosensitizing concentrations of FePcCl from 60 µg/ml to 100 µg/ml and 74 sec illumination (Figure 3.39).

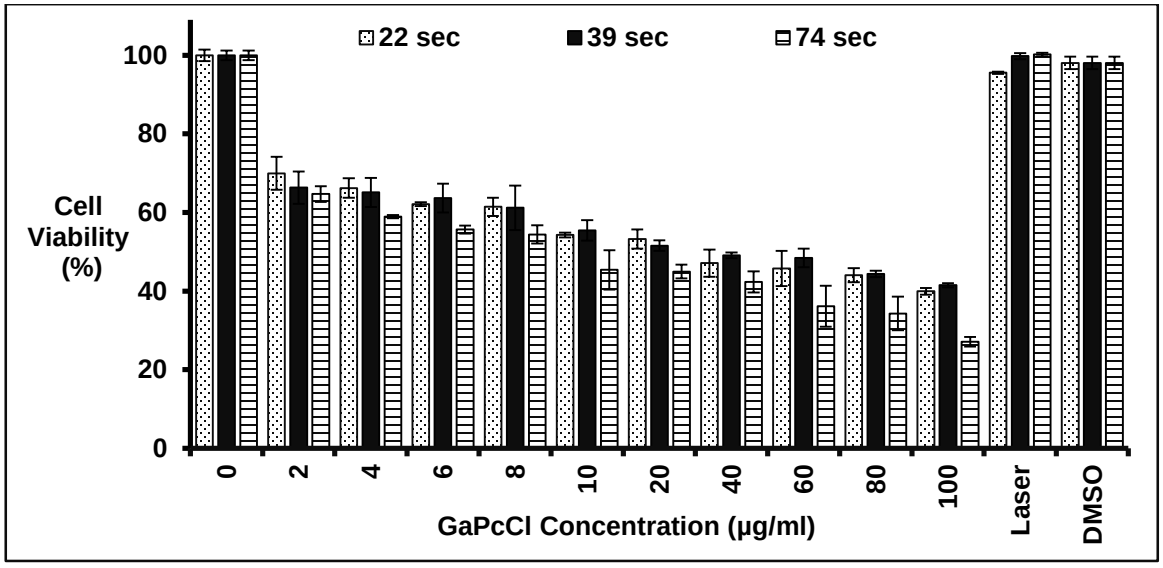

Figure 3.37 The cell viability (%) of Caco-2 cells after photosensitization with different concentrations of GaPcCl and photoirradiation (laser treatment) for 22 sec (2.5 J/cm^2), 39 sec (4.5 J/cm^2) and 74 sec (8.5 J/cm^2). 0 µg/ml = Caco-2 cells that were not exposed to GaPcCl and laser treatment (untreated control cells); Laser = Caco-2 cells that were photoirradiated without being exposed to GaPcCl (laser control); DMSO(control).

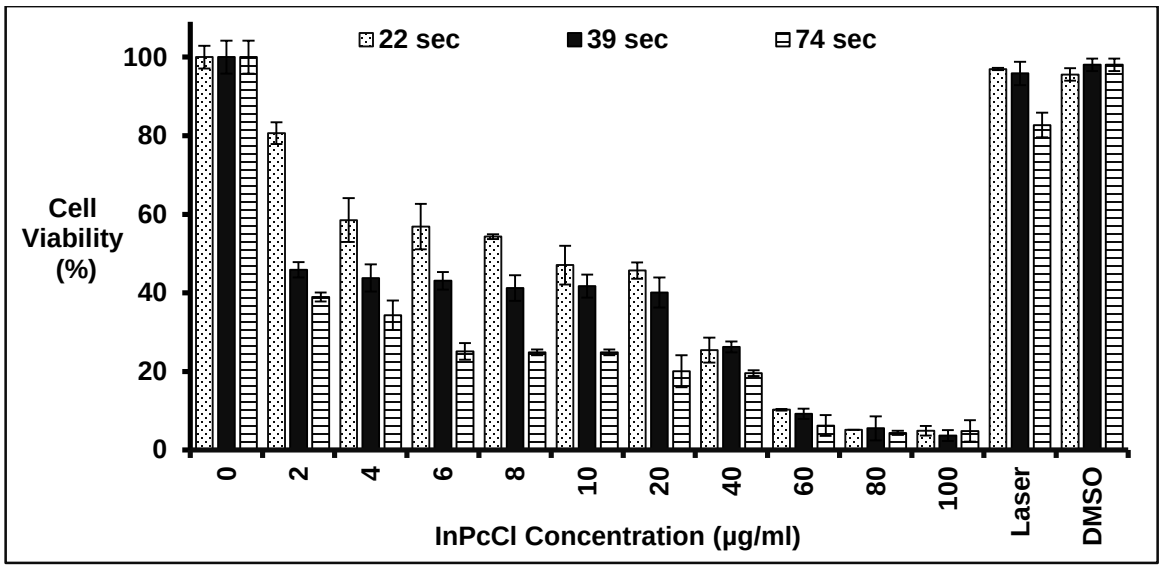

Figure 3.38 The cell viability (%) of Caco-2 cells after photosensitization with different concentrations of InPcCl and photoirradiation (laser treatment) for 22 sec (2.5 J/cm^2), 39 sec (4.5 J/cm^2) and 74 sec (8.5 J/cm^2). 0 µg/ml = Caco-2 cells that were not exposed to InPcCl and laser treatment (untreated control cells); Laser = Caco-2 cells that were photoirradiated without being exposed to InPcCl (laser control); DMSO (control).

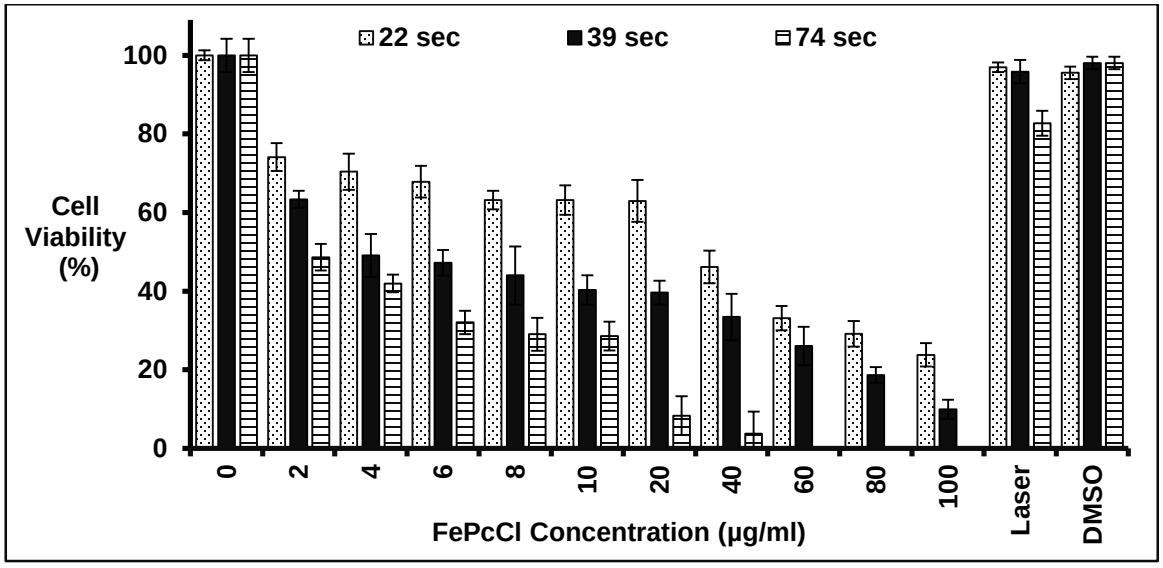

Figure 3.39 The cell viability (%) of Caco-2 cells after photosensitization with different concentrations of FePcCl and photoirradiation (laser treatment) for 22 sec (2.5 J/cm^2), 39 sec (4.5 J/cm^2) and 74 sec (8.5 J/cm^2). 0 µg/ml = Caco-2 cells that were not exposed to FePcCl and laser treatment (untreated control cells); Laser = Caco-2 cells that were photoirradiated without being exposed to FePcCl (laser control); DMSO = (control).

Figure 3.40 – Figure 3.42 show that as the photosensitizing concentration of GaPcCl, InPcCl and FePcCl increased the percentage of viable MCF-7 cells were proportionally decreasing after PDT treatment. The cell viability (%) of MCF-7 cells exposed to GaPcCl, InPcCl and FePcCl at a concentration of 2 µg/ml in combination with a treatment light dose of 2.5 J/cm^2 (22 sec) was 66%, 50% and 72% respectively. The resulting cell viability percentage for MCF-7 cells treated with 100 µg/ml of laser activated GaPcCl, InPcCl and FePcCl at a light dose of 2.5 J/cm^2 (22 sec) was 15%, 17% and 0% respectively. A 100% cell death of MCF-7 cancer cells was also detected when 20 µg/ml of FePcCl was photoactivated for 74 sec (Figure 3.42). Similarly, photoactivation for 39 sec and 74 sec of MCF-7 cancer cells photosensitized with FePcCl concentrations ranging from 40 µg/ml to 100 µg/ml resulted in 100% cell killing (Figure 3.42).

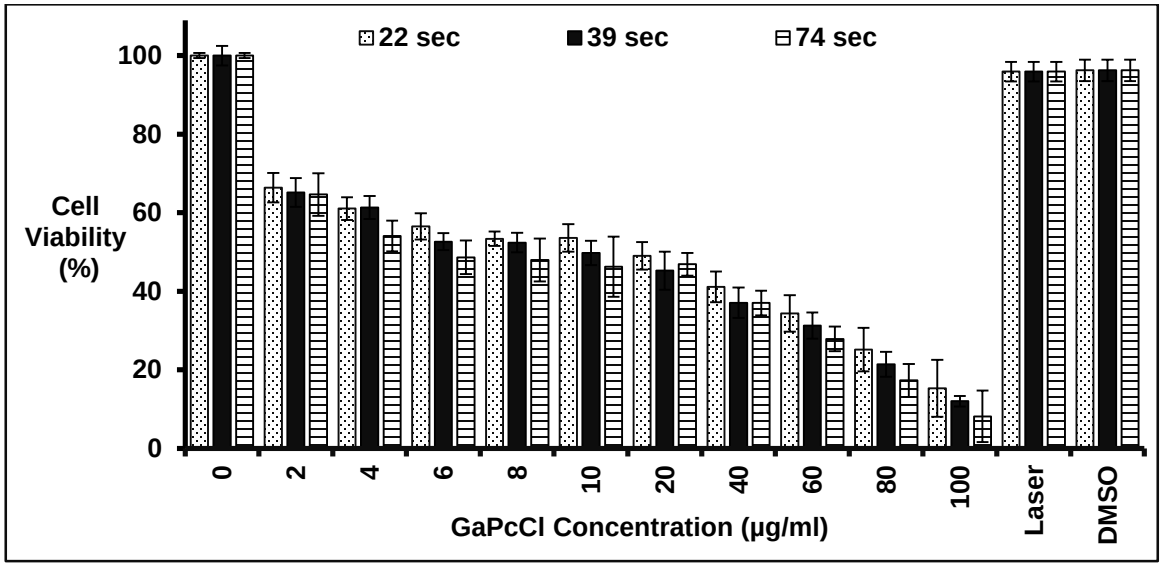

Figure 3.40 The cell viability (%) of MCF-7 cells after photosensitization with different concentrations of GaPcCl and photoirradiation (laser treatment) for 22 sec (2.5 J/cm2), 39 sec (4.5 J/cm2) and 74 sec (8.5 J/cm2). 0 µg/ml = MCF-7 cells that were not exposed to GaPcCl and laser treatment (untreated control cells); Laser = MCF-7 cells that were photoirradiated without being exposed to GaPcCl (laser control); DMSO = (control).

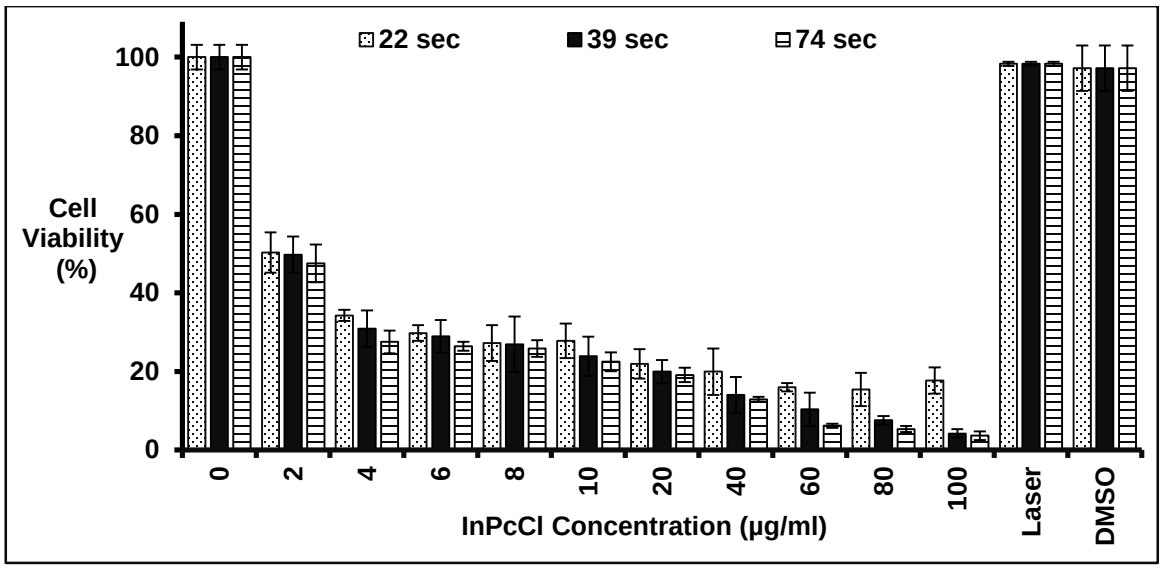

Figure 3.41 The cell viability (%) of MCF-7 cells after photosensitization with different concentrations of InPcCl and photoirradiation (laser treatment) for 22 sec (2.5 J/cm^2), 39 sec (4.5 J/cm^2) and 74 sec (8.5 J/cm^2). 0 µg/ml = MCF-7 cells that were not exposed to InPcCl and laser treatment (untreated control cells); Laser = MCF-7 cells that were photoirradiated without being exposed to InPcCl (laser control); DMSO (control).

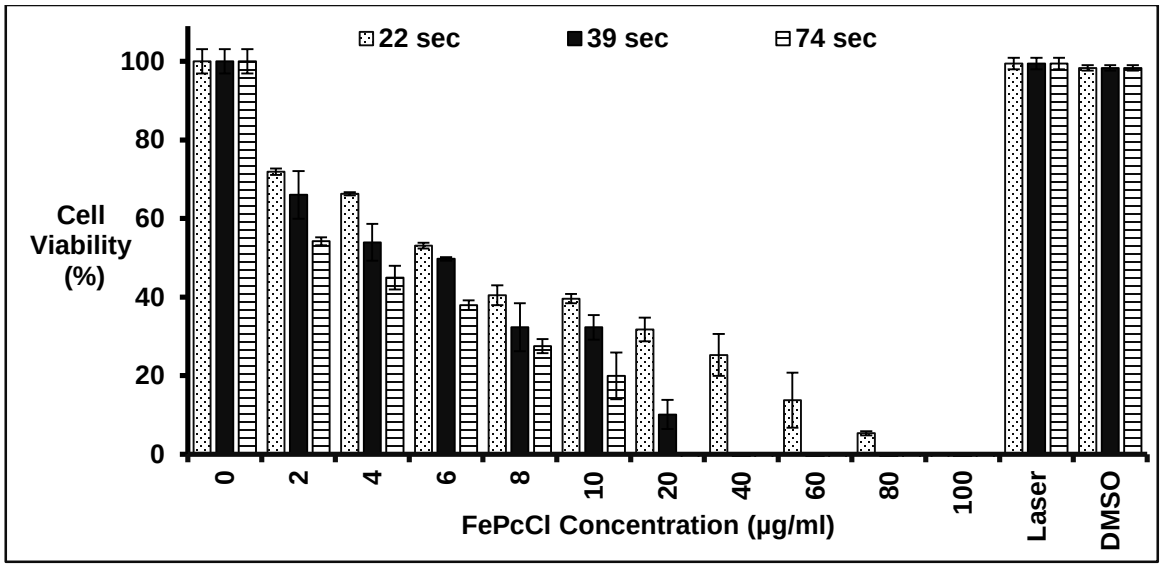

Figure 3.42 The cell viability (%) of MCF-7 cells after photosensitization with different concentrations of FePcCl and photoirradiation (laser treatment) for 22 sec (2.5 J/cm^2), 39 sec (4.5 J/cm^2) and 74 sec (8.5 J/cm^2). 0 µg/ml = MCF-7 cells that were not exposed to FePcCl and laser treatment (untreated control cells); Laser = MCF-7 cells that were photoirradiated without being exposed to FePcCl (laser control); DMSO = (control).

In Figure 3.43 – 3.45, different concentrations of GaPcCl, InPcCl and FePcCl were also observed to be potently cytotoxic towards melanoma cancer cells upon exposure to laser light doses of 2.5 J/cm^2, 4.5 J/cm^2 and 8.5 J/cm^2. Melanoma cells treated with GaPcCl (40 µg/ml), InPcCl (6 µg/ml) and FePcCl (8 µg/ml) with a treatment light dose of 2.5 J/cm^2 decreased the cell viability of the melanoma cells to 49%, 50% and 46% respectively. 40 µg/ml of GaPcCl activated with an increased light dose of 4.5 J/cm^2 and 8.5 J/cm^2 reduced melanoma cell viability to 40% and 31% respectively (Figure 3.43). InPcCl at a low concentration of 6 µg/ml activated with an increased light dose of 4.5 J/cm^2 and 8.5 J/cm^2 reduced melanoma cell viability to 42% and 24% respectively (Figure 3.44). Figure 3.45 shows that 8 µg/ml of FePcCl activated with a light dose of 4.5 J/cm^2 and 8.5 J/cm^2 reduced melanoma cell viability to 43% and 40% respectively. 100 µg/ml of GaPcCl, InPcCl and FePcCl in combination with a light dose of 8.5 J/cm^2 reduced cell viability of melanoma cancer cells to 16%, 10% and 15% respectively.

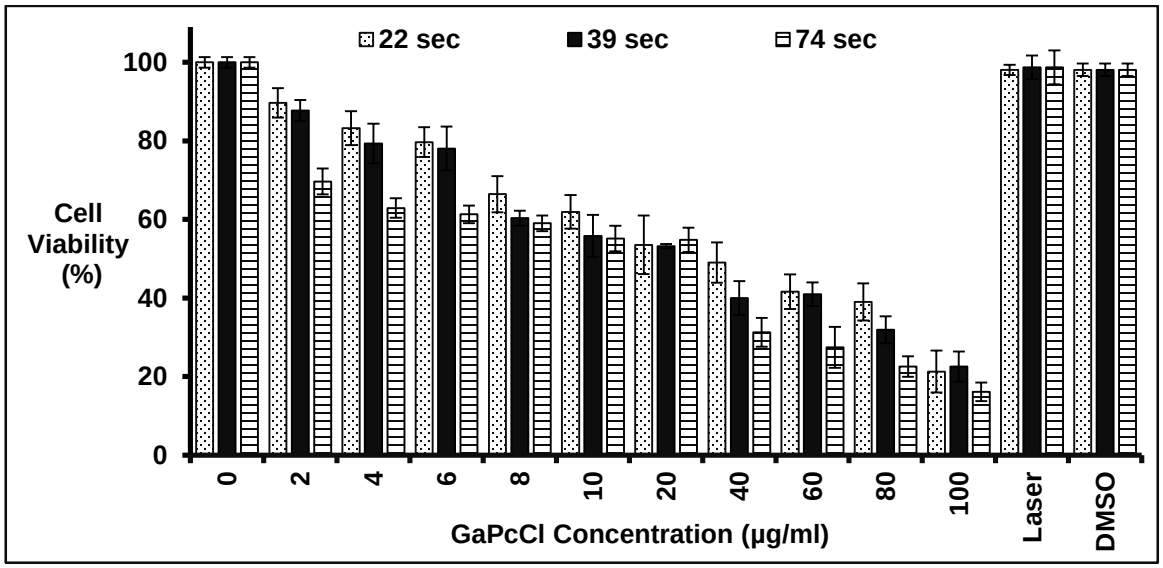

Figure 3.43 The cell viability (%) of melanoma cells after photosensitization with different concentrations of GaPcCl and photoirradiation (laser treatment) for 22 sec (2.5 J/cm^2), 39 sec (4.5 J/cm^2) and 74 sec (8.5 J/cm^2). 0 µg/ml = melanoma cells that were not exposed to GaPcCl and laser treatment (untreated control cells); Laser = melanoma cells that were photoirradiated without being exposed to GaPcCl (laser control); DMSO (control).

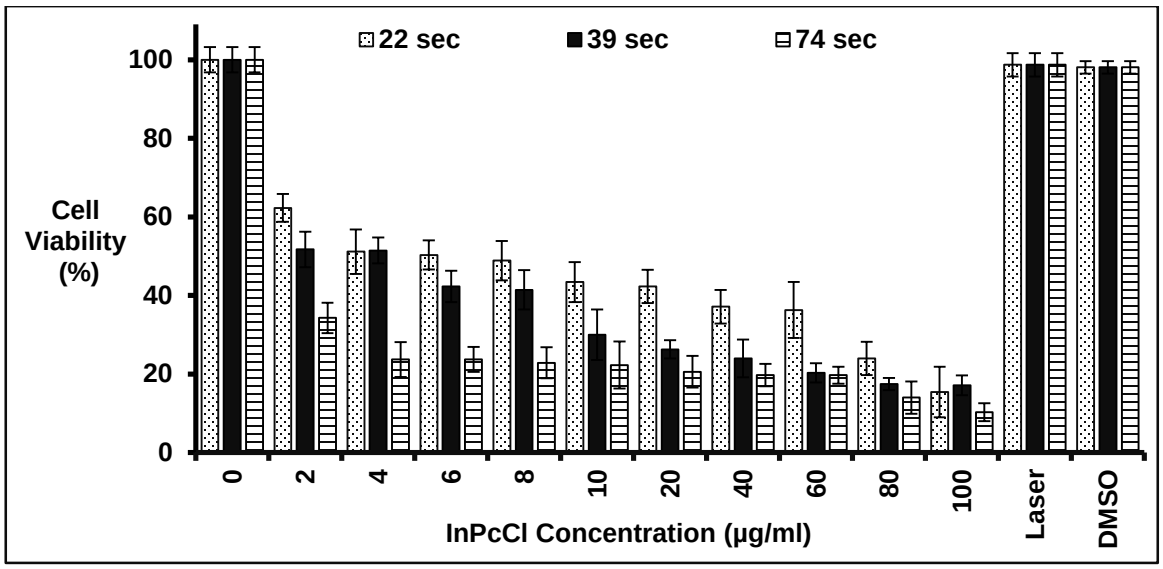

Figure 3.44 The cell viability (%) of melanoma cells after photosensitization with different concentrations of InPcCl and photoirradiation (laser treatment) for 22 sec (2.5 J/cm^2), 39 sec (4.5 J/cm^2) and 74 sec (8.5 J/cm^2). 0 µg/ml = melanoma cells that were not exposed to InPcCl and laser treatment (untreated control cells); Laser = melanoma cells that were photoirradiated without being exposed to InPcCl (laser control); DMSO (control).

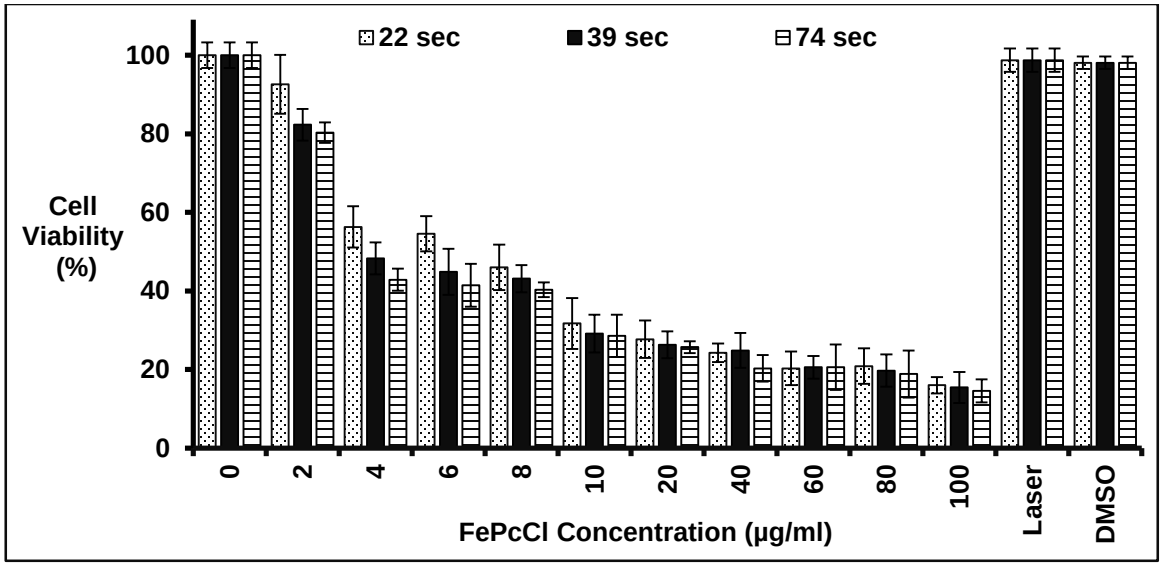

Figure 3.45 The cell viability (%) of melanoma cells after photosensitization with different concentrations of FePcCl and photoirradiation (laser treatment) for 22 sec (2.5 J/cm^2), 39 sec (4.5 J/cm^2) and 74 sec (8.5 J/cm^2). 0 µg/ml = melanoma cells that were not exposed to FePcCl and laser treatment (untreated control cells); Laser = melanoma cells that were photoirradiated without being exposed to FePcCl (laser control); DMSO (control).

Figures 3.46 – 3.48 show that PDT treatment with all three PSs at varying concentrations and different laser exposure times were highly toxic to A549 cancer cells. When comparing the cell viability of A549 cancer cells after treatment with the PSs (dark toxicity assay, figures 4.31 – 4.33) only and treatment with PS in combination with laser exposure (figures 3.46 – 3.48), it is clear that low viability is due to PDT treatment. The cell viability (%) of A549 cells exposed to GaPcCl, InPcCl and FePcCl at a low concentration of 2 µg/ml in combination with light exposure for 22 sec was 30%, 49% and 36% respectively. The cell viability of A549 cancer cells were further reduced or proportionally decreased for all three PSs as the PS concentration and laser exposure time increased. The resulting cell viability percentage for A549 cells treated with 40 µg/ml of FePcCl and 22 sec of laser exposure was 0%. Similarly, laser treatment times of 39 sec and 74 sec for photoactivation of A549 cells photosensitized with 20 µg/ml – 100 µg/ml of FePcCl also resulted in 100% cell killing (Figure 3.48).

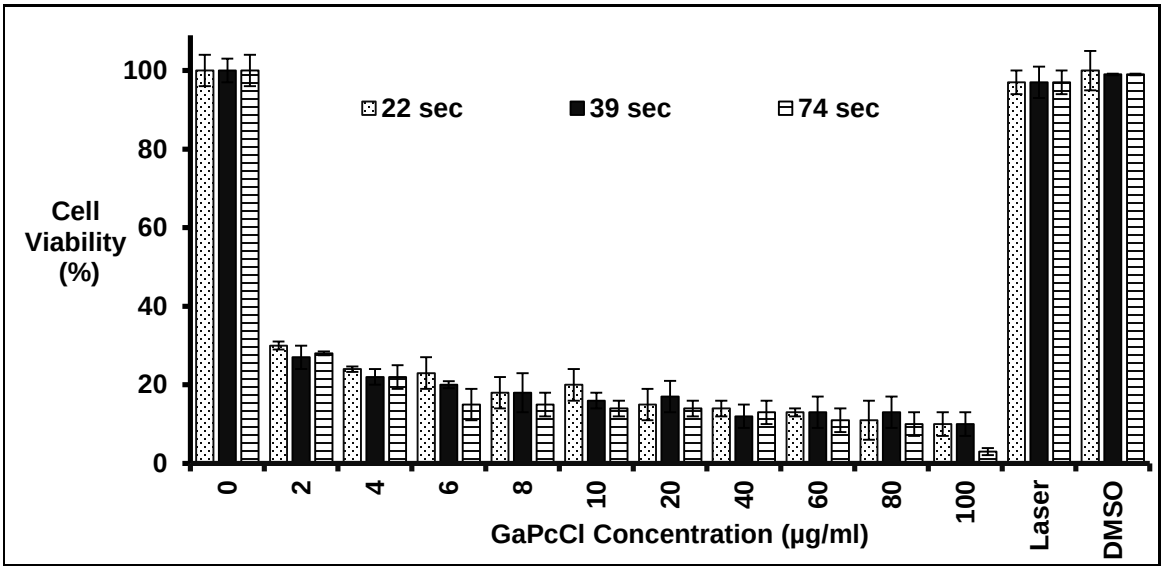

Figure 3.46 The cell viability (%) of A549 cells after photosensitization with different concentrations of GaPcCl and photoirradiation (laser treatment) for 22 sec (2.5 J/cm^2), 39 sec (4.5 J/cm^2) and 74 sec (8.5 J/cm^2). 0 µg/ml = A549 cells that were not exposed to GaPcCl and laser treatment (untreated control cells); Laser = A549 cells that were photoirradiated without being exposed to GaPcCl (laser control); DMSO (control).

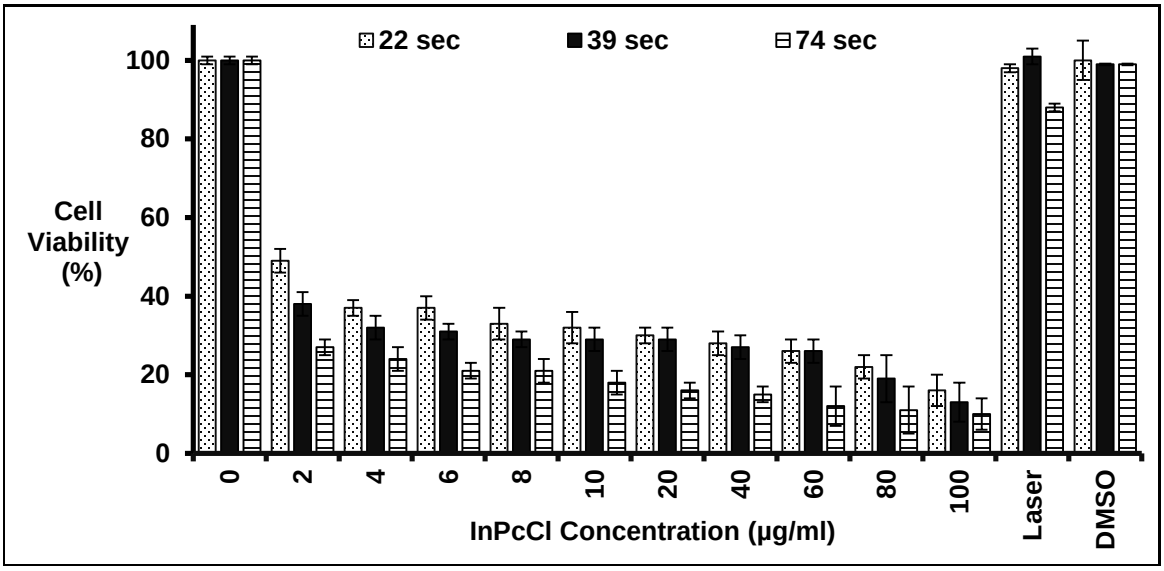

Figure 3.47 The cell viability (%) of A549 cells after photosensitization with different concentrations of InPcCl and photoirradiation (laser treatment) for 22 sec (2.5 J/cm^2), 39 sec (4.5 J/cm^2) and 74 sec (8.5 J/cm^2). 0 µg/ml = A549 cells that were not exposed to InPcCl and laser treatment (untreated control cells); Laser = A549 cells that were photoirradiated without being exposed to InPcCl (laser control); DMSO (control).

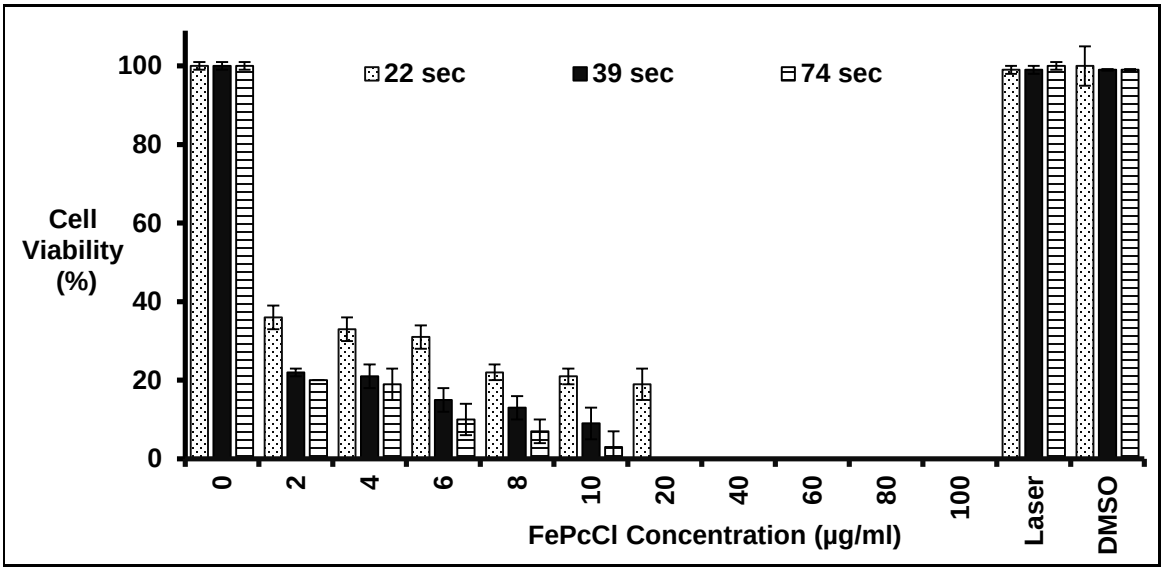

Figure 3.48 The cell viability (%) of A549 cells after photosensitization with different concentrations of FePcCl and photoirradiation (laser treatment) for 22 sec (2.5 J/cm^2), 39 sec (4.5 J/cm^2) and 74 sec (8.5 J/cm^2). 0 µg/ml = A549 cells that were not exposed to FePcCl and laser treatment (untreated control cells); Laser = A549 cells that were photoirradiated without being exposed to FePcCl (laser control); DMSO (control).

Figure 3.49 – Figure 3.51 indicates the photodynamic effect of GaPcCl, InPcCl and FePcCl on healthy normal fibroblast cells. These also show the effective concentration of GaPcCl, InPcCl and FePcCl that are acutely lethal to kill 50% of healthy normal fibroblast cells under controlled laboratory conditions. At the GaPcCl concentrations of 2 µg/ml, 60 µg/ml and 100 µg/ml with a treatment light dose of 2.5 J/cm^2 the cell viability of fibroblast cells was reduced to 66%, 47% and 38% respectively (Figure 3.49). In the case of fibroblast treated with InPcCl concentrations of 2 µg/ml and 100 µg/ml with a treatment light dose of 2.5 J/cm^2 the resulting cell viability was 97% and 48% accordingly (Figure 3.50). Similarly, the resulting cell viability for fibroblast cells treated with FePcCl concentrations of 2 µg/ml and 100 µg/ml with a treatment light dose of 2.5 J/cm^2 was 91% and 47% respectively (Figure 3.51). Results also showed that FePcCl at a photosensitizing concentration of 100 µg/ml photoactivated with a light dose of 8.5 J/cm^2 decreased cell viability of fibroblast cells to 25%, 42% and 42% respectively.

When comparing the cell viability (%) of fibroblast cells after treatment with the PSs (dark toxicity assay, Figures 4.34 – 4.36) only to treatment with PSs in combination with laser exposure (Figures 3.46 – 3.48), it is clear that illumination during PDT treatment reduces the cell viability of the normal healthy cells (fibroblast cells) as well. Also, a distinct correlation is seen between the pattern of PS uptake by fibroblast cells and survival of fibroblast cells after illumination. The high level of GaPcCl uptake by fibroblast cells (Figure 4.19) resulted in enhanced photokilling effects of fibroblast cells after PDT treatment in figure 4.49. Whereas, the low level of InPcCl and FePcCl uptake by fibroblast cells (Figures 4.20 – 4.21) resulted in good survival after PDT treatment as showed in Figures 4.50 – 4.51. The increase in the laser exposure time had a minor effect in reducing the cell viability of fibroblast cells during PDT treatment. Therefore, the survival of healthy

normal fibroblast after laser treatment during PDT was largely affected by the amount of PS being taken up.

Overall, results showed that healthy normal fibroblast cells survived *in vitro* PDT treatment with all three PSs much better than the cancer (Caco-2, MCF-7, melanoma and A549) cells. This illustrates the previously reported results that PSs such as Pcs and its metal-based Pc complexes preferentially accumulate in cancer cells compared to normal healthy cells.

A constant low treatment light dose of 2.5 J/cm^2 with optimum GaPcCl, InPcCl and FePcCl concentrations that reduced the cell viability of cancer cells to 50% were different for each of the cancer cell lines and these results are summarized in Table 3.1. The *in vitro* PDT effect of these optimum parameters for each of the cancer cells on the cell viability of healthy normal fibroblast cells are also depicted in Table 3.1. When comparing cell viability percentages for each of the cancer cell lines with the healthy normal cell line in Table 3.1 after *in vitro* PDT treatment; GaPcCl mediated PDT had the same killing effects on each of the cancer cell lines as well as healthy normal fibroblast cells. Therefore, it is noteworthy that for this *in vitro* study the best suited photosensitizers would be InPcCl and FePcCl for the PDT killing of cancer cells (Caco-2, MCF-7, melanoma and A549 cancer cells) with the sparing of the healthy normal fibroblast cells.

Table 3.1 Comparison of the cell viability (%) of cancer cells to healthy normal cells after *in vitro* PDT with the optimum PS concentrations of GaPcCl, InPcCl and FePcCl and a low light dose of 2.5 J/cm^2

	GaPcCl	**InPcCl**	**FePcCl**
Parameters	**40 µg/ml + 2.5 J/cm^2**	**10 µg/ml + 2.5 J/cm^2**	**40 µg/ml + 2.5 J/cm^2**
Caco-2 (Cell Viability)	47%	47%	46%
Fibroblast (Cell Viability)	51%	72%	60%
	GaPcCl	**InPcCl**	**FePcCl**
Parameters	**20 µg/ml + 2.5 J/cm^2**	**2 µg/ml + 2.5 J/cm^2**	**8 µg/ml + 2.5 J/cm^2**
MCF-7 (Cell Viability)	49%	50%	40%
Fibroblast (Cell Viability)	52%	97%	75%
	GaPcCl	**InPcCl**	**FePcCl**
Parameters	**40 µg/ml + 2.5 J/cm^2**	**6 µg/ml + 2.5 J/cm^2**	**8 µg/ml + 2.5 J/cm^2**
Melanoma (Cell Viability)	49%	50%	46%
Fibroblast (Cell Viability)	51%	85%	75%
	GaPcCl	**InPcCl**	**FePcCl**
Parameters	**2 µg/ml + 2.5 J/cm^2**	**2 µg/ml + 2.5 J/cm^2**	**2 µg/ml + 2.5 J/cm^2**
A549 (Cell Viability)	30%	49%	37%
Fibroblast (Cell Viability)	66%	97%	91%

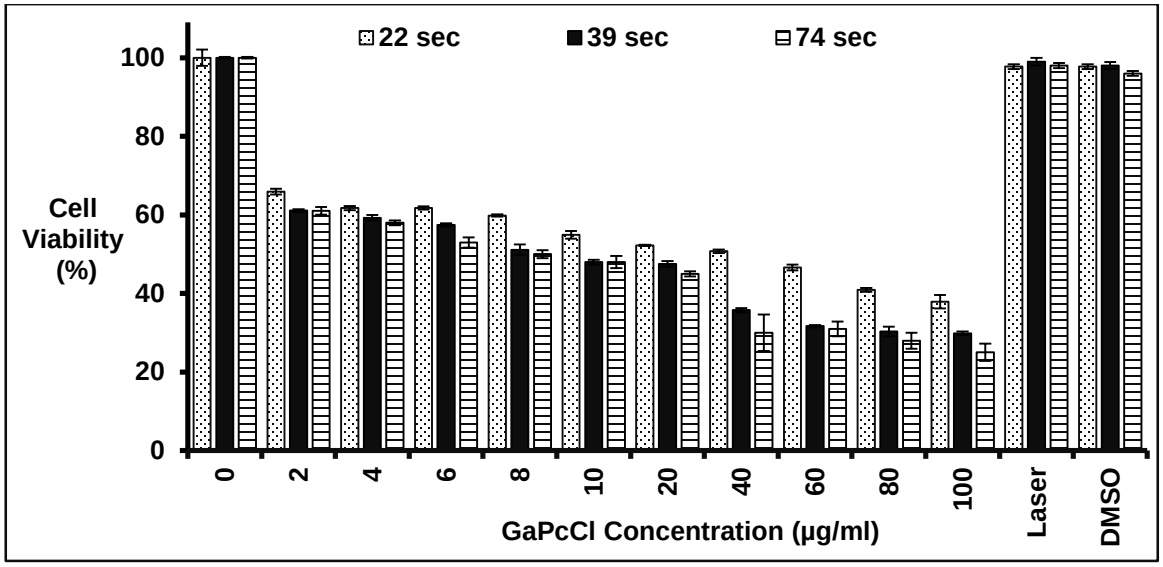

Figure 3.49 The cell viability (%) of fibroblast cells after photosensitization with different concentrations of GaPcCl and photoirradiation (laser treatment) for 22 sec (2.5 J/cm^2), 39 sec (4.5 J/cm^2) and 74 sec (8.5 J/cm^2). 0 µg/ml = fibroblast cells that were not exposed to GaPcCl and laser treatment (untreated control cells); Laser = fibroblast cells that were photoirradiated without being exposed to GaPcCl (laser control); DMSO (control).

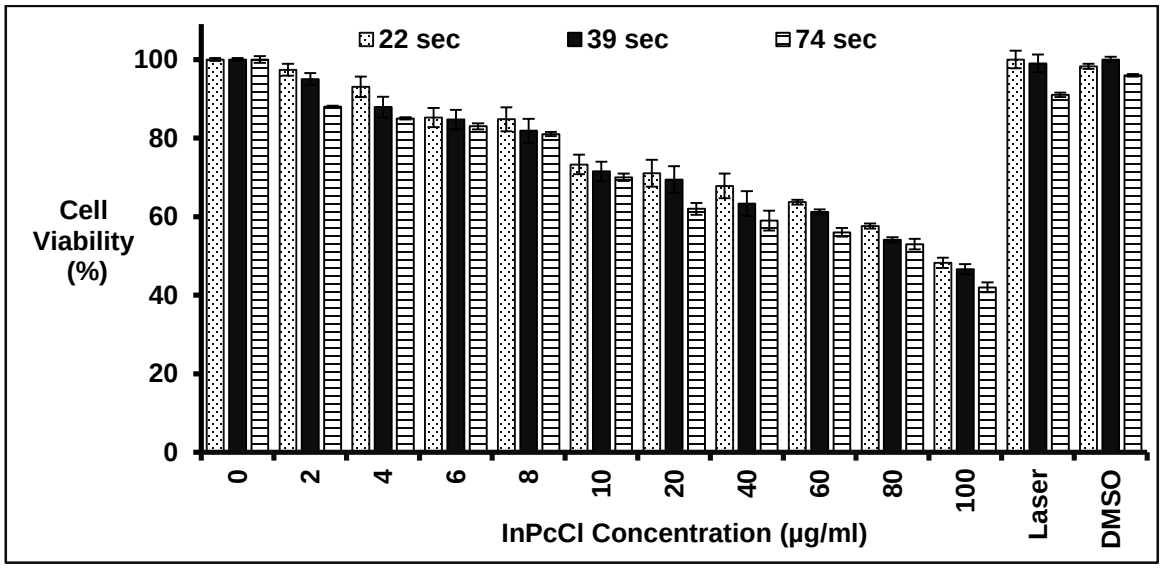

Figure 3.50 The cell viability (%) of fibroblast cells after photosensitization with different concentrations of InPcCl and photoirradiation (laser treatment) for 22 sec (2.5 J/cm^2), 39 sec (4.5 J/cm^2) and 74 sec (8.5 J/cm^2). 0 µg/ml = fibroblast cells that were not exposed to InPcCl and laser treatment (untreated control cells); Laser = fibroblast cells that were photoirradiated without being exposed to InPcCl (laser control); DMSO (control).

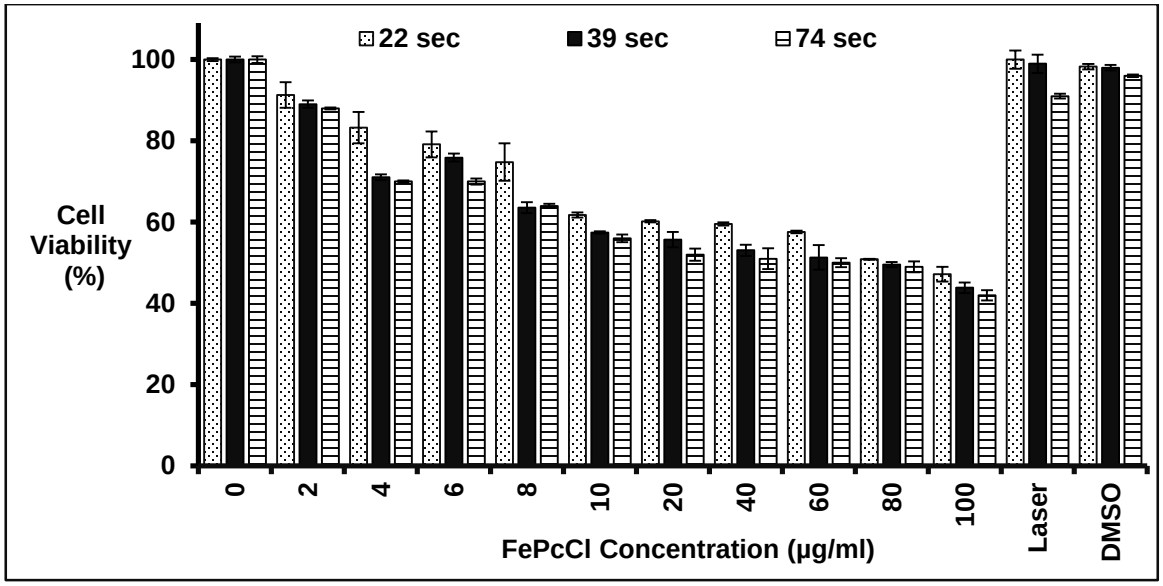

Figure 3.51 The cell viability (%) of fibroblast cells after photosensitization with different concentrations of FePcCl and photoirradiation (laser treatment) for 22 sec (2.5 J/cm^2), 39 sec (4.5 J/cm^2) and 74 sec (8.5 J/cm^2). 0 µg/ml = fibroblast cells that were not exposed to FePcCl and laser treatment (untreated control cells); Laser = fibroblast cells that were photoirradiated without being exposed to FePcCl (laser control); DMSO (control).

Lastly, it was also noted that the most lethal *in vitro* PDT treatment parameters which resulted in 100% cell death for each of the cancer cell lines was as follows:

- Caco-2 cell line – FePcCl (60 µg/ml – 100 µg/ml); treatment light dose 8.5 J/cm^2
- MCF-7 cell line – FePcCl (20 µg/ml); treatment light dose of 8.5 J/cm^2
- MCF-7 cell line – FePcCl (40 µg/ml - 100 µg/ml); treatment light dose of 4.5 or 8.5 J/cm^2
- MCF-7 cell line – FePcCl (100 µg/ml); treatment light dose of 2.5, 4.5 or 8.5 J/cm^2
- A549 cell line – FePcCl (20 µg/ml - 100 µg/ml); treatment light dose of 4.5 or 8.5 J/cm^2
- A549 cell line – FePcCl (40 µg/ml - 100 µg/ml); treatment light dose of 2.5, 4.5 or 8.5 J/cm^2

GaPcCl, InPcCl and FePcCl at the highest photosensitizing concentration (100 µg/ml) and light dose (8.5 J/cm^2) in this *in vitro* study resulted in reducing the cell viability of melanoma cells to 16%, 10% and 15% respectively.

3.5 CYTOLOGIC ANALYSIS OF PDT TREATED CELLS USING AN INVERTED MICROSCOPE

The change in cell morphology as a result of GaPcCl, InPcCl and FePcCl mediated PDT treatment were also monitored in the four different cancer cell lines using an inverted microscope. The PDT treated Caco-2 (Figure 3.52), MCF-7 (Figure 3.53), melanoma (Figure 3.54) and A549 (Figure 3.55) cancer cells showed morphological features that were not prominent in untreated control cells. The PDT cancer cells appeared round in shape; showed abrupt cell shrinkage and detachment from adjacent cells. Blebbing was also seen in MCF-7 cancer cells treated with 2 µg/ml or 100 µg/ml of GaPcCl in combination with 22 sec, 39 sec or 74 sec of laser treatment in Figure 3.53. Melanoma cancer cells treated with 100 µg/ml of GaPcCl and irradiated for 22 sec, 39 sec or 74 sec displayed blebbing (Figure 3.54). Blebbing was also observed in melanoma cancer cells treated with 2 µg/ml of InPcCl in combination with laser treatment for 39 sec or 74 sec; and 100 µg/ml of InPcCl photoactivated for 22 sec, 39 sec or 74 sec (Figure 3.54). 2 µg/ml or 100 µg/ml of FePcCl and 74 sec of laser treatment also produced blebbing in melanoma cancer cells as seen in Figure 3.54.

Morphology changes were also observed for untreated and PDT treated fibroblast cells (healthy normal cells) as depicted in Figure 3.56. Fibroblast cells photosensitized with 2 µg/ml of GaPcCl, InPcCl or FePcCl and laser treated for 22 sec, 39 sec or 74 sec showed no changes in cell morphology when compared to untreated controls. Whereas, PDT treated fibroblast cells exposed to 100 µg/ml of GaPcCl, InPcCl or FePcCl and laser

treatment for 22 sec, 39 sec or 74 sec showed profound changes in cell morphology. These changes included rounding of cells, shrinking of cells, blebbing and cells detaching from neighboring cells shown in Figure 3.56.

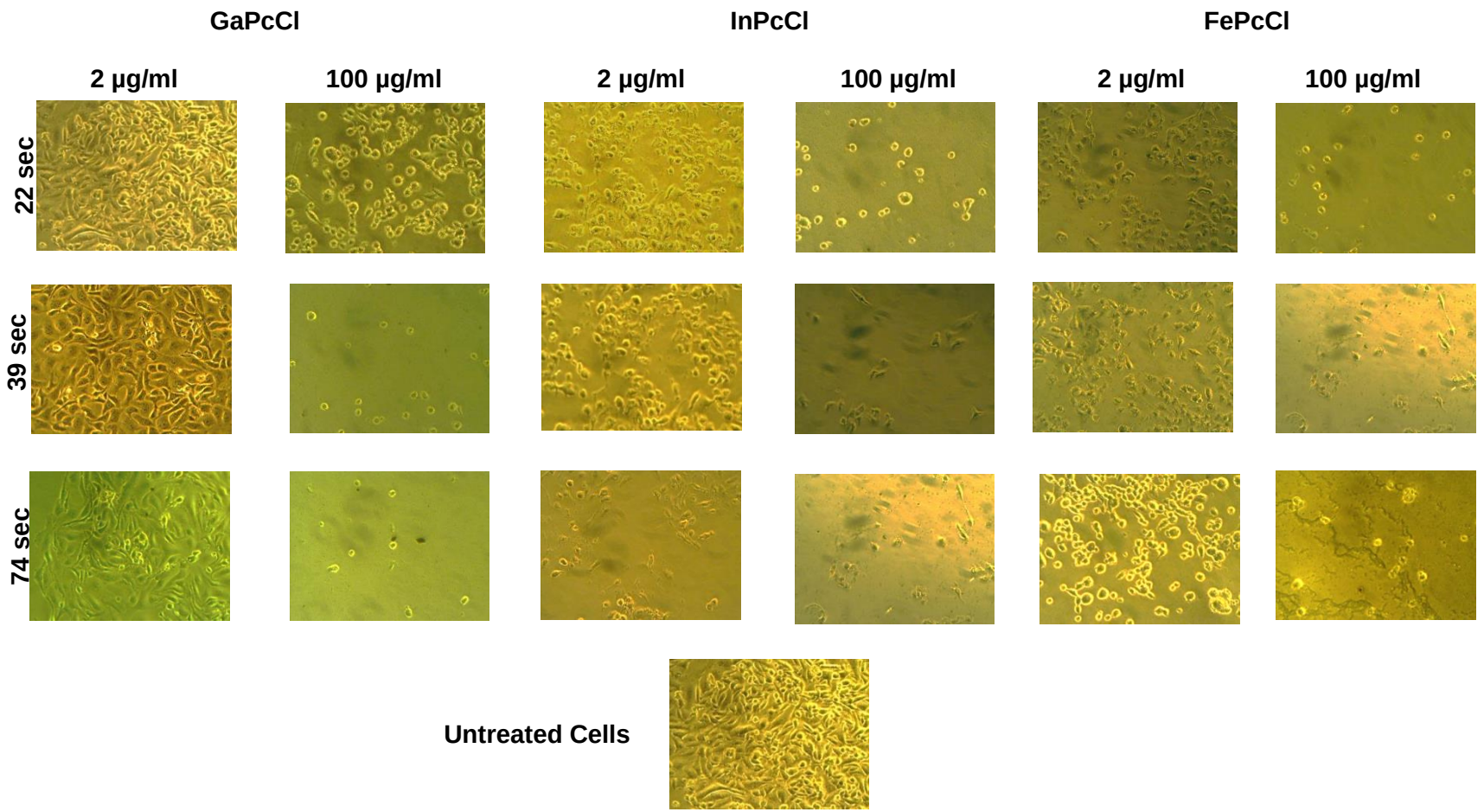

Figure 3.52 Micrographs showing the photodynamic effect of a low (2 µg/ml) and a high (100 µg/ml) concentration GaPcCl, InPcCl and FePcCl on Caco-2 cancer cells after laser treatment for 22 sec (2.5 J/cm^2); 39 sec (4.5 J/cm^2) and 74 sec (8.5 J/cm^2). Untreated control cells not exposed to photosensitizers and laser treatment. (Magnification = 10x).

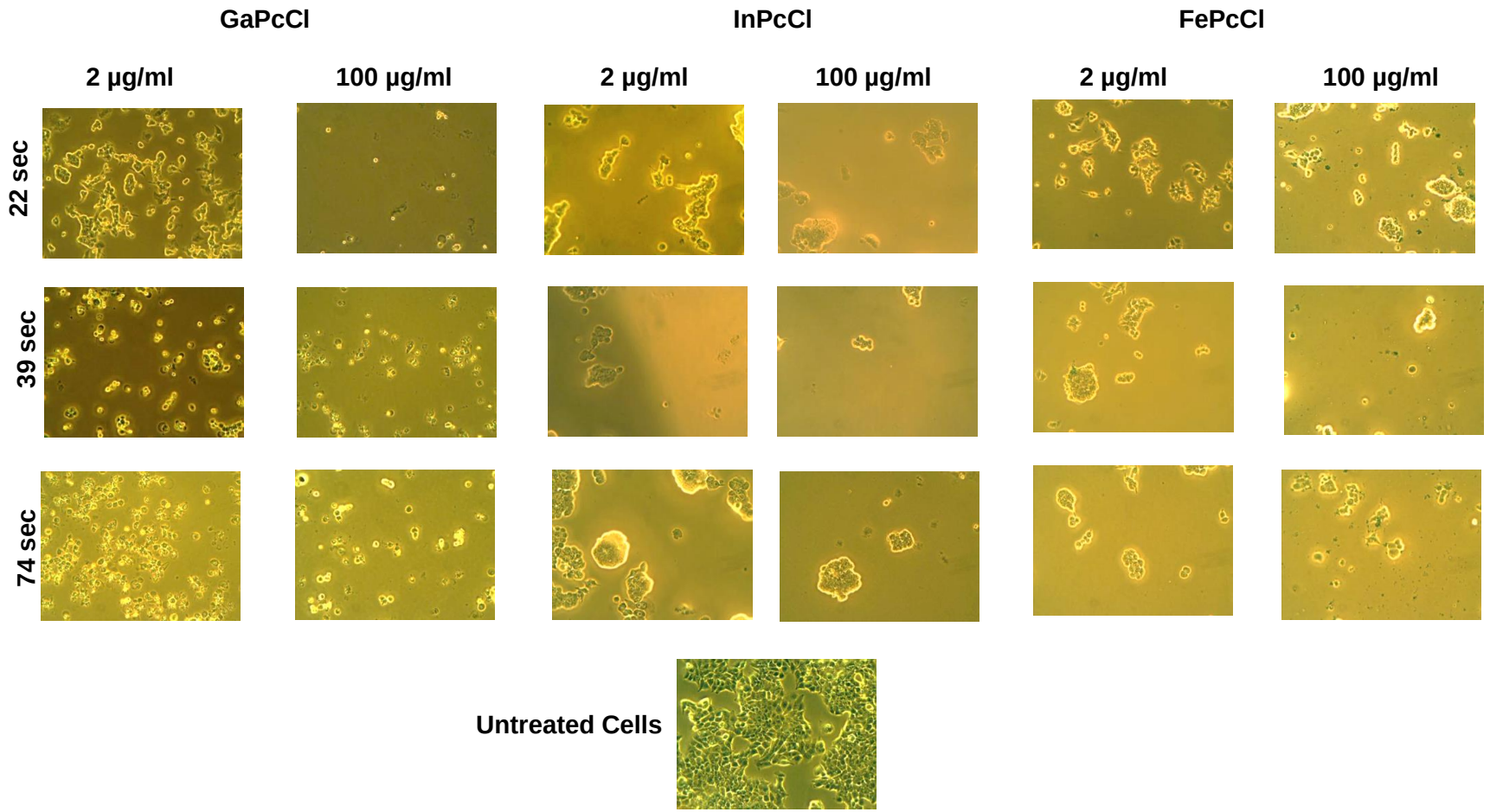

Figure 3.53 Micrographs showing the photodynamic effect of a low (2 µg/ml) and a high (100 µg/ml) concentration GaPcCl, InPcCl and FePcCl on MCF-7 cancer cells after laser treatment for 22 sec (2.5 J/cm^2); 39 sec (4.5 J/cm^2) and 74 sec (8.5 J/cm^2). Untreated control cells not exposed to photosensitizers and laser treatment. (Magnification = 10x).

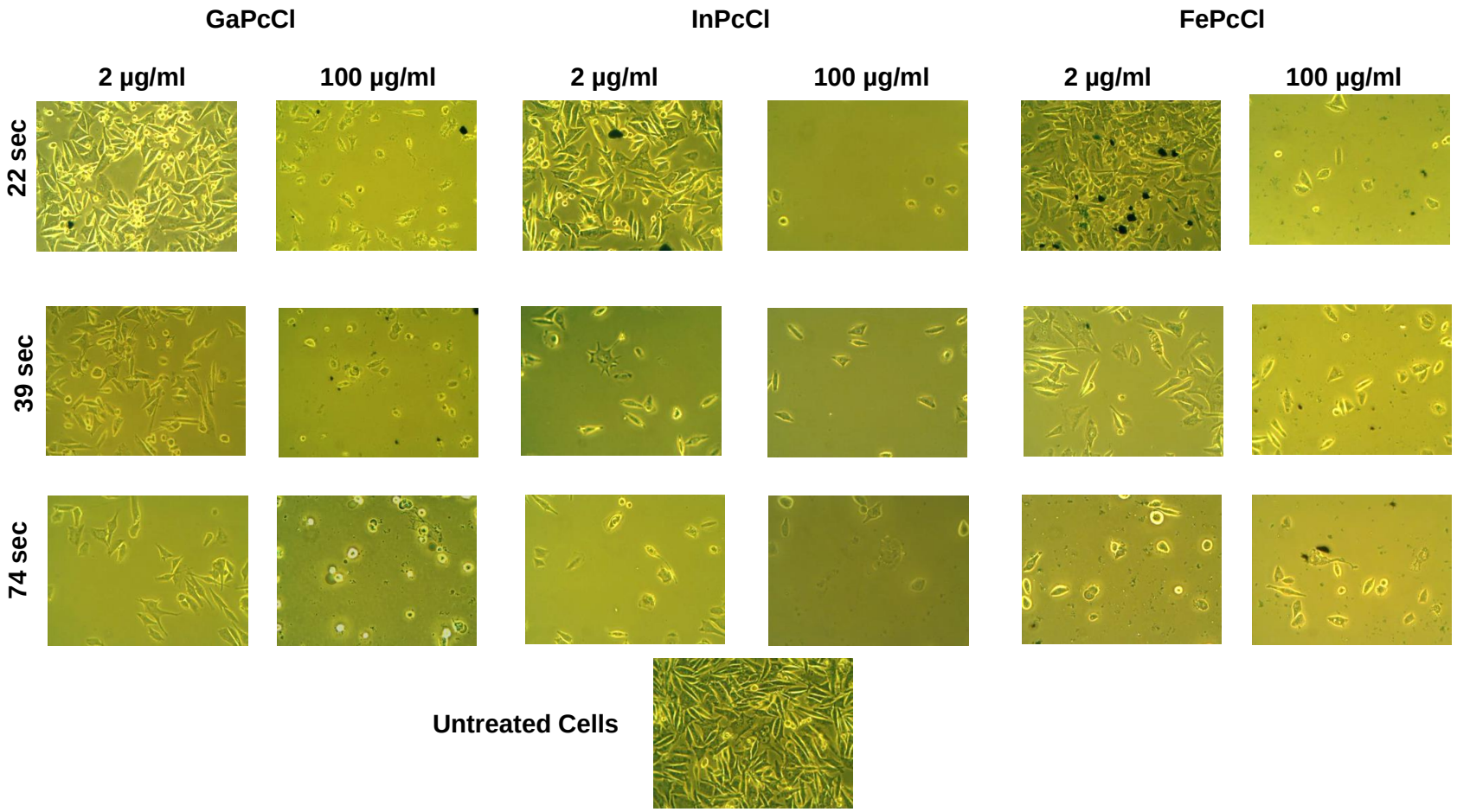

Figure 3.54 Micrographs showing the photodynamic effect of a low (2 µg/ml) and a high (100 µg/ml) concentration GaPcCl, InPcCl and FePcCl on melanoma cancer cells after laser treatment for 22 sec (2.5 J/cm^2); 39 sec (4.5 J/cm^2) and 74 sec (8.5 J/cm^2). Untreated control cells not exposed to photosensitizers and laser treatment. (Magnification = 10x).

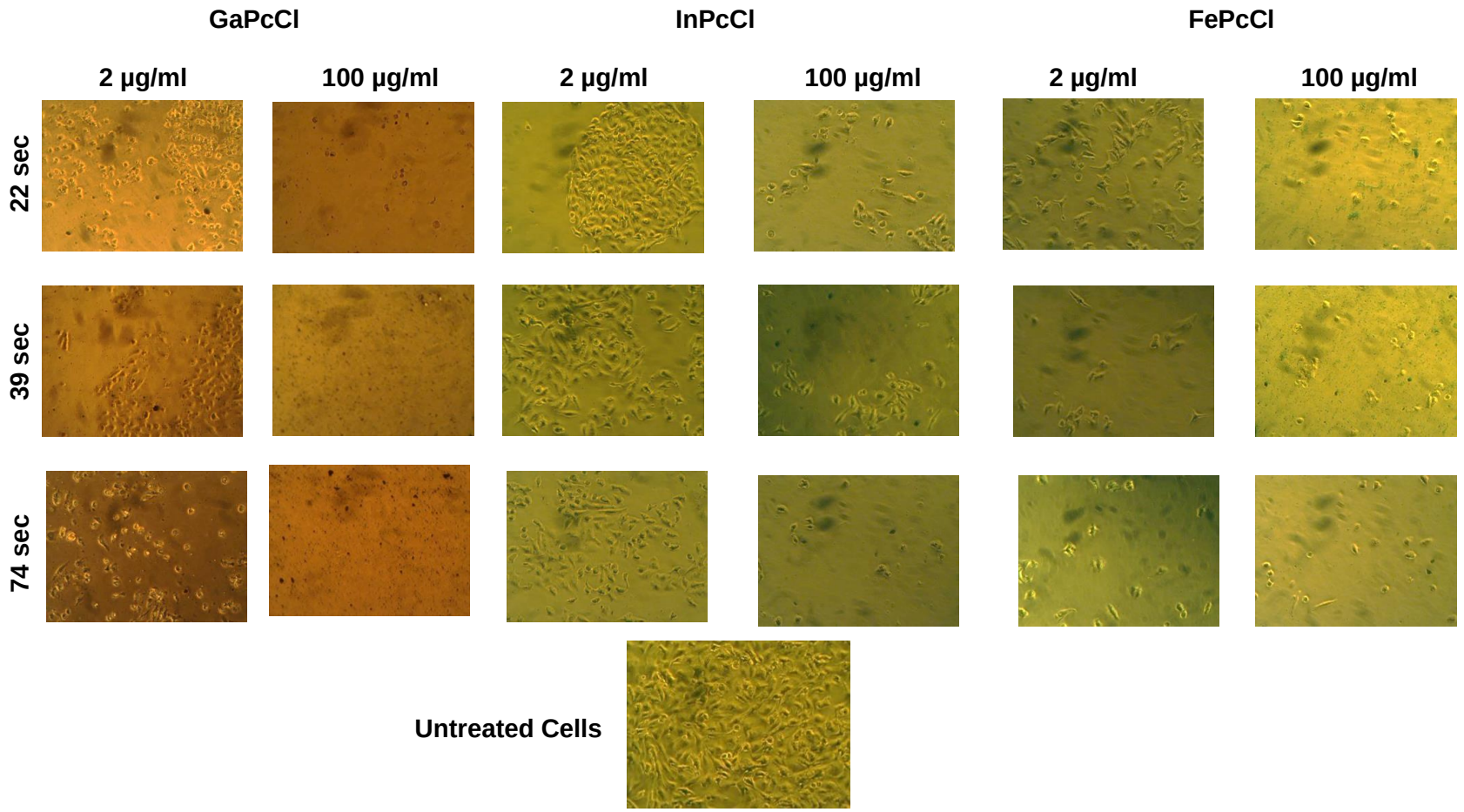

Figure 3.55 Micrographs showing the photodynamic effect of a low (2 µg/ml) and a high (100 µg/ml) concentration GaPcCl, InPcCl and FePcCl on A549 cancer cells after laser treatment for 22 sec (2.5 J/cm^2); 39 sec (4.5 J/cm^2) and 74 sec (8.5 J/cm^2). Untreated control cells not exposed to photosensitizers and laser treatment. (Magnification = 10x).

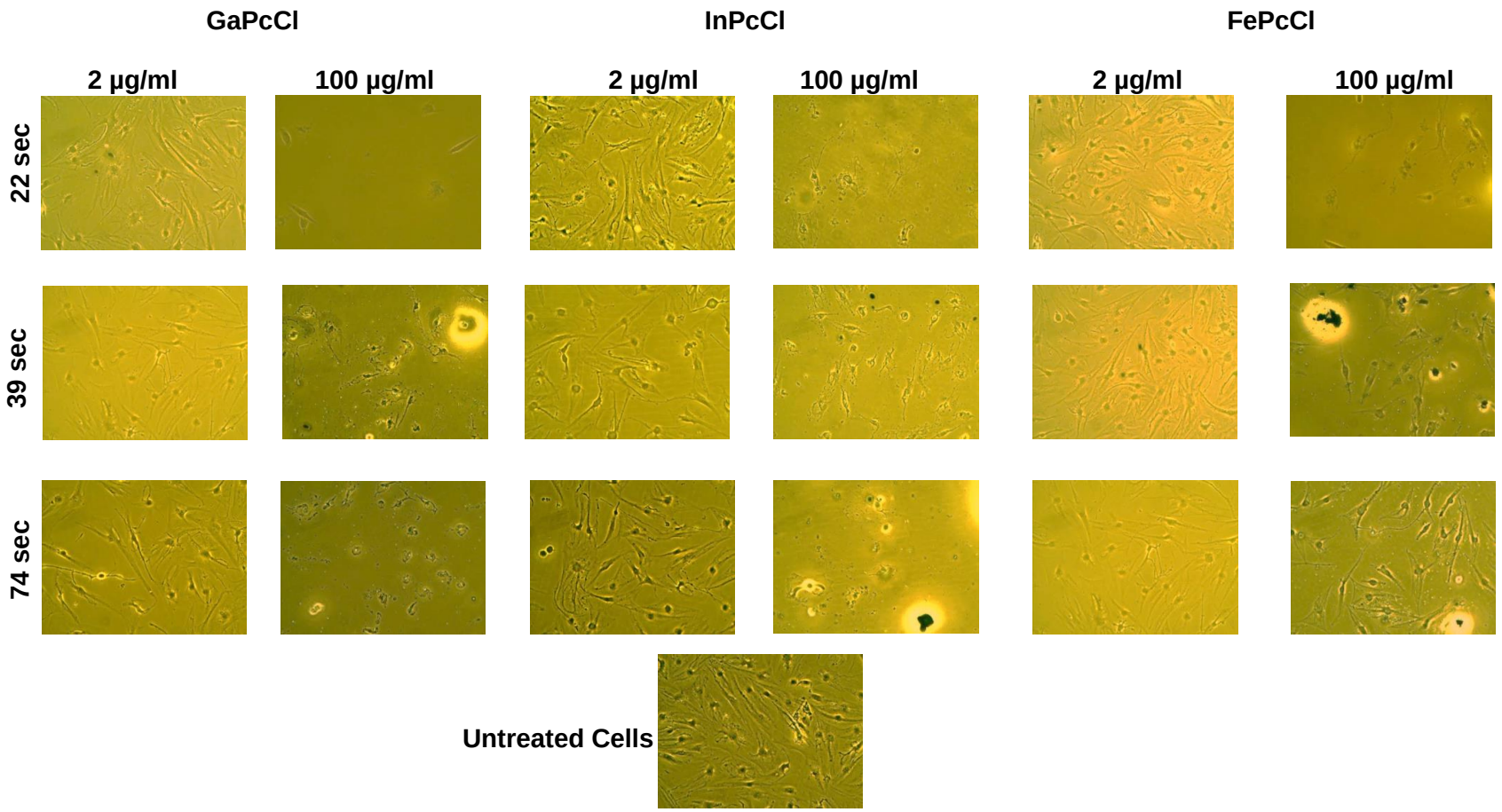

Figure 3.56 Micrographs showing the photodynamic effect of a low (2 µg/ml) and a high (100 µg/ml) concentration GaPcCl, InPcCl and FePcCl on fibroblast cells (healthy normal cells) after laser treatment for 22 sec (2.5 J/cm^2); 39 sec (4.5 J/cm^2) and 74 sec (8.5 J/cm^2). Untreated control cells not exposed to photosensitizers and laser treatment. (Magnification = 10x).

3.6 ULTRA-STRUCTURAL CHANGES IN CANCER CELLS AFTER PDT TREATMENT BY THE TEM

For the TEM and Annexin V-FITC/propidium iodide assay specific parameters were selected on the base of the EC_{50} (effective concentration that kills 50% of the cells) for each PS in each cell line. These were attained from the previous *in vitro* PDT study by selecting the first set of PDT treatment parameters that caused a 50% decrease in cell viability in combination with the lowest treatment light time. These parameters, presented in Table 3.2., were applied to investigate the mode of cell death induced by PDT for each of the cancer cell lines. Since, the focus was on cancer cell death, normal primary cultured fibroblasts were not included in these experiments.

Table 3.2 PS concentrations and treatment light doses used for cell death studies

Cancer Cell line	**[GaPcCl] + Light Time**	**[InPcCl] + Light Time**	**[FePcCl] + Light Time**
Caco-2	40 µg/ml + 22 sec	10 µg/ml + 22 sec	40 µg/ml + 22 sec
MCF-7	20 µg/ml + 22 sec	2 µg/ml + 22 sec	8 µg/ml + 22 sec
Melanoma	40 µg/ml + 22 sec	6 µg/ml + 22 sec	8 µg/ml + 22 sec
A549	2 µg/ml + 22 sec	2 µg/ml + 22 sec	2 µg/ml + 22 sec

TEM micrographs revealed that untreated control Caco-2 (Figure 3.57 A & B), MCF-7 (Figure 3.58 A), melanoma (Figure 3.59 A) and A549 (Figure 3.60 A) cancer cells (without PDT treatment) displayed the characteristics of normal cancer cell such as intact nucleus and undamaged cytoplasmic membrane. The different photosensitizers - mediated PDT treatments applied to Caco-2, MCF-7, melanoma and A549 cancer cells induced district ultrastructural alterations to nucleus, cytoplasmic membrane and plasma membrane as

seen in Figure 3.57 – Figure 3.60. After 24 h post-PDT treatment with GaPcCl, InPcCl and FePcCl, all four different cancer lines showed ultrastructural alterations that characterize either autophagy and/or apoptosis death cell mechanisms. Cancer cells (Caco-2, melanoma and A549) subjected to PDT induced apoptosis and autophagy exhibited a large number of autophagic vacuoles in the cytoplasm membrane; plasma membrane blebbing; spaces around the nucleus caused by irregular condensation of chromatin; and nuclear blebs pinching off to from fragments or nucleus undergoing fragmentation. In Figure 3.58, PDT treated MCF-7 cancer cells with GaPcCl (Figure 3.58 B), InPcCl (Figure 3.58 C) and FePcCl (Figure 3.58 D) induced similar apoptotic features only. However, PDT treated MCF-7 cancer cells lacked autophagic vacuoles in the cytoplasm membrane.

Thus, the ultrastructural changes in a dying Caco-2, melanoma and A549 cancer cells are characteristic of apoptosis and autophagy after treatment with GaPcCl, InPcCl or FePcCl followed by laser irradiation as indicated in Figures 3.57, Figure 3.59 and Figure 3.60. These distinguishable morphological ultrastructural apoptotic changes include blebbing, chromatin condensation and nucleus fragmentation, accompanied by autophagic vacuolization of the cytoplasm. Figure 3.58 shows that PDT treated MCF-7 cancer cell portrayed morphological features of apoptosis such as DNA fragmentation, spaces around the nucleus caused by irregular condensation of chromatin and an increased nuclear: cytoplasmic ratio.

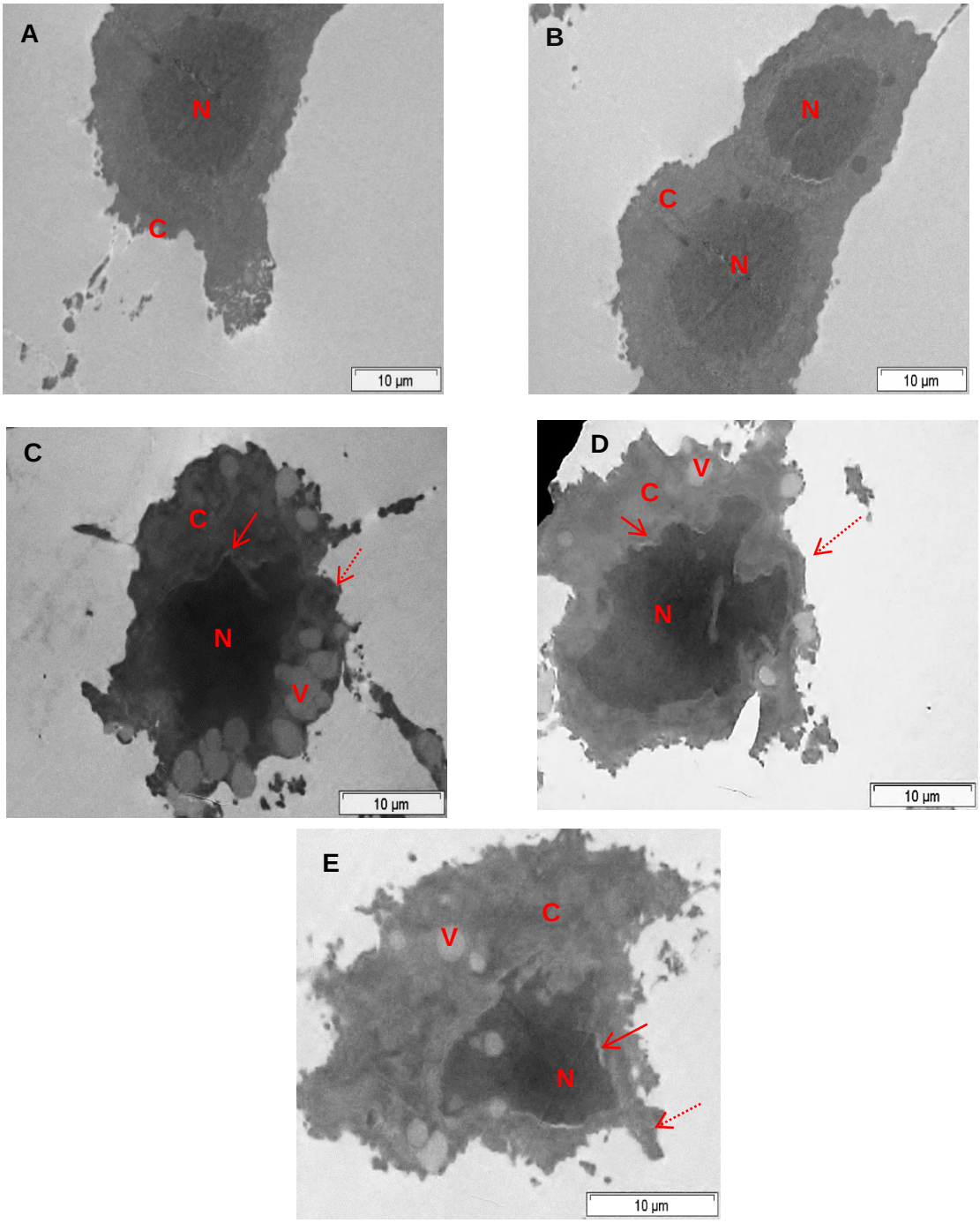

Figure 3.57 TEM micrographs showing the ultrastructural features in (A) untreated Caco-2 cancer cell, (B) untreated Caco-2 cancer cell, (C) GaPcCl mediated-PDT treated Caco-2 cancer cell, (D) InPcCl mediated-PDT treated Caco-2 cancer cell and (E) FePcCl mediated-PDT treated Caco-2 cancer cell. Magnification = (A) 5000x, (B) 5000x, (C) 8000x, (D) 6000x and (E) 6000x. N = nucleus; C = cytoplasmic membrane; V = vacuole; (→) = spaces around the nucleus; (⇜) = plasma membrane bleb.

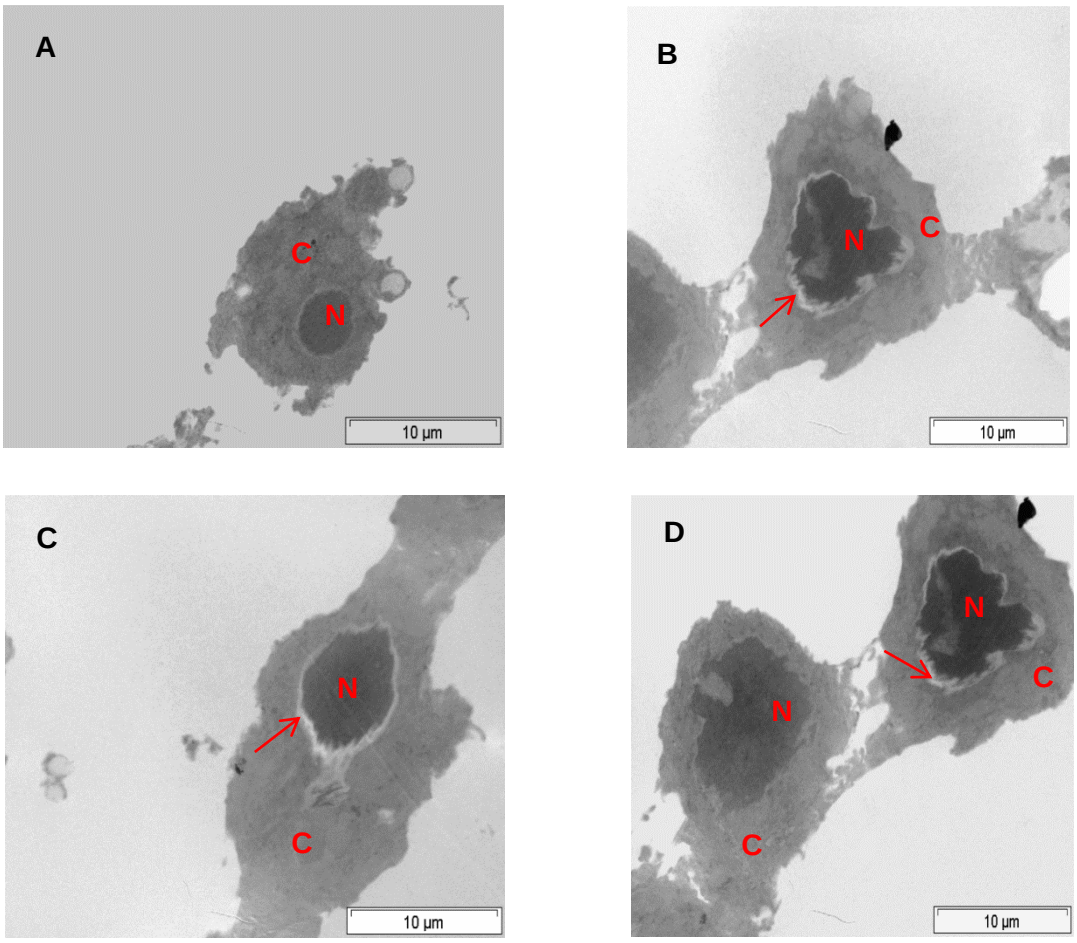

Figure 3.58 TEM micrographs showing the ultrastructural features in (A) untreated MCF-7 cancer cell, (B) GaPcCl mediated-PDT treated mcf cancer cell, (C) InPcCl mediated-PDT treated mcf cancer cell and (D) FePcCl mediated-PDT treated mcf cancer cells. Magnification = 8000x. N = nucleus; C = cytoplasmic membrane; (→) = space around the nucelus.

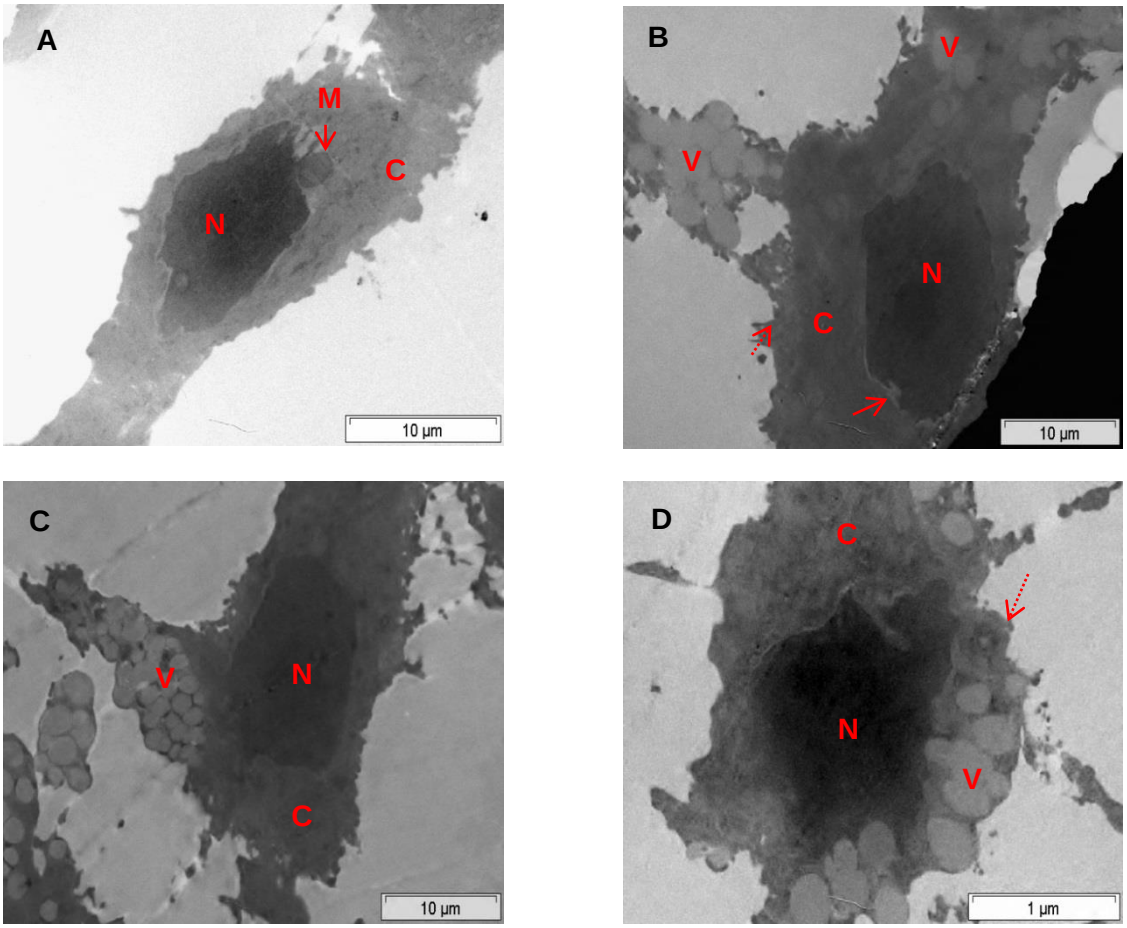

Figure 3.59 TEM micrographs showing the ultrastructural features in (A) untreated melanoma cancer cell, (B) GaPcCl mediated-PDT treated melanoma cancer cell, (C) InPcCl mediated-PDT treated melanoma cancer cell and (D) FePcCl mediated-PDT treated melanoma cancer cell. Magnification = (A) 8000x, (B) 8000x (C) 6000x (D) 8000x. N = nucleus; C = cytoplasmic membrane; V = vacuole; M = mitrochondria; (→) = spaces around the nucleus; (⇜) = plasma membrane bleb.

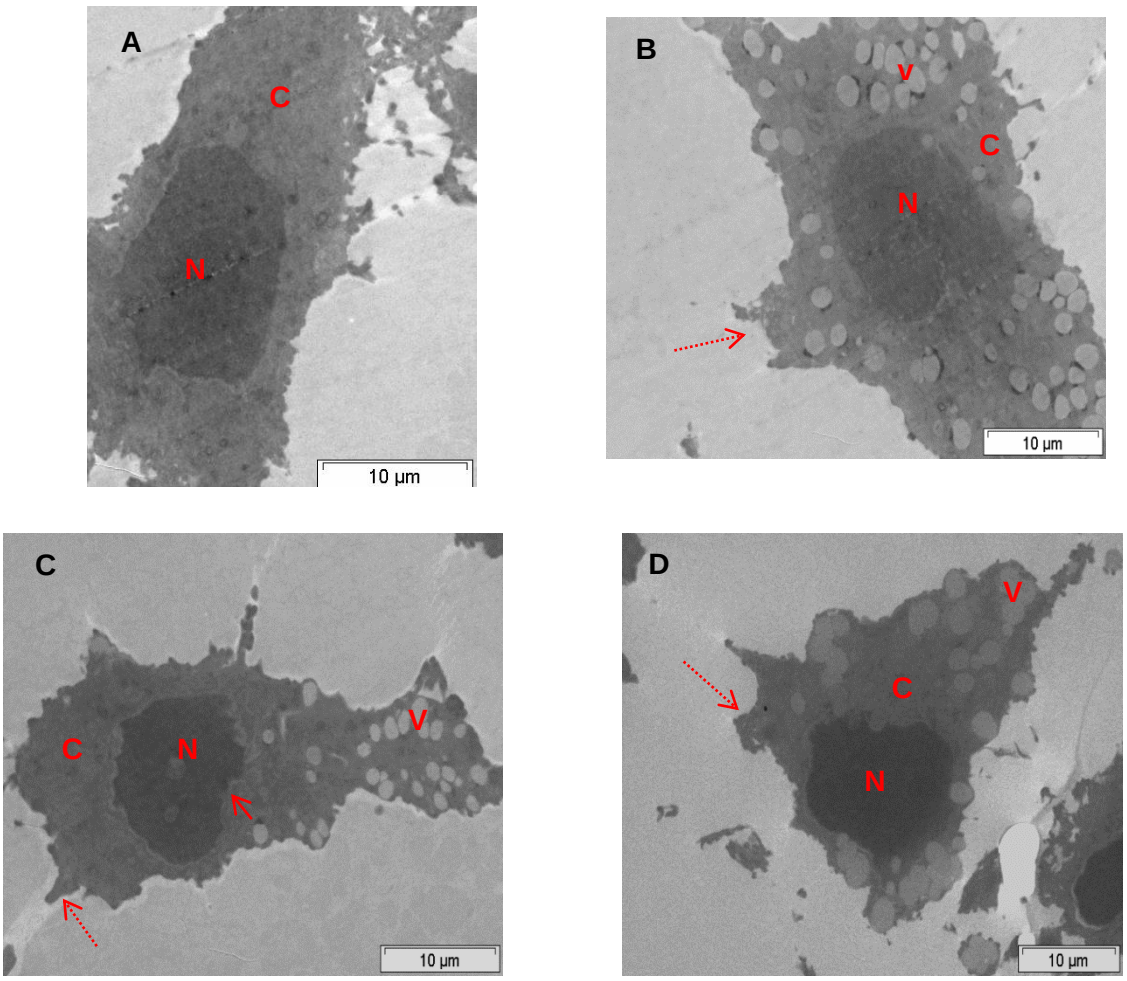

Figure 3.60 TEM micrographs showing the ultrastructural features in (A) untreated A549 cancer cell, (B) GaPcCl mediated-PDT treated A549 cancer cell, (C) InPcCl mediated-PDT treated A549 cancer cell and (D) FePcCl mediated-PDT treated A549 cancer cell. Magnification = (A) 6000x, (B) 6000x, (C) 6000x and (D) 5000x. N = nucleus; C = cytoplasmic membrane; V = vacuole; (→) = spaces around the nucleus; (≪····) = plasma membrane bleb.

3.7 ANALYSIS OF APOPTOSIS USING DUAL FITC ANNEXIN V AND PROPIDIUM IODIDE STAINS

Cell death was identified and quantified by flow cytometry using the FITC Annexin V and propidium iodide (PI) assays. FITC Annexin V is a membrane marker of apoptosis and PI enters the plasma membrane of damaged or dying cells to the stain the nucleus. Caco-2 (Figure 3.61), MCF-7 (Figure 3.62), melanoma (Figure 3.63) and A549 (Figure 3.64) cancer cells were assessed 24 h post-PDT treatment.

As shown in Figure 3.61 A, Figure 3.62 A, Figure 3.63 A and Figure 3.64 A the untreated control cancer cells were primarily FITC Annexin V and PI negative indicating that these cells were viable and not undergoing apoptosis. After treatment with GaPcCl, InPcCl or FePcCl in combination with laser treatment the induced cell death mode could be distinguished, based on three populations of Caco-2 cancer cells in Figure 3.61. These were low percentage of viable Caco-2 cells; Caco-2 cells undergoing late apoptosis and Caco-2 cell debris. Melanoma (Figure 3.63) cancer cells after GaPcCl, InPcCl or FePcCl mediated PDT treatment depicted four populations of cells namely, low percentage of viable cells; cells undergoing early apoptosis; cells undergoing late apoptosis and cell debris. PDT treated A549 cancer cells showed similar results as seen in Figure 3.64; except InPcCl mediated PDT treatment depicted low percentage of viable A549 cells; no A549 cells undergoing early apoptosis (0%); large percentage of A549 cells undergoing late apoptosis (65.4%) and A549 cell debris. PDT treated MCF-7 cancer cells displayed (Figure 3.62) only three populations of cells (viable, early apoptosis and late apoptosis cells) with no evidence of MCF-7 cell debris population. GaPcCl, InPcCl and FePcCl mediated PDT produced an increased population of apoptotic cells and a decrease in viable population for all four cancer cell lines. In addition, three cancer cell lines (MCF-7,

melanoma and A549 cancer cells) after 24 h post-PDT treatment displayed a pattern of treated cells moving from the early apoptotic stage into the late apoptotic stage.

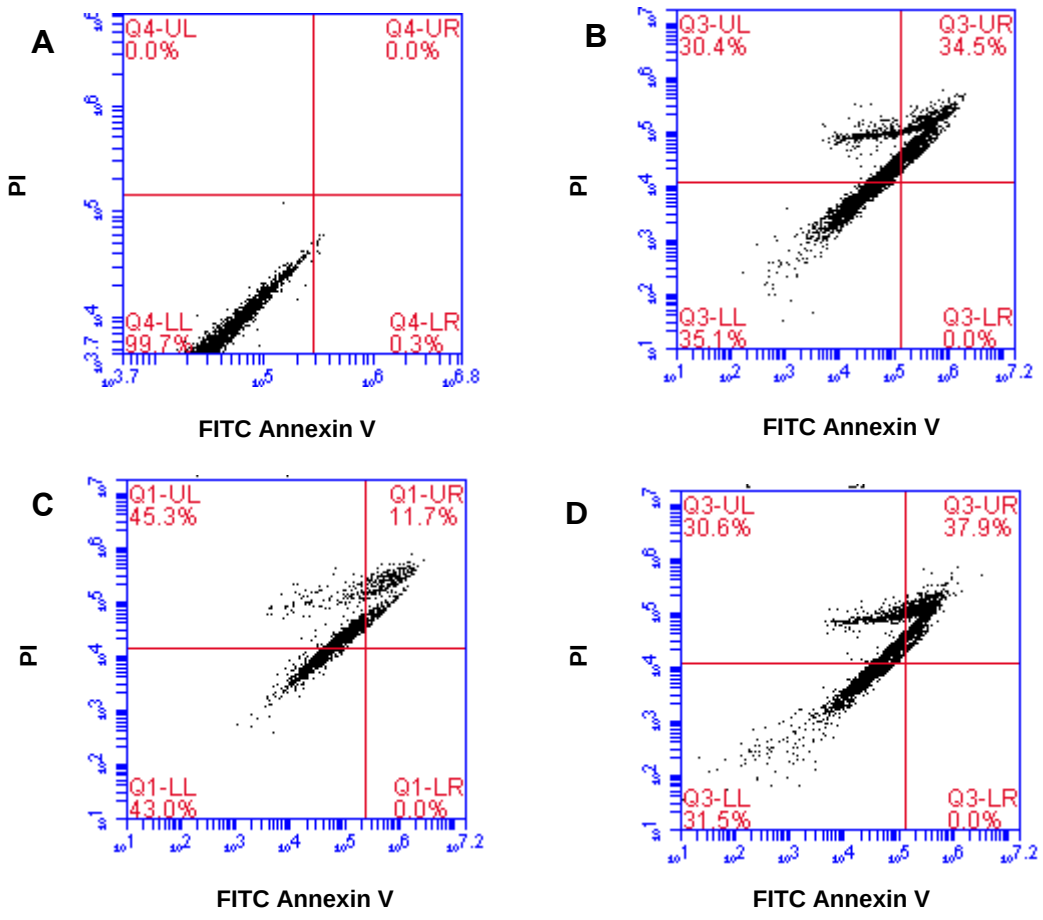

Figure 3.61 Representative FITC Annexin V/PI flow cytometric dot-plots of Caco-2 cancer cells after 24 post-PDT treatment. (A) Untreated control cells, (B) Caco-2 cells after photosensitization with 40 µg/ml of GaPcCl and photoactivation with a treatment light dose of 2.5 J/cm^2, (C) Caco-2 cells after photosensitization with 10 µg/ml of InPcCl and photoactivation with a treatment light dose of 2.5 J/cm^2, (D) Caco-2 cells after photosensitization with 40 µg/ml of FePcCl and photoactivation with a treatment light dose of 2.5 J/cm^2. Percentage (%) of viable cells, early apoptotic cells, late apoptotic cells and cellular debris are shown in the lower left, lower right, upper left and upper right quadrant respectively.

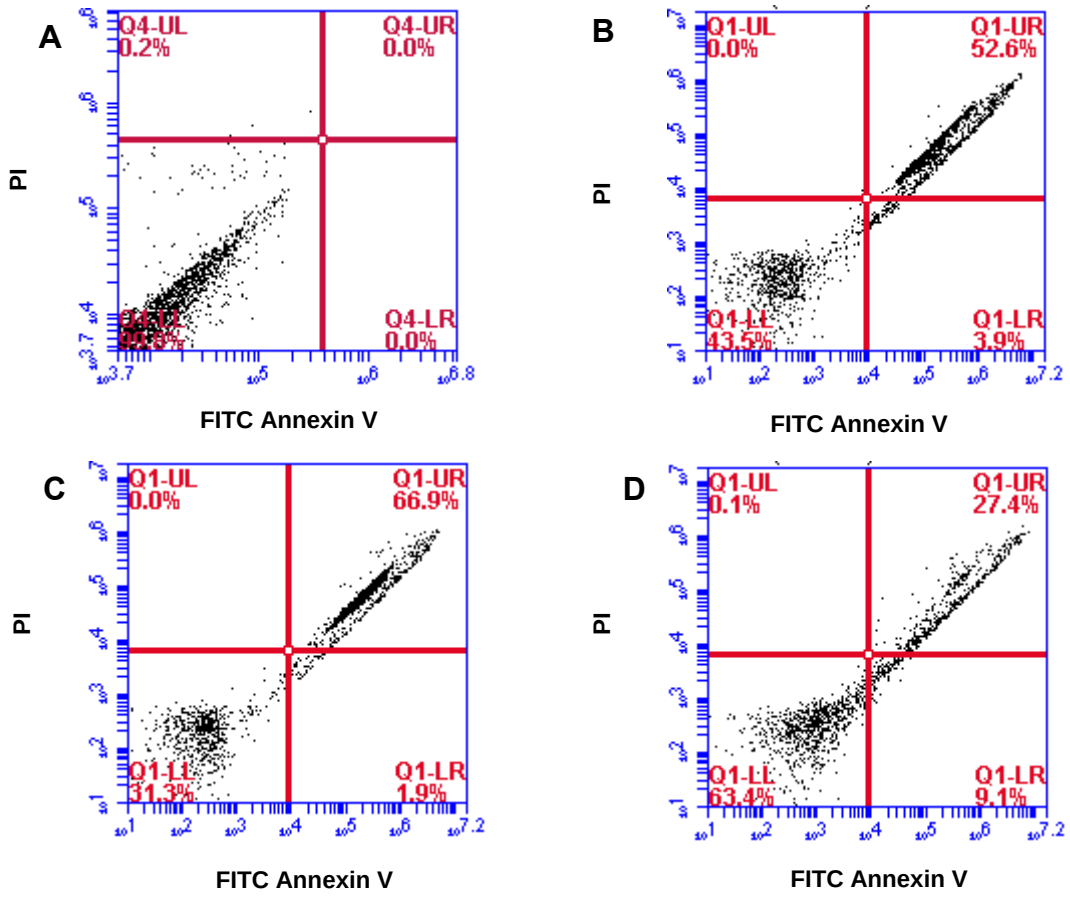

Figure 3.62 Representative FITC Annexin V/PI flow cytometric dot-plots of MCF-7 cancer cells after 24 post-PDT treatment. (A) Untreated control cells, (B) MCF-7 cells after photosensitization with 20 µg/ml of GaPcCl and photoactivation with a treatment light dose of 2.5 J/cm^2, (C) MCF-7 cells after photosensitization with 2 µg/ml of InPcCl and photoactivation with a treatment light dose of 2.5 J/cm^2, (D) MCF-7 cells after photosensitization with 8 µg/ml of FePcCl and photoactivation with a treatment light dose of 2.5 J/cm^2. Percentage (%) of viable cells, early apoptotic cells, late apoptotic cells and cellular debris are shown in the lower left, lower right, upper left and upper right quadrant respectively.

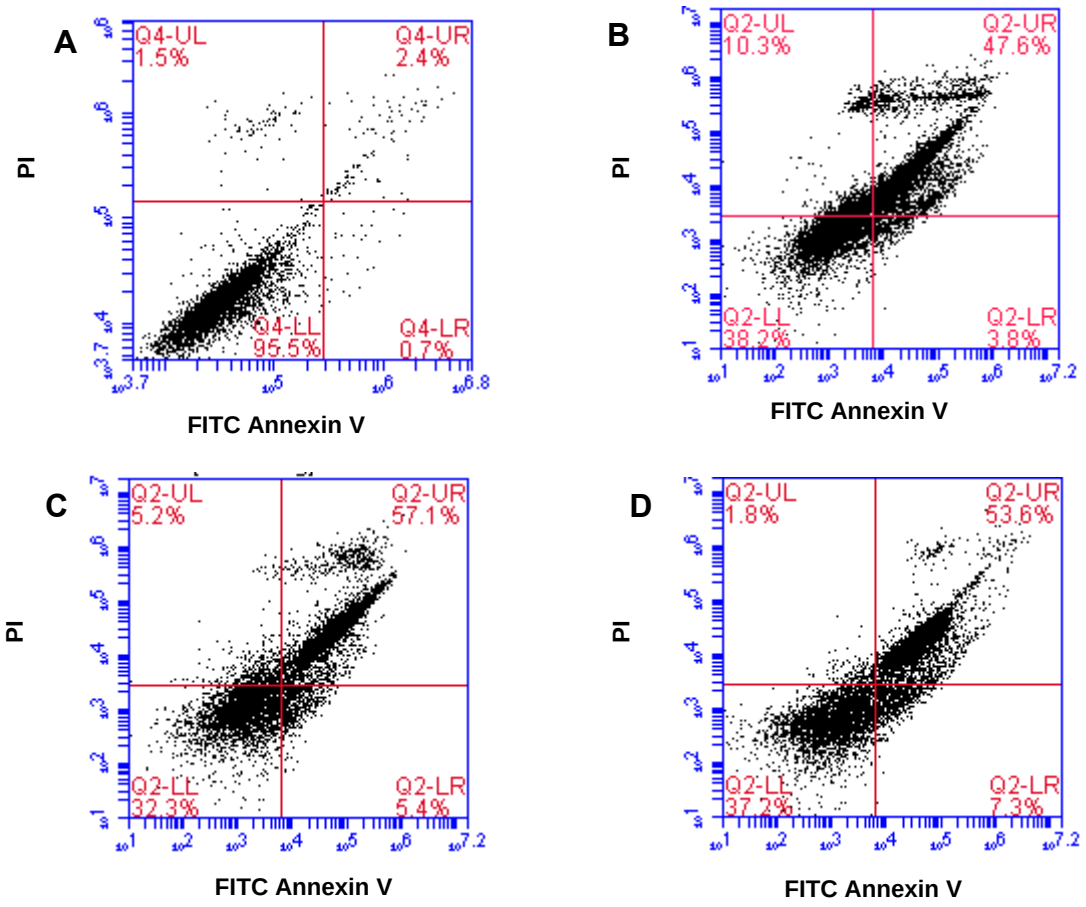

Figure 3.63 Representative FITC Annexin V/PI flow cytometric dot-plots of melanoma cancer cells after 24 post-PDT treatment. (A) Untreated control cells, (B) melanoma cells after photosensitization with 40 µg/ml of GaPcCl and photoactivation with a treatment light dose of 2.5 J/cm^2, (C) melanoma cells after photosensitization with 6 µg/ml of InPcCl and photoactivation with a treatment light dose of 2.5 J/cm^2, (D) melanoma cells after photosensitization with 8 µg/ml of FePcCl and photoactivation with a treatment light dose of 2.5 J/cm^2. Percentage (%) of viable cells, early apoptotic cells, late apoptotic cells and cellular debris are shown in the lower left, lower right, upper left and upper right quadrant respectively.

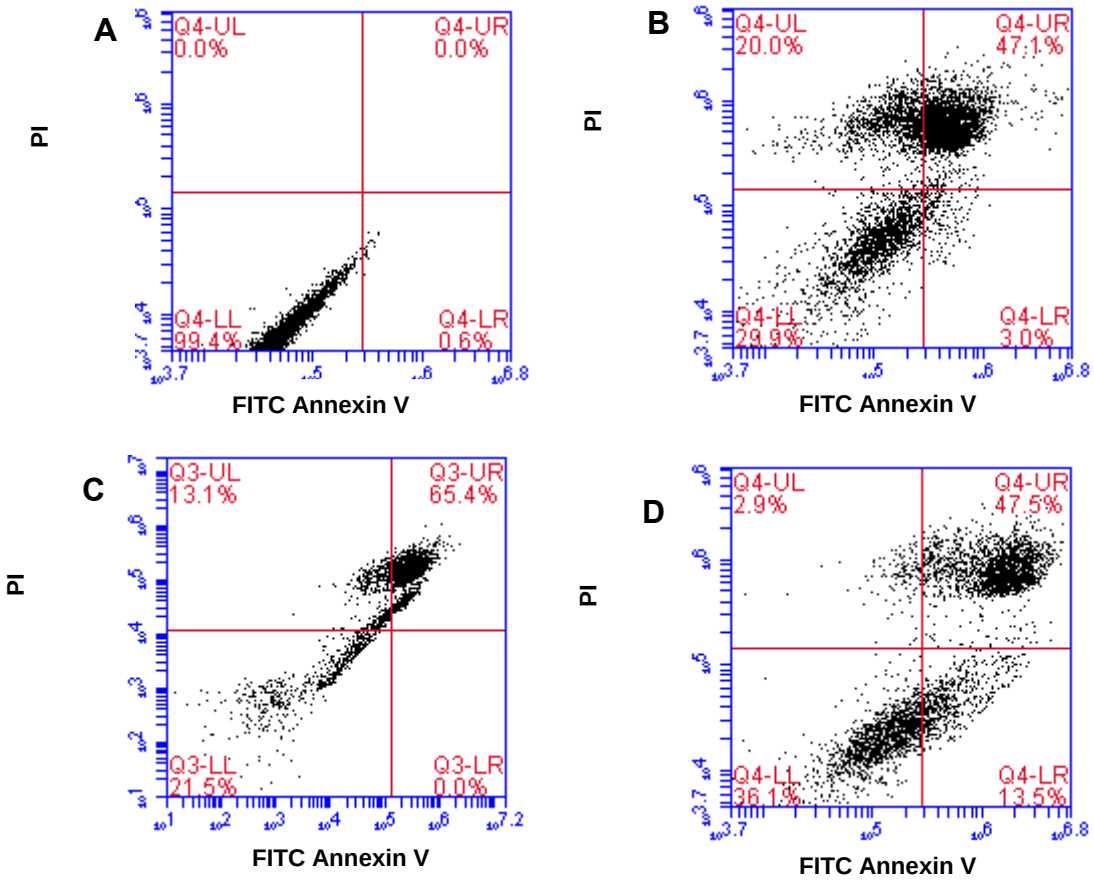

Figure 3.64 Representative FITC Annexin V/PI flow cytometric dot-plots of A549 cancer cells after 24 post-PDT treatment. (A) Untreated control cells, (B) A549 cells after photosensitization with 2 µg/ml of GaPcCl and photoactivation with a treatment light dose of 2.5 J/cm^2, (C) A549 cells after photosensitization with 2 µg/ml of InPcCl and photoactivation with a treatment light dose of 2.5 J/cm^2, (D) A549 cells after photosensitization with 2 µg/ml of FePcCl and photoactivation with a treatment light dose of 2.5 J/cm^2. Percentage (%) of viable cells, early apoptotic cells, late apoptotic cells and cellular debris are shown in the lower left, lower right, upper left and upper right quadrant respectively.

3.8 SUBCELLULAR LOCALIZATION OF PHOTOSENSTIZERS

The effective uptake of GaPcCl, InPcCl and FePcCl as well as its initial sites of localization in Caco-2, MCF-7, melanoma and A549 cancer cells after 2 h incubation period are shown in Figures 3.65 – 3.72. Each of the different types of cancer cells were stained with mitotracker, lysotracker and DAPI dyes to detect nucleus, mitochondria and lysosomes respectively. The fluorescent patterns of each of the organelle dyes were compared to the fluorescent patterns of cancer cells treated with GaPcCl, InPcCl and FePcCl to identify the localization site of each of these photosensitizers.

The micrographs in Figure 3.65 and Figure 3.66 revealed that GaPcCl, InPcCl and FePcCl localized in mitochondria and lysosomes of the Caco-2 cancer cells. Similarly, the same PSs also localized in mitochondria and lysosomes of the MCF-7 (Figure 3.67 – Figure 3.68) and A549 (Figure 3.71 – Figure 3.72) cancer cells. Also, all three PSs seem to have localized in the mitochondria of melanoma cancer cells as shown in Figure 3.69. However, there was no evidence of GaPcCl (Figure 3.70) and FePcCl (Figure 3.70) localization in lysosomes of melanoma cancer cells. In addition, InPcCl localized to greater extent in lysosomes (Figure 3.70, B) than mitochondria (Figure 3.69, B) of melanoma cancer cells.

Thus, the fluorescent patterns observed in this *in vitro* study indicate that GaPcCl, InPcCl and FePcCl localize in both the mitochondria and lysosomes at different degrees in three of the cancer (Caco-2, MCF-7 and A549) cell lines. These PSs also localized in the mitochondria of melanoma cancer cells. Results also indicated that GaPcCl, InPcCl and FePcCl didn’t localize in nucleus of all four cancer cell lines.

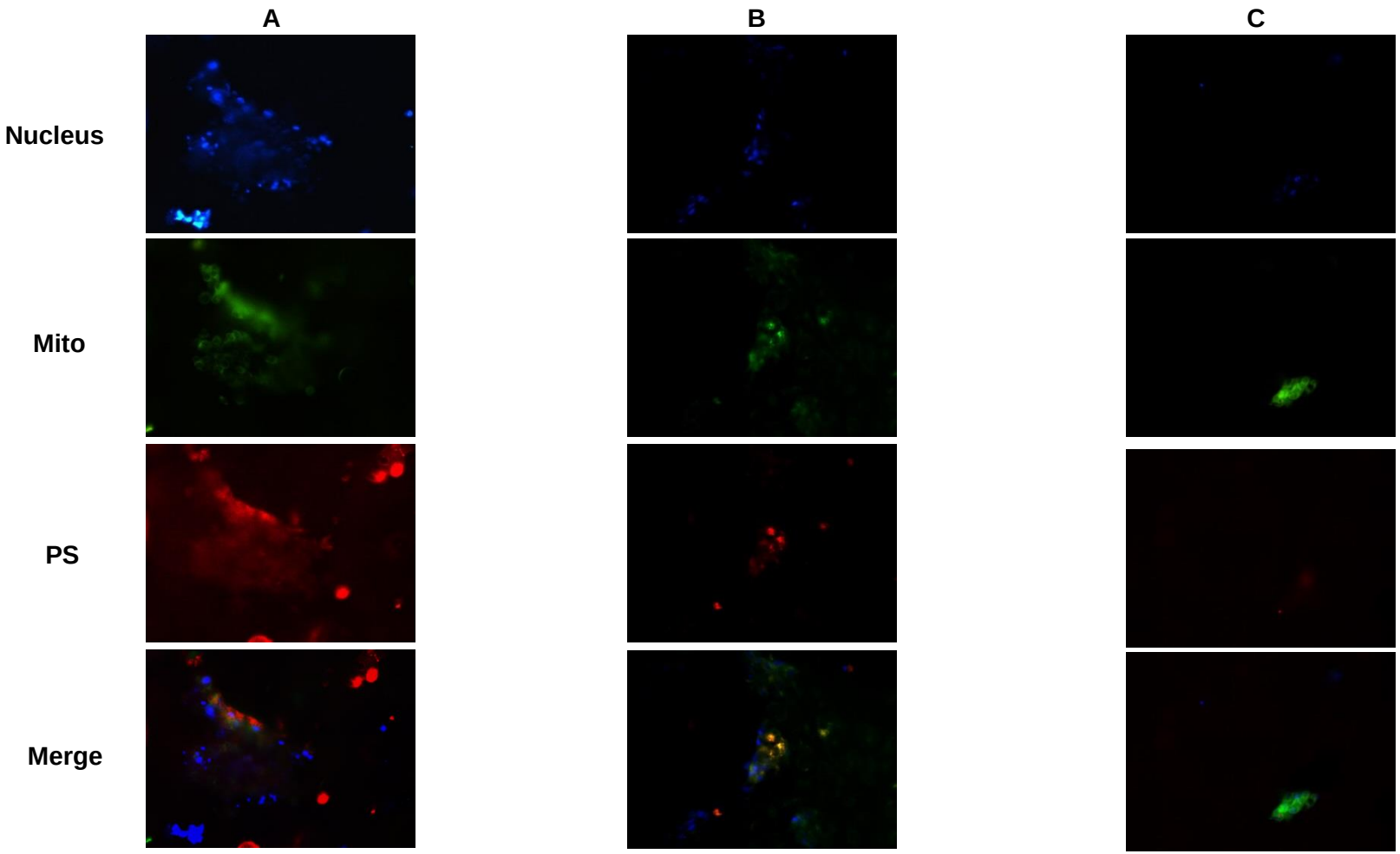

Figure 3.65 Mitochondrial localization of 100 µg/ml of (A) GaPcCl, (B) InPcCl, (C) FePcCl in Caco-2 cancer cells. DAPI stained nuclei (blue - nucleus); mitotracker stained mitochondria (green – mito) and PSs localized in the mitochondria (red – PS). Fluorescence distribution patterns of PSs are similar to that of the mitotracker. Magnification = 40 x. Scale bar = 20 µm

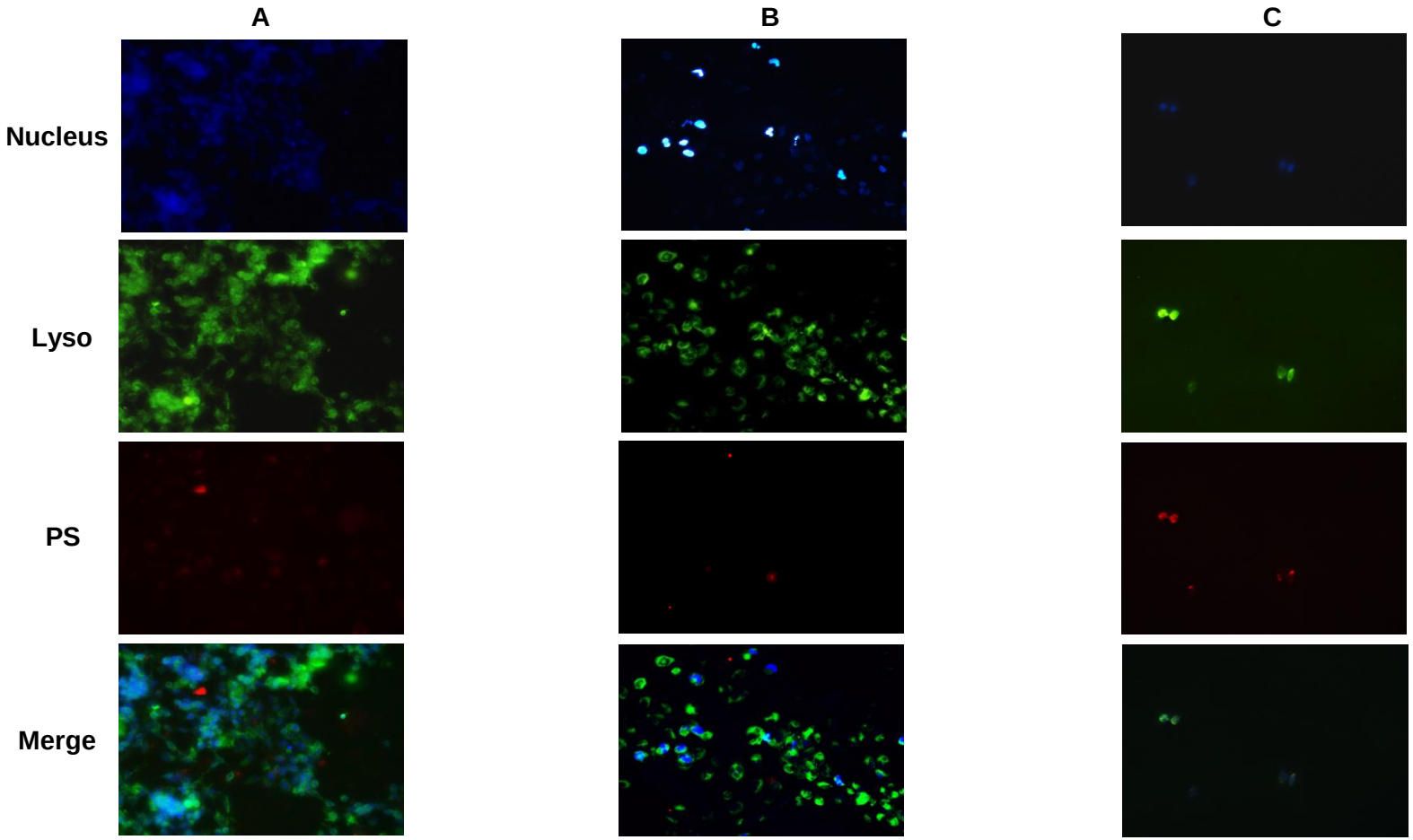

Figure 3.66 Lysosomal localization of 100 µg/ml of (A) GaPcCl, (B) InPcCl, (C) FePcCl in Caco-2 cancer cells. DAPI stained nuclei (blue - nucleus); lysotracker stained lysosome (green – lyso) and PSs localized in the lysosome (red – PS). Fluorescence distribution patterns of photosensitizers are similar to that of the lysotracker. Magnification = 40 x.

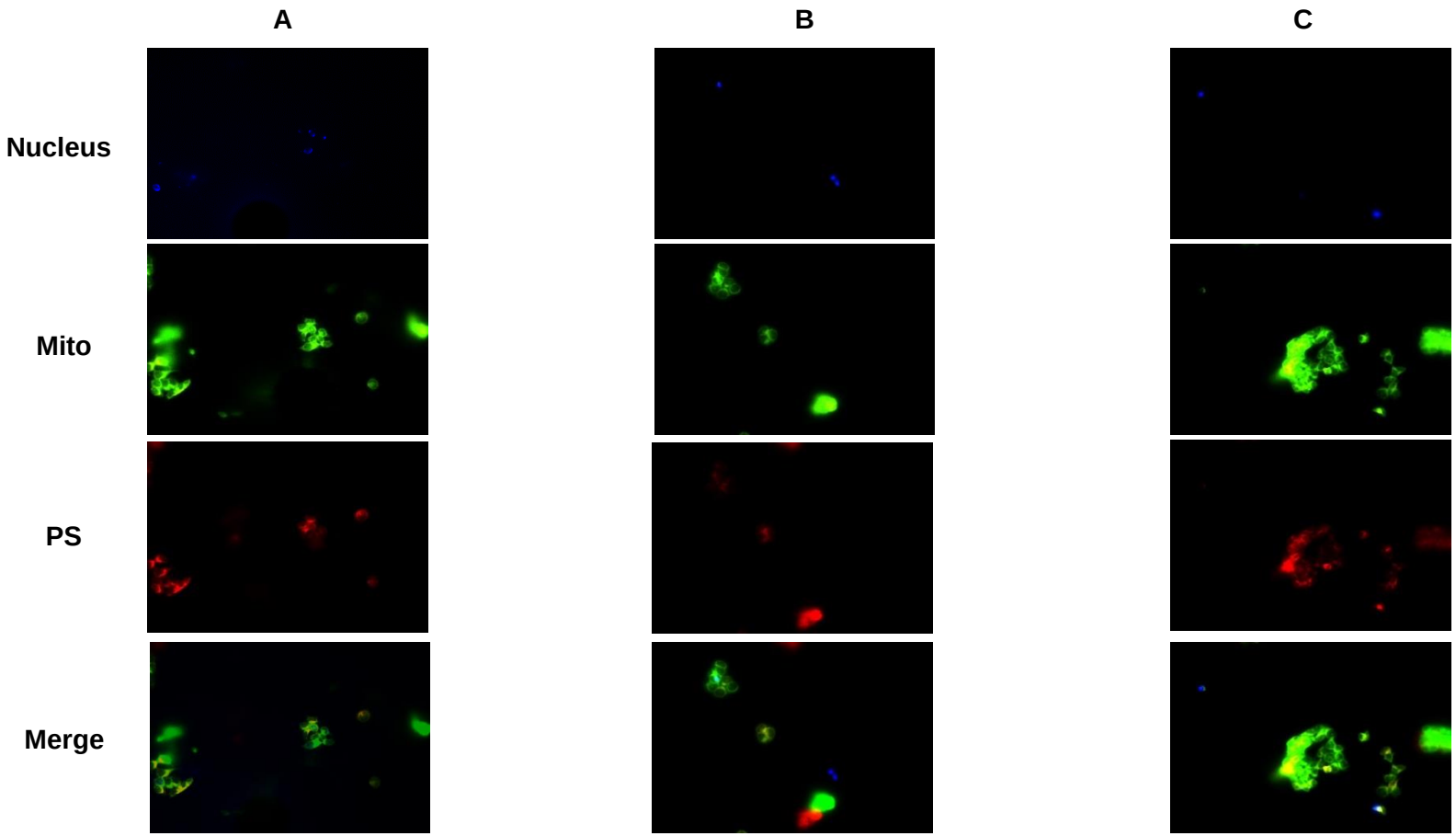

Figure 3.67 Mitochondrial localization of 100 µg/ml of (A) GaPcCl, (B) InPcCl, (C) FePcCl PSs in MCF-7 cancer cells. DAPI stained nuclei (blue - nucleus); mitotracker stained mitochondria (green – mito) and PSs localized in the mitochondria (red – PS). Fluorescence distribution patterns of PSs are similar to that of the mitotracker. Magnification = 40 x. Scale bar = 15 µm.

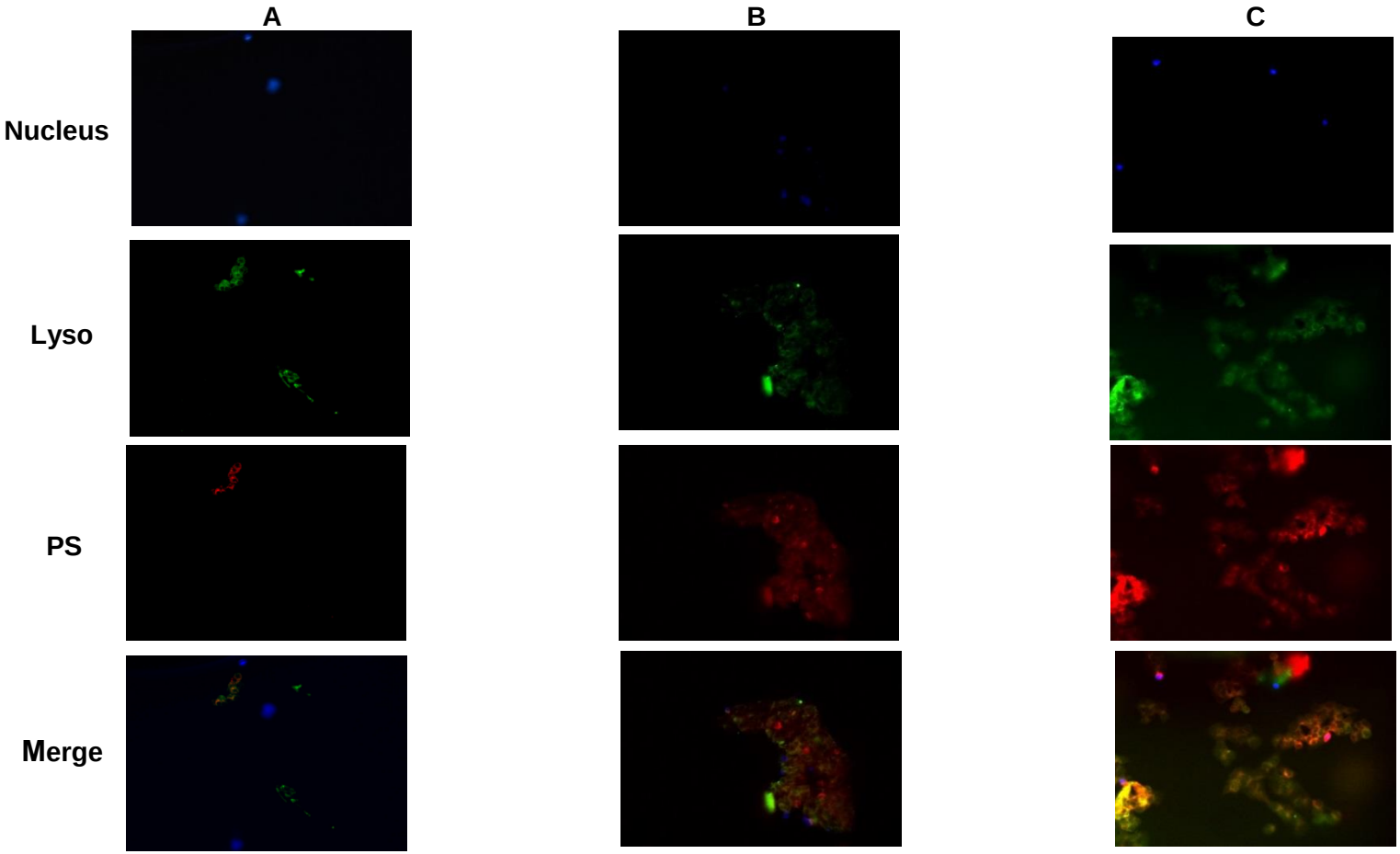

Figure 3.68 Lysosomal localization of 100 µg/ml of (A) GaPcCl, (B) InPcCl, (C) FePcCl MCF-7 cancer cells. DAPI stained nuclei (blue - nucleus); lysotracker stained lysosome (green – lyso) and PSs localized in the lysosome (red – PS). Fluorescence distribution patterns of PSs are similar to that of the lysotracker. Magnification = 40 x.

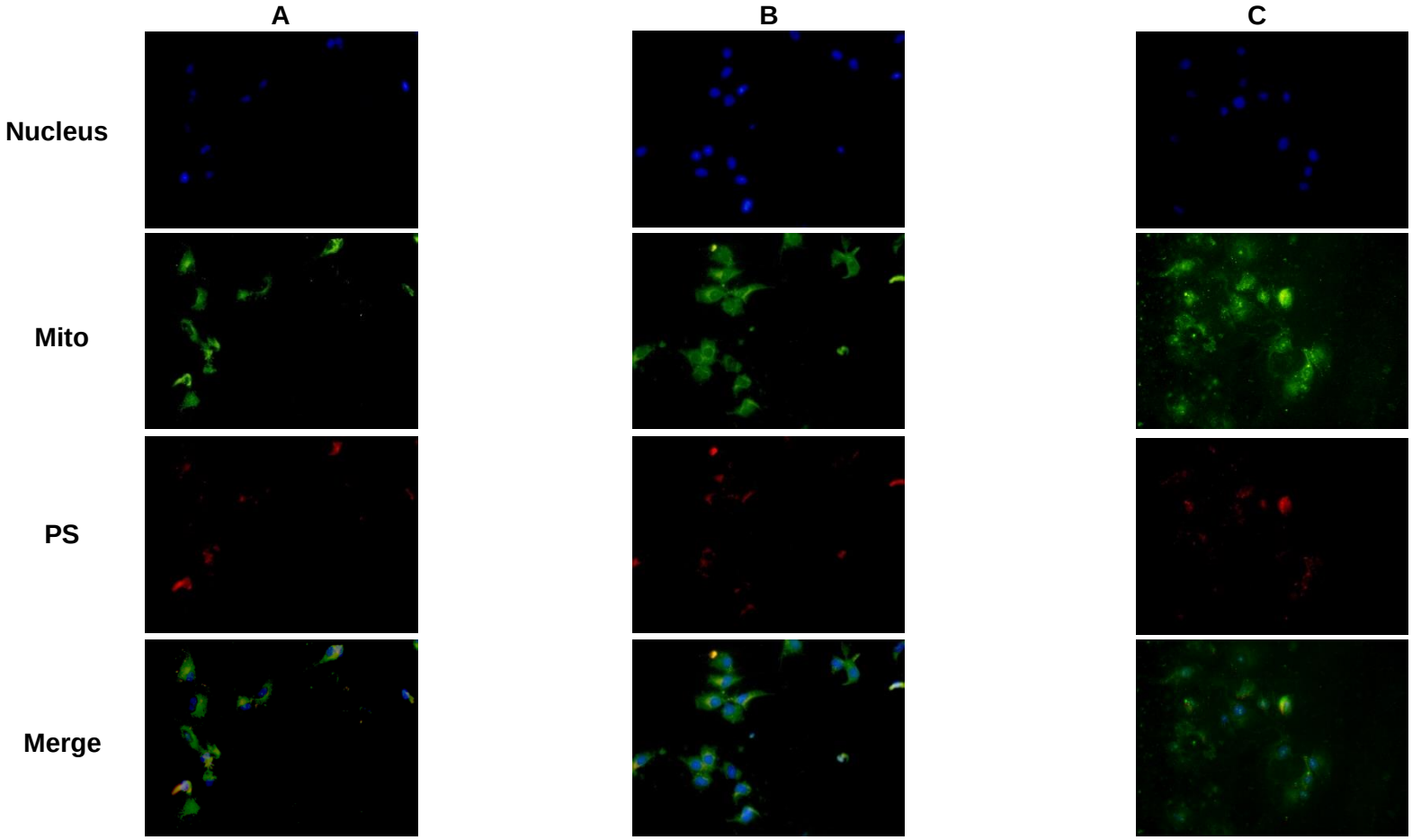

Figure 3.69 Mitochondrial localization of 100 µg/ml of (A) GaPcCl, (B) InPcCl, (C) FePcCl in melanoma cancer cells. DAPI stained nuclei (blue - nucleus); mitotracker stained mitochondria (green – mito) and PSs localized in the mitochondria (red – PS). Fluorescence distribution patterns of PSs are similar to that of the mitotracker. Magnification = 40 x. Scale bar = 40 µm.

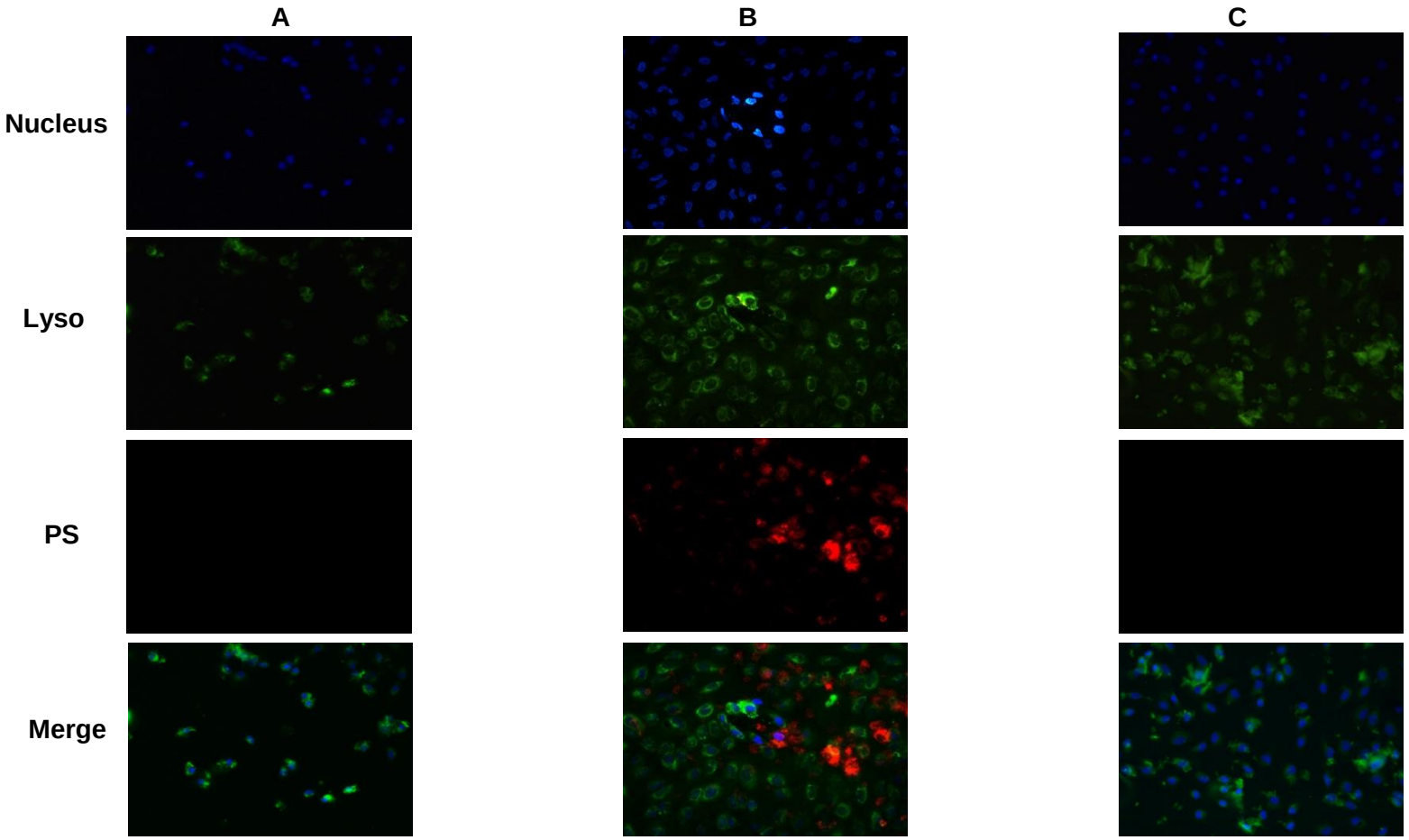

Figure 3.70 Lysosomal localization of 100 µg/ml of (A) GaPcCl, (B) InPcCl, (C) FePcCl PSs in melanoma cancer cells. DAPI stained nuclei (blue - nucleus); lysotracker stained lysosome (green – lyso) and PSs localized in the lysosome (red – PS). Fluorescence distribution pattern of FePcCl is similar to that of the lysotracker. Magnification = 40 x.

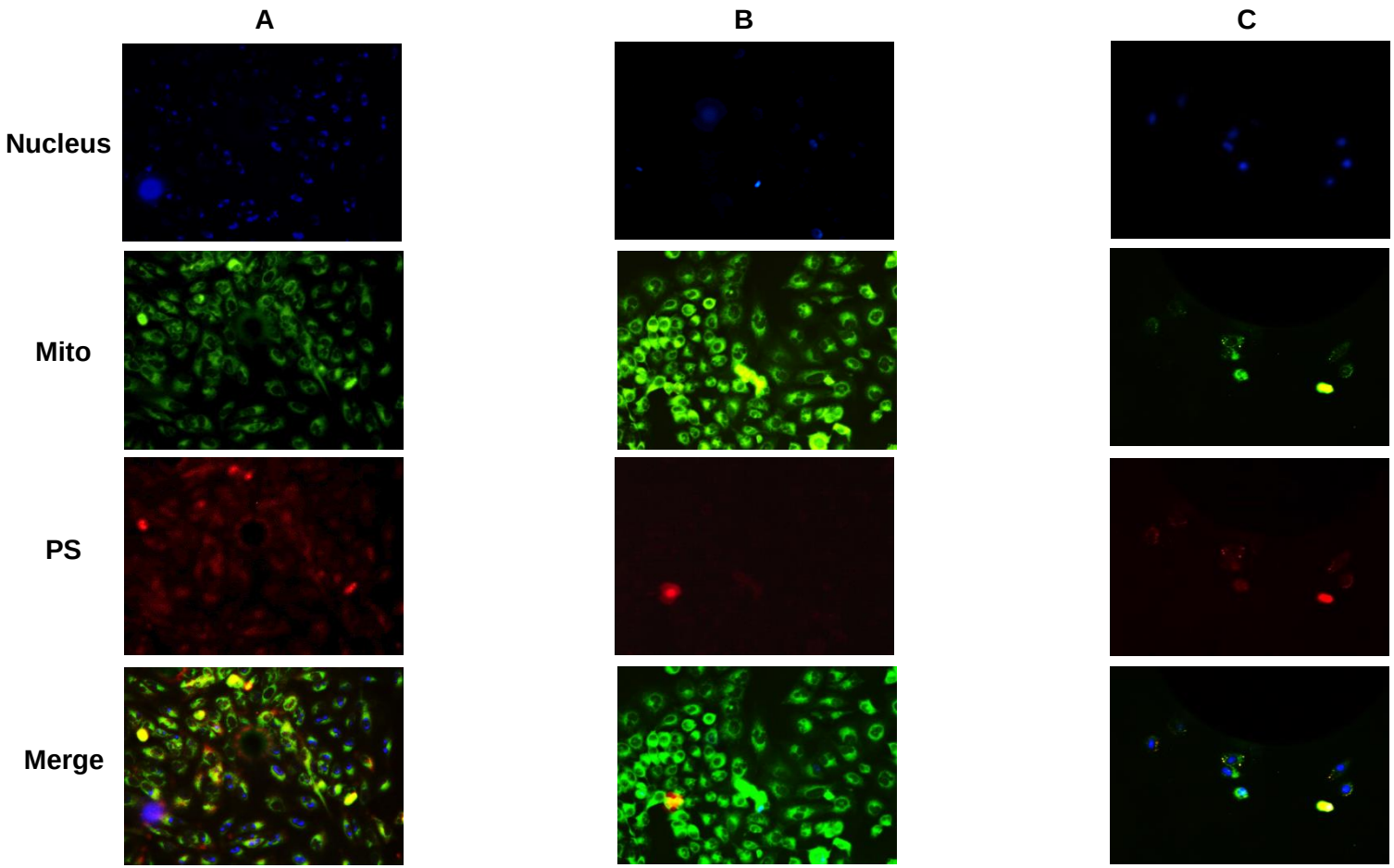

Figure 3.71 Mitochondrial localization of 100 µg/ml of (A) GaPcCl, (B) InPcCl, (C) FePcCl in A549 cancer cells. DAPI stained nuclei (blue - nucleus); mitotracker stained mitochondria (green – mito) and PSs localized in the mitochondria (red – PS). Fluorescence distribution pattern of PSs is similar to that of the mitotracker. Magnification = 40 x. Scale bar = 20 µm.

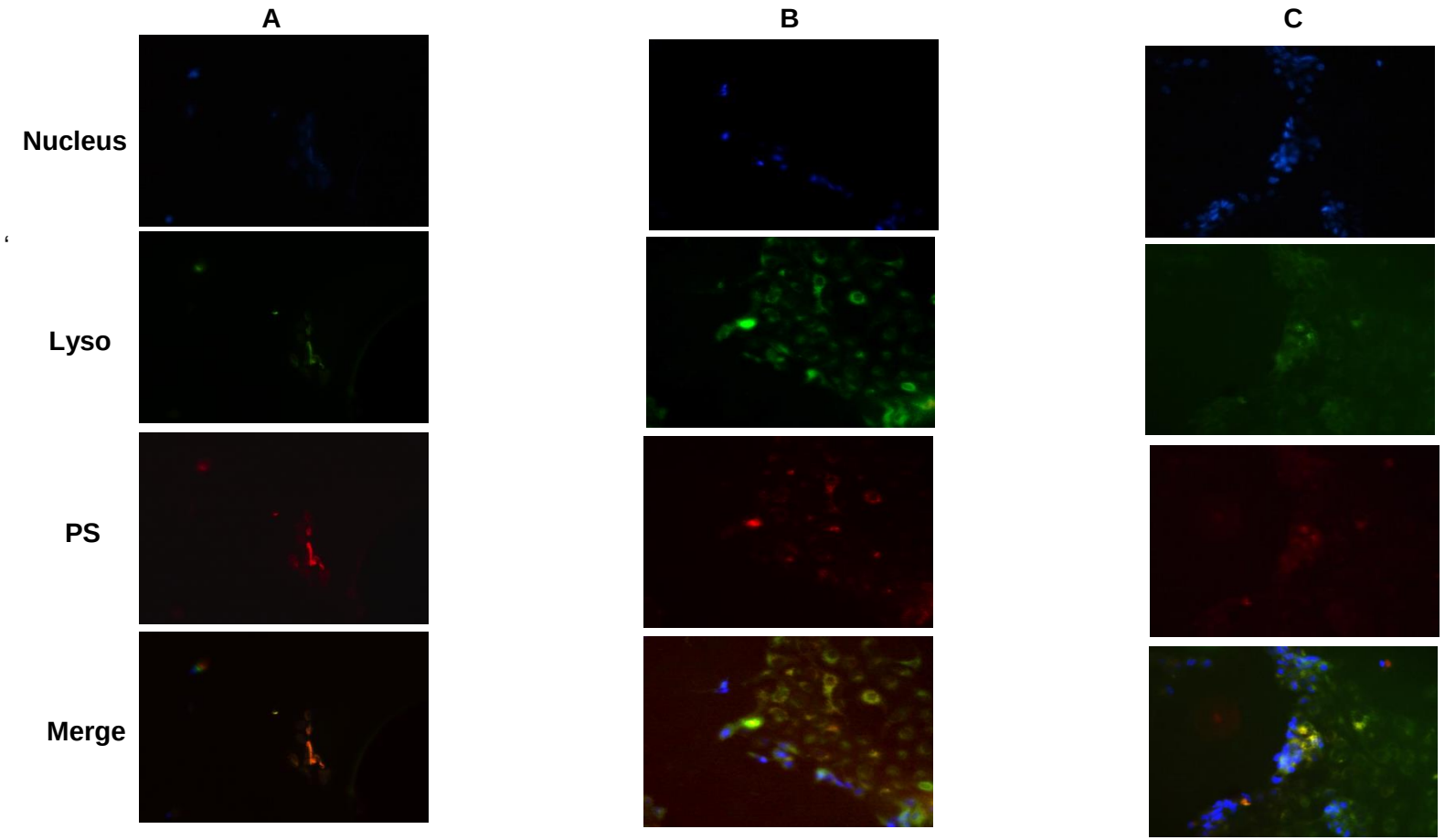

Figure 3.72 Lysosomal localization of 100 µg/ml of (A) GaPcCl, (B) InPcCl, (C) FePcCl in A549 cancer cells. DAPI stained nuclei (blue - nucleus); lysotracker stained lysosome (green – lyso) and PSs localized in the lysosome (red – PS). Fluorescence distribution pattern of PSs is similar to that of the lysotracker. Magnification = 40 x.

CHAPTER 4

DISCUSSION

PDT is a less invasive, painless procedure employed as an alternative to chemotherapy or radiotherapy. Due to the potential disadvantages of most approved PDT photosensitizing agents, establishment of promising second-generation photosensitizing agents is clinically required. From a pharmaceutical and clinical point of view the composition, stability, peak absorption wavelength, selective uptake by cancer cells, low dark toxicity of PSs and low administration concentrations must be taken into consideration when choosing appropriate photosensitizing agents for PDT.

In vivo, the PDT effect at the tumor site depends on the concentration of the PS and the radiant energy density at the site which together determines the energy absorbed per unit volume at the target site. Therefore, knowledge regarding different treatment light doses and different concentrations of PS is essential for safe and effective treatment. Also, influence of the different PS concentrations and treatment light doses on the cancer cells as well as healthy normal cells needs to be evaluated.

In literature, Prof Nyokong and her research group at Rhode University has defined, studied and reported on the characteristics of Pcs and many metal-based Pc complexes (Nyokong, 2007, Nyokong, 2011, Sekkat et al., 2011). These reports highlight the good stability (photochemical and chemical) and photophysical properties of Pcs including different metal-based Pc complexes. For example, Pc complexes containing transition metals such as Fe offer a photosensitizing agent with short lifetimes. Whereas, Pc complexes containing diamagnetic ions such as Ga have high triplet quantum yields and long triplet lifetimes. Also, large metal ions such as In Pc complexes have high triplet and

singlet oxygen quantum yields which are valuable for PDT treatment. A high triplet and singlet oxygen quantum yields are important for efficient PDT treatment, and so that the PSs can also be administrated at lower concentrations.

This study demonstrates that PDT following photosensitization using these PSs (low and high concentrations) is able to directly photokill Caco-2 (colon), MCF-7 (breast), melanoma (skin) and A549 (lung) cancer cells *in vitro*. Our results confirm previous studies that demonstrate that metal-based Pcs are effective photosensitizing agents in PDT for the eradication of cancerous cells (Refer to Table 1.3).

The measured peak absorbance of the photosensitizing agent GaPcCl, InPcCl and FePcCl were 678 nm, 685 nm and 675 nm respectively. PSs that are capable of absorbing light at these wavelengths display deep tissue penetration. Thus, PSs with this feature is considered clinically beneficial for it can be used for PDT of superficial tumors as well as for large or deep-seated tumors.

In Caco-2 cells, inactive FePcCl was not toxic (dark toxicity assay) at low concentrations (2 µg/ml – 10 µg/ml) but laser treatment reduced cell viability to as low as 30%, and this reduction at all concentrations dependent on the laser treatment time. These findings correlate very well with our initial results that showed best uptake of FePcCl, followed GaPcCl and least uptake of InPcCl by Caco-2 cancer cells. Although, GaPcCl uptake was slightly lower than FePcCl by Caco-2 cancer cells, it seem toxic at all concentrations in its inactive form. InPcCl was taken up at low levels and displayed low toxic effects in its inactive form. PDT treatment with InPcCl was more effectively in reducing cell survival of Caco-2 cells than activated GaPcCl. While all three Pcs in its inactive form negatively affected MCF-7 cell viability, GaPcCl was the least toxic to MCF-7 cells (dark toxicity

assay). PDT treated with GaPcCl had very little additional effects on these cells, other than FePcCl or InPcCl, but then only with longer laser treatment times. FePcCl was best absorbed by MCF-7 cancer cells, followed by GaPcCl and InPcCl was least absorbed by MCF-7 cancer cells. However, InPcCl and FePcCl were the most effective upon illumination in decreasing the survival rate of MCF-7 cancer cells.

Both InPcCl and FePcCl were very effective in reducing viability of melanoma cells after PDT treatment, especially highlighted by the fact that high levels of survival was observed in this cell line when exposed to the inactive InPcCl and FePcCl. Increasing the light doses to activate InPcCl and FePcCl proportionally decreased the cell viability of melanoma cancer cells. Uptake results indicated that both InPcCl and FePcCl were taken up in lower amounts than GaPcCl by melanoma cancer cells. The best results were obtained with all three PSs in A549 cells. Inactive GaPcCl, InPcCl and FePcCl seemed to have low toxicity in these cells, especially at low concentrations. However, at all concentrations and even with the shortest illumination periods, the increase in cell death was a minimum of 60% with further reduction in cell viability with longer illumination periods. FePcCl mediated PDT was able to reduce cell survival to 0% with concentrations ranging from 40 µg/ml – 80 µg/ml in combination with laser treatment times of 39 sec and 74 sec. Similarly, 20 µg/ml of FePcCl activated for 22 sec resulted in no surviving A549 cancer cells (lung). While all three PSs gave excellent PDT results, the uptake patterns varied. FePcCl showed the best uptake, GaPcCl lower uptake than FePcCl and InPcCl displayed the lowest uptake by A549 cancer cells.

GaPcCl (100 µg/ml) showed the best uptake by healthy normal fibroblast cells. For the dark toxicity assay cell viability was at 57% after treatment with GaPcCl (100 µg/ml) only. At the same photosensitizing concentration of GaPcCl (100 µg/ml) after PDT with

increasing light treatment doses, viability dropped to 25%. InPcCl and FePcCl (100 µg/ml) had a low uptake by fibroblast cells. Even with low uptakes of inactive InPcCl and FePcCl, Subsequently, illumination with various time periods resulted in similarly low survival rate of fibroblast cells. This is an indication that InPcCl and FePcCl is also toxic to normal fibroblast cells at high concentrations. Fibroblast cells, when treated with low concentrations (2 µg/ml – 8 µg/ml) of inactive InPcCl and FePcCl, were least affected compared to GaPcCl. Upon illumination for 22 sec, 39 sec and 74 sec survival remained well above 75%, 64% and 64%. The type of metal-based Pc chloride complex, the concentration and light dose largely influenced the survival rate of the healthy normal fibroblast cells.

Overall, these *in vitro* PDT results indicate that the efficacy of metal-based Pc chloride complexes mediated PDT photokilling of cancer cells is dependent on the type of metal-based PS being selected, PS concentration administrated and the treatment light doses applied. Results also indicate that GaPcCl, InPcCl and FePcCl exhibit dark toxicity which can be minimized by using low concentrations of the PS and considering shorter photosensitizing incubation times during PDT treatment. As literature states that the use of low PS concentrations can be the key solution to minimize or eradicate any dark cytotoxicity that can be initiated by the PS in its inactive state (without laser activation) to cancerous and healthy normal surrounding tissue (Castano *et al*., 2005). Also, the exposure or incubation time of PS with cells before laser treatment can be decreased to minimize its dark cytotoxicity effects on cells (Decréau *et al*., 1999).

PDT treatment can lead to three forms of cell death, namely apoptosis, necrosis and autophagy (Mroz *et al*., 2011, Kessel, 2006, Castano *et al*., 2004, Chiaviello *et al*., 2011). The cell death and main damages induced by PDT depends on the type of PSs being

used and where those PSs localize within the cell (Mroz *et al*., 2011; Kessel, 2006; Castano *et al*., 2004; Chiaviello *et al*., 2011). Mitochondria have been found to be a very important and common subcellular target for many photosensitizing agents used in PDT. Many photosensitizing agents that localize in the mitochondria tend to trigger apoptosis by mitochondrial damage after laser treatment. Recently, lysosomes were proposed to be a critical intracellular target for localization of PSs. It has been reported that several PSs target autophagy-related organelles such as lysosomes and endosomes (Mroz *et al*., 2011). Also, PSs that localize in the lysosome activate apoptotic pathways via mitochondrial destabilization following the damage of lysosomes during PDT. PSs localizing in plasma membrane, Golgi apparatus and endoplasmic reticulum were found to be relatively uncommon in the PDT (Castano *et al*., 2004).

Literature also states that autophagy may play a role in PDT induced apoptosis and that these two processes can also occur independently of one another (Mroz *et al*., 2011). This simple role is to promote cell death in PDT treated cells. An *in vitro* study conducted on murine leukaemia cells (L1210) found signs of autophagy occurring immediately before apoptosis (Mroz *et al*., 2011). Based on results from other PDT studies with various cancer cell lines and different photosensitizers it can be concluded that PDT directly induces autophagy; and that apoptosis often occurs in cells that are already undergoing autophagy as a result of PDT (Mroz *et al*., 2011). The rates of autophagy and apoptosis largely depends on the type of cancer cell, photosensitizer and treatment light dose applied. In cells that are capable to undergoing apoptosis, autophagy is known to enhance the destructive effects of PDT by recycling damaged organelles (Mroz *et al*., 2011). This shows a close link between induced cell death modes and localisation of PS in the various organelles.

There were observable morphological changes between untreated control cells and PDT treated cancer cells as well as PDT treated healthy normal fibroblast cells. The treated cancer cells showed features of apoptosis (programmed cell death) which was not prominent in untreated control cancer cells. Features of apoptosis like the occurrence of scattered single cells indicate that treated cancer cells lost contact with and detached from neighbouring cells due to cell shrinkage. Micrographs indicating apoptotic characteristics (blebbing) in MCF-7 cancer cells treated with 2 µg/ml or 100 µg/ml of GaPcCl in combination with 22 sec, 39 sec or 74 sec of laser treatment. Blebbing was also seen in MCF-7 cancer cells treated with 2 µg/ml or 100 µg/ml of GaPcCl in combination with 22 sec, 39 sec or 74 sec of laser treatment. Melanoma cancer cells treated with GaPcCl, InPcCl or FePcCl mediated PDT also displayed apoptotic blebbing. The formation of apoptotic bodies were revealed in melanoma cancer cells PDT treated with GaPcCl (100 µg/ml) and 22 sec or 39 sec or 74 sec of laser treatment; InPcCl (100 µg/ml) and 74 sec of laser treatment; FePcCl (2 µg/ml) and 74 sec of laser treatment; and FePcCl (100 µg/ml) and 22 sec, 39 sec or 74 sec of laser treatment. The formation of apoptotic bodies were also seen with Caco-2 cancer cells after treatment with 100 µg/ml of InPcCl and 74 sec of laser treatment. These apoptotic morphology changes were also observed for some of the PDT treated fibroblast cells (healthy normal cells). Fibroblast cells photosensitized with 2 µg/ml of GaPcCl, InPcCl or FePcCl and laser treated for 22 sec, 39 sec or 74 sec showed no changes in cell morphology when compared to untreated cell controls. Whereas, PDT treated fibroblast cells treated with 100 µg/ml of GaPcCl, InPcCl or FePcCl and laser treated for 22 sec, 39 sec or 74 sec showed profound changes in cell morphology. These changes included rounding of cells, shrinking of cells, blebbing and cells detaching from neighboring cells. Therefore, the evidence of cell shrinkage, blebbing and formation of apoptotic bodies confirms that PDT treatment mediated by

photosensitization with GaPcCl, InPcCl and FePcCl can effectively kill cancer cells via programmed cell death known as apoptosis.

Micrographs also confirmed that PDT is a concentration-dependent treatment because as the photosensitizing concentration of GaPcCl, InPcCl and FePcCl increased (from 2 µg/ml to 100 µg/ml) with a constant treatment light dose of 2.5 J/cm^2 (22 sec) a proportional decrease in cancer cell numbers were seen. It was also observed that PDT is a light dose-dependent treatment because increased treatment light doses of 4.5 J/cm^2 (39 sec) and 8.5 J/cm^2 (74 sec) enhanced PDT killing of cancer cells.

The morphological appearance of cancer cells undergoing apoptosis are both defined and precise (Allen *et al*., 1997). All experimentation, which intends on qualifying mode of cell death should include TEM work (Allen *et al*., 1997). TEM is the only definitive method to detail ultrastructural changes occurring in dying cell undergoing apoptosis, necrosis or autophagy (Allen *et al*., 1997). TEM micrographs shown intact nucleus and intact cytoplasm for the untreated control Caco-2, MCF-7, melanoma and A549 cancer cells. PDT treated Caco-2, melanoma and A549 cancer cells showed distinct apoptotic and autophagic features. These features include plasma membrane blebbing, spaces around the nucleus caused by irregular condensation of chromatin, nuclear blebs pinching off to from fragments or nucleus undergoing fragmentation and large number of autophagic vacuoles in cytoplasmic membrane. However, PDT treated MCF-7 cancer cells demonstrated apoptotic characteristics such as spaces around the nucleus, nuclear blebs are pinching off to from fragments or nucleus undergoing fragmentation and no autophagic features. This concludes on a positive note that GaPcCl, InPcCl and FePcCl mediated PDT induces apoptosis in MCF-7 cancer cells; and apoptosis simultaneously with

autophagy in the other three cancer cell lines (Caco-2, melanoma and A549 cancer cells) under *in vitro* conditions.

In addition to confirm and quantify this mode of cell death in PDT treated samples flow cytometric analysed using dual FITC Annexin V and propidium iodide staining was performed. After PDT treatment with GaPcCl, InPcCl and FePcCl the percentage of Caco-2 cells undergoing late apoptosis was 34.5%, 11.7% and 37.9% respectively. Similarly, melanoma cancer cells after GaPcCl, InPcCl and FePcCl mediated PDT treatment revealed late apoptosis populations of 45.2%, 54.7% and 51.2% respectively. PDT treatment with GaPcCl, InPcCl and FePcCl also revealed an early apoptosis population of 3.1%, 4.7% and 6.6% respectively. PDT treated MCF-7 cancer cells displayed similar results. MCF-7 cancer cells after GaPcCl, InPcCl and FePcCl mediated PDT treatment displayed late apoptosis populations of 52.6%, 66.9% and 27.4% respectively. The percentage of early apoptosis populations of 3.9%, 1.9% and 9.1% was seen with PDT treatment with GaPcCl, InPcCl and FePcCl accordingly. GaPcCl mediated PDT treated A549 cancer cells demonstrated an early apoptosis (2.4%) and late apoptosis (47.1%) populations. Whereas, PDT treatment with InPcCl showed a population of late apoptotic A549 cells (65.4%). Early apoptosis (12.9%) and late apoptosis (47.5%) were distinguished in A549 cells treated with laser activated FePcCl.

The fluorescence pattern in this *in vitro* study suggests that all three metal-based Pc chlorides (GaPcCl, InPcCl and FePcCl) localizes in both the mitochondria and lysosomes for the Caco-2 (colon cancer), MCF-7 (breast cancer) and A549 (lung cancer) cancer cell lines. Similar results using Zn phthalocyanine were found by (Manoto *et al*., 2012) in DLD-1 (colon) and A549 (lung) cell line, and (Tynga *et al*., 2013) in breast cancer cell line (MCF-7). Whereas, the mitochondria was the only primary site of localization for GaPcCl

and FePcCl for melanoma (skin cancer) cancer cell line. Our results (organelle localization) revealed that mitochondria and lysosomes in melanoma cancer cells are primary sites of InPcCl. These findings reveal that GaPcCl, InPcCl and FePcCl is taken and retained in the organelle or organelles of the cancer cells, and upon laser treatment induces cell death. Localization of GaPcCl, InPcCl and FePcCl in the mitochondria can lead to damage of mitochondrial ion pumps due to reactive oxygen species (ROS) formed during PDT, resulting in changes in the cytosolic calcium (Ca^{2+}) concentrations and result in irreversible apoptosis (Mroz et al., 2011). Therefore, PS localization in the mitochondria is known to be essential for PDT to be the most effective as compared to other organelles. PS localization to the lysosome results in lysosomal enzymes becoming inactivated before the membrane ruptures, allowing for specific targeting of the lysosome without causing damage to the rest of the cell. On the other hand, PSs that bind to lysosomal membranes causes it to rupture upon laser treatment. This releases proteases via mitochondria that can cause induction of apoptosis by cathespin-mediated cleavage of Bid. Therefore, PS localization in lysosome of cells can induce apoptosis or autophagy as cell death mechanisms (Mroz *et al*., 2011).

This *in vitro* PDT study demonstrated that GaPcCl, InPcCl and FePcCl are effective second-generation PSs due to its ability to localize in cellular organelles (mitochondria and lysosome) vital for cell function (mitochondria and lysosome); rapidly accumulates and once activated by red light at a long wavelength of 661 nm induces irreversible cell death (apoptosis) in four different cancer cell lines.

CHAPTER 5

CONCLUSION

This study concludes that low concentrations of GaPcCl, InPcCl and FePcCl activated with low light doses at a long wavelength of 661 nm can be used for the effective *in vitro* killing of different cancer cells. This enables pairing of these drugs to the appropriate cancer types for maximal PDT effect:

- GaPcCl was the best photosensitizing agent for the effective PDT killing of MCF-7 cancer cells (proliferative breast cancer cell line)
- InPcCl and FePcCl was more effective for the invasive cancer cell lines such as Caco-2 (colon), melanoma (skin) and A549 (lung).

The PDT effect of these metal-based Pc complexes also depends on the PS uptake, PS concentration, localization site of PS and light dose applied during treatment. The potential of inactive GaPcCl, InPcCl and FePcCl to induce dark toxicity effects at high concentrations and even low concentrations depends on the cell type. This can be minimized by decreasing the incubation periods (drug-light interval periods) with the PSs before laser treatment. Also, during PDT treatment with these PSs the damage to healthy normal cells can be prevented by using low light treatment doses (short illumination times), low PS concentrations and short drug-light interval periods. More recently, targeting strategies using nanotechnology have shown to increase affinity of the PSs for tumor tissue. Therefore, combining PDT principles with nanotechnology enhances specificity of the PSs and efficiency of PDT.

Metal-based Pc complexes are highly valued for its photodynamic properties. GaPcCl, InPcCl and FePcCl are starting to be explored as photosensitizing agents for PDT and

further investigations will be performed to understand fully the photodynamic mechanistic details stimulated by these metal-based Pc chloride complexes on other cancer cell lines. This small amount of data is encouraging and suggests that full scale studies should be conducted on other metal-based Pc complexes as possible photosensitizing agents for PDT. Presently, the obvious ways to improve PDT efficacy requires the development of new PSs, the use of nanotechnology techniques, precise dosimetry and optimization of protocols using second-generation PSs through ongoing *in vitro* and *in vivo* research. Therefore, PSs like metal-based Pcs can be of value to improve the current efficacy of PDT even further.

CHAPTER 6

REFERENCES

AGOSTINIS, P., BERG, K., CENGEL, K. A., FOSTER, T. H., GIROTTI, A. W., GOLLNICK, S. O., HAHN, S. M., HAMBLIN, M. R., JUZENIENE, A. & KESSEL, D. 2011. Photodynamic therapy of cancer: an update. CA: a cancer journal for clinicians, 61, 250-281.

AGOSTINIS, P., VANTIEGHEM, A., MERLEVEDE, W. & DE WITTE, P. A. 2002. Hypericin in cancer treatment: more light on the way international journal of biochemistry & cell biology, 34, 221-241.

ALISON, M. R. 2001. Cancer. Encyclopedia of Life Sciences. Nature Publisihing Group.

ALLEN, C. M., SHARMAN, W. M. & VAN LIER, J. E. 2001. Current status of phthalocyanines in the photodynamic therapy of cancer. Journal of Porphyrins and Phthalocyanines, 5, 161-169.

ALLEN, R. T., HUNTER III, W. J. & AGRAWAL, D. K. 1997. Morphological and biochemical characterization and analysis of apoptosis. Journal of pharmacological and toxicological methods, 37, 215-228.

ALLISON, R. R., DOWNIE, G. H., CUENCA, R., HU, X.-H., CHILDS, C. J. & SIBATA, C. H. 2004a. Photosensitizers in clinical PDT. Photodiagnosis and photodynamic therapy, 1, 27-42.

ALLISON, R. R., SIBATA, C., MANG, T. S., BAGNATO, V. S., DOWNIE, G. H., HU, X. H. & CUENCA, R. 2004b. Photodynamic therapy for chest wall recurrence from breast cancer. Photodiagnosis and Photodynamic Therapy, 1, 157-171.

ALLISON, R. R. & SIBATA, C. H. 2010. Oncologic photodynamic therapy photosensitizers: a clinical review. Photodiagnosis and photodynamic therapy, 7, 61-75.

ALY, H. A. 2012. Cancer therapy and vaccination. Journal of immunological methods, 382, 1-23.

ANDERSON, C. Y., FREYE, K., TUBESING, K. A., LI, Y. S., KENNEY, M. E., MUKHTAR, H. & ELMETS, C. A. 1998. A comparative analysis of silicon phthalocyanine photosensitizers for in vivo photodynamic therapy of RIF-1 tumors in C3H mice. journal of Photochemistry and Photobiology B: Biology, 67, 332-336.

BANFI, S., CARUSO, E., BUCCAFURNI, L., RAVIZZA, R., GARIBOLDI, M. & MONTI, E. 2007. Zinc phthalocyanines-mediated photodynamic therapy induces cell death in adenocarcinoma cells. Journal of organometallic chemistry, 692, 1269-1276.

BERLANDA, J., KIESSLICH, T., ENGELHARDT, V., KRAMMER, B. & PLAETZER, K. 2010. Comparative in vitro study on the characteristics of different photosensitizers employed in PDT. Journal of Photochemistry and Photobiology B: Biology, 100, 173-180.

CABUY, E. 2012. Photodynamic therapy in cancer treatment. Reliable Cancer Therapies. Energy - based therapies 3, 1-54.

ÇAMUR, M., AHSEN, V. & DURMUŞ, M. 2011. The first comparison of photophysical and photochemical properties of non-ionic, ionic and zwitterionic gallium (III) and indium (III) phthalocyanines. Journal of Photochemistry and Photobiology A: Chemistry, 219, 217-227.

CASTANO, A. P., DEMIDOVA, T. N. & HAMBLIN, M. R. 2004. Mechanisms in photodynamic therapy: part one—photosensitizers, photochemistry and cellular localization. Photodiagnosis and Photodynamic Therapy, 1, 279-293.

CELLI, J. P., SPRING, B. Q., RIZVI, I., EVANS, C. L., SAMKOE, K. S., VERMA, S., POGUE, B. W. & HASAN, T. 2010. Imaging and photodynamic therapy: mechanisms, monitoring, and optimization. Chemical reviews, 110, 2795-2838.

CHAN, W.-S., BRASSEUR, N., MADELEINE, G. L., QUELLET, R. & VAN LIER, J. 1997. Efficacy and mechanism of aluminium phthalocyanine and its sulphonated derivatives mediated photodynamic therapy on murine tumours. European Journal of Cancer, 33, 1855-1859.

CHAN, W., SVENSEN, R., PHILLIPS, D. & HART, I. 1986. Cell uptake, distribution and response to aluminium chloro sulphonated phthalocyanine, a potential anti-tumour photosensitizer. British journal of cancer, 53, 255.

CHAUKE, V., DURMUŞ, M. & NYOKONG, T. 2007. Photochemistry, photophysics and nonlinear optical parameters of phenoxy and tert-butylphenoxy substituted indium (III) phthalocyanines. Journal of Photochemistry and Photobiology A: Chemistry, 192, 179-187.

CHIAVIELLO, A., POSTIGLIONE, I. & PALUMBO, G. 2011. Targets and mechanisms of photodynamic therapy in lung cancer cells: a brief overview. Cancers, 3, 1014-1041.

CLAESSENS, C. G., BLAU, W. J., COOK, M., HANACK, M., NOLTE, R. J., TORRES, T. & WOÈHRLE, D. 2001. Phthalocyanines and phthalocyanine analogues: the quest for applicable optical properties. Monatshefte für Chemie/Chemical Monthly, 132, 3-11.

CUBEDDU, R., CANTI, G., D'ANDREA, C., PIFFERI, A., TARONI, P., TORRICELLI, A. & VALENTINI, G. 2001. Effects of photodynamic therapy on the absorption properties of disulphonated aluminium phthalocyanine in tumor-bearing mice journal of Photochemistry and Photobiology B: Biology, 60, 73-78.

DANIAL, N. N. & KORSMEYER, S. J. 2004. Cell death: Critical control points Cell 116, 205-219.

DE CASTROPAZOS, M., PACHECO-SOARES, C., SOARES DA SILVA, N., DAMATTA, R. A. & PACHECO, M. T. T. 2003. Ultrastructural effects of two phthalocyanines in CHO-K1 and HeLa cells after laser irradiation. Biocell, 27, 301-309.

DE OLIVEIRA, C. A., KOHN, L. K., ANTONIO, M. A., CARVALHO, J. E., MOREIRA, M. R., MACHADO, A. E. & PESSINE, F. B. 2010. Photoinactivation of different human tumor cell lines and sheep red blood cells in vitro by liposome-bound Zn (II) Phthalocyanine: Effects of cholesterol. Journal of Photochemistry and Photobiology B: Biology, 100, 92-99.

DECRÉAU, R., RICHARD, M. J., VERRANDO, P., CHANON, M. & JULLIARD, M. 1999. Photodynamic activities of silicon phthalocyanines against achromic M6 melanoma cells and healthy human melanocytes and keratinocyte. journal of Photochemistry and Photobiology B: Biology, 48, 48-56.

DOLMANS, D. E., FUKUMURA, D. & JAIN, R. K. 2003. Photodynamic therapy for cancer. Nature Reviews Cancer, 3, 380-387.

DURMUŞ, M., ERDOĞMUŞ, A., OGUNSIPE, A. & NYOKONG, T. 2009. The synthesis and photophysicochemical behaviour of novel water-soluble cationic indium (III) phthalocyanine. Dyes and Pigments, 82, 244-250.

DURMUŞ, M. & NYOKONG, T. 2007a. The synthesis, fluorescence behaviour and singlet oxygen studies of new water-soluble cationic gallium (III) phthalocyanines. Inorganic Chemistry Communications, 10, 332-338.

DURMUŞ, M. & NYOKONG, T. 2007b. Synthesis, photophysical and photochemical properties of tetra-and octa-substituted gallium and indium phthalocyanines. Polyhedron, 26, 3323-3335.

DURMUŞ, M. & NYOKONG, T. 2007c. Synthesis, photophysical and photochemical studies of new water-soluble indium (III) phthalocyanines. Photochemical & Photobiological Sciences, 6, 659-668.

ETHIRAJAN, M., CHEN, Y., JOSHI, P. & PANDEY, R. K. 2011. The role of porphyrin chemistry in tumor imaging and photodynamic therapy. Chemical Society Reviews, 40, 340-362.

FABRIS, C., SONCIN, M., MIOTTO, G., FANTETTI, L., CHITI, G., DEI, D., RONCUCCI, G. & JORI, G. 2006. Zn (II)-phthalocyanines as phototherapeutic agents for cutaneous diseases. Photosensitization of fibroblasts and keratinocytes. Journal of Photochemistry and Photobiology B: Biology, 83, 48-54.

GAO, L., QIAN, X., ZHANG, L. & ZHANG, Y. 2001. Tetra-trifluoroethoxyl zinc phthalocyanine: potential photosensitizer for use in the photodynamic therapy of cancer. Journal of Photochemistry and Photobiology B: Biology, 65, 35-38.

GLASSBERG, E., LEWANDOWSKI, L., LASK, G. & UITTO, J. 1990. Laser-induced photodynamic therapy with aluminum phthalocyanine tetrasulfonate as the photosensitizer: differential phototoxicity in normal and malignant human cells in vitro. Journal of investigative dermatology, 94.

GOMES, E., CRUZ, T., LOPES, C., CARVALHO, A. & DUARTE, C. 1999. Photosensitization of lymphoblastoid cells with phthalocyanines at different saturating incubation times. Cell biology and toxicology, 15, 249-260.

GROBOSCH, M., SCHMIDT, C., KRAUS, R. & KNUPFER, M. 2010. Electronic properties of transition metal phthalocyanines: The impact of the central metal atom (d^5 - d^{10}). Organic Electronics, 11, 1483-1488.

GUEDES, R. C. & ERIKSSON, L. A. 2005. Theoretical study of hypericin. Journal of Photochemistry and Photobiology A: Chemistry, 172, 293-299.

HASAN, T., ORTEL, B., MOOR, A. C. E. & POGUE, B. W. 2011. Photodynamic therapy of cancer. Radiation Oncology, 9, 605-622.

HAYWOOD-SMALL, S., VERNON, D., GRIFFITHS, J., SCHOFIELD, J. & BROWN, S. 2006. Phthalocyanine-mediated photodynamic therapy induces cell death and a G0/G1 cell cycle arrest in cervical cancer cells. Biochemical and biophysical research communications, 339, 569-576.

HORNE, T., ABRAHAMSE, H. & CRONJÉ, M. J. 2012. Investigating the efficiency of novel metallo-phthalocyanine PDT-induced cell death in MCF-7 breast cancer. Photodiagnosis and Photodynamic Therapy 9, 215-224.

HU, Y. & FU, L. 2012. Targeting cancer stem cells: a new therapy to cure cancer patients. American journal of cancer research, 2, 340.

HUANG, Z. 2005. A review of progress in clinical photodynamic therapy. Technology in cancer research & treatment, 4, 283.

JOSEFSEN, L. & BOYLE, R. 2008a. Photodynamic therapy: novel third-generation photosensitizers one step closer? British journal of pharmacology, 154, 1-3.

JOSEFSEN, L. B. & BOYLE, R. W. 2008b. Photodynamic therapy and the development of metal-based photosensitisers. Metal-based drugs, 2008.

JOSEFSEN, L. B. & BOYLE, R. W. 2012. Unique diagnostic and therapeutic roles of porphyrins and phthalocyanines in photodynamic therapy, imaging and theranostics. Theranostics, 2, 916.

JUARRANZ, Á., JAÉN, P., SANZ-RODRÍGUEZ, F., CUEVAS, J. & GONZÁLEZ, S. 2008. Photodynamic therapy of cancer. Basic principles and applications. Clinical and Translational Oncology, 10, 148-154.

JUZENIENE, A., PENG, Q. & MOAN, J. 2007. Milestones in the development of photodynamic therapy and fluorescence diagnosis. Photochemical & Photobiological Sciences, 6, 1234-1245.

KALKA, K., MERK, H. & MUKHTAR, H. 2000. Photodynamic therapy in dermatology. Journal of the American Academy of Dermatology, 42, 389-413.

KARIOTI, A. & BILIA, A. R. 2010. Hypericins as potential leads for new therapeutics. International journal of molecular sciences, 11, 562-594.

KESSEL, D. 2006. Death pathways associated with photodynamic therapy. Medical Laser Application, 21, 219-224.

KOLAROVA, H., LENOBEL, R., KOLAR, P. & STRNAD, M. 2007. Sensitivity of different cell lines to phototoxic effect of disulfonated chloroaluminium phthalocyanine. Toxicology in Vitro, 21, 1304-1306.

KOLAROVA, H., MACECEK, J., NEVRELOVA, P., HUF, M., TOMECKA, M., BAJGAR, R., MOSINGER, J. & STRNAD, M. 2005. Photodynamic therapy with zinc-tetra (p-sulfophenyl) porphyrin bound to cyclodextrin induces single strand breaks of cellular DNA in G361 melanoma cells. Toxicology in vitro, 19, 971-974.

KONOPKA, K. & GOSLINSKI, T. 2007. Photodynamic therapy in dentistry. Journal of Dental Research, 86, 694-707.

KOREN, H., SCHENK, G., IINDRA, R., ALTH, G., EBERMANN, R., KUBIN, A., KODERHOLD, G. & KREITNER, M. 1996. Hypericin in phototherapy. Journal of Photochemistry and Photobiology B: Biology, 36, 113-119.

KRESFELDER, T. L., CRONJÉ, M. J. & ABRAHAMSE, H. 2009. The Effects of Two Metallophthalocyanines on the Viability and Proliferation of an Esophageal Cancer Cell Line. Photomedicine and laser surgery, 27, 625-631.

KROEMER, G., EL-DEIRY, W., GOLSTEIN, P., PETER, M., VAUX, D., VANDENABEELE, P., ZHIVOTOVSKY, B., BLAGOSKLONNY, M., MALORNI, W. & KNIGHT, R. 2005. Classification of cell death: recommendations of the Nomenclature Committee on Cell Death. Cell Death & Differentiation, 12, 1463-1467.

KUBIN, A., WIERRANI, F., BURNER, U., ALTH, G. & GRUNBERGER, W. 2005. Hypericin-the facts about a controversial agent. Current pharmaceutical design, 11, 233-253.

KUDINOVA, N. & BEREZOV, T. 2010. Photodynamic therapy of cancer: Search for ideal photosensitizer. Biochemistry (Moscow) Supplement Series B: Biomedical Chemistry, 4, 95-103.

KYRIAZI, M., ALEXANDRATOU, E., YOVA, D., RALLIS, M. & TREBST, T. 2008. Topical photodynamic therapy of murine non-melanoma skin carcinomas with aluminum phthalocyanine chloride and a diode laser: pharmacokinetics, tumor response and cosmetic outcomes. Photodermatology, photoimmunology & photomedicine, 24, 87-94.

LIU, W., CHEN, N., JIN, H., HUANG, J., WEI, J., BAO, J., LI, C., LIU, Y., LI, X. & WANG, A. 2007. Intravenous repeated-dose toxicity study of $ZnPcS_2P_2$-based-photodynamic therapy in beagle dogs. Regulatory Toxicology and Pharmacology, 47, 221-231.

LO, P.-C., LENG, X. & NG, D. K. 2007. Hetero-arrays of porphyrins and phthalocyanines. Coordination Chemistry Reviews, 251, 2334-2353.

MACDONALD, I. J. & DOUGHERTY, T. J. 2001. Basic principles of photodynamic therapy. Journal of Porphyrins and Phthalocyanines, 5, 105-129.

MACHADO, A. H. A., MORAES, K. C., SOARES, C. P., JUNIOR, M. B. & DA SILVA, N. S. 2010. Cellular changes after photodynamic therapy on HEp-2 cells using the new ZnPcBr8 phthalocyanine. Photomedicine and laser surgery, 28, S-143-S-149.

MACHADO, A. H. A., PACHECO SOARES, C., DA SILVA, N. S. & MORAES, K. 2009. Cellular and molecular studies of the initial process of the photodynamic therapy in HEp-2 cells using LED light source and two different photosensitizers. Cell biology international, 33, 785-795.

MADURAY, K., KARSTEN, A., ODHAV, B. & NYOKONG, T. 2011. In vitro toxicity testing of zinc tetrasulfophthalocyanines in fibroblast and keratinocyte cells for the treatment of melanoma cancer by photodynamic therapy. Journal of Photochemistry and Photobiology B: Biology, 103, 98-104.

MADURAY, K., ODHAV, B. & NYOKONG, T. 2012. In vitro photodynamic effect of aluminumtetrasulfophthalocyanines on melanoma skin cancer and healthy normal skin cells. Photodiagnosis and Photodynamic Therapy, 9, 32-39.

MAFTOUM-COSTA, M., NAVES, K. T., OLIVEIRA, A. L., TEDESCO, A. C., DA SILVA, N. S. & PACHECO-SOARES, C. 2008. Mitochondria, endoplasmic reticulum and actin filament behavior after PDT with chloroaluminum phthalocyanine liposomal in HeLa cells. Cell biology international, 32, 1024-1028.

MAIURI, M. C., CRIOLLO, A. & KROEMER, G. 2010. Crosstalk between apoptosis and autophagy within the Berlin 1 interactome. EMBO, 29, 515-516.

MANOTO, S. L., SEKHEJANE, P. R., HOURELD, N. N. & ABRAHAMSE, H. 2012. Localization and phototoxic effect of zinc sulfophthalocyanine photosensitizer in human colon (DLD-1) and lung (A549) carcinoma cells (in vitro). Photodiagnosis and photodynamic therapy, 9, 52-59.

MIHAELA, C., CRISTINA, C. & EMIL, P. 2009. Optical Techniques for Monitoring Tumour Response to Photodynamic Therapy. European Journal of Interdisciplinary Studies, 1, 40-49.

MOOR, A. C. 2000. Signaling pathways in cell death and survival after photodynamic therapy. Journal of Photochemistry and Photobiology B: Biology, 57, 1-13.

MROZ, P., YAROSLAVSKY, A., KHARKWAL, G. B. & HAMBLIN, M. R. 2011. Cell death pathways in photodynamic therapy of cancer. Cancers, 3, 2516-2539.

NYMAN, E. S. & HYNNINEN, P. H. 2004. Research advances in the use of tetrapyrrolic photosensitizers for photodynamic therapy. Journal of Photochemistry and Photobiology B: Biology, 73, 1-28.

NYOKONG, T. 2007. Effects of substituents on the photochemical and photophysical properties of main group metal phthalocyanines. Coordination chemistry reviews, 251, 1707-1722.

NYOKONG, T. 2011. Desired properties of new phthalocyanines for photodynamic therapy. Pure & Applied Chemistry, 83, 1763-1779.

PASZKO, E., EHRHARDT, C., SENGE, M. O., KELLEHER, D. P. & REYNOLDS, J. V. 2011. Nanodrug applications in photodynamic therapy. Photodiagnosis and photodynamic therapy, 8, 14-29.

PENG, Q., JUZENIENE, A., CHEN, J., SVAASAND, L. O., WARLOE, T., GIERCKSKY, K.-E. & MOAN, J. 2008. Lasers in medicine. Reports on Progress in Physics, 71, 056701.

PLAETZER, K., KIESSLICH, T., KRAMMER, B. & HAMMERL, P. 2002. Characterization of the cell death modes and the associated changes in cellular energy supply in response to AlPcS 4-PDT. Photochemical & Photobiological Sciences, 1, 172-177.

POSTIGLIONE, I., CHIAVIELLO, A. & PALUMBO, G. 2011. Enhancing photodynamyc therapy efficacy by combination therapy: dated, current and oncoming strategies. Cancers, 3, 2597-2629.

RATHMELL, J. C. & THOMPSON, C. B. 1999. The central effectors of cell death in the immune system Annual Review: Immunology 17, 781-828.

RUSTIN, P. 2002. Mitrochondria, from cell death to proliferation Nature Genet., 30, 352-353.

SAN, S. E., OKUTAN, M., NYOKONG, T., DURMUŞ, M. & OZTURK, B. 2011. Temperature activated ionic conductivity in gallium and indium phthalocyanines. Polyhedron, 30, 1023-1026.

SAVILL, J. & FADOK, V. 2000. Corpse clearance defines the meaning of cell death Nature, 407, 784-788.

SEKKAT, N., BERGH, H. V. D., NYOKONG, T. & LANGE, N. 2011. Like a bolt from the blue: phthalocyanines in biomedical optics. Molecules, 17, 98-144.

SEOTSANYANA-MOKHOSI, I., KRESFELDER, T., ABRAHAMSE, H. & NYOKONG, T. 2006. The effect of Ge, Si and Sn phthalocyanine photosensitizers on cell proliferation and viability of human oesophageal carcinoma cells. Journal of Photochemistry and Photobiology B: Biology, 83, 55-62.

SHAO, J., XUE, J., DAI, Y., LIU, H., CHEN, N., JIA, L. & HUANG, J. 2012. Inhibition of human hepatocellular carcinoma HepG2 by phthalocyanine photosensitiser PHOTOCYANINE: ROS production, apoptosis, cell cycle arrest. European Journal of Cancer, 48, 2086-2096.

SHARMAN, W. M., ALLEN, C. M. & VAN LIER, J. E. 1999. Photodynamic therapeutics: basic principles and clinical applications. Drug discovery today, 4, 507-517.

SIBATA, C., COLUSSI, V., OLEINICK, N. & KINSELLA, T. 2000. Photodynamic therapy: a new concept in medical treatment. Brazilian Journal of Medical and Biological Research, 33, 869-880.

SOUKOS, N. S., GRANT, W. E. & SPEIGHT, P. M. 1994. Photodynamic effects of di-sulphonated aluminium phthalocyanine on human epidermal keratinocytes in vitro. Lasers in medical Science, 9, 183-190.

SPIKES, J. D. 1986. Phthalocyanines as photosensitizers in biological systems and for the photodynamic therapy of tumors. Photochemistry and photobiology, 43, 691-699.

STRANADKO, E. P., MESHKOV, V. M., KORABOYEV, U. M. & RIABOV, M. V. Clinical photodynamic therapy using Russian photosensitizers Photoheme and Photosense: six-year experience. Selected Papers on Laser Use in Oncology II, 1999. International Society for Optics and Photonics, 25-31.

STUKAVEC, J., DUCHAC, V., HORAK, L. & POUCKOVA, P. 2009. Photodynamic therapy of human colorectal carcinoma cell line. Photomedicine and laser surgery, 27, 107-110.

STYLLI, S., HILL, J., SAWYER, W. & KAYE, A. 1995. Aluminium phthalocyanine mediated photodynamic therapy in experimental malignant glioma. Journal of Clinical Neuroscience, 2, 146-151.

TAPAJÓS, E., LONGO, J., SIMIONI, A., LACAVA, Z., SANTOS, M., MORAIS, P., TEDESCO, A. & AZEVEDO, R. 2008. In vitro photodynamic therapy on human oral keratinocytes using chloroaluminum-phthalocyanine. Oral oncology, 44, 1073-1079.

TYNGA, I., HOURELD, N. & ABRAHAMSE, H. 2013. The primary subcellular localization of Zinc phthalocyanine and its cellular impact on viability, proliferation and structure of breast cancer cells (MCF-7). Journal of Photochemistry and Photobiology B: Biology, 120, 171-176.

URRUTICOECHEA, A., ALEMANY, R., BALART, J., VILLANUEVA, A., VINALS, F. & CAPELLA, G. 2010. Recent advances in cancer therapy: an overview. Current pharmaceutical design, 16, 3-10.

VITTAR, N. B. R., AWRUCH, J., AZIZUDDIN, K. & RIVAROLA, V. 2010. Caspase-independent apoptosis, in human MCF-7c3 breast cancer cells, following photodynamic therapy, with a novel water-soluble phthalocyanine. The international journal of biochemistry & cell biology, 42, 1123-1131.

WIKTOROWICZ, K., COFTA, J., DUDKOWIAK, A., WASZKOWIAK, A. & FRACKOWIAK, D. 2004. Preliminary studies of phthalocyanine sensitizers incorporated into human leukemia cells from two cell-lines. ACTA BIOCHIMICA POLONICA-ENGLISH EDITION-, 703-710.

WOJTYK, J. T., GOYAN, R., GUDGIN-DICKSON, E. & POTTIER, R. 2006. Exploiting tumour biology to develop novel drug delivery strategies for PDT. Medical laser application, 21, 225-238.

YANıK, H., AYDıN, D., DURMUŞ, M. & AHSEN, V. 2009. Peripheral and non-peripheral tetrasubstituted aluminium, gallium and indium phthalocyanines: Synthesis, photophysics and photochemistry. Journal of Photochemistry and Photobiology A: Chemistry, 206, 18-26.

YANO, S., HIROHARA, S., OBATA, M., HAGIYA, Y., OGURA, S.-I., IKEDA, A., KATAOKA, H., TANAKA, M. & JOH, T. 2011. Current states and future views in photodynamic therapy. Journal of Photochemistry and Photobiology C: Photochemistry Reviews, 12, 46-67.

YSLAS, E. I., DURANTINI, E. N. & RIVAROLA, V. A. 2007. Zinc-(II) 2, 9, 16, 23-tetrakis (methoxy) phthalocyanine: potential photosensitizer for use in photodynamic therapy in vitro. Bioorganic & medicinal chemistry, 15, 4651-4660.

ZHOU, C., SHUNJI, C., JINSHENG, D., JUNLIN, L., JORI, G. & MILANESI, C. 1996. Apoptosis of mouse MS-2 fibrosarcoma cells induced by photodynamic therapy with Zn (II)-phthalocyanine. Journal of Photochemistry and Photobiology B: Biology, 33, 219-223.

ZHU, T. C. & FINLAY, J. C. 2008. The role of PDT physics. Medical Physics, 35, 3127-36.

ZONG, W.-X. & THOMPSON, C. B. 2006. Necrotic death as a cell fate. Genes & development, 20, 1-15.

APPENDIX

Photosensitizers

GaPcCl: $C_{32}H_{16}ClGaN_8$; 662, 79 g/mol

InPcCl: $C_{32}H_{16}ClFeN_8$; 662, 79 g/mol

FePcCl: $C_{32}H_{16}ClInN_8$; 603, 82 g/mol

Reagents for TEM

0.2 M Phosphate Buffer, pH 7.4

Na_2HPO_4 ---------- 43.6 g

NaH_2PO_4 ---------- 12.8 g

Distilled water ---------- 1000 ml

Fixative (2.5% Glutaraldehyde in 0.2 M Phosphate Buffer, pH 7.4)

0.2 M Phosphate Buffer, pH 7.4 ---------- 95 ml

Glutaraldehyde ---------- 5 ml

0.5% Osmium in 0.2 M Phosphate Buffer

2% Aqueous Osmium ---------- 2.5 ml

0.2 M Phosphate Buffer, pH7.4 ---------- 2.5 ml

5% Uranyl Acetate Solution

To prepare 50 ml, add 2.5 g of uranyl acetate to 50 ml of distilled water. Cover with foil and stir overnight. Add 10 drops of glacial acetic acid. Store at 4 ºC. This solution is stable for at least 6 months at 4 ºC.

Reynold’s Lead Citrate Solution

To prepare 50 ml, add chemicals in distilled water in following order

Lead nitrate ---------- 1.33 g

Sodium citrate, dihydrate ---------- 1.76 g (solution becomes cloudy when sodium citrate is added and stir for 30 minutes)

1 M NaOH ---------- 8 ml (solution becomes clear when NaOH is added)

Distilled water ---------- 30 ml

Stir for another 10 minutes and add additional 15 ml of distilled water. Store solution for 3-6 months at 4 ºC. Note: the mount of NaOH is very important. The solution should have pH 12.

Table A-1 Statistical difference between the untreated controls (0 µg/ml of PS and 0 J/cm^2) and their respective experimental groups are shown as (*) P ≤ 0.05, (**) P ≤ 0.01, (***) P ≤ 0.001 and (ns) non-significant.

PS Conc. (µg/ml)	Caco-2									MCF-7								
	GaPcCl			InPcCl			FePcCl			GaPcCl			InPcCl			FePcCl		
	2.5 J/cm^2	4.5 J/cm^2	8.5 J/cm^2	2.5 J/cm^2	4.5 J/cm^2	8.5 J/cm^2	2.5 J/cm^2	4.5 J/cm^2	8.5 J/cm^2	2.5 J/cm^2	4.5 J/cm^2	8.5 J/cm^2	2.5 J/cm^2	4.5 J/cm^2	8.5 J/cm^2	2.5 J/cm^2	4.5 J/cm^2	8.5 J/cm^2
0 vs 2	***	***	***	*	***	***	**	***	***	***	***	***	***	***	***	***	***	***
0 vs 4	***	***	***	***	***	***	***	***	***	***	***	***	***	***	***	***	***	***
0 vs 6	***	***	***	***	***	***	***	***	***	***	***	***	***	***	***	***	***	***
0 vs 8	***	***	***	***	***	***	***	***	***	***	***	***	***	***	***	***	***	***
0 vs 10	***	***	***	***	***	***	***	***	****	****	***	***	***	***	***	***	***	***
0 vs 20	***	***	***	***	***	***	***	***	***	***	***	***	***	***	***	***	***	***
0 vs 40	***	***	***	***	***	***	***	***	***	***	***	***	***	***	***	***	***	***
0 vs 60	***	***	***	***	***	***	***	***	***	***	***	***	***	***	***	***	***	***
0 vs 80	***	***	***	***	***	***	***	***	***	***	***	***	***	***	***	***	***	***
0 vs 100	***	***	***	***	***	***	***	***	***	***	***	***	***	***	***	***	***	***
0 vs laser	ns	ns	ns	ns	ns	**	ns	ns	ns	ns	ns	ns	ns	ns	ns	ns	ns	ns
2 vs 4	ns	ns	ns	**	ns	ns	ns	ns	ns	ns	ns	ns	ns	ns	**	ns	ns	ns

2 vs 6	ns	ns	ns	**	ns	*	ns	ns	ns	ns	ns	ns	*	ns	***	**	ns	**
2 vs 8	ns	ns	ns	***	ns	*	ns	ns	ns	ns	ns	ns	*	*	***	***	***	***
2 vs 10	ns	**	**	***	ns	*	ns	*	ns	ns	ns	ns	*	*	***	***	***	***
2 vs 20	ns	**	**	***	ns	**	ns	*	*	ns	**	ns	**	**	***	***	***	***
2 vs 40	**	***	***	***	**	**	***	**	*	**	***	**	***	***	****	****	***	***
2 vs 60	**	***	***	***	***	***	***	***	***	***	***	***	***	***	***	***	***	***
2 vs 80	***	***	***	***	***	***	***	***	***	***	***	***	***	***	***	***	***	***
2 vs 100	***	***	***	***	***	***	***	***	***	***	***	***	***	***	***	***	***	***
2 vs laser	***	***	***	ns	***	***	**	***	***	***	***	**	***	***	***	****	***	***
4 vs 6	ns	ns	ns	ns	ns	ns	ns	ns	ns	ns	ns	ns	ns	ns	ns	ns	ns	ns
4 vs 8	ns	ns	ns	ns	ns	ns	ns	ns	ns	ns	ns	ns	ns	ns	ns	***	**	***
4 vs 10	ns	ns	*	ns	ns	ns	ns	ns	ns	ns	ns	ns	ns	ns	ns	***	**	***
4 vs 20	ns	*	*	ns	ns	*	ns	ns	ns	ns	*	ns	ns	ns	ns	***	***	***
4 vs 40	*	***	**	***	**	*	**	ns	ns	*	***	ns	ns	ns	ns	***	***	***
4 vs 60	**	***	***	***	***	***	***	*	***	**	***	*	ns	ns	**	***	***	***

4 vs 80	***	***	***	***	***	***	***	**	***	***	***	***	ns	*	**	***	***	***
4 vs 100	***	***	***	***	***	***	***	***	***	***	***	***	ns	**	**	***	***	***
4 vs laser	***	***	***	***	***	***	***	***	***	***	***	***	ns	***	***	***	***	***
6 vs 8	ns	ns	ns	ns	ns	ns	ns	ns	ns	ns	ns	ns	***	ns	ns	ns	*	ns
6 vs 10	ns	ns	ns	ns	ns	ns	ns	ns	ns	ns	ns	ns	ns	ns	ns	ns	*	***
6 vs 20	ns	ns	ns	ns	ns	ns	ns	ns	ns	ns	ns	ns	ns	ns	ns	**	***	***
6 vs 40	*	*	*	***	**	ns	**	ns	ns	ns	*	ns	ns	ns	ns	***	***	***
6 vs 60	*	**	**	***	***	**	***	ns	*	*	**	ns	ns	ns	*	***	***	***
6 vs 80	**	**	***	***	***	***	***	**	**	***	***	**	ns	*	**	***	***	***
6 vs 100	***	***	***	***	***	***	***	***	*	***	***	***	ns	*	**	***	***	***
6 vs laser	***	***	***	***	***	***	***	***	***	***	***	***	***	***	***	***	***	***
8 vs 10	ns	ns	ns	ns	ns	ns	ns	ns	ns	ns	ns	ns	ns	ns	ns	ns	ns	ns
8 vs 20	ns	ns	ns	ns	ns	ns	ns	ns	ns	ns	ns	ns	ns	ns	ns	ns	**	***
8 vs 40	ns	*	ns	***	*	ns	ns	ns	ns	ns	ns	ns	ns	ns	ns	*	***	***
8 vs 60	ns	*	**	***	***	**	***	ns	*	ns	**	ns	ns	ns	*	***	***	***

8 vs 80	**	**	**	***	***	***	***	*	***	**	***	**	ns	ns	**	***	***	***
8 vs 100	**	***	***	***	***	***	***	***	*	***	***	***	ns	*	**	***	***	***
8 vs laser	***	***	***	***	***	***	***	***	***	***	***	***	***	***	***	***	***	***
10 vs 20	ns	ns	ns	ns	ns	ns	ns	ns	ns	ns	ns	ns	ns	***	ns	ns	**	***
10 vs 40	ns	ns	ns	**	*	ns	ns	ns	ns	ns	ns	ns	ns	ns	ns	*	***	***
10 vs 60	ns	ns	ns	***	***	**	***	ns	*	*	**	ns	ns	ns	ns	***	***	***
10 vs 80	ns	ns	ns	***	***	***	***	ns	**	***	***	**	ns	ns	*	***	***	***
10 vs 100	ns	*	**	***	***	***	***	**	*	***	***	***	ns	ns	*	***	***	***
10 vs laser	***	***	***	***	***	***	***	***	***	***	***	***	***	***	***	***	***	***
20 vs 40	ns	ns	ns	**	*	ns	ns	ns	ns	ns	ns	ns	ns	ns	ns	ns	ns	ns
20 vs 60	ns	ns	ns	***	***	*	***	ns	ns	ns	ns	ns	ns	ns	ns	**	***	ns
20 vs 80	ns	ns	ns	***	***	*	***	ns	ns	**	***	**	ns	ns	ns	***	***	ns
20 vs 100	ns	*	**	***	***	*	***	**	ns	***	***	***	ns	ns	ns	***	***	***
20 vs laser	***	***	***	***	***	***	***	***	***	***	***	***	***	***	***	***	***	***
40 vs 60	ns	ns	ns	ns	**	*	ns	ns	ns	ns	ns	ns	ns	ns	ns	ns	**	ns

40 vs 80	ns	ns	ns	*	**	*	ns	ns	ns	**	*	ns	ns	ns	ns	**	***	ns
40 vs 100	ns	ns	*	*	***	*	**	*	ns	**	***	***	ns	ns	ns	***	***	***
40 vs laser	***	***	***	***	***	***	***	***	***	***	***	***	***	***	***	***	***	***
60 vs 80	ns	ns	ns	ns	ns	ns	ns	ns	ns	ns	ns	ns	ns	ns	ns	ns	ns	ns
60 vs 100	ns	ns	ns	ns	ns	ns	ns	ns	ns	ns	**	ns	ns	ns	ns	*	***	***
60 vs laser	***	***	***	***	***	***	***	***	***	***	***	***	***	***	***	***	***	***
80 vs 100	ns	ns	ns	ns	ns	ns	ns	ns	ns	ns	ns	ns	***	ns	ns	ns	***	**
80 vs laser	***	***	***	***	***	***	***	***	***	***	***	***	ns	***	***	***	***	***
100 vs laser	***	***	***	***	***	***	***	***	***	***	***	***	***	***	***	***	***	***

Table A-2 Statistical difference between the untreated controls (0 µg/ml of PS and 0 J/cm^2) and their respective experimental groups are shown as (*) P ≤ 0.05, (**) P ≤ 0.01, (***) P ≤ 0.001 and (ns) non-significant.

PS Conc. (µg/ml)	Melanoma									A549								
	GaPcCl			InPcCl			FePcCl			GaPcCl			InPcCl			FePcCl		
	2.5 J/cm^2	4.5 J/cm^2	8.5 J/cm^2	2.5 J/cm^2	4.5 J/cm^2	8.5 J/cm^2	2.5 J/cm^2	4.5 J/cm^2	8.5 J/cm^2	2.5 J/cm^2	4.5 J/cm^2	8.5 J/cm^2	2.5 J/cm^2	4.5 J/cm^2	8.5 J/cm^2	2.5 J/cm^2	4.5 J/cm^2	8.5 J/cm^2
0 vs 2	ns	ns	***	***	***	***	ns	ns	*	***	***	***	***	***	***	***	***	***
0 vs 4	ns	**	***	***	***	***	***	***	***	***	***	***	***	***	***	***	***	***
0 vs 6	ns	***	***	***	***	***	***	***	***	***	***	***	***	***	***	***	***	***
0 vs 8	***	***	***	***	***	***	***	***	***	***	***	***	***	***	***	***	***	***
0 vs 10	***	***	***	***	***	***	***	***	***	***	***	***	***	***	***	***	***	***
0 vs 20	***	***	***	***	***	***	***	***	***	***	***	***	***	***	***	***	***	***
0 vs 40	***	***	***	***	***	***	***	***	***	***	***	***	***	***	***	***	***	***
0 vs 60	***	***	***	***	***	***	***	***	***	***	***	***	***	***	***	***	***	***
0 vs 80	***	***	***	***	***	***	***	***	***	***	***	***	***	***	***	***	***	***
0 vs 100	***	***	***	***	***	***	***	ns	***	***	***	***	***	***	***	***	***	***
0 vs laser	ns	ns	ns	ns	ns	ns	ns	***	ns	ns	ns	ns	ns	ns	ns	ns	ns	ns

2 vs 4	ns	ns	ns	ns	ns	ns	***	***	***	ns	ns	ns	ns	ns	ns	ns	ns	ns
2 vs 6	ns	***	ns	ns	ns	ns	***	***	***	ns	ns	ns	ns	ns	ns	ns	ns	ns
2 vs 8	*	***	ns	ns	ns	ns	***	***	***	ns	ns	ns	*	ns	ns	**	ns	*
2 vs 10	**	***	ns	ns	*	ns	***	***	***	ns	ns	ns	*	ns	ns	**	**	***
2 vs 20	***	***	ns	ns	**	ns	***	***	***	ns	ns	ns	**	ns	ns	***	***	***
2 vs 40	***	***	***	*	***	ns	***	***	***	*	ns	*	**	ns	ns	***	***	***
2 vs 60	***	***	***	*	***	ns	***	***	***	*	ns	*	***	ns	ns	***	***	***
2 vs 80	***	***	***	***	***	*	***	***	***	*	ns	**	***	*	ns	***	***	***
2 vs 100	***	***	***	***	***	**	***	***	***	**	*	***	***	***	*	***	***	***
2 vs laser	ns	ns	***	***	***	***	ns	ns	ns	***	***	***	***	***	***	***	***	***
4 vs 6	ns	*	ns	ns	ns	ns	ns	ns	ns	ns	ns	ns	ns	ns	ns	ns	ns	ns
4 vs 8	ns	**	ns	ns	ns	ns	ns	ns	ns	ns	ns	ns	ns	ns	ns	*	ns	*
4 vs 10	ns	**	ns	ns	*	ns	*	ns	ns	ns	ns	ns	ns	ns	ns	*	**	**
4 vs 20	**	***	ns	ns	**	ns	**	*	ns	ns	ns	ns	ns	ns	ns	**	***	***
4 vs 40	***	***	***	ns	**	ns	**	*	*	ns	ns	ns	ns	ns	ns	***	***	***

4 vs 60	***	***	***	ns	***	ns	***	**	*	ns	ns	ns	ns	ns	ns	***	***	***
4 vs 80	***	***	***	*	***	ns	***	**	**	ns	ns	ns	*	ns	ns	***	***	***
4 vs 100	***	***	***	***	***	ns	***	***	**	ns	ns	**	**	*	ns	***	***	***
4 vs laser	ns	*	***	***	***	***	***	***	***	***	***	***	***	***	***	***	***	***
6 vs 8	ns	ns	ns	ns	ns	ns	ns	ns	ns	ns	ns	ns	ns	ns	ns	ns	ns	ns
6 vs 10	ns	ns	ns	ns	ns	ns	ns	ns	ns	ns	ns	ns	ns	ns	ns	ns	ns	ns
6 vs 20	**	*	ns	ns	ns	ns	*	ns	ns	ns	ns	ns	ns	ns	ns	*	***	ns
6 vs 40	**	*	***	ns	ns	ns	**	*	*	ns	ns	ns	ns	ns	ns	***	***	***
6 vs 60	***	***	***	ns	*	*	***	**	*	ns	ns	ns	ns	ns	ns	***	***	***
6 vs 80	***	***	***	*	**	*	***	**	*	ns	ns	ns	*	ns	ns	***	***	***
6 vs 100	***	***	***	***	**	*	***	***	**	ns	ns	ns	**	*	ns	***	***	***
6 vs laser	ns	***	***	***	***	***	***	***	***	***	***	***	***	***	***	***	***	***
8 vs 10	ns	ns	ns	ns	ns	ns	ns	ns	ns	ns	ns	ns	ns	ns	ns	ns	ns	ns
8 vs 20	ns	ns	ns	ns	ns	ns	ns	ns	ns	ns	ns	ns	ns	ns	ns	ns	***	ns
8 vs 40	ns	ns	***	ns	ns	ns	ns	ns	*	ns	ns	ns	ns	ns	ns	***	***	***

8 vs 60	*	**	***	ns	*	ns	*	*	ns	ns	ns	ns	ns	ns	ns	***	***	***
8 vs 80	**	***	***	*	**	ns	*	*	*	ns	ns	ns	ns	ns	ns	***	***	***
8 vs 100	***	***	***	**	**	ns	**	**	**	ns	ns	ns	*	ns	ns	***	***	***
8 vs laser	***	***	***	***	***	***	***	***	***	***	***	***	***	***	***	***	***	***
10 vs 20	ns	ns	ns	ns	ns	ns	ns	ns	ns	ns	ns	ns	ns	ns	ns	ns	***	ns
10 vs 40	ns	ns	***	ns	ns	ns	ns	ns	ns	ns	ns	ns	ns	ns	ns	***	***	***
10 vs 60	ns	*	***	ns	ns	ns	ns	ns	ns	ns	ns	ns	ns	ns	ns	***	***	***
10 vs 80	*	***	***	ns	ns	ns	ns	ns	ns	ns	ns	ns	ns	ns	ns	***	***	***
10 vs 100	***	***	***	*	ns	ns	ns	ns	ns	ns	ns	ns	*	ns	ns	***	***	***
10 vs laser	***	***	***	***	***	***	***	***	***	***	***	***	***	***	***	***	***	***
20 vs 40	ns	ns	***	ns	ns	ns	ns	ns	ns	ns	ns	ns	ns	ns	ns	***	***	***
20 vs 60	ns	ns	***	ns	ns	ns	ns	ns	ns	ns	ns	ns	ns	ns	ns	***	***	***
20 vs 80	ns	ns	***	ns	ns	ns	ns	ns	ns	ns	ns	ns	ns	ns	ns	***	***	***
20 vs 100	***	*	***	*	ns	ns	ns	ns	ns	ns	***	***	ns	ns	ns	***	***	***
20 vs laser	***	***	***	***	***	***	***	***	***	***	ns	ns	***	***	***	***	***	***

40 vs 60	ns	ns	ns	ns	ns	ns	ns	ns	ns	ns	ns	ns	ns	ns	ns	***	***	ns
40 vs 80	ns	*	ns	ns	ns	ns	ns	ns	ns	ns	ns	ns	ns	ns	ns	**	***	***
40 vs 100	**	*	ns	ns	ns	ns	ns	ns	ns	ns	***	***	**	ns	ns	***	***	ns
40 vs laser	***	***	***	***	***	***	***	***	***	***	ns	ns	**	***	***	***	***	***
60 vs 80	***	ns	ns	ns	ns	ns	ns	ns	ns	ns	ns	ns	ns	ns	ns	ns	***	***
60 vs 100	ns	ns	ns	ns	ns	ns	ns	ns	ns	ns	ns	ns	ns	ns	ns	**	ns	ns
60 vs laser	***	***	***	***	***	***	***	***	***	***	***	***	***	***	***	***	***	***
80 vs 100	ns	ns	ns	ns	ns	ns	ns	ns	ns	ns	ns	ns	ns	ns	ns	***	***	***
80 vs laser	***	***	***	***	***	***	***	***	***	***	***	***	***	***	***	***	***	***
100 vs laser	***	***	***	***	***	***	***	***	***	***	***	***	***	***	***	***	***	***

Table A-3 Statistical difference between the untreated controls (0 µg/ml of PS and 0 J/cm^2) and their respective experimental groups are shown as (*) P ≤ 0.05, (**) P ≤ 0.01, (***) P ≤ 0.001 and (ns) non-significant.

PS Conc. (µg/ml)	Fibroblast								
	GaPcCl			InPcCl			FePcCl		
	2.5 J/cm^2	4.5 J/cm^2	8.5 J/cm^2	2.5 J/cm^2	4.5 J/cm^2	8.5 J/cm^2	2.5 J/cm^2	4.5 J/cm^2	8.5 J/cm^2
0 vs 2	***	***	**	ns	***	**	***	***	**
0 vs 4	***	***	**	ns	***	**	***	***	**
0 vs 6	***	***	***	***	***	***	***	***	***
0 vs 8	***	***	***	***	***	***	***	***	***
0 vs 10	***	***	***	***	***	***	***	***	***
0 vs 20	***	***	***	***	***	***	***	***	***
0 vs 40	***	***	***	***	***	***	***	***	***
0 vs 60	***	***	***	***	***	***	***	***	***
0 vs 80	***	***	***	***	***	***	***	***	***
0 vs 100	***	***	***	***	***	***	***	***	***
0 vs laser	ns	ns	ns	ns	ns	ns	ns	ns	ns

2 vs 4	ns	ns	ns	ns	ns	ns	ns	ns	ns
2 vs 6	ns	ns	ns	**	ns	ns	ns	ns	ns
2 vs 8	*	ns	ns	**	ns	ns	*	ns	ns
2 vs 10	***	ns	ns	***	ns	ns	***	ns	ns
2 vs 20	***	ns	ns	***	ns	ns	***	ns	ns
2 vs 40	***	***	*	***	***	**	***	***	ns
2 vs 60	***	***	ns	***	***	ns	***	***	ns
2 vs 80	***	***	*	***	***	*	***	***	*
2 vs 100	***	***	*	***	***	*	***	***	*
2 vs laser	***	***	*	ns	***	*	***	***	*
4 vs 6	ns	ns	ns	ns	ns	ns	ns	ns	ns
4 vs 8	ns	ns	ns	***	ns	ns	ns	ns	ns
4 vs 10	*	ns	ns	***	ns	ns	*	ns	ns
4 vs 20	***	ns	ns	***	ns	ns	***	ns	ns
4 vs 40	***	**	ns	***	**	ns	***	**	ns

4 vs 60	***	***	ns	***	***	ns	***	***	ns
4 vs 80	***	***	ns	***	***	ns	***	***	ns
4 vs 100	***	***	*	***	***	*	***	***	*
4 vs laser	***	***	**	ns	***	**	***	***	**
6 vs 8	ns	ns	ns	ns	ns	ns	ns	ns	ns
6 vs 10	*	ns	ns	**	ns	ns	*	ns	ns
6 vs 20	***	ns	ns	***	ns	ns	***	ns	ns
6 vs 40	***	**	ns	***	**	ns	***	**	ns
6 vs 60	***	***	ns	***	***	ns	***	***	ns
6 vs 80	***	***	ns	***	***	ns	***	***	ns
6 vs 100	***	***	ns	***	***	ns	***	***	ns
6 vs laser	***	***	**	***	***	**	***	***	**
8 vs 10	ns	ns	ns	**	ns	ns	ns	ns	ns
8 vs 20	**	ns	ns	***	ns	ns	**	ns	ns
8 vs 40	***	ns	ns	***	ns	ns	***	ns	ns

8 vs 60	***	**	ns	***	**	ns	***	**	ns
8 vs 80	***	**	ns	***	**	ns	***	**	ns
8 vs 100	***	**	ns	***	**	ns	***	**	ns
8 vs laser	***	***	***	***	***	***	***	***	***
10 vs 20	ns	ns	ns	ns	ns	ns	ns	ns	ns
10 vs 40	ns	ns	ns	ns	ns	ns	ns	ns	ns
10 vs 60	**	*	ns	***	*	ns	**	*	ns
10 vs 80	***	*	ns	***	*	ns	***	*	ns
10 vs 100	***	*	ns	***	*	ns	***	*	ns
10 vs laser	***	***	***	***	***	***	***	***	***
20 vs 40	ns	ns	ns	ns	ns	ns	ns	ns	ns
20 vs 60	ns	*	ns	*	*	ns	ns	*	ns
20 vs 80	***	*	ns	**	***	**	***	***	***
20 vs 100	***	*	**	***	***	***	***	**	***
20 vs laser	***	***	***	***	***	***	***	***	***

40 vs 60	ns	ns	ns	ns	ns	ns	ns	ns	ns
40 vs 80	***	ns	***	*	***	*	***	***	***
40 vs 100	***	ns	**	***	***	***	***	**	***
40 vs laser	***	***	***	***	***	***	***	***	***
60 vs 80	*	ns	ns	ns	*	ns	*	ns	*
60 vs 100	***	ns	ns	***	***	***	***	ns	***
60 vs laser	***	***	***	***	***	***	***	***	***
80 vs 100	ns	ns	ns	*	ns	*	ns	**	ns
80 vs laser	***	***	***	***	***	***	***	***	***
100 vs laser	***	***	***	***	***	***	***	***	***

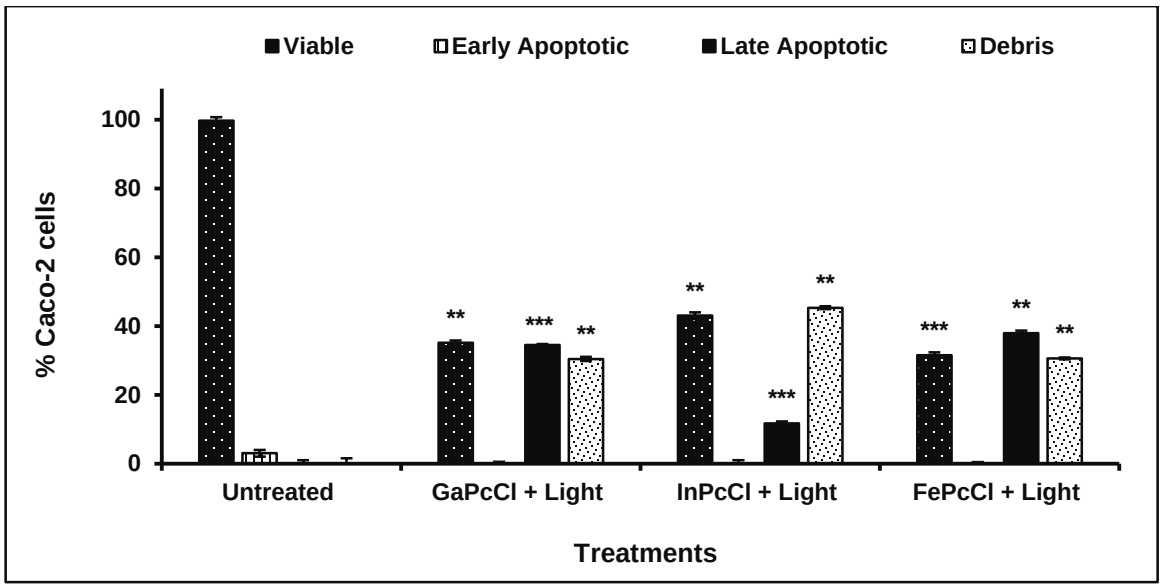

Figure A-1 FITC Annexin V/PI apoptosis analysis by flow cytometry of Caco-2 cancer cells after 24 post-PDT treatment. Percentage (%) of viable cells, early apoptotic cells, late apoptotic cells and cellular debris are compared with the untreated control. (**) $P \leq 0.01$ and (***) $P \leq 0.001$.

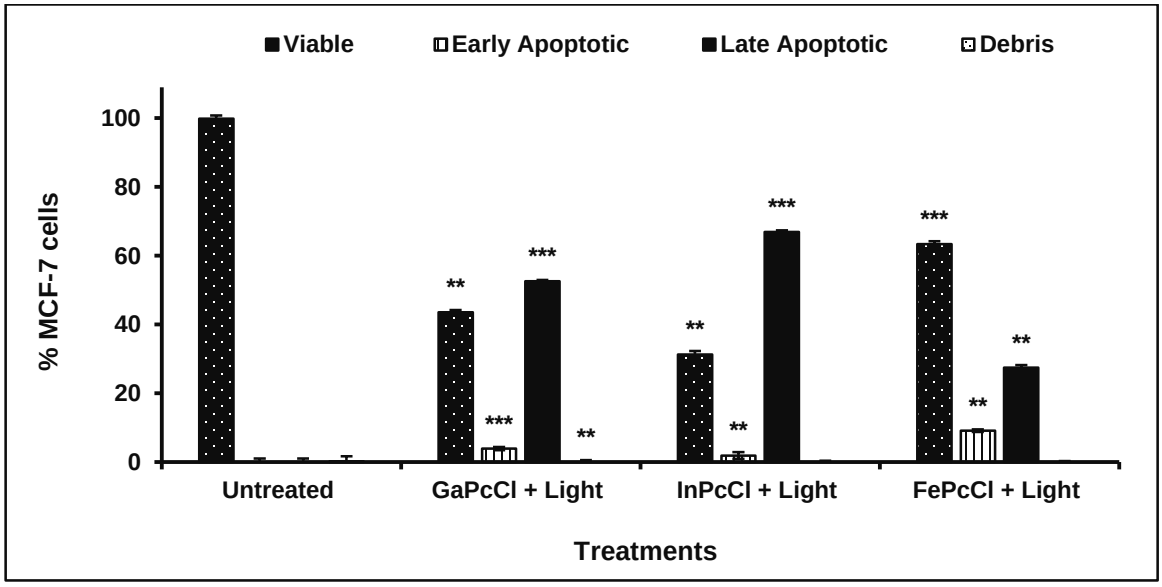

Figure A-2 FITC Annexin V/PI apoptosis analysis by flow cytometry of MCF-7 cancer cells after 24 post-PDT treatment. Percentage (%) of viable cells, early apoptotic cells, late apoptotic cells and cellular debris are compared with the untreated control. (**) $P \leq 0.01$ and (***) $P \leq 0.001$.

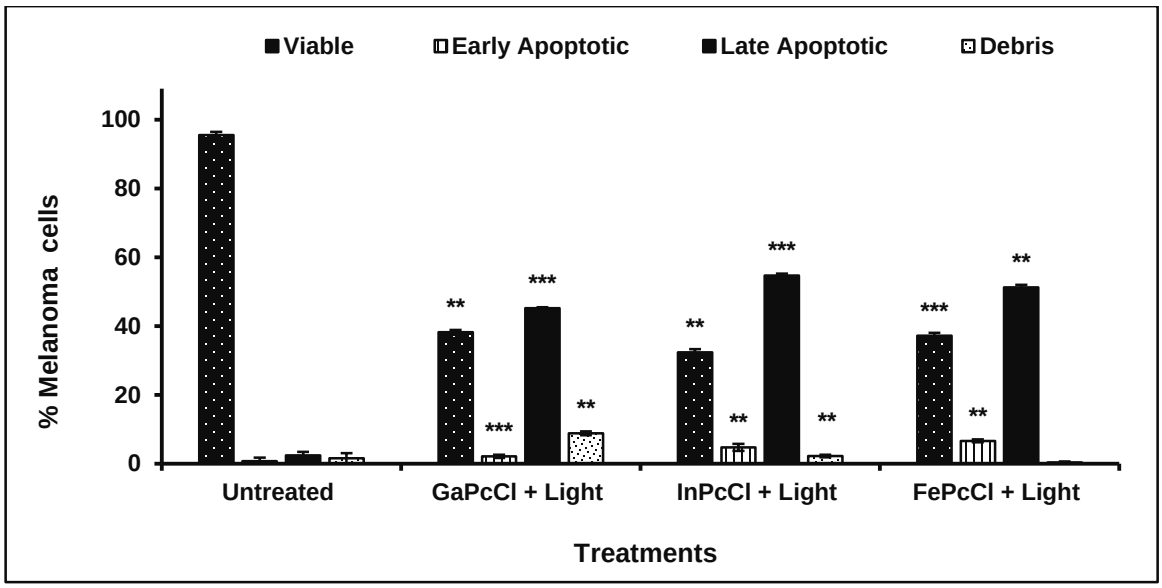

Figure A-3 FITC Annexin V/PI apoptosis analysis by flow cytometry of melanoma cancer cells after 24 post-PDT treatment. Percentage (%) of viable cells, early apoptotic cells, late apoptotic cells and cellular debris are compared with the untreated control. (**) $P \leq 0.01$ and (***) $P \leq 0.001$.

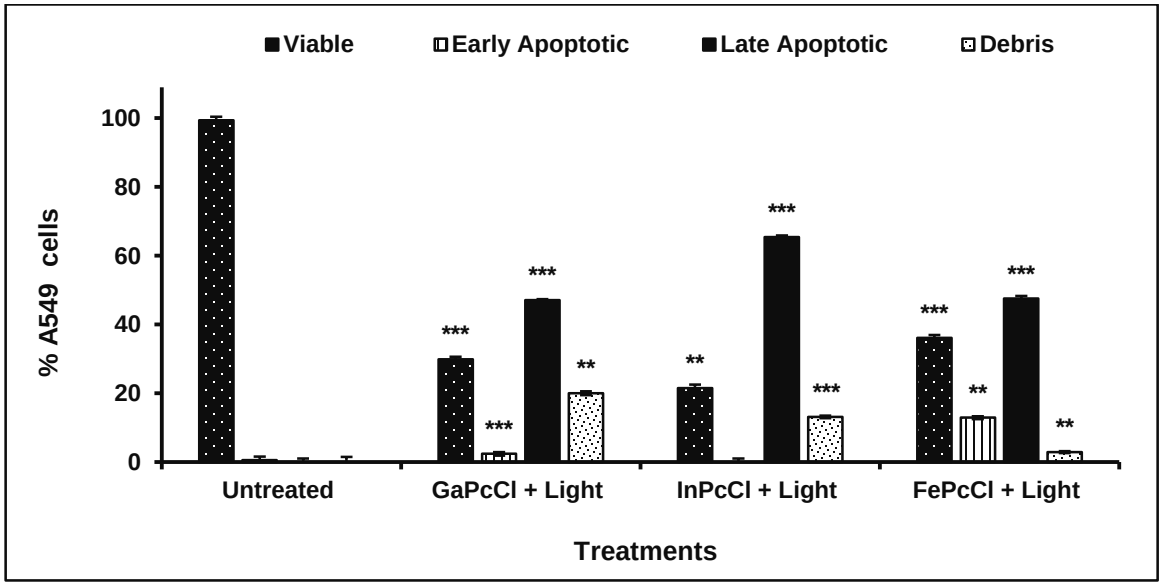

Figure A-4 FITC Annexin V/PI apoptosis analysis by flow cytometry of A549 cancer cells after 24 post-PDT treatment. Percentage (%) of viable cells, early apoptotic cells, late apoptotic cells and cellular debris are compared with the untreated control. (**) $P \leq 0.01$ and (***) $P \leq 0.001$.

Efficacy of gallium phthalocyanine as a photosensitizing agent in photodynamic therapy for the treatment of cancer

Kaminee Maduray*[a], Bharti Odhav[a]
[a]Durban University of Technology; Department of Biotechnology and Food Technology, 41/43 ML Sultan Road, Durban, 4001, South Africa

ABSTRACT

Photodynamic therapy is a revolutionary treatment aimed at treating cancers without surgery or chemotherapy. It is based on the discovery that certain chemicals known as photosensitizing agents (e.g. porphyrins, phthalocyanines, etc.) can kill cancerous cells when exposed to low level laser light at a specific wavelength. The present study investigates the cellular uptake and photodynamic effect of gallium (III) phthalocyanine chloride (GaPcCl) on Caco-2 cancer cells. Caco-2 cells were treated with different concentrations of GaPcCl for 2 h before treatment with a diode laser (λ = 661 nm, laser power = 90 mW) delivering a light dose of 2.5 J/cm^2, 4.5 J/cm^2 or 8.5 J/cm^2. After 24 h, the cell viability of post-irradiated cells was measured using the MTT assay. Cellular uptake studies were performed by photosensitizing cells with GaPcCl for 30 min, 2 h, 10 h, 12 h, 18 h and 24 h before lysing the treated cells into solution to measure the GaPcCl fluorescence emission at an excitation wavelength of 600 nm. Results showed an increase in fluorescence intensity of emission peaks at longer incubation times, indicating a greater cellular uptake of GaPcCl by Caco-2 cells at 24 h in comparison to 30 min. GaPcCl at a concentration of 100 µg/ml activated with a laser light dose of 8.5 J/cm^2 reduced the cell viability of Caco-2 cells to 27%. This concludes that GaPcCl activated with low level laser light can be used as a photosensitizing agent for the *in vitro* PDT treatment of colon cancer.

Keywords: gallium phthalocyanine, photodynamic therapy, photosensitizer, colon cancer, laser treatment

1. INTRODUCTION

Photodynamic therapy (PDT) is clinically approved in several countries for the treatment of dermatological diseases and various cancers (e.g. head, neck, brain, lung, oesophageal, gastric, cervical, bronchi and bladder cancer). It is a minimally invasive treatment that requires an inactive photosensitive drug/dye termed a photosensitizer (PS), light usually between 600 nm and 900 nm generated from a low power laser source and molecular oxygen from biological tissue. The PS is applied topically or administrated systemically to preferentially accumulate in the diseased/cancerous tissue before light at a specific wavelength is precisely delivered to the affected area or entire body to activate the PS.[1-2] The activated PS can directly react with a substrate (e.g. cell membrane or molecule) and transfer a proton or hydrogen atom to form free radicals. These radicals will react with oxygen present in the tissue to produce reactive oxygen species (ROS). Alternatively, the activated PS can transfer its energy directly to molecular oxygen (a triplet form in the ground state), to form an excited state singlet oxygen. This highly reactive form of oxygen (excited state singlet oxygen) will react with many biological molecules (e.g. lipids, proteins or nucleic acids). Both these photochemical reactions can occur simultaneously to produce ROS and excited state singlet oxygen, which are the primary cytotoxic agents responsible for the eradication of cancerous tissue (tumor) making PDT highly dependent on the amount of ROS and excited state singlet oxygen produced by these photochemical reactions.[3-4]

Phthalocyanines (Pcs) are industrial dyes[5] which have proven to be promising as photosensitizing agents for PDT, due to its versatility, chemical and thermal stability.[6-7] The PDT properties of the Pc dyes can be influenced by the presence and nature of the incorporated metal ion.[8] For example, Pcs containing transition metals tend to have short triplet lifetimes.[8]

*madurayk@yahoo.com; phone 083 6129541

Optics in Health Care and Biomedical Optics V, edited by Qingming Luo, Ying Gu, Xingde D. Li,
Proc. of SPIE Vol. 8553, 85530G · © 2012 SPIE · CCC code: 1605-742/12/$18
doi: 10.1117/12.2001266

The closed shell, diamagnetic ions such as Zn^{2+} (zinc), Al^{3+} (aluminum) and Ga^{3+} (gallium) provide Pc complexes with high triplet quantum yields and long triplet lifetimes, resulting in efficient generation of singlet molecular oxygen. Pc complexes that contain Ga^{3+} as a central metal ion and axial ligands which act as spacers between the rings display reduced aggregation.[8] Generally, metal Pc complexes are known to have minimal dark toxicity and low solubility in most organic solvents. However, the solubility can be improved in non-polar solvents by introducing different substituents such as alkyl, alkoxy and alkylthio chains on the Pc ring. The presence of sulfo or quaternary ammonium groups enhances its solubility in aqueous media at different pH values.[9] Metal Pc complexes are well characterized by a distinct intense absorption at a wavelength of ± 600 nm (Q band) accompanied by a weak absorption at a wavelength of ± 400 nm (B band).[10] These characteristics of metal Pc complexes suggest that it may be the ideal photosensitizing agent for PDT.

The photophysical and photochemistry of all metal Pc complexes are well documented.[11] Most *in vitro* and *vivo* PDT studies have used aluminum, zinc and silicon Pc complexes or derivatives as photosensitizing agents[12] which has lead to several Pc complexes such as the silicon (IV) Pc complex and a liposomal preparation of zinc (II) Pc complex into the clinical trial stages.[13] Currently, sulfonated aluminum Pc complex (Photosens®) is being clinically used as a PDT agent in Russia for the treatment of a range of cancers[13] with no PDT-related pain reported during treatment.[5] Nonetheless, the photodynamic activity of many metal Pc complexes (e.g. gallium Pcs, germanium Pcs, tin Pcs, etc.) appears not to have been fully explored especially when compared to aluminum, zinc and silicon Pc complexes.[6]

Gallium being diamagnetic[8], should exhibit excellent photosensitizing ability desirable for PDT applications and it is known to accumulate in tumors.[14] At present time gallium is being used in cancer treatments and radioactive gallium compounds are used as tumor imaging agents.[14] Therefore, the anti-cancer activity of gallium Pc complexes is of fundamental importance, hence this study investigates the *in vitro* photodynamic effect of gallium (III) phthalocyanine chloride activated with a continuous wave laser at a wavelength of 661 nm on human Caco-2 (colorectal) cancer cells.

2. METHODOLOGY

2.1 Spectrophotometric analysis of GaPcCl

Gallium (III) phthalocyanine chloride (GaPcCl) was purchased from Sigma-Aldrich and used as a photosensitizer without further purification. Spectrophotometric experiments were carried out in dimethylsulfoxide (DMSO, Sigma). The electronic absorption spectrum of GaPcCl was recorded on the Cary 100 UV-Vis spectrophotometer in the spectral range of 300-900 nm at room temperature. The fluorescence emission spectrum of GaPcCl was measured by using a Varian Eclipse Fluorescence Spectrophotometer with an excitation wavelength set at 600 nm.

2.2 Cell culture of Caco-2 cancer cells

Human colon carcinoma (Caco-2) cells (passage 4) were routinely maintained in Dulbecco's modified Eagle's medium (DMEM, Biochrom) supplemented with 10% fetal calf serum (FCS, Highveld Biological) and 1% Penicillin-Streptomycin (pen/strep, Biochrom) at 37°C in a 5% CO_2 incubator. For experimental assays, 80% confluent flasks with Caco-2 cells from passage 7 to 9 were seeded in 24-well tissue culture plates (Costar) at a density of 2 x 10^4 cells per a well in 1 ml supplemented DMEM.

2.3 Cellular uptake of GaPcCl by Caco-2 cells

Caco-2 cells seeded in 24-well tissue culture plates were photosensitized with 100 µg/ml of GaPcCl for uptake times of 30 min, 2 h, 10 h, 12 h, 14 h, 18 h and 24 h at 37 °C in a 5% CO_2 incubator under dark conditions. After incubation with GaPcCl for 30 min, 2 h, 10 h, 12 h, 14 h, 18 h, and 24 h, cells were washed with phosphate buffer (PBS, Sigma) before collecting pellets of the cells for the extraction of intracellular GaPcCl using DMSO. Then the samples were centrifuged

and the supernatants were collected for fluorescence detection using Fluorescence Spectrophotometer with an excitation wavelength set at 600 nm.

2.4 Dark toxicity assay

A PS (in its inactive form) without laser treatment may have anti-proliferative and/or cytotoxic effects, referred as dark toxicity. A stock solution GaPcCl at a concentration of 100 µg/ml was prepared using DMEM and DMSO. The stock solution of GaPcCl was further diluted in DMEM medium supplemented with 10% FCS and 1% pen/strep to prepare treatment concentrations ranging from 2 µg/ml – 90 µg/ml. Caco-2 cells seeded in 24-well tissue culture plates were incubated for 2 h with different GaPcCl concentrations at 37 °C in a 5% CO_2 incubator under dark conditions. Cell culture media (DMEM), cells treated with DMSO and untreated cells served as controls. After 2 h the photosensitized cells were washed with PBS and cell viability was measured by 3-[4, 5-dimethylthiazolyl]-2, 5-diphenyltetrazolium bromide (MTT) assay. 500 µl of DMEM with 100 µl of MTT (5 mg/ml) was added to each well for 4 h at 37 °C in a 5% CO_2 atmosphere. After 4 h, MTT was replaced with 500 µl of DMSO to dissolve the formazan crystals and the resulting absorbance was measured using a plate reader (Biohit) at a wavelength of 490 nm with a reference wavelength at 630 nm simultaneously.

2.5 *In vitro* photodynamic therapy

Caco-2 cells at a density of 2 x 10^4 cells/ml were seeded onto 24-well tissue culture plates and allowed to attach overnight before treatment with different concentrations of GaPcCl (2 µg/ml-100 µg/ml). After 2 h the photosensitized cells were irradiated in the dark. Irradiation was performed using a continuous wave diode laser (Cube Laser System, Coherent) with a wavelength of 661 nm. A spot size of 1 cm with a measured output power of 90 mW was used to deliver treatment light doses of 2.5 J/cm^2, 4.5 J/cm^2 and 8.5 J/cm^2 to specific wells on the 24-well plates containing a monolayer of photosensitized cells in 22 sec, 39 sec, and 74 sec of irradiation time accordingly. The control cells contained no photosensitizer and were not exposed to laser treatment. A laser control was set-up for each treatment light dose by irradiating cells without photosensitizer for 22 sec, 39 sec or 74 sec. After irradiation, plates were incubated at 37 °C in a 5% CO_2 incubator under dark conditions for 24 h before cell viability was measured using the MTT assay as described above. The results of all experiments were expressed as percentage reduction of the number of viable cells, when compared to the untreated controls. PDT treated , untreated and laser treated (control) Caco-2 cells were viewed under an inverted microscopy (Nikon, Japan) at 10x magnification to observe changes in cell morphology that may have occurred after 24 h, before cell viability was measured.

3. DATA

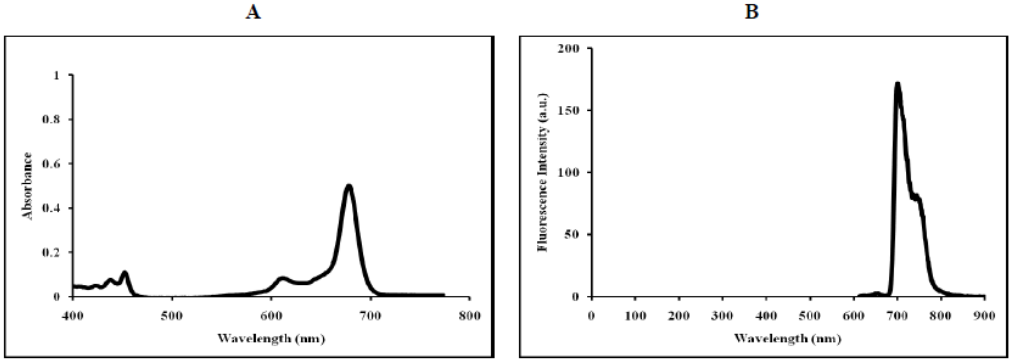

Figure 1. (A) The absorption spectrum of GaPcCl in DMSO (B) A fluorescence emission spectrum GaPcCl in DMSO determined by using a fixed excitation wavelength of 600 nm.

The UV-Vis spectrum of GaPcCl in DMSO is seen in **Figure 1A** and **Figure 1B** shows the emission spectrum of GaPcCl in DMSO determined by using a fixed excitation wavelength of 600 nm.

Figure 2A shows the emission peak and emission or fluorescence intensity (excitation wavelength = 600 nm) of intracellular GaPcCl in DMSO extracted from Caco-2 cells at uptake times of 30 min, 2 h and 10 h; with **Figure 2B** showing uptake times of 12 h,18 h and 24 h.

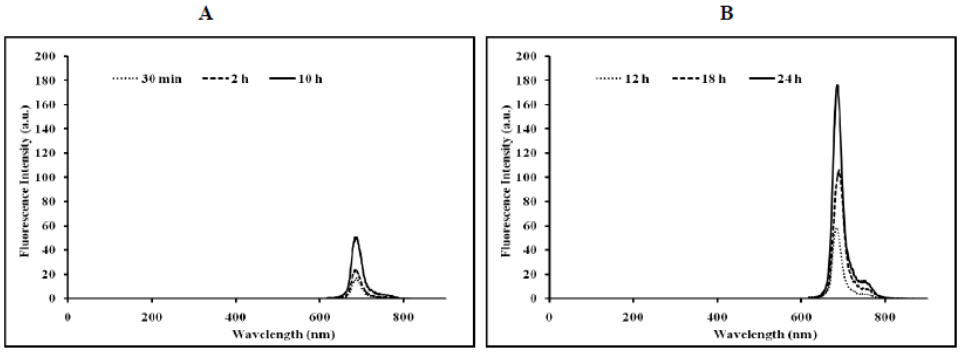

Figure 2. The emissiom peak and fluorescence intensity of extracted intracellular GaPcCl (100 μg/ml) from Caco-2 cancer cells after an incubation period of 30 min, 2 h, 10 h (A); 12 h, 18 h and 24 h (B) measured using a spectrofluorometer with a excitation wavelenght set at 600 nm.

The cytotoxic effect of different concentrations of GaPcCl in its inactive state (without laser treatment) on the cell viability of Caco-2 cancer cells is presented in **Figure 3**.

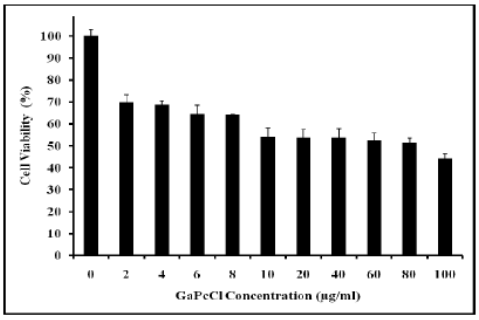

Figure 3. The cell viability (%) of Caco-2 cells after photosensitization with different concentrations of GaPcCl without laser treatment. 0 = Caco-2 cells that were not exposed to GaPcCl (untreated control). Data points represent the mean of ± standard deviation, n =3.

Caco-2 cancer cells were photosensitized with different concentrations GaClPc (2 µg/ml - 100 µg/ml) before laser treatment for 22 sec (2.5 J/cm^2), 34 sec (4.5 J/cm^2) and 74 sec (8.5 J/cm^2) with continuous wave laser at a wavelength of 672 nm. Post-irradiated cells were incubated for 24 h before cell viability was measured using MTT assay (**Figure 4**). The change in cell morphology of Caco-2 cells as a result of GaPcCl-mediated PDT was observed using an inverted microscope and is shown in **Figure 5**.

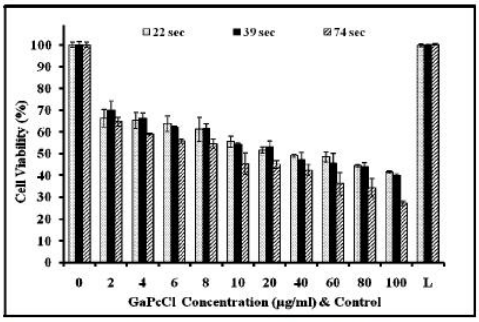

Figure 4. The cell viability (%) of Caco-2 cells photosensitized with different concentrations of GaPcCl and laser treatment for 22 sec (2.5 J/cm^2), 34 sec (4.5 J/cm^2) and 74 sec (8.5 J/cm^2). 0 = Caco-2 cells that were not exposed to GaPcCl and laser treatment (untreated control); L = Caco-2 cells that were irradiated without being exposed to GaPcCl (laser control). Data points represent the mean of ± standard deviation, n =3.

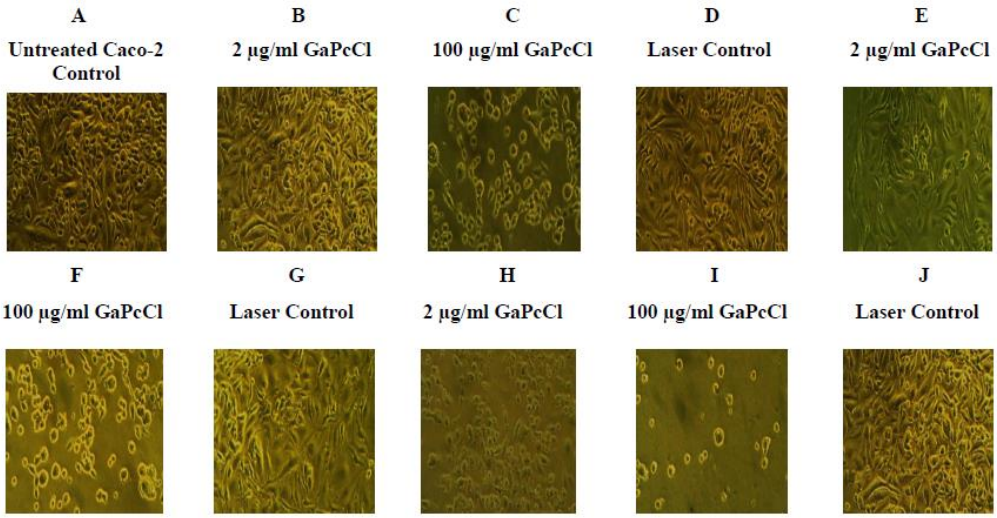

Figure 5: Micrographs showing the photodynamic effect of activated GaPcCl on Caco-2 cancer cells 24 h after irradiation for 22 sec (B-C), 39 sec (E-F) and 74 sec (H-I). Untreated Caco-2 cells not exposed to GaPcCl and laser treatment (A). Caco-2 cancer cells irradiated for 22 sec (D), 39 sec (G) and 74 sec (J) without being exposed to GaPcCl (laser control). (Magnification =10 x).

4. RESULTS

The ground state electronic absorption spectra of GaPcCl in DMSO showed a sharp single Q band at a wavelength of 678 nm accompanied by a few shoulder bands at 452 nm and 438 nm (**Figure 1A**). Fluorescence compounds can be identified and quantified on the basis of their excitation and emission properties. As shown in **Figure 1B** this PS has a detectable emission at 701 nm and 754 nm at a unique excitation wavelength of 600 nm. Emitted fluorescence is observed at 701 nm and 754 nm for the DMSO supernatant collected from treated Caco-2 cells at uptake times of 30 min, 2 h, 10 h, 12 h, 18 h and 24 h (**Figure 2A & 2B**) when excited at 600 nm; however maximum emission or fluorescence intensity is observed at an uptake time of 24 h. Dark toxicity studies were conducted to determine the cytotoxicity effects of GaPcCl in its inactive state (without laser treatment) on the Caco-2 cancer cells. The data in **Figure 3** indicated that inactive GaPcCl concentrations higher than 10 μg/ml decreased the cell viability of Caco-2 cells below 60% and inactive GaPcCl at a concentration of 100 μg/ml decreased cell viability to 44%.

Caco-2 cancer cells photosensitized with different concentrations of GaPcCl showed a significant decrease in the cell viability when irradiated for 22 sec (2.5 J/cm^2), 34 sec (4.5 J/cm^2) and 74 sec (8.5 J/cm^2). At a GaPcCl concentration of 2 μg/ml cell viability was decreased to 60%, 70% and 65 %; 24 h after treatment with a light dose of 2.5 J/cm^2, 4.5 J/cm^2 and 8.5 J/cm^2 respectively (**Figure 4**). In comparison to a higher treatment concentration of 100 μg/ml cell viability was further decreased to 41%, 40% and 27%; 24 h after treatment with a light dose of 2.5 J/cm^2, 4.5 J/cm^2 and 8.5 J/cm^2 respectively (**Figure 4**). Morphology changes were observed under an inverted microscope and micrographs are depicted in **Figure 5**. Cells photosensitized with higher concentrations of GaPcCl and laser treated with varying light doses showed profound changes in cell morphology (**Figure 5C, 5F & 5I**) when compared to the morphology of untreated Caco-2 cancer cells (**Figure 5A**). PDT treated Caco-2 cancer cells became round and detached from neighboring cells (**Figure 5C, 5F & 5I**). Cells treated with the laser at different light doses excluding GaPcCl remained healthy and undamaged after 24 h (**Figure 5D, 5G & 5J**).

5. CONCLUSION

The present study shows that gallium (III) phthalocyanine chloride is a potent and effective photosensitizer for *in vitro* PDT treatment of colorectal carcinoma cells.

ACKNOWLEDGMENTS

The authors wish to thank Dr Yen-Ju (Hollis) Shen (MRC, Medical Research Council) for providing the Caco-2 cancer cells. This work was funded by the National Research Funding (NRF) of South Africa and Durban University of Technology.

REFERENCES

1. Nowis, D., Makowski, M., Stoklosa, T., Legat, M. and Issat, T., Golab, J., "Direct tumor damage mechanisms of photodynamic therapy," Acta Biochimica Polonica 52(2), 339-352 (2005).
2. Huang, Z., "A review progress in clinical photodynamic therapy, "Technol Cancer Res Treat. 4(3), 283-293 (2005).
3. Jiménez-Banzo, A., Sagrista, M.L., Mora, M. and Nonell, S., "Kinetics of singlet oxygen photosensitization in human skin fibroblasts," Free Radical Biology & Medicine 44 (2008).
4. Plaetzer, K., Krammer, B., Berlanda, J., Berr, F. and Kiesslich, T., "Photophysics and photochemistry of photodynamic therapy: fundamental aspects, " Lasers Med Sci. 24, 259-268 (2009).
5. Allison, R.R., Downie, G.H., Cuenca, R., Hu, X., Childs, C.J.H. and Sibata, C.H., "Photosensitizers in clinical PDT," Photodiagnosis and Photodynamic Therapy 1, 27-42 (2004).
6. Durmuş, M. and Nykong, T., "Synthesis, photophysical and photochemical properties of aryloxy tetra-substituted gallium and indium phthalocyanine derivatives," Tetrahedron 63, 1385-1394 (2007).

7. Grobosch, M., Schmidt, C., Kraus, R. and Knupfer, M. "Electronic properties of transition metal Pcs: The impact of the central metal atom, " Organic Electronics 11, 1483-1488 (2010).
8. Durmuş, M. and Nykong, T., "The synthesis, fluorescence behavior and singlet oxygen studies of new water-soluble cationic gallium (III) phthalocyanines," Inorganic Chemistry Communications 10, 332-338 (2007).
9. Durmuş, M. and Nykong, T., "Synthesis, photophysical and photochemical properties of tetra- and octa-substituted gallium and indium phthalocyanines," Polyhedron 26, 3323-3335 (2007).
10. Chen, J., Gan, Q., Li, S., Gong, F., Wang, Q., Yang, Z., Wang, S., Xu, H., Ma, J.S. and Yang, G., "The effects of central metals and peripheral substituents on the photophysical properties and optical limiting performance of phthalocyanines with axial chloride ligand, " Journal of Photochemistry and Photobiology A: Chemistry 207, 58-65 (2009).
11. Nykong, T. "Effects of substituents on the photochemical and photophysical properties of main group metal phthalocyanines, "Coordination Chemistry Reviews 251, 1707-1722 (2007).
12. Sekkat, N., Van Den Bergh, H., Nykong, T. and Lange N., "Like a Bolt from the Blue: Phthalocyanines in Biomedical Optics, "Molecules 17, 98-144 (2012).
13. Çamur, M. and Durmuş, M., "The first comparison of photophysical and photochemical properties of non-ionic, ionic and zwitterionic gallium (III) and indium (III) phthalocyanines," Journal of Photochemistry and Photobiology A: Chemistry 219, 217-227 (2011).
14. Lessa, J.A., Parrilha, G.L. and Beraldo, H., "Gallium complexes as new promising metallodrug candidates, "Inorganica Chimica Acta, In Press (2012).

Journal of Photochemistry and Photobiology B: Biology 128 (2013) 58–63

Contents lists available at ScienceDirect

Journal of Photochemistry and Photobiology B: Biology

journal homepage: www.elsevier.com/locate/jphotobiol

The *in vitro* photodynamic effect of laser activated gallium, indium and iron phthalocyanine chlorides on human lung adenocarcinoma cells

K. Maduray *, B. Odhav

Durban University of Technology, Department of Biotechnology and Food Technology, Steve Biko Campus, Durban 4001, South Africa

ARTICLE INFO

Article history:
Received 13 June 2013
Received in revised form 18 July 2013
Accepted 2 August 2013
Available online 17 August 2013

Keywords:
Photodynamic therapy
Gallium phthalocyanines
Indium phthalocyanines
Iron phthalocyanines
Lung cancer
A549 cells

ABSTRACT

Metal-based phthalocyanines currently are utilized as a colorant for industrial applications but their unique properties also make them prospective photosensitizers. Photosensitizers are non-toxic drugs, which are commonly used in photodynamic therapy (PDT), for the treatment of various cancers. PDT is based on the principle that, exposure to light shortly after photosensitizer administration predominately leads to the production of reactive oxygen species for the eradication of cancerous cells and tissue. This *in vitro* study investigated the photodynamic effect of gallium (GaPcCl), indium (InPcCl) and iron (FePcCl) phthalocyanine chlorides on human lung adenocarcinoma cells (A549). Experimentally, 2×10^4 cells/ml were seeded in 24-well tissue culture plates and allowed to attach overnight, after which cells were treated with different concentrations of GaPcCl, InPcCl and FePcCl ranging from 2 μg/ml to 100 μg/ml. After 2 h, cells were irradiated with constant light doses of 2.5 J/cm^2, 4.5 J/cm^2 and 8.5 J/cm^2 delivered from a diode laser (λ = 661 nm). Post-irradiated cells were incubated for 24 h before cell viability was measured using the MTT Assay. At 24 h after PDT, irradiation with a light dose of 2.5 J/cm^2 for each photosensitizing concentration of GaPcCl, InPcCl and FePcCl produced a significant decrease in cell viability, but when the treatment light dose was further increased to 4.5 J/cm^2 and 8.5 J/cm^2 the cell survival was less than 40%. Results also showed that photoactivated FePcCl decreased cell survival of A549 cells to 0% with photosensitizing concentrations of 40 μg/ml and treatment light dose of 2.5 J/cm^2. A 20 μg/ml photosensitizing concentration of FePcCl in combination with an increased treatment light dose of either 4.5 J/cm^2 or 8.5 J/cm^2 also resulted in 0% cell survival. This PDT study concludes that low concentrations on GaPcCl, InPcCl and FePcCl activated with low level light doses can be used for the effective *in vitro* killing of lung cancer cells.

1. Introduction

Photodynamic therapy (PDT) has been used both as an investigational tool and as a treatment modality for lung cancer since the 1980s [1]. The procedure is relatively simple and treatment does not require the cutting through ribs, nerves and healthy lung parenchyma tissue; making it less invasive than conventional surgery [1,2]. High risk patients with poor pulmonary and/or cardiac function that have been refused surgery and suffer from multiple lung cancers become ideal candidates for PDT treatment [3]. Due to the fact that treatment involves the systemic administration of a cancerous tissue photosensitizing drug (photosensitiser; PS) such as porfimer sodium (Photofrin®) and photoirradiation through a fibreoptic bronchoscope. The light sources (e.g. broad spectrum lights, diode lamps and lasers) used in PDT for photoirradiation are at a specific wavelength that corresponds to the peak absorption of the PS [4–6]. During photoirradiation, the PS in its singlet ground state becomes activated to an excited singlet state, which is followed by intersystem crossing to an excited triplet state (a relatively long-lived excited state). The energy of the excited PS in its excited triplet state can be transferred to biological substrates and molecular oxygen present in the lung tissue via photochemical reactions (type I and type II) to generate reactive oxygen species (ROS). ROS is the cytotoxic agent in PDT responsible for triggering cell death mainly by apoptosis, necrosis or autophagy, resulting in the eradication of the cancerous tissue (tumor) [6,7].

Photofrin® has been approved for clinical treatment of lung, esophageal, bladder and cervical cancer [8] in several countries (e.g. European countries, Canada, United Kingdom, Netherlands and Japan) [9]. It is administrated via intravenous injection at a drug concentration of 2–5 mg/kg followed by irradiation with light dose of 100–200 J/cm^{-2} (λ = 630 nm) at 24–48 h after injection [10]. Although Photofrin® is still the most widely used PS, the prolonged skin photosensitivity after PDT treatment (4–12 weeks) and relatively low absorbance at 630 nm are considered potential disadvantages [11]. Due to these concerns newly and potentially improved photosensitizers (PSs) were discovered such as

* Corresponding author.
E-mail address: maduraysk@yahoo.com (K. Maduray).

1011-1344/$ - see front matter © 2013 Elsevier B.V. All rights reserved.
http://dx.doi.org/10.1016/j.jphotobiol.2013.08.003

benzoporphyrin derivatives (BPD-MA), meta-tetrahydroxyphenylchlorin (m-THPC), δ-aminolaevulinic acid (5-ALA) and phthalocyanines (Pcs). These newly discovered PSs do not cause prolonged photosensitivity and are activated by longer wavelengths (660–690 nm) that penetrate more deeply into tissue [12,13]. Most of these newly improved developed PSs are not yet approved for clinical use as these are still under investigation to determine treatment-related parameters, such as optimal PS dose, time interval between administration of the PS and laser treatment, optimal light dose, photodynamic efficacy of PSs for various cancers, cytotoxicity effects of each PS on healthy normal tissue and optimal wavelength excitation [12].

A great interest is currently focused on phthalocyanines, naphthalocyanines and their metal complexes for PDT, since they not only resemble porphyrins but are made up of isoindoles rather than pyrroles, have a longer conjugate pathway around the ring structure, and therefore absorb at longer wavelengths than porphyrins [14]. Pcs tend to exhibit low absorption at wavelengths between 300 nm and 400 nm (spectral range where daylight intensity is the highest) leading potentially to a low or no skin photosensitivity when exposed to sunlight after PDT treatment [15]. Another desirable feature of Pcs is its strong absorbance in the visible region between 600 nm and 700 nm which favors the optimal penetration of the light through tissue, thus allowing for more efficient treating of deeper lying lesions or deep-seated tumors by PDT. These compounds are also considered to be chemically and photochemically stable compounds [14,16,17].

Naphthalocyanines (extended Pc derivatives) advantageously absorb at a higher wavelength (740–780 nm) than Pcs, further increasing the light penetration through skin [18,19]. This absorption range of naphthalocyanines makes them potential *in vivo* imaging agents and photosensitizing agents for the PDT treatment of highly pigmented tumors (e.g. melanomas) [18, 19]. Unfortunately, naphthalocyanines are generally less stable than their Pc counterparts as they readily decompose in the presence of light and oxygen [18,20].

In contrast, the metal-based Pc complexes are known to be more stable in the presence of light and oxygen. These are formed by incorporating one of 70 different kinds of metals or metalloid atoms into the central ring of the Pc structure, replacing the two hydrogens normally present in non-metal Pcs [21]. Interestingly, the nature and the presence of the inserted central metal ion in Pc strongly influence its PDT properties [16,22]. For example, diamagnetic ions that contain a closed shell such as zinc (Zn^{2+}), aluminum (Al^{3+}), gallium (Ga^{3+}) and silicon (Si^{4+}) give Pc complexes high triplet quantum yields and long triplet lifetimes, which are essential for efficient photosensitization during PDT treatment [16,22]. Pcs containing Al, Zn and Si as central metal ions have been the most extensively studied for their PDT activity because of their desirable photophysical properties [23]. To date, Photosens® (mixture of aluminum chloride Pcs with sulphonated side-groups) is clinically used in Russia to treat a range of cancers (e.g. skin, breast, lung, head, neck, cervical, etc.) [15]. Photosens®-mediated PDT is performed according to a procedure similar to that described for Photofrin® but using considerably lower drug (0.5–0.8 mg/kg) concentrations and lower level light doses ranging from 150 J/cm^{-2} to 200 J/cm^{-2} (peak λ = 675 nm) at 24–72 h after intravenous injection [10]. Silicon (IV) phthalocyanine Pc4 and a liposomal preparation of zinc (II) phthalocyanine are currently under clinical trials [23,24].

The main disadvantages of most Pcs including some metal Pc complexes are their low solubility potential and its ability to aggregate in certain solvents (e.g. water and organic solvents) [24]. Aggregation reduces the lifetimes of the MPc excited state, quantum yields and singlet-oxygen generation. Altering the peripheral substitution of the macrocyclic ring in Pc structure is one way of improving the solubility of these photosensitizers. On the other hand, MPc complexes that contain hydrophilic groups as axial ligands, which coordinate to central metal ions, facilitate them to be water-soluble [24]. In addition, MPc complexes containing metals like Ga^{3+} that can coordinate axial ligands is beneficial in that axial ligation prevents aggregation [16]. Likewise, large metals such as indium (In) are also useful central metals in MPc complexes as it is diamagnetic and able to host axial ligands [22,25]. The well documented information available on the architectural flexibility, photophysics and photochemistry properties of various metal-based Pc complexes shows clearly that these compounds could make valuable photosensitizers for the PDT treatment of tumors [14–25]. Unfortunately, only a small amount of preliminary data seems to be available on the photodynamic activity of GaPcs, InPcs and a variety of other metal-based Pcs. Thus, the present work studied the cellular uptake and *in vitro* photodynamic effect of three different metal-based phthalocyanines: gallium (III) phthalocyanine chloride, indium (III) phthalocyanine chloride and iron (III) phthalocyanine chloride using lung carcinoma cells (A549).

2. Materials and methods

2.1. Photosensitizers

Gallium (III) phthalocyanine chloride (GaPcCl); indium (III) phthalocyanine chloride (InPcCl) and iron (III) phthalocyanine chloride (FePcCl) were purchased from Sigma Aldrich®. Stock solutions (100 μg/ml) of each photosensitizer was prepared using dimethylsulfoxide (DMSO) and Dulbecco's modified eagle's medium (DMEM) culture media, which was further diluted in DMEM to obtain treatment concentrations ranging from 2 μg/ml to 100 μg/ml.

2.2. Spectrophotometric analysis of the photosensitizers

All spectrophotometric experiments were carried out using DMSO as a solvent. The absorption spectrum for GaPcCl, InPcCl and FePcCl were recorded on a spectrophotometer (Cary 100) in the spectral range of 300–900 nm at room temperature. Fluorescence excitation and emission spectrum for GaPcCl, InPcCl and FePcCl were measured using a fluorescence spectrophotometer (Eclipse, Varian) at room temperature.

2.3. Cell culture

Human lung carcinoma cells (A549) were kindly provided by Dr. Bronwyn C. Joubert from University of Kwazulu Natal, Nelson Mandela Medical School. A549 cancer cells were routinely grown in DMEM supplemented with 10% fetal calf serum (FCS) and 1% antibiotics (Penicillin/Streptomycin) at 37 °C in humidified atmosphere with 5% CO_2. All experiments were performed with cells of passage numbers from 48 to 57.

2.4. Cellular uptake of photosensitizers by A549 cancer cells

A549 cells were seeded in 24-well tissue culture plates at a density of approximately 2×10^4 cells/ml. Cells were allowed to attach overnight at 37 °C in a humidified atmosphere with 5% CO_2. After 24 h, cells were exposed to GaPcCl, InPcCl or FePcCl at a concentration of 100 μg/ml for 30 min, 1 h, 2 h, 4 h, 8 h, 10 h, 12 h, 14 h, 16 h, 18 h, 20 h, 22 h and 24 h. At the end of each exposure time, the photosensitized cells were thoroughly washed in phosphate buffered saline (PBS) before detaching the cells from the surface of the plate by trypsinization for the harvesting of cells by centrifugation.

The harvested cells were resuspended in DMSO at room temperature for 10 min followed by centrifugation for 2 min at 6000 rpm. The cell lysis solution or DMSO supernatant were analyzed for traces of intracellular accumulated GaPcCl, InPcCl or FePcCl using a fluorescence spectrophotometer at specific excitation wavelengths of 600 nm, 605 nm and 680 nm respectively. Emitted fluorescence peaks are an indication of the PS uptake by A549 cancer cells and fluorescence intensity (arbitrary units, a.u.) of emitted peaks will be proportional to the concentration of the PS. Simultaneously, cell lysis from untreated A549 cells (not pre-incubated with the metal-based phthalocyanines) were measured as a control at similar excitation wavelengths for each exposure time.

2.5. Dark toxicity assay (cytotoxic effect of the photosensitizers without laser irradiation)

A549 cells were seeded in 24-well tissue culture plates at a density of approximately 2×10^4 cells/ml. Cells were allowed to attach overnight at 37 °C in a humidified atmosphere with 5% CO_2. After 24 h, cells were incubated with various concentrations (2–100 μg/ml) of GaPcCl, InPcCl or FePcCl at 37 °C in humidified atmosphere with 5% CO_2 in the dark for 2 h. A control (untreated cells) containing A549 cells that were not exposed to GaPcCl, InPcCl or FePcCl (0 μg/ml) was included for each set of experiments. After 2 h, the photosensitized cells were washed twice with PBS and the cell viability was measured using the MTT (methyl-thiazolyl-tetrazolium) colorimetric assay. For the MTT assay, 500 μl of fresh culture medium was added together with 100 μl of MTT (methyl-thiazolyl-tetrazolium) solution (1 mg/ml in PBS) to each well. The plates were incubated for 4 h allowing for the MTT to be metabolised to formazan by the succinate-tetrazolim reductase system that is active only in viable cells. At the end of the fourth hour, the formed formazan crystals at the bottom of each well were dissolved in DMSO and the absorbance of each well was measured at a wavelength 490 nm simultaneously with a reference wavelength at 630 nm using a microplate reader (Biohit). The percentage of viable cells for each well was calculated using the formula [1].

$$\text{Cell viability}(\%) = (\text{absorbance of sample}/\text{absorbance control}) \times 100 \quad (1)$$

2.6. In vitro photodynamic therapy

For the photodynamic therapy experiments, cells after 24 h incubation for full attachment in 24-well tissue culture plates were treated with GaPcCl, InPcCl or FePcCl at different photosensitizing concentrations (2–100 μg/ml) for 2 h. After 2 h, cells in monolayer cultures were irradiated with a red light diode laser (Cube System, Coherent) at a wavelength of 661 nm. A spot size of 1 cm in diameter was used to deliver a light dose of 2.5 J/cm^2, 4.5 J/cm^2 or 8.5 J/cm^2 with an output power of 90 mW to the respective wells. Laser parameters for each light dose are clearly shown in Table 1 and all irradiations were performed at room temperature in the dark. Cells to be used as untreated controls were not exposed to the photosensitizers and laser irradiation. Laser irradiated cells not pretreated with the photosensitizers served as the laser controls. Post-irradiated and control cells were incubated for 24 h before cell viability was measured using the MTT cell viability assay as described above.

Table 1
Laser parameters.

Parameters	Duration of irradiation		
	22 s	39 s	74 s
Wavelength (nm)	661	661	661
Wave emission	Continuous	Continuous	Continuous
Power output (mW)	90	90	90
Power density (mW/cm^2)	114.5913×10^{-3}	114.5913×10^{-3}	114.5913×10^{-3}
Spot size (cm^2)	0.7854	0.7854	0.7854
Fluence (J/cm^2)	2.5	4.5	8.5

2.7. Statistical analysis

Each test was done in triplicate. The mean, standard deviation and standard error were calculated using Microsoft Excel 2010 software. Further, statistical analysis was performed using Instat software (GraphPad prism 6) by one-way analysis of Variance (ANOVA). The Tukey–Kramer Multiple Comparisons Test was used to determine the significant changes between experimental groups and respective controls.

3. Results

the ground state electronic spectra of GaPcCl, InPcCl and FePcCl in DMSO showed characteristic absorption in the Q band region at a wavelength (λ_{max}) of 678 nm, 685 nm and 675 nm respectively. Each PS also showed an extra band at 611 nm (GaPcCl), 616 nm (InPcCl) and 642 nm (FePcCl) due to aggregation in the DMSO. Fluorescence emission peaks were observed at: 700 nm and 746 nm for GaPcCl with an excitation wavelength of 600 nm; 701 nm and 750 nm for InPc with an excitation wavelength of 605 nm and 750 nm for FePcCl with an excitation wavelength of 680 nm in DMSO.

Fluorescence compounds like phthalocyanines can be identified on the basis of its excitation and emission properties. As shown in Figs. 1–3, GaPcCl, InPcCl and FePcCl displayed detectable emission peaks/fluorescence when excited at a fixed wavelength of 600 nm, 605 nm and 680 nm respectively. Emission peaks were observed at specific wavelengths for the DMSO supernatant (cell lysis solution) collected from GaPcCl, InPcCl and FePcCl photosensitized A549 cancer cells after 30 s, 1 h, 2 h, 4 h, 8 h, 10 h, 12 h, 14 h, 16 h, 18 h, 20 h, 22 h and 24 h. However, maximum fluorescence intensity (a.u.) for the emission peaks of GaPcCl (Fig. 1), InPcCl (Fig. 2) and FePcCl (Fig. 3) was observed at an uptake time of 24 h.

The cytotoxic effect of inactive GaPcCl, InPcCl and FePcCl at different photosensitizing concentrations (without laser treatment) on the cell viability of A549 cancer cells is presented in Figs. 4–6. Negligible cytotoxicity was detected with lower concentrations of inactive GaPcCl, InPcCl and FePcCl. 100 μg/ml of GaPcCl and InPcCl in its inactive state decreased cell viability of A549 cancer cells to 46% (Fig. 4) and 55% (Fig. 5) respectively. At the same photosensitizing concentration FePcCl (inactive state) decreased cell viability of A549 cancer cells to 26%.

Figs. 7–9 illustrates that photodynamic therapy is a concentration-dependant treatment because as the photosensitizing concentration of GaPcCl, InPcCl and FePcCl increased the percentage of viable A549 cancer cells were proportionally decreasing after laser irradiation with a constant light dose of 2.5 J/cm^2. It was also observed that increased treatment light doses of 4.5 J/cm^2 and 8.5 J/cm^2 for the photoactivation of the different photosensitizing concentrations of GaPcCl, InPcCl and FePcCl were able to further reduce the cell viability of A549 cancer cells. The cell viability (%) of A549 cancer cells exposed to GaPcCl, InPcCl and FePcCl at a concentration of 2 μg/ml in combination with a treatment light dose of 2.5 J/cm^2 were 30%, 49% and 36% respectively. The resulting cell viability percentage for A549 cancer cells treated with 40 μg/ml of FePcCl and a light dose of 2.5 J/cm^2 was 0% (Fig. 9). Similarly, treatment light doses of 4.5 J/cm^2 and 8.5 J/cm^2 for photoactivation of A549 cancer cell photosensitized with 20 μg/ml of FePcCl resulted in 100% cell killing.

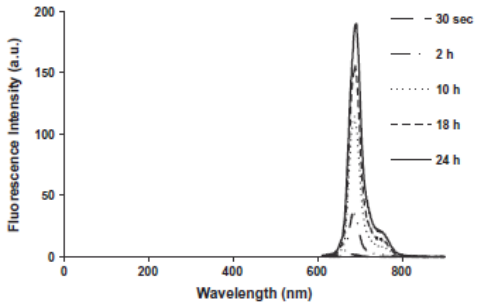

Fig. 1. The emission peak and fluorescence intensity (arbitrary units) of extracted intracellular GaPcCl from A549 cancer cells after an incubation period of 30 s, 2 h, 10 h, 18 h and 24 h with 100 μg/ml of GaPcCl measured using a fluorescence spectrophotometer with a excitation wavelength set at 600 nm.

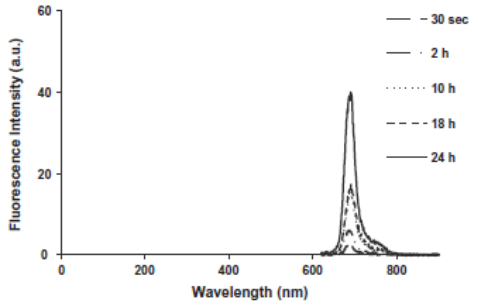

Fig. 2. The emission peak and fluorescence intensity (arbitrary units) of extracted intracellular InPcCl from A549 cancer cells after an incubation period of 30 s, 2 h, 10 h, 18 h and 24 h with 100 μg/ml of InPcCl measured using a fluorescence spectrophotometer with a excitation wavelength set at 605 nm.

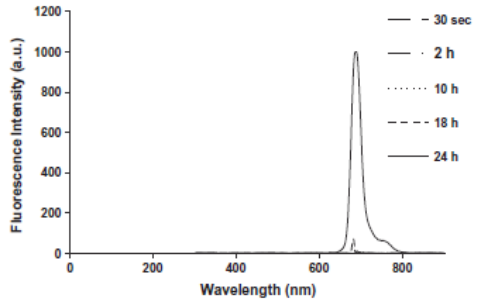

Fig. 3. The emission peak and fluorescence intensity (arbitrary units) of extracted intracellular FePcCl from A549 cancer cells after an incubation period of 30 s, 2 h, 10 h, 18 h and 24 h with 100 μg/ml of FePcCl measured using a fluorescence spectrophotometer with a excitation wavelength set at 680 nm.

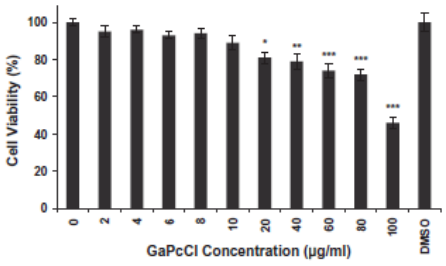

Fig. 4. The cell viability (%) of A549 cancer cells after photosensitization with different concentrations of GaPcCl for 2 h without laser treatment. 0 μg/ml = A549 cancer cells that were not exposed to GaPcCl (untreated cells-control); DMSO = dimethylsulfoxide (control). Data points represent the mean of ±SEM, $n = 3$. Significant differences between the untreated control and each of the different treatment concentrations are represented in graph as (*) $P \leqslant 0.05$, (**) $P \leqslant 0.01$ and (***) $P \leqslant 0.001$.

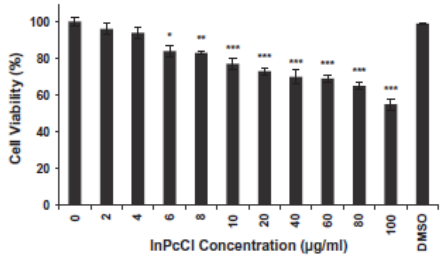

Fig. 5. The cell viability (%) of A549 cancer cells after photosensitization with different concentrations of InPcCl for 2 h without laser treatment. 0 μg/ml = A549 cancer cells that were not exposed to InPcCl (untreated cells-control); DMSO = dimethylsulfoxide (control). Data points represent the mean of ±SEM, $n = 3$. Significant differences between the untreated control and each of the different treatment concentrations are represented in graph as (*) $P \leqslant 0.05$, (**) $P \leqslant 0.01$ and (***) $P \leqslant 0.001$.

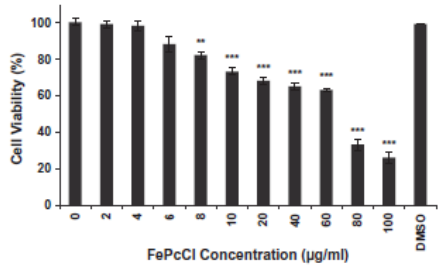

Fig. 6. The cell viability (%) of A549 cancer cells after photosensitization with different concentrations of FePcCl for 2 h without laser treatment. 0 μg/ml = A549 cancer cells that were not exposed to FePcCl (untreated cells-control); DMSO = dimethylsulfoxide (control). Data points represent the mean of ±SEM, $n = 3$. Significant differences between the untreated control and each of the different treatment concentrations are represented in graph as (**) $P \leqslant 0.01$ and (***) $P \leqslant 0.001$.

4. Discussion

In the present study, the cellular uptake and photodynamic effect of three different photosensitizers (GaPcCl, InPcCl and FePcCl) on A549 cancer cells were investigated. The minimal time course for the uptake of GaPcCl, InPcCl and FePcCl (100 μg/ml) by A549 cancer cells is shown in Figs. 1–3. Each photosensitizer had a very fast uptake since emission peaks with low fluorescence intensity (arbitrary units) was achieved after 30 s incubation with A549 cells. For periods of incubation longer than 30 s, the emission peaks

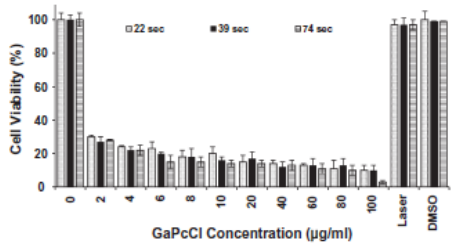

Fig. 7. The cell viability (%) of A549 cells after photosensitization with different concentrations of GaPcCl and photoirradiation (laser treatment) for 22 s (2.5 J/cm^2), 34 s (4.5 J/cm^2) and 74 s (8.5 J/cm^2). 0 μg/ml = A549 cells that were not exposed to GaPcCl and laser treatment (untreated cells-control); Laser = A549 cells that were photoirradiated without being exposed to GaPcCl (laser control); DMSO = dimethylsulfoxide (control). Data points represent the mean of ±SEM, $n = 3$. The differences between the untreated control and the respective experimental groups for each concentration were significant ($P \leqslant 0.001$).

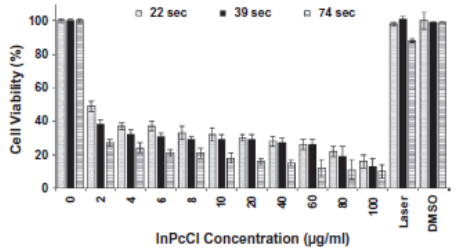

Fig. 8. The cell viability (%) of A549 cells after photosensitization with different concentrations of InPcCl and photoirradiation (laser treatment) for 22 s (2.5 J/cm^2), 34 s (4.5 J/cm^2) and 74 s (8.5 J/cm^2). 0 μg/ml = A549 cells that were not exposed to InPcCl and laser treatment (untreated cells-control); Laser = A549 cells that were photoirradiated without being exposed to InPcCl (laser control); DMSO = dimethylsulfoxide (control). Data points represent the mean of ±SEM, $n = 3$. The differences between the untreated control and the respective experimental groups for each concentration were significant ($P \leqslant 0.001$).

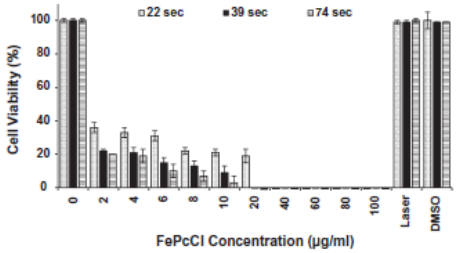

Fig. 9. The cell viability (%) of A549 cells after photosensitization with different concentrations of FePcCl and photoirradiation (laser treatment) for 22 s (2.5 J/cm^2), 34 s (4.5 J/cm^2) and 74 s (8.5 J/cm^2). 0 μg/ml = A549 cells that were not exposed to FePcCl and laser treatment (untreated cells-control); Laser = A549 cells that were photoirradiated without being exposed to FePcCl (laser control); DMSO = dimethylsulfoxide (control). Data points represent the mean of ±SEM, $n = 3$. The differences between the untreated control and the respective experimental groups for each concentration were significant ($P \leqslant 0.001$).

associated with GaPcCl, InPcCl and FePcCl showed increased fluorescence intensity indicating an increased cellular uptake of photosensitizer by A549 cancer cells. The results also indicate that the cellular uptake of GaPcCl, InPcCl and FePcCl by A549 cancer cells is time-dependant. At an uptake time of 24 h, the emission peak for extracted intracellular FePcCl from A549 cells (Fig. 3) showed the highest fluorescence intensity when compared to the emission peaks for extracted intracellular GaPcCl and InPcCl from A549 cells. However, in this study for the *in vitro* PDT experiments the A549 cancer cells were incubated with GaPcCl, InPcCl and FePcCl for 2 h instead of 24 h (when uptake of these photosensitizers were higher), to minimize the dark toxicity effects of these photosensitizers.

Phthalocyanines in its inactive state are inherently less or non-cytotoxic in the dark (absence of ambient light and laser photoactivation) depending on the photosensitizing concentration being used. This was seen with the percentage of viable A549 cancer cells after photosensitization with different concentrations of GaPcCl, InPcCl and FePcCl for 2 h under dark conditions displayed in Figs. 4–6 respectively. Negligible cytotoxicity was observed with low photosensitizing concentrations of GaPcCl (2–20 μg/ml), InPcCl (2–8 μg/ml) and FePcCl (2–10 μg/ml). Interestingly, 2 μg/ml photosensitizing concentration of GaPcCl, InPcCl and FePcCl were able to reduce the cell viability of A549 cancer cells to 95%, 96% and 99% respectively. A 100 μg/ml photosensitizing concentration of GaPcCl, InPcCl and FePcCl were able to reduce the cell viability of A549 cancer cells to 46%, 55% and 26% respectively. It is significantly evident ($P \geqslant 0.001$) that a 100 μg/ml photosensitizing concentration of GaPcCl, InPcCl and FePcCl was highly cytotoxic to A549 cancer cells than that of 2 μg/ml. On the other hand, these photosensitizers at a concentration of 2 μg/ml were found to be potently cytotoxic towards A549 cancer cells upon exposure to low laser light doses of 2.5 J/cm^2, 4.5 J/cm^2 and 8.5 J/cm^2 (Figs. 7–9). A549 cancer cells treated with 2 μg/ml of GaPcCl, InPcCl and FePcCl photoactivated with a treatment light dose of 2.5 J/cm^2 decreased the cell viability of the A549 cancer cells to 30%, 36% and 49% respectively (Figs. 7–9). It is also noteworthy to mention that GaPcCl, InPcCl and FePcCl mediated PDT is shown to be a concentration-dependent treatment. As the Pc concentration increased the cell viability of A549 cancer cells proportionally decreased as shown in Figs. 7–9. Concentrations of GaPcCl, InPcCl and FePcCl greater than 2 μg/ml photoactivated with light doses higher than 2.5 J/cm^2 (i.e. 4.5 J/cm^2 and 8.5 J/cm^2) were found to further decrease the survival of A549 cancer cells. Thus, indicating that the efficacy of GaPcCl, InPcCl or FePcCl mediated photokilling of A549 cancer cells is dependent of both the Pc concentration and the treatment light doses applied. In comparison to GaPcCl and InPcCl, FePcCl (40–100 μg/ml) was able to attain a 100% cell death when photoactived with a light dose of 2.5 J/cm^2, 4.5 J/cm^2 and 8.5 J/cm^2 (Fig. 9). A 100% cell death of A549 cancer cells was also detected when 20 μg/ml of FePcCl was photactivated with light doses of 4.5 J/cm^2 and 8.5 J/cm^2.

It is noteworthy to mention that GaPcCl, InPcCl and FePcCl displayed dark toxicity under the current experimental conditions at concentrations of 20 μg/ml and higher. This dark toxicity most likely contributes to the decrease in cell viability of the PDT treated A549 cancer cells. However, the presence of dark toxicity does not necessarily have to interfere with the possible future *in vivo* or clinical application of GaPcCl, InPcCl and FePcCl as photosensitizing agents for the PDT treatment of lung cancer, especially if these Pcs exhibit little or no dark toxicity effects on normal healthy cells or normal healthy surrounding tissue.

5. Conclusion

GaPcCl, InPcCl and FePcCl mediated PDT has a significant killing effect on human lung carcinoma cells (A549). The PDT effect of these metal-based phthalocyanines was influenced by PS concentration and the applied treatment light dose. Photosensitizing

concentrations of FePcCl ranging from 40 μg/ml to 100 μg/ml activated with light doses of 2.5 J/cm^2, 4.5 J/cm^2 and 8.5 J/cm^2 were the best parameters for this *in vitro* experiment. This small amount of data is encouraging and suggests that full scale studies should be made on these photosensitizers as well as a wide variety of other MPCs as possible photosensitizing agents for PDT. Several authors have reported that metal-based phthalocyanines are highly valued for its photodynamic properties and safety. These authors also report that PDT is not associated with any complications and, in addition prevent or minimize the need for many invasive oncology procedures. Moreover, PDT is currently highly effective for the treatment of primary lung cancer, and obstructing endobronchial lesions and debulking of large tumors. PDT can be used as a stand-alone therapy or in combination with other oncologic therapies (e.g. chemotherapy) including surgery. The obvious ways to improve PDT efficacy require the development of new PSs, optimization of protocols and precise dosimetry. Photosensitizers like GaPcCl, InPcCl and FePcCl can offer to improve the current efficacy of PDT even further.

6. Abbreviations

PDT	photodynamic therapy
PS	photosensitizer
PSs	photosensitizers
ROS	reactive oxygen species
Pc	phthalocyanine
Pcs	phthalocyanines
GaPcCl	gallium (III) phthalocyanine chloride
InPcCl	indium (III) phthalocyanine chloride
FePcCl	iron (III) phthalocyanine chloride

Acknowledgements

The authors wish to thank Dr. Bronwyn C. Joubert (Nelson Mandela Medical School, University of Kwazulu Natal) for providing the A549 cancer cells and Renata Bianca Maduray for proof-reading this manuscript. This work was funded by the National research Funding (NRF) of South Africa and Durban University of Technology.

References

[1] S. Lam, Photodynamic therapy for lung cancer, Thorax 48 (1993) 469.
[2] A. Chiaviello, I. Postiglione, G. Palumbo, Targets and mechanisms of photodynamic therapy in lung cancer cells: a brief overview, Cancers 3 (2011) 1014–1041.
[3] T.G. Sutedja, P.E. Postmus, Photodynamic therapy in lung cancer, A review, Journal of Photochemistry and Photobiology: Biology 36 (1996) 199–204.
[4] C.B. Simone, J.S. Friedberg, E. Glatstein, J.P. Stevenson, D.H. Sterman, S.M. Hahn, K.A. Cengel, Photodynamic therapy for the treatment of non-small cell lung cancer, Journal of Thoracic Disease 1 (2012) 63–75.
[5] R. Allison, K. Moghissi, G. Downie, K. Dixon, Photodynamic therapy (PDT) for lung cancer, Photodiagnosis Photodynamic Therapy 8 (2011) 231–239.
[6] M.C. Issa, M. Manela-Azulay, Photodynamic therapy: a review of the literature and image documentation, An Bras Dermatology 4 (2010) 501–511.
[7] A. Juarranz, P. Jaén, F. Sanz-Rodríguez, J. Cuevas, S. González, Photodynamic therapy of cancer: basic principles and applications, Clinical Translational Oncology 10 (2008) 148–154.
[8] C. Hopper, Photodynamic therapy: a clinical reality in the treatment of cancer, Lancet Oncology 1 (2000) 212–219.
[9] J.T. Dougherty, C.J. Gomer, B.W. Henderson, G. Jori, D. Kessel, M. Korbelik, J. Moan, Q. Peng, Photodynamic Therapy, Journal National Cancer Institute 90 (1998) 889–905.
[10] S. Yanoa, S. Hirohara, M. Obata, Y. Hagiya, S. Ogura, A. Ikeda, H. Kataoka, M. Tanaka, T. Joh, Current states and future views in photodynamic therapy, Journal of Photochemistry and Photobiology C: Photochemistry Reviews 12 (2011) 46–67.
[11] M. Triesscheijn, P. Baas, J.H.M. Schellens, F.A. Stewart, Photodynamic therapy in oncology, Oncologist 11 (2006) 1034–1044.
[12] W.M. Sharman, C.M. Allen, J.E. Van Lier, Photodynamic therapeutics: basic principles and clinical applications, DDT 4 (1999) 507–517.
[13] G.J. Stables, D.V. Ash, Photodynamic therapy, Cancer Treatment Reviews 21 (1995) 311–323.
[14] J.D. Spikes, Phthalocyanines as photosensitizers in biological systems and for the photodynamic therapy of tumors, Journal of Photochemistry and Photobiology 43 (1986) 691–699.
[15] N. Sekkat, H. Van den Bergh, T. Nyokong, N. Lange, Like a bolt from the blue: phthalocyanines in biomedical optics, Molecules 17 (2012) 98–144.
[16] M. Durmuş, T. Nyokong, The synthesis, fluorescence behaviour and singlet oxygen studies of new water-soluble cationic gallium(III) phthalocyanines, Inorganic Chemistry Communications 10 (2007) 332–338.
[17] T. Nyokong, Desired properties of new phthalocyanines for photodynamic therapy, Pure and Applied Chemistry 83 (2011) 1763–1779.
[18] L.B. Josefsen, R.W. Boyle, Unique diagnostic and therapeutic roles of porphyrins and phthalocyanines in photodynamic therapy, Imaging and Theranostics, Theranostics 9 (2012) 916–966.
[19] S. Ogura, K. Tabata, K. Fukushima, T. Kamachi, I. Okura, Development of phthalocyanines for photodynamic therapy, Journal of Porphyrins and Phthalocyanines 10 (2006) 1116–1124.
[20] L.B. Josefsen, R.W. Boyle, Photodynamic therapy and the development of metal-based phthalocyanines, Metal-Based Drugs (2008) 1–24.
[21] C.G. Claessens, W.J. Blau, M. Cook, M. Hanack, R.J.M. Nolte, T. Torres, D. Wohrle, Phthalocyanines and phthalocyanines analogues: the quest for applicable optical properties, Chemical Monthly 132 (2001) 3–11.
[22] M. Durmuş, T. Nyokong, Synthesis, photophysical and photochemical studies of new water-soluble indium(III) phthalocyanines, Photochem Photobiol Science 6 (2007) 659–668.
[23] H. Yanık, D. Aydın, M. Durmuş, V. Ahsen, Peripheral and non-peripheral tetrasubstituted aluminium, gallium and indium phthalocyanines: synthesis, photophysics and photochemistry, Journal of Photochemistry and Photobiology A: Chemistry 206 (2009) 18–26.
[24] M. Çamura, V. Ahsena, M. Durmuşa, The first comparison of photophysical and photochemical properties of non-ionic, ionic and zwitterionic gallium (III) and indium (III) phthalocyanines, Journal of Photochemistry and Photobiology A: Chemistry 219 (2011) 217–227.
[25] S. Moeno, T. Nyokong, Solvent and central metal effects on the photophysical and photochemical properties of peripherally tetra mercaptopyridine substituted metallophthalocyanines, Journal of Photochemistry and Photobiology A: Chemistry 203 (2009) 204–210.

Metal-based phthalocyanines as a potential photosensitizing agent in photodynamic therapy for the treatment of melanoma skin cancer

Kaminee Maduray*[a], Bharti Odhav[a]
[a]Durban University of Technology; Department of Biotechnology and Food Technology, Steve Biko Road, Durban, 4001, South Africa

ABSTRACT

Photodynamic therapy (PDT) is an emerging medical treatment that uses photosensitizers (drug) which are activated by laser light for the generation of cytotoxic free radicals and singlet oxygen molecules that cause tumor cell death. In the recent years, there has been a focus on using and improving an industrial colorant termed phthalocyanines as a prospective photosensitizer because of its unique properties. This *in vitro* study investigated the photodynamic effect of indium (InPcCl) and iron (FePcCl) phthalocyanine chlorides on human skin cancer cells (melanoma). Experimentally, 2 x 10^4 cells/ml were seeded in 24-well tissue culture plates and allowed to attach overnight, after which cells were treated with different concentrations (2 µg/ml – 100 µg/ml) of InPcCl and FePcCl. After 2 h, cells were irradiated with constant light doses of 2.5 J/cm^2, 4.5 J/cm^2 and 8.5 J/cm^2 delivered from a diode laser. Post-irradiated cells were incubated for 24 h before cell viability was measured using the MTT Assay. At 24 h after PDT, irradiation with a light dose of 2.5 J/cm^2 for each photosensitizing concentration of InPcCl and FePcCl produced a significant decrease in cell viability, but when the treatment light dose was further increased to 4.5 J/cm^2 and 8.5 J/cm^2 the cell survival was less than 55% for photosensitizing concentrations of InPcCl and FePcCl from 4 µg/ml to 100 µg/ml. This PDT study concludes that low concentrations on InPcCl and FePcCl activated with low level light doses can be used for the effective *in vitro* killing of melanoma cancer cells.

Keywords: photodynamic therapy, indium phthalocyanine chlorides, iron phthalocyanine chlorides, melanoma cancer, photosensitizers, cancer, phthalocyanines, laser

1. INTRODUCTION

Malignant melanoma is a neoplasm (cancer) that originates in the melanocytes which are found randomly throughout the basal cells or in the deepest portions of the epidermis. Melanocytes are responsible for producing melanin (pigment and photoprotector) which is the primary determinant of skin color.[1] There are several known risk factors for the development of melanoma in individuals. For example, the duration of exposure to ultraviolet (UV) radiation from the sun over one's life has shown to be a major risk factor in the development of melanoma. Also, a patient that has been diagnosed with basal cell or squamous cell skin cancer is at high risk of developing another skin cancer such as melanoma cancer and approximately 8-12% of reported cutaneous melanoma cancer cases are hereditary.[1-2] The standard primary treatments for melanoma cancer are surgery, chemotherapy and radiation therapy.[3-5] Furthermore, chemotherapy and radiation therapy can also be used as an adjuvant therapy in combination with other cancer treatments (e.g. surgery) or as a stand-alone therapy. Unfortunately, chemotherapy and radiation therapy possesses many side effects, which can be more severe if chemotherapy is received in addition to radiation therapy. Newer therapies such as cytokine biotherapy, antibody biotherapy and vaccines are now also being used as an adjuvant therapy for the treatment of melanoma cancer.[1]

*madurayk@yahoo.com; phone 083 6129 541

These biological therapies differ from chemotherapy because it aids the immune system in fighting cancer. It is mostly used to stop or slow growth which makes it easier for the immune system to destroy the cancer cells.[1] Surgery, chemotherapy, radiation therapy and biological therapy can be used in any combinations to varying degrees of success. Since, melanoma cancer is typically a highly aggressive and metastatic in nature many of these treatment options act as deterrents rather than cures. However, melanoma can be curable when it is found in its very early stages. [5]

Photodynamic therapy (PDT) is an emerging alternative to radiation therapy, chemotherapy, surgery and biological therapy. It is based on the principle that, a photosensitive drug (photosensitizer, PS) in its inactive state is administrated to the patient, which preferentially accumulates in the cancerous tissue rather than normal healthy tissue. Subsequently, light from a laser source at a specific wavelength which generally correlates to the peak absorption of PS is applied to the cancerous tissue (containing the PS). During light treatment, the activated PS generates a photochemical reaction that leads to the production of free radicals and reactive oxygen species (ROS), mostly singlet oxygen, which is cytotoxic and causes irreversible tumor cell death via necrosis, apoptosis or autophagy.[1,6-7] PDT has been around since the 1980s and has been successfully used to treat non-cancerous diseases (e.g. cardiovascular, dermatological, ophthalmic and infectious diseases), several precancerous diseases and specific types of cancers including non-melanoma skin cancers.[6] Although, it has been around for over three decades, PDT has not received as much attention clinically as a therapeutic treatment for melanoma cancer. The major reason for this lack of attention stems from the fact that the wavelength of light used to activate these clinically approved first-generation PSs (e.g. photofrin and porphyrins) overlaps with the absorption spectra of melanin. Therefore, melanin playing a major role in photoprotection blocks light during laser treatment making PDT less effective.[1] Interestingly, a great deal of research is ongoing towards improving PDT and developing second-generation PSs that have intense absorptions in the wavelength range of 600 nm to 900 nm which fits within the photodynamic or therapeutic window required for efficient PDT. This research has certainly been useful for the PDT treatment of melanoma cancer. For instance, phthalocyanines (Pcs) and its derivatives are second- generation PSs that have been extensively studied as a potential photosensitizing agent for the treatment of melanoma cancer and are continually being developed for the PDT treatment of various tumors. [6-7]

Phthalocyanines (Pcs) represent another form of macrocycle, similar to porphyrins[1] and may be regarded as azaporphyrins.[8] These compounds also have the ability to coordinate metal ions within their nitrogen core to form metal- based phthalocyanine (MPc) complexes. The type of the metal ion strongly influences the photophysical or PDT properties of the MPc complex.[9] MPc complexes containing transition metals (e.g. Fe, Mn, Co, Ni or Cu) offer a PS with short lifetimes, whereas diamagnetic metal ions that contain a closed shell such as zinc (Zn^{2+}), aluminium (Al^{3+}), gallium (Ga^{3+}) and silicon (Si^{4+}) give MPc complexes high triplet quantum yields and long triplet lifetimes, which are essential for efficient photosensitization during PDT treatment.[8-10] The electronic spectrum of MPc complexes reveals a distinct intense absorption at ± 600 nm (Q band) accompanied by a weak absorption at ± 400 nm (B band).[8] Whereas, naphthalocyanines (an extend Pc derivative) advantageously absorb at higher wavelengths (740 nm – 780 nm) than MPcs. This absorption range of naphthalocyanines makes them potential *in vivo* imaging agents and photosensitizing agents for the PDT treatment of highly pigmented tumors (e.g. melanomas).[11] To date, Photosens® (mixture of aluminium chloride Pcs with sulphonated side – groups) is clinically used in Russia to treat a range of cancers (e.g. skin, breast, lung, head, neck, cervical, etc.). Silicon (IV) phthalocyanine Pc4 and a liposomal preparation of zinc (II) phthalocyanine are currently under clinical trials.[12-13]

The architectural flexibility, photophysics and photochemistry properties of the different MPc complexes shows clearly that these compounds are valuable photosensitizing agents in PDT for the treatment of various cancers including melanoma cancer, but further *in vitro* and *in vivo* studies investigating the photodynamic activity of many of these MPc complexes for different cancers still needs to performed. Therefore, the present work studied the cellular uptake and *in vitro* photodynamic effect of two different MPc complexes: indium (III) phthalocyanine chloride and iron (III) phthalocyanine chloride using a malignant melanoma cell line.

2. METHODOLOGY

2.1 Spectrophotometric analysis of InPcCl and FePcCl

Indium (III) phthalocyanine chloride (InPcCl) and iron (III) phthalocyanine chloride (FePcCl) was purchased from Sigma-Aldrich and used as a photosensitizer without further purification. Spectrophotometric experiments were carried out in dimethylsulfoxide (DMSO, Sigma). The electronic absorption spectrum of InPcCl and FePcCl was recorded on the Cary 100 UV-Vis spectrophotometer in the spectral range of 300-900 nm at room temperature. The fluorescence emission spectrum of InPcCl and FePcCl was measured by using a Varian Eclipse Fluorescence Spectrophotometer with an excitation wavelength set at 605 nm and 680 nm respectively.

2.2 Cell culture of melanoma cancer cells

Human malignant melanoma cells (UCAA-62) were routinely maintained in Dulbecco's modified Eagle's medium (DMEM, Biochrom) supplemented with 10% fetal calf serum (FCS, Highveld Biological) and 1% Penicillin-Streptomycin (pen/strep, Biochrom) at 37°C in a 5% CO_2 incubator. For experimental assays, 80% confluent flasks with melanoma cells from passage 9 to12 were seeded in 24-well tissue culture plates (Costar) at a density of 2 x 10^4 cells per a well in 1 ml supplemented DMEM.

2.3 Cellular uptake of InPcCl and FePcCl by melanoma cancer cells

Melanoma cancer cells seeded in 24-well tissue culture plates were photosensitized with 100 µg/ml of InPcCl or FePcCl for uptake times of 30 min, 2 h, 10 h, 18 h and 24 h at 37 °C in a 5% CO_2 incubator under dark conditions. After incubation with PS for 30 min, 2 h, 10 h, 18 h and 24 h; cells were washed with phosphate buffer (PBS, Sigma) before collecting pellets of the cells for the extraction of intracellular InPcCl or FePcCl using DMSO. Thereafter, the samples were centrifuged and the DMSO supernatants were collected and analyzed for traces of intracellular accumulated InPcCl and FePcCl using a fluorescence spectrophotometer at specific excitation wavelengths of 605 nm and 680 nm respectively. Simultaneously, DMSO supernatant from untreated melanoma cancer cells (not pre-incubated with InPcCl and FePcCl) were measured as a control at the excitation wavelengths of 605 nm and 680 nm for each exposure time.

2.4 Dark toxicity assay

A PS (in its inactive form) without laser treatment may have anti-proliferative and/or cytotoxic effects, referred to as dark toxicity. A stock solution InPcCl and FePcCl at a concentration of 100 µg/ml was prepared using DMEM and DMSO. Each stock solution of InPcCl and FePcCl was further diluted using DMEM medium supplemented with 10% FCS and 1% pen/strep to prepare treatment concentrations ranging from 2 µg/ml – 90 µg/ml. Melanoma cancer cells seeded in 24-well tissue culture plates were incubated for 2 h with either different InPcCl or FePcCl concentrations at 37 °C in a 5% CO_2 incubator under dark conditions. Cell culture media (DMEM) only, cells treated with DMSO only and cells that were not exposed to InPcCl or FePcCl (0 µg/ml; untreated cells) served as controls. After 2 h the photosensitized cells were washed with PBS and cell viability was measured by 3-[4, 5-dimethylthiazolyl]-2, 5-diphenyltetrazolium bromide (MTT) assay. 500 µl of DMEM with 100 µl of MTT (5 mg/ml) was added to each well for 4 h at 37 °C in a 5% CO_2 atmosphere. After 4 h, MTT was replaced with 500 µl of DMSO to dissolve the formazan crystals and the resulting absorbance was measured using a plate reader (Biohit) at a wavelength of 490 nm with a reference wavelength at 630 nm simultaneously. The relative cell viability (%) was expressed as a percentage relative to the untreated control cells.

2.5 *In vitro* photodynamic therapy treatment

Melanoma cancer cells at a density of 2 x 10^4 cells/ml were seeded onto 24-well tissue culture plates and allowed to attach overnight before treatment with different concentrations of InPcCl or FePcCl (2 µg/ml-100 µg/ml). After 2 h the photosensitized cells were irradiated under dark conditions. Irradiation was performed using a continuous wave diode laser (Cube Laser System, Coherent) with a wavelength of 661 nm. A spot size of 1 cm with a measured output power of

90 mW was used to deliver treatment light doses of 2.5 J/cm^2, 4.5 J/cm^2 and 8.5 J/cm^2 to specific wells on the 24-well plates containing a monolayer of photosensitized cells in 22 sec, 39 sec, and 74 sec of irradiation time accordingly. The untreated control cells were not exposed to InPcCl or FePcCl and laser irradiation. A laser control was set-up for each treatment light dose by irradiating cells without InPcCl or FePcCl for 22 sec, 39 sec or 74 sec. After irradiation, plates were incubated at 37 °C in a 5% CO_2 incubator under dark conditions for 24 h before cell viability was measured using the MTT assay as described above. The relative cell viability (%) was expressed as a percentage relative to the untreated control cells.

2.6 Statistical analysis

Each test was done in triplicate. Statistical analysis was performed using Instat software of GraphPad prism 6 by one-way analysis of Variance (ANOVA). The Tukey-Kramer Multiple Comparisons Test was used to determine the significant changes between experimental groups and respective controls.

3 DATA

The absorption spectrum of InPcCl and FePcCl in DMSO is seen in **Figure 1A** and **Figure 1B** respectively. **Figure 2A and 2B** shows the emission profile of InPcCl and FePcCl in DMSO determined by using a fixed excitation wavelength of 605 nm and 680 nm respectively.

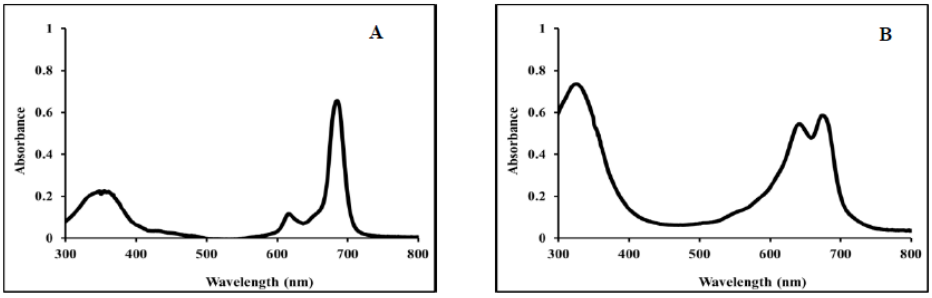

Figure 1. The absorption spectrum of (A) InPcCl and (B) FePcCl in DMSO.

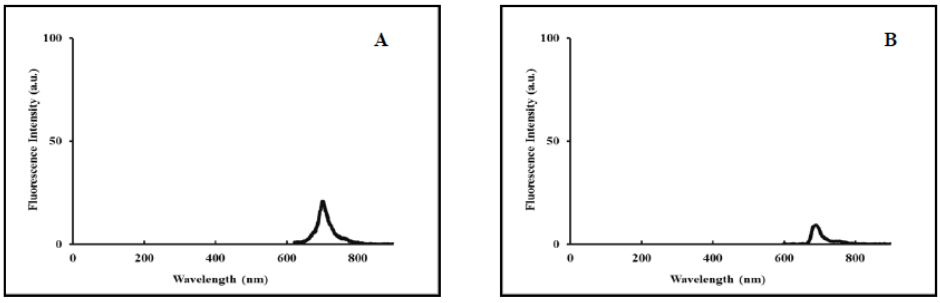

Figure 2. The fluorescence emission spectrum (A) InPcCl and (B) FePcCl in DMSO determined by using a fixed excitation wavelength of 605 nm and 680 nm respectively.

Figure 3A shows the emission peak and emission or fluorescence intensity (excitation wavelength = 605 nm) of intracellular InPcCl in DMSO extracted from melanoma cancer cells at uptake times of 30 min, 2 h, 10 h, 18 h and 24 h; with **Figure 3B** showing the emission peak and emission or fluorescence intensity (excitation wavelength = 680 nm) of intracellular FePcCl in DMSO extracted from melanoma cancer cells at similar uptake times of 30 min, 2 h, 10 h, 18 h and 24 h.

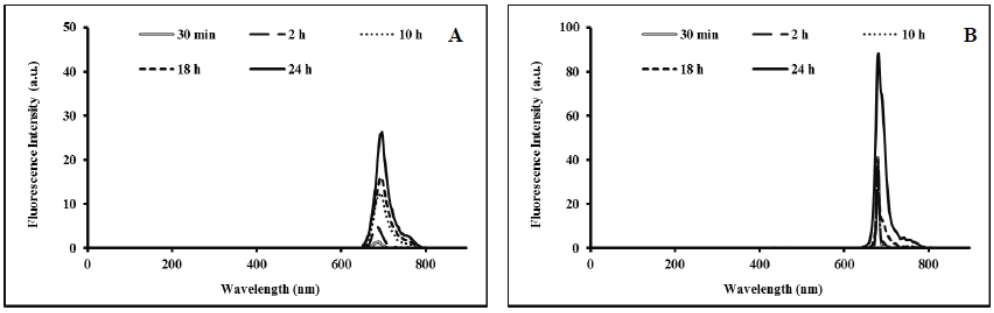

Figure 3. The emission peak and fluorescence intensity (a.u.) of intracellular InPcCl and FePcCl taken up by melanoma cancer cells at different incubation times measured using a fluorescence spectrophotometer with an excitation wavelength set at 605 nm and 680 nm respectively.

The cytotoxic effect of different concentrations of InPcCl and FePcCl in its inactive state (without laser treatment) on the cell viability of melanoma cancer cells is presented in **Figure 4A and 4B** respectively.

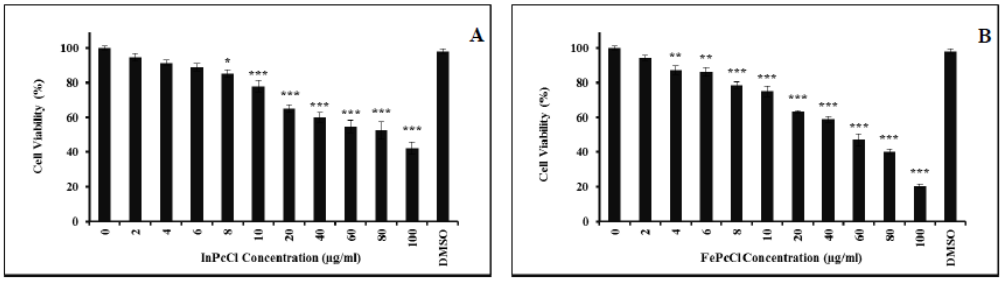

Figure 4. The cell viability (%) of melanoma cancer cells after photosensitization for 2 h with inactive (A) InPcCl and (B) FePcCl at different concentrations without exposure to ambient light and laser treatment. Cell viability was expressed as a percentage of the untreated control cells not exposed to InPcCl or FePcCl. 0 µg/ml = melanoma cancer cells that were not exposed to photosensitizers (untreated control cells); DMSO = melanoma cancer cells treated with dimethylsulfoxide (DMSO) only. Data points represent the mean of ±SEM, n = 3. Significant differences between the untreated cell control and each of the different treatment concentrations are represented in the graph as (**) $P \leq 0.01$ and (***) $P \leq 0.001$.

Melanoma cancer cells were photosensitized with different concentrations InPcCl and FePcCl before laser treatment for 22 sec (2.5 J/cm^2), 34 sec (4.5 J/cm^2) and 74 sec (8.5 J/cm^2) with continuous wave diode laser at a wavelength of 661 nm. Post-irradiated cells were incubated for 24 h before cell viability was measured using MTT assay as seen in **Figure 5A** and **5B**.

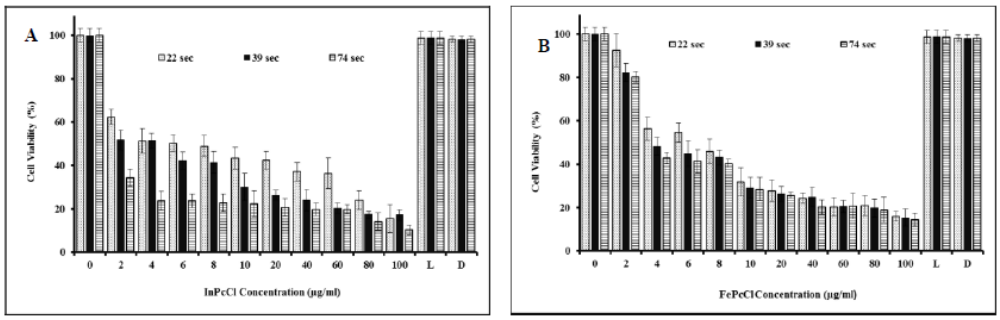

Figure 5. The cell viability (%) of melanoma cells after photosensitization with different concentrations of (A) InPcCl ; (B) FePcCl and laser treatment for 22 sec (2.5 J/cm^2), 34 sec (4.5 J/cm^2) and 74 sec (8.5 J/cm^2). 0 µg/ml = melanoma cells that were not exposed to InPcCl or FePcCl and laser treatment (untreated cells); L = melanoma cells that were laser treated but not exposed to InPcCl or FePcCl (laser control); D = DMSO control. The differences between the untreated control and the respective experimental groups for each concentration were significant ($P \leq 0.001$).

4 RESULTS

The electronic spectra of InPcCl dissolved in DMSO showed the highest absorption peak at 685 nm accompanied by lower absorption peaks at 350 nm and 616 nm (Figure 1A). FePcCl dissolved in DMSO displayed absorption at 325 nm, 642 nm and 675 nm (Figure 1B). As shown in Figure 2A and 2B, InPcCl and FePcCl displayed detectable emission peaks when excited at a fixed wavelength of 605 nm and 680 nm respectively. The fluorescence profile of InPcCl in DMSO exhibits two distinct emission peaks at: 701 nm and 750 nm with an excitation wavelength of 605 nm (Figure 2A). A fluorescence emission peak was observed at 750 nm for FePcCl with an excitation wavelength of 680 nm in DMSO (Figure 2B). In the present study, the cellular uptake of InPcCl and FePcCl by melanoma cancer cells were also investigated. The minimal time course for the uptake of InPcCl and FePcCl (100 µg/ml) by melanoma cancer cells is shown in Figure 3A and 3B respectively. Each photosensitizer had a very fast uptake since emission peaks with low fluorescence intensity (arbitrary units) was achieved after 30 min incubation with melanoma cancer cells. For periods of incubation longer than 30 min, the emission peaks associated with InPcCl and FePcCl showed increased fluorescence intensity indicating an increased cellular uptake of photosensitizer by melanoma cancer cells. The results also indicate that the cellular uptake of InPcCl and FePcCl by melanoma cancer cells is time-dependant.

Dark toxicity studies were conducted to determine the cytotoxicity effects of InPcCl (Figure 4A) and FePcCl (Figure 4B) in its inactive state (without laser treatment) on the melanoma cancer cells. Negligible cytotoxicity was observed with low photosensitizing concentrations of InPcCl (2 µg/ml – 10 µg/ml) and FePcCl (2 µg/ml – 10 µg/ml). Interestingly, 2 µg/ml photosensitizing concentration of InPcCl and FePcCl were able to reduce the cell viability of melanoma cancer cells to 94% and 94% respectively. A 100 µg/ml photosensitizing concentration of InPcCl and FePcCl were able to reduce the cell viability of melanoma cancer cells to 42% and 21% respectively. It is significantly evident ($P \geq 0.001$) that a 100 µg/ml photosensitizing concentration of InPcCl and FePcCl was highly cytotoxic to melanoma cancer cells than that of 2 µg/ml. On the other hand, these photosensitizers at a concentration of 2 µg/ml were found to be potently cytotoxic towards melanoma cancer cells upon exposure to low laser light doses of 2.5 J/cm^2, 4.5 J/cm^2 and 8.5 J/cm^2 (Figure 5A & 5B). Melanoma cancer cells treated with 4 µg/ml of InPcCl and FePcCl photoactivated with a treatment light dose of 2.5 J/cm^2 decreased the cell viability of the melanoma cancer cells to 51% and 56% respectively. Concentrations of InPcCl and FePcCl greater than 4 µg/ml photoactivated with light doses higher than 2.5 J/cm^2 (i.e. 4.5 J/cm^2 and 8.5 J/cm^2) were found to further decrease the survival of melanoma cancer cells. It is also noteworthy to mention that InPcCl and FePcCl mediated PDT is shown to be a concentration - dependent treatment. As the InPcCl and FePcCl concentration increased the cell viability of melanoma cancer cells proportionally decreased as shown in Figure

5A and 5B. This indicates that the *in vitro* PDT efficacy of InPcCl or FePcCl for melanoma cancer is dependent of both the PS concentration and the treatment light doses applied.

5 CONCLUSION

This *in vitro* study has demonstrated that InPcCl and FePcCl mediated PDT is an option for melanoma skin cancer. The PDT efficiency of these metal - based phthalocyanine complexes depends on the photosensitizer concentration and light dose applied during treatment. The obvious ways to improve PDT efficacy requires the development of new PSs, optimization of protocols and precise dosimetry. Photosensitizers like InPcCl and FePcCl can offer to improve the current efficacy of PDT even further.

ACKNOWLEDGMENTS

The authors wish to thank Natasha Kolesnikova (Biosciences, CSIR) for providing the human malignant melanoma cell line. The National Research Funding (NRF) of South Africa and Durban University of Technology (DUT) for financial support.

REFERENCES

[1] Swavey, S., Tran, M., "Porphyrin and phthalocyanine photosensitizers as PDT agents: A new modality for the treatment of melanoma," Recent Advances in the biology, therapy and management of melanoma, 253-282 (2013).
[2] Baldea, I., Filip, A.G.,"Photodynamic therapy in melanoma- an update" Journal of Physiology and pharmacology 63 (2), 109-118 (2012).
[3] Lawson, D.H., "Choices in adjuvant therapy of melanoma" Cancer control 12 (4), 236-241 (2005).
[4] Berk, L.B., "Radiation therapy as primary and adjuvant treatment for local and regional melanoma" Cancer control 15 (3), 233-237 (2008).
[5] Elias, E.G., Hassksmp, J.H., Sharma, B.K., "Biology of human cutaneous melanoma" Cancers 2, 165-189 (2010).
[6] Van Den Bergh, H., Ballini, J.P., "Principles of photodynamic therapy" PDT of oculars diseases, 11-42 (2004).
[7] Zhu, T.C., Finlay, J.C., "The role of photodynamic therapy physics" Medical Physics 35 (7), 3127-3136 (2008).
[8] Spikes, J.D., "Phthalocyanines as photosensitizers in biological systems and for the photodynamic therapy of tumors" Journal of Photochemistry and Photobiology 43, 691-699 (1986).
[9] Durmuş, M., Nyokong, T., "The synthesis, fluorescence behaviour and singlet oxygen studies of new water-soluble cationic gallium (III) phthalocyanines" Inorganic Chemistry Communication 10, 332-338 (2007).
[10] Durmuş, M., Nyokong, T., "Synthesis, photophysical and photochemical studies of new water-soluble indium (III) phthalocyanines" Photochem Photobiol Science 6, 659-68 (2007).
[11] Ogura, S., Tabata, K., Fukushima, K., Kamachi, T., Okura, I., "Development of phthalocyanines for photodynamic therapy" Journal of Porphyrins and Phthalocyanines 10, 1116-1124 (2006).
[12] Sekkat, N., Van den Bergh, H., Nyokong, T., Lange, N., "Like a bolt from the blue: phthalocyanines in biomedical optics" Molecules 17, 98-144 (2012).
[13] Yanik, H., Aydin, D., Durmuş, M., Ahsen, V., "Peripheral and non-peripheral tetrasubstituted aluminum, gallium and indium phthalocyanines: Synthesis, photophysics and photochemistry" Journal of Photochemistry and Photobiology A: Chemistry 206, 18–26 (2009).